PALEOLIMNOLOGY IN AN URBAN ENVIRONMENT: THE HISTORY OF ENVIRONMENTAL CHANGE IN ST. JOHN'S, NEWFOUNDLAND

TERRY CHRISTOPHER


CENTRE FOR NFLD. STUDIES
MEMORIAL UNIVERSITY
OF NEWFOUNDLAND

PALEOLIMNOLOGY IN AN URBAN ENVIRONMENT: THE HISTORY OF ENVIRONMENTAL CHANGE IN ST. JOHN'S, NEWFOUNDLAND

by

Terry Christopher

A thesis submitted to the

School of Graduate Studies

in partial fulfilment of the

requirements for the degree of

Doctor of Philosophy

Department of Earth Sciences
Memorial University of Newfoundland

March 1999

St. John's Newfoundland

Dedicated to Stella
You are hope and
hope shall let fall
from Heaven
a shower of roses

Abstract

Lake sediment cores from St. John's and surrounding areas were used to document anthropogenic impacts since European settlement. Environmental indicators preserved in the sediment including, geochemical characteristics, pollen, diatoms, soot and charcoal were analyzed in a chronological sequence to document the physical, chemical and biological impacts over time.

Two broad-scale eras of direct soil disturbance were identified and related to farming and urban growth. During the farming era, between 1750 and 1950, the natural vegetation cover was removed and lake sedimentation rates increased. The urban era, which began about 1910, resulted in rapid soil erosion and high lake sedimentation rates. During the most intense period of urban development, the mid-1960s, the dry sediment influx rate was 160 times pre-European rates. Storm sewers and pavement played an important role in the urban environment, providing a direct path to the lakes for pollutants.

Superimposed on these disturbances are atmospheric contributions from coal and automobile emissions. Coal combustion, which began about 1800 and increased to the mid-1950s, emitted soot and toxic metals, as observed in the lake sediment records. Automobile pollution, through leaded gasoline combustion, contributed significant levels of lead.

Lake sediment records show the highest inputs and concentrations of lead occurred about 1970. Lead isotopic ratios suggest two or three different gasoline types were used in this area.

The most notable aquatic impact is a pH increase through the last few decades. Reconstructing water pH in Quidi Vidi Lake from diatom assemblages showed that the earliest farming had little influence on the pH, while an increase of about 1.2 units was observed to the 1980s. The recent high pH has been attributed to increased buffering capacity, believed to be caused by an increase in Mg and Ca contributions from the dissolution of concrete in the watershed.

The long history of coal combustion and leaded gasoline combustion has probably left the local soils charged with soot and heavy metals. Although the extent of influence is unknown, these soils may be continuous suppliers of contaminants for centuries to come. Any attempt to ameliorate the urban lakes and their watershed soils should consider all consequences, since the lakes appear to be in a 'city-equilibrium'.

Acknowledgements

Thanks go out to Martin Blake, Rick Bourgeois and Skip Pile who provided assistance during sampling in the cold winter months of 1992. Many more thanks to Martin who spent so many more hours helping with the extrusion of the lake cores.

Helen Gillespie, Chris Finch and Dr. John Kingston are thanked for their guidance in the laboratory at different stages.

Mr. Robert McNealy is thanked for sharing so willingly his great knowledge of the historical aspects of St. John's.

Dr. Joyce Macpherson, Dr. Moire Wadleigh, Dr. Ali Aksu and Dr. Jun Abrajano are thanked for allowing the use of their laboratory space and equipment, and for guidance and assistance in the laboratory and otherwise.

A special thanks is extended to Dr. Elliott Burden and Dr. Peter Davenport, who provided much assistance and at the same time a certain autonomy allowing me to mould this thesis the way I wanted it. Their patience is also noted.

Both the Department of Graduate Studies and Department of Earth Sciences are thanked for their financial assistance. Gratitude is extended to the Department of Mines and Energy, Newfoundland Branch, for their financial assistance for data acquisition and access to laboratory and computer facilities. Without both of these funding sources this project would never

have started.

The Geological Survey of Canada is thanked for providing five ^{14}C dates.

A special thanks is extended to my mother. You have taught me the meaning of perseverance.

Table of Contents

Chapter 1 1

1.1 Introduction 1

1.2 Purpose, Scope 1

1.3 Present Day St. John's 6

1.4 Previous Work 7

1.5 Climate 16

1.6 Geology 16

1.7 Historical Aspects of St. John's 17
1.7.1 Farming and Forestry 17
1.7.2 Population 21
1.7.3 Urban Growth 21
1.7.5 Transportation Systems 24
1.7.6 Industrialization in St. John's 24
1.7.7 Fuel Sources 25

1.8 Thesis Layout 27

Chapter 2: Methods 29

2.1 Lake Core Sampling 29

2.2 Core Components 29

2.3 Coring Operation 33
2.3.1 Core extrusion 35
2.3.2 Sediment Sampling 36

2.4 Sample preparation and Geochemical Analysis 38
2.4.1 Total and Acid Extractable Analysis 39

2.5 Palynomorph and Diatom Preparation and Analysis . . 40
2.5.1 Frequency Calculations and pH reconstruction 42

2.6 Common Pb Isotopic Ratios; $^{206}Pb/^{207}Pb$, $^{208}Pb/^{204}Pb$, $^{206}Pb/^{204}Pb$ 43

2.7 Clay and Mineral Analysis 43

2.8 Radiometric dates (^{210}Pb, ^{137}Cs and ^{14}C) 44

2.9 Statistical analysis 44

2.10 Analytical accuracy 48

Chapter 3: Geochemical Results 49

3.1 Introduction 49

3.2 Defining the Major Geochemical Associations 49

3.3 Results from Statistical Analysis on Geochemical data 53
3.3.1 Core QV2; the main variations 53
3.3.1.a Principal component 1; core QV2 . . . 55
3.3.1.b Principal component 2; Core QV2 . . . 59
3.3.1.c Principal component 3; Core QV2 . . . 59
3.3.1.d Principal component 4; Core QV2 . . . 60
3.3.2 Discriminant function groupings of cores QV1, 3 and 4 60
3.3.3 Discriminant function groupings of Long Pond cores 63
3.3.4 Discriminant function groupings of Mundy Pond 65
3.3.5 Discriminant groupings of Georges Pond . . . 65
3.3.6 Discriminant groupings of Long Pond, Witless Bay Line 68

3.4 Statistical summary 68

3.5 Common Lead Isotopic Ratios 71
3.5.1 Common Lead Isotopic Ratios from Quidi Vidi Lake, core QV2 71
3.5.2 Common Lead Isotopic Ratios in Long Pond Witless Bay Line, core LPW 73

Chapter 4: Biological and physical parameters recorded in the lake sediment cores. 75

4.1 Palynology 75

4.2 Pollen Zonation 75
4.2.1 Urban palynology of St. John's 76
4.2.2 Pollen assemblage from Quidi Vidi Lake . . . 76
4.2.3 Pollen assemblage from core LP5 79
4.2.4 Pollen and spore assemblage from Georges

Pond 82
4.2.5 Pollen and spore assemblage from Mundy Pond 85
4.2.6 Pollen and Spore assemblage from Long Pond Witless Bay Line 87
4.3 Results of Diatom analysis from core QV2 90
4.3.1 Individual Taxa 90
4.3.2 Morphological and Ecological Changes 92
4.3.3 pH reconstruction 94

4.4 Charcoal and soot from sediment cores 96
4.4.1 Charcoal and soot from core QV2 96
4.4.2 Charcoal and soot from core LP5 98
4.4.3 Charcoal and soot from core MP1 98
4.4.4 Charcoal and soot from core GP1 100
4.4.5 Charcoal from core LPW 103

4.5 Radiometric dates 103
4.5.1 ^{14}C from lake cores 103
4.5.2 ^{137}Cs profile from QV2 105
4.5.3 ^{210}Pb dating from QV2 106
4.5.4 Radiometric dates from Long Pond, St. John's 113
4.5.4.a ^{137}Cs from LP5 and LP3 113

4.6 Clay mineralogy from Quidi Vidi Lake, core QV2 . . 113
4.6.1 Peak identification for clay minerals . . . 116
4.6.2 Semi-quantitative analysis of clay mineralogy 118
4.6.3 Results from > 2 μm fraction 121

4.7 Sedimentation and Influx Rates 124

Chapter 5: Discussion 129

5.1 General Introduction 129

5.2 Presentation of geochemical data 129

5.3 Chapter format 133

5.4 Record of impacts related to watershed soil disturbances 133
5.4.1 The Earliest Settlers 134
5.4.2 The dawn of farming 134
5.4.3 The Farming Era 136
5.4.3.i Lithophilic composition of sediment through the main farming era 140
5.4.3.ii Pollen percentages through the upper farming interval 141

5.4.3.iii Clay through upper farming interval 143
5.4.3.iv Lacustrine impacts associated with farming (1757-1949) 143
5.4.4 Suburban/urban development 147
5.4.4.i Sediment influx through the urban era 147
5.4.4.ii Chemical profiles through the urban era 150
5.4.4.iii Pollen changes through the urban era 155
5.4.4.iv Lacustrine Impacts associated with urban sprawl 155
5.4.5 Farming and urban growth in Mundy Pond and Long Pond 158

5.5 Element signatures of fossil fuel emissions 160
5.5.1 General introduction 160
5.5.2 Emission signatures for fuel use in St. John's 161
5.5.3 Impacts discerned from heavy metals concentrations 163
5.5.3.i Impacts discerned form Pb changes . . 163
5.5.3.ii Other metals above the coal peak . . 175

5.6 History and spatial distribution of airborne pollution in St. John's 177

Chapter 6: Summary and Conclusions 183

References 194

Appendix A Core locations, water depth and core lengths 219

Appendix B Sample preparation 220

Appendix C Lake sediment geochemical data 226

Appendix D Pollen and Spore data 320

Appendix E Diatom data for core QV2 334

Appendix F Dating methods for core QV2 337

Appendix G Relative and absolute analytical accuracy . 346

Appendix H Dry sediment influx and wet sedimentation rates 352

List of Figures

Fig 1.1 Schematic map of Canada, showing the location for St. John's, Newfoundland. 2

Fig 1.2 Spatial growth lines superimposed on a road map of St. John's dated ca. 1976. The crest of a feature, Freshwater Hill, is noted in the heavy fill area. Learys Brook feeds into Long Pond, Rennies River runs from Long Pond to Quidi Vidi Lake and Virginia River runs from Virginia Lake to Quidi Vidi Lake. 5

Fig 1.3 Location map of the north-east Avalon with sampled lakes, geology (from King, 1990) and an outline of the present urban core. 18

Fig 1.4 Farm distribution in St. John's and vicinity between 1780 and 1810 (From MacKinnon, 1981). Note: U. Long Pond is now Long Pond, Middle Long Pond is now Kents Pond. The stars represent fortifications (Fort William - East star, Fort Townshend - West star). 20

Fig 1.5 Farm distribution in St. John's and vicinity between 1810 and 1840. (From MacKinnon, 1981). . . 22

Fig 1.6 Population and automobile growth in St. John's. Automobile growth only includes data from 1903 to 1958. 23

Fig 1.7 Number of occupied dwellings by principal heating fuel in Newfoundland and Labrador between 1951 and 1986. Data from Historical Statistics of Newfoundland and Labrador (1988). 26

Fig 2.1 Core locations from urban lakes. 30

Fig 2.2 Location of core from Long Pond, Witless Bay Line. 31

Fig 2.3 Schematic of corer modified from Reasoner (1986). 32

Fig 2.4 Schematic of horizontal sediment extrusion into a trough. 37

Fig 3.1 Principal component profiles and cluster sections for core QV2. 56

Fig 3.2 Principal component 1 and selected profiles for core QV2. 57

Fig 3.3 Principal component 4 and selected profiles for core QV2. 61

Fig 3.4 Section profiles for Quidi Vidi Lake cores, computed using a discriminant function derived from core QV2. 62

Fig 3.5 Section profiles for Long Pond cores, computed using a discriminant function derived from core QV2. The circles denote samples which classify into section 2. 64

Fig 3.6 Section profiles for Mundy Pond cores, computed using a discriminant function derived from core QV2. 66

Fig 3.7 Element profiles from cores MP1 and MP2 depicting the prominent Cr peak and the depth contrast of individual features between the cores. 67

Fig 3.8 Section profiles for Georges Pond cores, computed using a discriminant function derived from core QV2. 69

Fig 3.9 Section profile for core LPW, computed using a discriminant function derived from core QV2. . . . 70

Fig 3.10 Common lead isotopic ratio profiles from core QV2. 72

Fig 3.11 Common lead isotopic ratio profiles from core LPW. 74

Fig 4.1 Stratigraphic profiles for the most abundant pollen and spores types in core QV2. 77

Fig 4.2 Stratigraphic profiles for the most abundant pollen and spores types in core LP5. 80

Fig 4.3 Stratigraphic profiles for the most abundant pollen and spores types in core GP1. 83

Fig 4.4 Stratigraphic profiles for the most abundant pollen and spores types in core MP1. 86

Fig 4.5 Stratigraphic profiles for the most abundant pollen and spores types in core LPW. 89

Fig 4.6 Stratigraphic profiles for the most abundant diatom species in core QV2. 91

Fig 4.7 Morphological form and ecological characteristics represented by the diatom community in core QV2. 93

Fig 4.8 Reconstructed lake water pH from core QV2. . . 95

Fig 4.9 Charcoal and soot particle profiles from core QV2. 97

Fig 4.10 Charcoal and soot particle profiles from core LP5. 99

Fig 4.11 Charcoal and soot particle profiles from core MP1. 101

Fig 4.12 Charcoal and soot particle profiles from core GP1. 102

Fig 4.13 Charcoal particle profile from core LPW. . . 104

Fig 4.14 ^{137}Cs versus depth profile for core QV2. . . 107

Fig 4.15 Total and supported ^{210}Pb activities versus depth profiles from core QV2. 109

Fig 4.16 The unsupported ^{210}Pb activity versus depth profile from core QV2. 110

Fig 4.17 Dry bulk density versus depth profile from core QV2. 111

Fig 4.18 The ^{137}Cs versus depth profiles from cores LP5 and LP3. 114

Fig 4.19 Diffractograms for the clay size fraction for selected samples from core QV2. The sample depth for each diffractogram is shown in the upper right hand corner. 117

Fig 4.20 Profiles of the ratio of peak intensities versus depth for illite, chlorite and quartz in the < 2 μm size fraction from core QV2. 120

Fig 4.21 Diffractograms for the > 2 μm size fraction for selected samples from core QV2. The sample depth for each diffractogram is shown in the upper right hand corner. 122

Fig 4.22 Profiles of the counts per second versus depth for quartz and albite in the > 2 μm size fraction from core QV2. 123

Fig 4.23 Influx and sedimentation rates for core QV2, with and without the ^{14}C date of 917 A.D. at 102.5 cm. 125

Fig 5.1 Profiles of selected elements in different formats to illustrate the effectiveness for data interpretation. The filled area is element influx, the unfilled area is element ratios, the thick line is sediment influx and the thin line is element concentration. 130

Fig 5.2 Charcoal in core QV2. The inset probably shows the earliest increase related to human use. . . 135

Fig 5.3 Selected lithophilic element concentration profiles (Al, Ca, Fe, K, Mg, Na and LOI) from Principal Component 1, core QV2. 137

Fig 5.4 Clay and mineral XRD data, Al and Na concentrations from core QV2. 138

Fig 5.5 Selected pollen percentage profiles and Al concentration profile from core QV2. 139

Fig 5.6 Pollen influx profiles showing the influx peak at about 1830. This peak may represent an early intense period of soil erosion. 142

Fig 5.7 Diatom reconstructed pH, selected diatom species, morphological and ecological data and *Isoetes* from core QV2 145

Fig 5.8 Dry sediment influx profile for core QV2. . . 148

Fig 5.9 Dry sediment influx for core QV2 and residential construction starts in St. John's for the interval between 1950 and 1970. (Source: Newfoundland Statistics of Newfoundland and Labrador, 1981). 151

Fig 5.10 Pre-European concentrations of lithophilic

elements in the five sampled lakes. All concentrations are in percent. 153

Fig 5.11 Influx and concentration profiles of selected elements and dry sediment influx rate from core QV2. The filled area is the element influx, the thin line is element concentration and the thick line is sediment influx. Sediment influx units are g $cm^{-2}yr^{-1}$ and g $100g^{-1}cm^{-2}yr^{-1}$ for the element influx. 154

Fig 5.12 Sediment columns and selected concentration profiles from cores MP1 (left) and LP5 (right). The sharp sediment and concentration changes at about 20 cm are probably post-1950. 159

Fig 5.13 Al, Au, Pb, lead isotopic data, excess lead and soot profiles from core QV2. 164

Fig 5.14 As, Au, Hg, Pb, Sb and Zn profiles from core QV2 showing elevated metal levels from coal combustion. 167

Fig 5.15 Lead concentration, isotope ratio and sediment influx profiles for core QV2 to illustrate changes in lead input and sources between 1930 and 1990. 172

Fig 5.16 Cr, Cu, Fe, Sb and Zn profiles and sediment influx profile from core QV2, showing metal increases in the upper sediments. 176

Fig 5.17 Soot, As, Au, Hg and Pb profiles from core GP1 to illustrate the distribution of airborne pollution from coal combustion. 179

Fig 5.18 Soot, As, Au, Hg and Pb profiles from core LP5 to illustrate the distribution of airborne pollution from coal combustion. 180

Fig 5.19 Soot, As, Au, Hg and Pb profiles from core MP1 to illustrate the distribution of airborne pollution from coal combustion. 181

Fig 6.1 Theoretical time projection for the decline of element concentrations and influxes, and sediment influx to pre-1750 levels. Projections are based on the linear decline between 1973 and 1989. . . . 190

List of Tables and Plates

Table 2.1 Univariate data, distribution (normal or lognormal), F values and variability expressed as a percentage for each element. Note: element symbols are followed by a number representing the analytical method used; 1 represents INAA, 2 is ICP and 3 is AA. Other numbers such as 2A (Cr), 5 (Mo), 6 (Ag), and 18 (Hg) represent special digestions or analytical procedures. Refer to Appendix B for particular procedures. 45-46

Table 3.1 Element loadings in each Principal Component, computed from the four Quidi Vidi Lake cores. Percent variance is displayed at the bottom. . . . 51

Table 3.2 A discriminant function derived from the four Quidi Vidi Lake cores (the predicted group) was tested on core QV2 (the computed group) for its effectiveness. The 'computed data' compared well to the 'predicted data', and thus the discriminant functions derived from the four Quidi Vidi Lake cores were applied to the whole data set. 54

Table 4.1 ^{14}C and calculated dates from QV2, LP5, GP1 and LPW. 105

Table 4.2 Calculated age dates from core QV2, based on ^{210}Pb analysis. See appendix F for age calculation procedures. 115

Plate 1 Photographs of charcoal, soot, 'oil droplet' and Soot 'A'. 218

Chapter 1

1.1 Introduction

This study was carried out to measure and document the extent of environmental change associated with agricultural and industrial development in St. John's. This was accomplished by using records preserved in sediment cores from urban lakes. The geochemical signature, placed in a chronological sequence, is the nucleus of this study and records of pollen, diatoms, mineralogy and human-produced particulates are used to assist in data interpretation.

The city of St. John's is located on the east coast Newfoundland, Canada, an island in north Atlantic Ocean, at 47°35' latitude and 52°45' longitude (Fig 1.1). The city, the largest in Newfoundland with a population of about 174,000, is dominantly a service centre covering 50 to 60 square kilometres. Within the city and its suburbs are numerous lakes including; Quidi Vidi Lake, Georges Pond, Kents Pond, Kennys Pond, Long Pond, Mundy Pond, Oxen Pond, Branscombes Pond and Virginia Lake. Most of the river systems, except that related to Mundy Pond and Branscombes Pond, feed into Quidi Vidi Lake.

1.2 Purpose, Scope

Long-term multidisciplinary environmental data are required for effective analysis and management of natural systems. In many cases only one 'environmental indicator' is

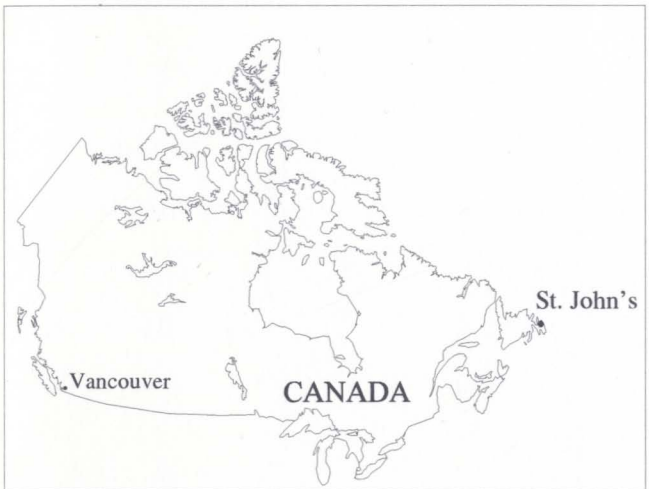

Fig 1.1. Schematic map of Canada, showing the location for St. John's, Newfoundland.

measured, and the data are sometimes interpreted by the reader to be representative of the whole system. Such studies, however, are merely snap-shots and more detail of the natural variability is needed. This could fluctuate over periods ranging from hours to decades.

Robust reconstructions and assessments of past environmental change are best achieved by using indirect proxy methods to firstly, determine the natural signature and variability and secondly, to show the timing and magnitude of anthropogenic changes. Lake sediments, an indirect proxy for measuring environmental change, provide a powerful tool for this type of multidisciplinary approach. The biological, chemical and physical indicators in the sediment cores enable the reconstruction and assessment of watershed changes. The use of lake sediments to reconstruct past conditions is known as paleolimnology (Smol, 1992).

Previously, Christopher (1991) showed elevated metal levels in lake sediments in the urban core of St. John's, compared to the surrounding rural areas which provided the background signature. Lead values, for example, in grab samples from urban lakes were as much as 10 times those in the surrounding area, and above the 99th percentile for the island of Newfoundland (Davenport et al., 1993). Likewise, Blake (1992) showed a similar pattern for the lake water geochemistry, with elevated levels in the urban lakes.

The purpose of this study is to investigate the nature, intensity and chronology of geochemical changes in the watersheds of St. John's. This was achieved by:

1. establishing a record of the natural geochemical signatures and variability in St. John's catchments using long lake sediment cores,
2. documenting and reconstructing the extent of anthropogenic impacts relative to the natural signature,
3. using other records in the lake sediment, including pollen (vegetation change), diatoms (lake water pH and chemistry), soot (coal combustion), charcoal (wood combustion), clay mineralogy (erosion sources), common lead isotopic signatures (lead source changes) and radiometric isotopes (dating), in conjunction with the historical and geochemical data, to ascertain possible anthropogenic impacts recorded in the lake sediment.

Quidi Vidi Lake is the nucleus for this study (Fig 1.2). It is the focal point of the largest watershed in St. John's, and is adjacent to the oldest part of the city where anthropogenic impacts to the landscape have continued for the longest period of time. Several other lakes were sampled to document local disturbances and to account for observations recorded in Quidi Vidi Lake. For example, Georges Pond which lies above the city, in an undeveloped National Historic Park, has not been impacted by urbanization to the same extent as

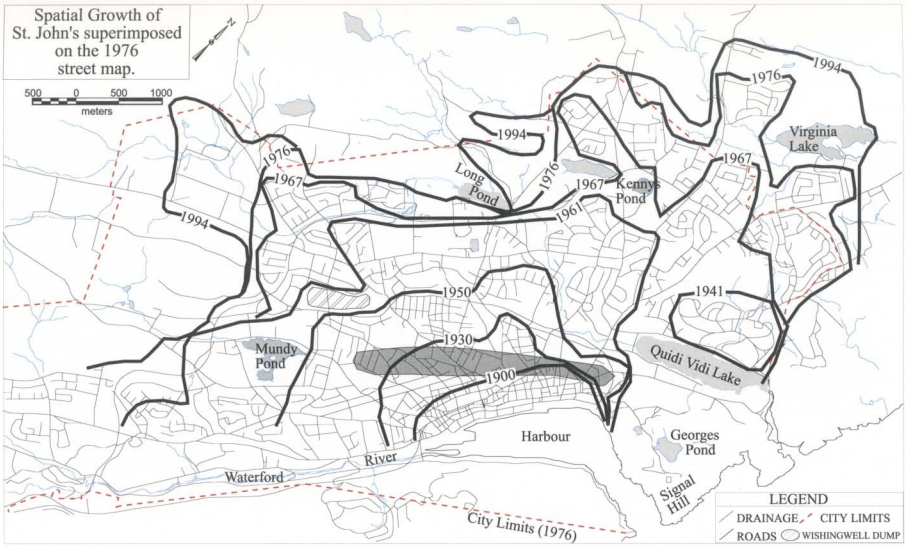

Fig 1.2. Spatial growth lines superimposed on a road map of St. John's dated ca. 1976. The crest of a feature, Freshwater Hill, is noted in the heavy fill area. Learys Brook feeds into Long Pond, Rennies River runs from Long Pond to Quidi Vidi Lake and Virginia River runs from Virginia Lake to Quidi Vidi Lake.

other urban ponds. Changes to this pond, located so close to the urban centre, should provide evidence of airborne pollutants from St. John's. A distinctive signal from Georges Pond could aid data interpretation from Quidi Vidi Lake, as well as the other urban lakes.

The other lakes, including Mundy Pond and Long Pond within the city limits, and Long Pond Witless Bay Line also provide important information. Long Pond and Mundy Pond should record many of the general anthropogenic impacts as observed in Quidi Vidi Lake, only later in sediment chronology. This should help to re-enforce or discredit observations from Quidi Vidi Lake, as well showing the migration of certain events, such as cultivation, across the natural landscape. Long Pond Witless Bay Line, in the same geological sequence as Quid Vidi Lake, should show similar geochemistry with much less disturbance in light of its remote location.

1.3 Present Day St. John's

The oldest parts of the city extend from the harbour area in a SSW direction. To the West and North, the city rises up the steep sided slope of Freshwater Hill, and down into Freshwater Valley. More recently, the city extended from this valley over a series of gentle slopes to its present limit. Figure 1.2 shows the chronological growth of the city, from the harbour outwards.

One of the major urban watercourses is the Rennies River system. It flows from a protected marshland and ponds, into Long Pond on the university campus, through suburban housing to the western end of Quidi Vidi Lake. Virginia River, which is fed from Virginia Lake and the surrounding marshlands, flows through a different suburban area and enters Quidi Vidi Lake on the north side.

Being mostly a service centre, city infrastructure is dominated by a network of roads, residential housing, light industry and office buildings. Little heavy industry is located in St. John's; thus the city appears to enjoy low levels of air pollution when compared to other cities in Canada.

1.4 Previous Work

A landmark paper by Engstrom and Wright (1984) reviewed how lake sediments provide an effective tool for palaeoecological reconstructions. Their examination shows that complex interactions of watershed processes are responsible for the chemical stratigraphy of lake sediments. Processes of, and changes in, lake water redox, lake sediment redox, trophic level, erosion intensity, vegetation, local and regional climate and watershed conditions (soil, bedrock geology and drainage) all combine to contribute to lake sediment chemical stratigraphy. Unless catastrophic in nature, single events are

rarely recorded, since most sediments tend to record widespread long-term changes. Laminated lake sediments have the potential to provide annual resolution of changes, but such deposits are rare in small, shallow lakes.

Engstrom and Wright (1984) show that analytical separation of the allogenic and authigenic fractions elucidate processes responsible for changes. Allogenic fractions are those derived from outside the lake such as soil or vegetation detritus, while authigenic fractions are those derived and deposited from within the lake such as pigments from aquatic matter or Fe and Mn depositions from changes in lake water and sediment conditions. Soil erosion, for example, would be marked by increases in element concentrations associated with clastic minerals, while the authigenic phases of elements such as P, Fe and Mn may document lake redox conditions. A striking theme throughout their study is that all lakes are unique and to fully appreciate the chemical changes recorded in the sediment, many facets need to be examined.

Although Engstrom and Wright (1984) show the effectiveness of a multi-disciplinary approach, few such approaches exist in the literature. In the St. John's area, there have been numerous environmental studies which, though limited in scope, provide important insights into the biological and chemical conditions found at different locations.

Butler (1990) examined pollen and a limited suite of elements in a sediment core from Branscombes Pond, Mount Pearl. The first human impacts are noted by pollen abundance changes coinciding with a LOI (loss on ignition) decline at 100 cm. Increases in Al, Fe, Mg, Ca, Na, K and P were attributed to local land clearance and cultivation. Increases in soot and elevated lead concentrations were attributed to inputs from modern fossil fuel combustion.

MacPherson and Mackinnon (1988) recognized and identified a sequence of anthropogenic events from pollen and chemical profiles from Kennys Pond (Fig 1.2). Impacts of land clearance, determined from changes in pollen and geochemical profiles at a depth of 80 cm, started in 1820 and continued to 1884 (35 cm). Increased Pb concentrations in 1833 (33 cm) were attributed to foundries and tinsmithing operations. Eutrophication which began about 1910, inferred from changes to C, K and P profiles, reached a maximum around 1945 (13 cm), when P and aquatic spores peaked. Starting in 1950 (10 cm) the decline of agriculture and encroaching suburban development is recorded from pollen profiles. Nearby road and hotel construction in 1965 (7.5 cm) is identified from increased Si.

Several biological investigations have been completed on city waterways. Marrie (1984) identified high levels of faecal coliform bacteria in inflow streams and ponds in the city, especially Mundy Pond, Long Pond and Quidi Vidi Lake. Buchanan

and Houlihan (1987) identified channelling and culverting as one of the major impacts on the urban waterways. Raw sewage, treated sewage, debris, de-icing practices and possible agricultural impacts were noted as inputs to the system.

Recently, O'Mally et al., (1996) examined the Polycyclic Aromatic Hydrocarbon (PAH) signatures from St. John's harbour, showing that automobile emissions accounted for 50%-80% of the PAH input. Transport of these emissions was attributed to urban run-off rather than direct aerial inputs. The remaining 20%-50% is apparently from crankcase oil contributions. Bieger et al., (1996) examined trace constituents of lubricating oils. They showed that the dominant petroleum biomarkers from Mundy Pond were derived from automotive oil.

Drover (1993) completed a comprehensive examination of the movement and sources of contaminants in a watershed approximately 20 km outside St. John's. The watershed contains a rendering plant, sewage treatment facility, incinerator, dump site, local and regional road systems and two road salt storage facilities. Stream water pH, conductivity and alkalinity all increase downstream, roughly correlating with identifiable anthropogenic influences. The highest levels were found in the area of greatest development. In contrast, sediment cores from a small pond within the industrial area did not show significant metal enrichments. The lack of any discernable metal increases in surface sediments is surprising

in light of the near-by incinerator.

In a remote area of Newfoundland, Vardy (1991) cored five lakes and examined chemical and palynological stratigraphies to determine the timing and characteristics of deglaciation. Cores were collected from ponds which lay in a number of different geologic units. Core chemistry showed that natural background, controlled by geology, is also the main contributor to the natural variation. This variation is clearly observed in the Digital Geochemical Atlas of Newfoundland (Davenport et al., 1996) which was produced from 'grab' samples collected from more than 17,000 lakes.

In an attempt to assess the impact of recent acid deposition, lake water pH reconstructions based on diatom assemblages were completed from lake sediment cores of two different acidic ponds in remote areas of Newfoundland (Scruton et al., 1990). Both lakes show acidification and according to the authors, the timing (approximately 1930) and magnitude (0.3 and 0.4 units) of change suggest anthropogenic acid deposition. Both lakes show a pH increase since about 1970, which is attributed to declining acid deposition.

Outside Newfoundland, and elsewhere in Atlantic Canada, Rogers and Ogden (1991) examined a lake system in rural Nova Scotia. They suggested that anthropogenic causes were responsible for metal increases in lacustrine surface sediments. These increases coincided with a decline in the

reconstructed lake water pH. In another study, Rodgers et al., (1991) examined pollen, diatoms, cladocera and lake sediment geochemistry. Lead and V increases were attributed to automobiles and the use of home heating oil, respectively; a Cu spike was inferred to represent modern plumbing.

Beyond Atlantic Canada, lake sediment cores have been used to assess the level of recent anthropogenic impact. Some studies focus on urban impacts. For instance, in Connecticut, Brugam (1978a) examined diatom, zooplankton, chemical and pollen profiles in Linsley Pond to document rural and urban development in a small watershed. Being one of the few multi-disciplinary studies in the literature it is also unique in that limnologists have studied Linsley Pond since the 1930's.

Brugam (1978b) examined P, Fe, Mn and Ca profiles from the same sediment core. Phosphorus did not correlate well with known periods of eutrophication (sewage input), but seemed to be correlated with Mn. Bortleson and Lee (1974) showed that P in Lake Mendota, Wisconsin sediment did not reflect the overlying lake water P concentration, but rather was controlled by adsorption on FeO_x and MnO_x precipitates. Iron and Mn sedimentation was controlled by the lake redox conditions and the sediment influx rate. Calcium in the sediment showed some correlation with organic matter, rather than rates of erosion.

The diatom stratigraphy of Linsley Pond proved to be

quite sensitive to anthropogenic disturbances. An early rise in *Melosira ambigua* correlates with the arrival of Europeans. Later, in the early 1800s, a large rise in *Melosira ambigua* coincided with development of a house and farm. An early increase *Asterionella formosa* correlated with one period of sewage pollution. With continued eutrophication the Centrales gave way to the Araphidineae, as Araphidineae are better at scavenging Si from the water during eutrophic conditions.

Mathewes and D'Auria (1982) examined the pollen and chemical profiles of Deer Lake, in Burnaby, British Columbia. Though the watershed has endured a shorter anthropogenic history than St. John's, it has progressed from an agricultural setting (initiated in 1862), increased logging activities (early 1900's), to a present day urban environment, not unlike St. John's. The authors were able to correlate historical watershed changes with observations in the pollen and chemical profiles. Lead contamination in the surface sediments was attributed to aerosol input and run-off from urban streets, while changes in Pb profile correlated with increases in post-war traffic. Increases in recent sedimentation rates were attributed to housing construction.

Fortescue and Vida (1991) showed the importance of establishing the natural background signature. By measuring the background prehistoric levels for metals in several hundred cores they attributed increased levels of As and Sb to

plume fallout from a sintering plant some 20 km away. In contrast, increased Pb levels in surface sediments suggested a widespread pollution source.

Extensive paleolimnological work has been completed by Smol (1980, 1981, 1983, 1988 and 1992), Smol et al., (1983 and 1986) and Dixit et al., (1992) on the use of paleoindicators for establishing past ecological conditions. Most of this work has focused on the use of diatoms and lake acidification throughout North America. Diatom assemblages have been shown effective in monitoring lake acidification and eutrophic conditions as a result of both natural and anthropogenic conditions. Diatoms have also been used to reconstruct other lake water conditions such as monomeric Al concentrations, acid neutralizing capacity and dissolved organic conditions. This body of research is one of the most advanced in the field of paleolimnology.

Worldwide, lake acidification has been the focus of numerous studies. Berge et al., (1990) examined records from a remote acid sensitive environment in Norway, and showed that sedimentary records suggest a close relationship with acid deposition and recent lake water acidification. So too, Rippey (1990) examined patterns of atmospheric contamination in lakes subject to high and low acid deposition in the UK and Scandinavia. The results showed lower levels of PAHs in areas of low acid deposition. In addition, recent declines of S and

PAHs correlated to declines in some of the trace metals through the last 10-30 years of sediment.

The impacts of mining on two large Swedish lakes were examined by Qvarfort (1983). Given detailed historical accounts and lake sediment metal profiles, Qvarfort was able to show the influx of ore metals in the lake sediment increased by orders of magnitude as a result of mining.

The impact of fossil fuel combustion on lake sediments has been extensively examined. Goldberg et al., (1981) examined charcoal, fly-ash and metal profiles from Lake Michigan. Results show that charcoal and metals increased to peak at 1955 and 1968, respectively. The fact that metals peak at depth and subsequently decline, has been attributed to metal dilution effects as a result of increased erosion, and atmospheric reductions of metal loadings due to the installation of scrubbers in smoke stacks. Edgington and Robbins (1976) also examined lead profiles from Lake Michigan. Their lead profile corresponded to historical use of coal and leaded gasoline. Paetzel et al., (1994) studied recent metal declines through the last 15-30 years of sediment in Skagerrak, to determine if the observed metal decline was due to decreased fossil fuel pollution. Metal accumulation rates, however, showed an increase and the observed concentration decline was attributed to dilution from increased clastic input.

Other studies have been element specific. For example, Meger (1986) examined high Hg levels in fish in remote lakes. No link was found between sediment Hg levels and the high levels recorded in the fish. Instead, Hg in fish was linked to factors including acid-sensitive lake water, the natural acid-neutralizing capacity and area/lake volume ratios. Sediment Hg levels were linked to thermal stratification and complexation-adsorption mechanisms within the lakes. In another single element study, Renberg et al., (1994) examined Pb to show that pre-industrial lead was being deposited in Swedish lakes more than 2600 years ago. This pollution was presumably airborne and derived from production and use of Pb in Europe.

1.5 Climate

St. John's experiences a marine climate with cool summers and mild winters. The mean annual temperature is 5°C and the mean annual precipitation is 1420 mm. The warmest month, July, has a mean temperature of 16° C compared to February, the coldest month, with a mean temperature of - 4°C (Environment Canada, 1981). January, the wettest month, has a mean precipitation of 165 mm compared to the driest month, July, with a mean precipitation of 61 mm.

1.6 Geology

The geology of this area consists of upper Precambrian

sediments which are thought to have originated from a large turbidite-fronted delta, which becomes younger progressively to the east (King, 1990). The geology strikes nearly north-south parallel to the eastern side of the Avalon Peninsula (Figure 1.3, adapted from King, 1990).

The study area is underlain by three main rock groups. The oldest, the Conception Group, is composed of chert, sandstone, conglomerate, tuffaceous siltstone and sandstones. Eastward and higher in this succession lies the St. John's Group, a sequence of grey and black sandstones and shales. The Signal Hill Group, the highest and youngest unit in this area, is composed of conglomerate, siltstone, sandstone and tuff.

Surficial deposits are mainly discontinuous till beds ranging 1-3 metres in thickness. All tills are locally derived and correlate in composition with the bedrock (King, 1990).

1.7 Historical Aspects of St. John's

1.7.1 Farming and Forestry

The earliest local use of the forest, while poorly documented, was for firewood, home building and fish flakes. O'Neill (1976) indicates that as early as 1676 timber was imported from New England to supplement local timber for dwelling construction. One can assume that the most accessible forest along the harbour was cut first and harvesting proceeded outwards. Early records suggest that the forest was

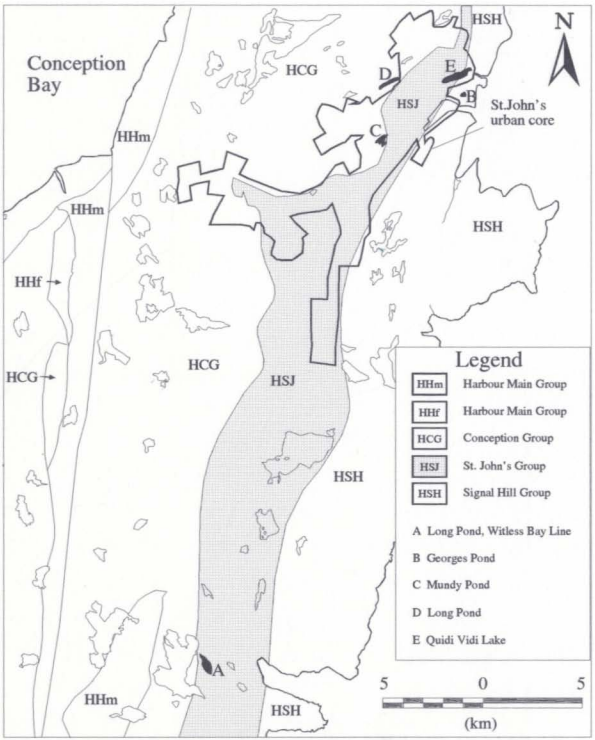

Figure 1.3 Location map of the north-east Avalon with sampled lakes, geology (from King, 1990) and an outline of the present urban core.

rapidly removed. As early as 1700, and during the construction of Fort William (Fig 1.4), timber was being cut as far back as Long Pond (O'Neill, 1976).

Forest clearance on Signal Hill was dictated by early military development. Its defensibility was partially attributed to the forest of fir and spruce which stood between 5' and 15' high (Candow, 1979). Much deforestation probably occurred between 1797 and 1806 when, according to Candow (1979), military construction on Signal Hill was intensive. In addition to construction uses, the forest was also used as firewood.

Farming and its growth has been documented in detail by MacKinnon (1981). He provides a summary of the data on the economic and spatial growth of farming over time. Initially, farming was for subsistence, but eventually became more economic. As with forest clearance, farms were initially restricted to the harbour's edge and expanded outwards. Local conditions were amenable to cool weather crops such as potatoes, cabbage, turnips and hay (for dairying).

The earliest documented farm, was established around 1730, and included 4 acres of cleared land on what is now Merrymeeting Road (MacKinnon, 1981) (this location is approximate to the location of '1930' in Fig 1.2). By 1757 there were two farms near Quidi Vidi Lake for a total of 40 acres; the largest was located on the north shore. MacKinnon

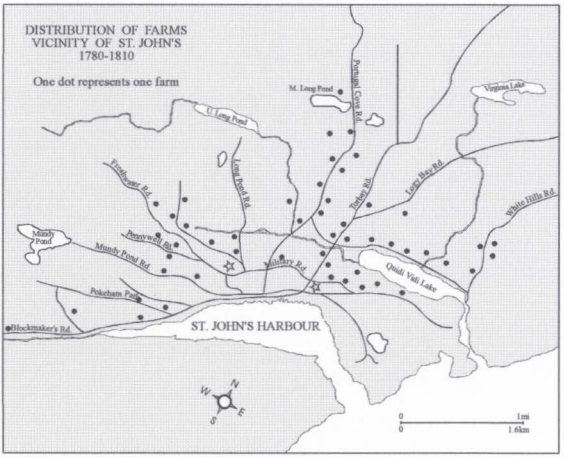

Figure 1.4 Farm distribution in St. John's and vicinity between 1780 and 1810 (From MacKinnon, 1981). Note; U. Long Pond is now Long Pond, Middle Long Pond is now Kents Pond. The stars represent fortifications. (Fort William - East star, Fort Townshend - West star)

mapped the spatial growth of agriculture in the St. John's area from 1780 to 1840 (Figures 1.4 and 1.5). Between 1757 and 1810, farms grew outward along the roads; most within 1.6 km of Quidi Vidi Lake. In 1810 there were no farms located in the vicinity of either Mundy Pond or Long Pond; however, several were located near Kents Pond. Between 1810 and 1840 farming expanded rapidly, and by 1850 agricultural development covered most of what is now the city.

Agricultural production peaked in the interval between 1911 and 1921. After this time, the city encroached rapidly upon the fringe gardens and dairy farms (MacKinnon 1981).

1.7.2 Population

The population growth of St. John's is depicted in Figure 1.6. It shows a slow growth between 1603 and 1779 (1792 persons) with a modest and consistent growth to 1945 (44,603 persons). Beyond 1945 the profile shows a sharper rate of increase to 1981, remaining steady to 1992 (approximately 96,000 persons).

1.7.3 Urban Growth

Urban growth, as used here, is simply the spatial spread of the city, which is chronologically displayed in Fig 1.2. Up until about 1900 most of the population was located along the harbour up to the crest of Freshwater Hill. From that time

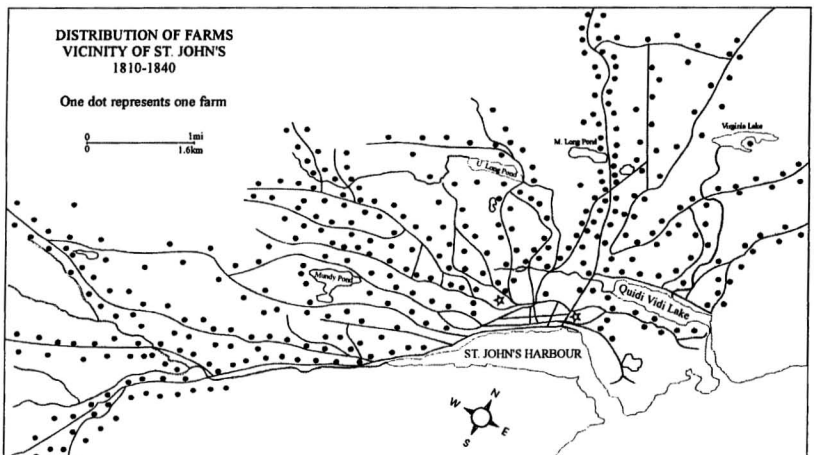

Figure 1.5 Farm distribution in St. John's and vicinity between 1810 and 1840. (From MacKinnon, 1981)

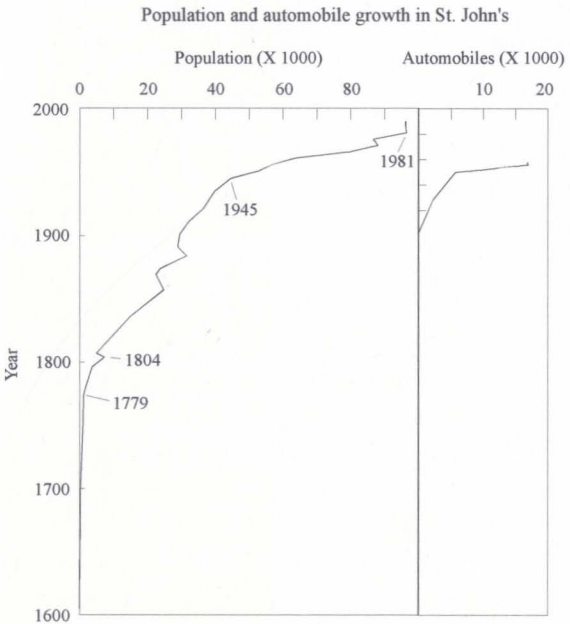

Figure 1.6 Population and automobile growth in St. John's. Automobile growth only includes data from 1903 to 1958.

urban growth continued outward to reach its present spatial distribution.

1.7.5 Transportation Systems

With an expanding population and the spatial growth of the city, transportation became important. The movement of agriculture products to market was one of the earliest uses of for a road system. It was not until Confederation in 1949 that the city's road system took on a more modern appearance, and included pavement.

The gasoline-powered automobile was first introduced to St. John's in 1903 (O'Neill, 1976). The number of automobiles grew steadily to 1950 when there were 5705 registered vehicles in St. John's (Fig 1.6). A notable increase in automobiles occurred during the years of 1925-26, when taxis were introduced (Adams, 1991). However, according to Mr. Robert McNealy (pers. comm 1993), automobiles did not become popular until after 1950.

1.7.6 Industrialization in St. John's

The present level of industrialization in St. John's is low compared to earlier times. The first heavy industry in St. John's was the Gas Works (established in 1842) near the harbour. From that time onward numerous heavy industries were built. By the 1880's most industries were run on steam engines

fuelled by imported coal (Baker et al., 1990). Historical records show that small local industries survived until shortly after Confederation (1949), when competition from Canadian markets caused many to close.

Among the larger industries was 'The Newfoundland Consolidated Foundry Company, Limited'. Built in 1847, it was one of the longest-standing foundries in St. John's (Joy 1977). Joy, in examining trade and manufacturing in St. John's, noted that "small foundries and blacksmith shops appeared and disappeared regularly" between 1870 and 1910. Other industries present in St. John's included tanneries, a cordage factory and cooperages. Most industries were located along the harbour area with several in the Mundy Pond area (Fig 1.2).

1.7.7 Fuel Sources

The earliest fuel source, for cooking and heat, would logically have been wood. Wood, which is still used today in outports, was probably used extensively in St. John's for centuries. Coal became a popular fuel after its earliest importation in 1803 (Head, 1976).

Coal was used for residential heating up until the late 1950's and early 1960's, when oil furnaces became popular (Mr. Robert McNealy, pers. com., 1993). Figure 1.7 shows the number of occupied dwellings by principal heating source for all of

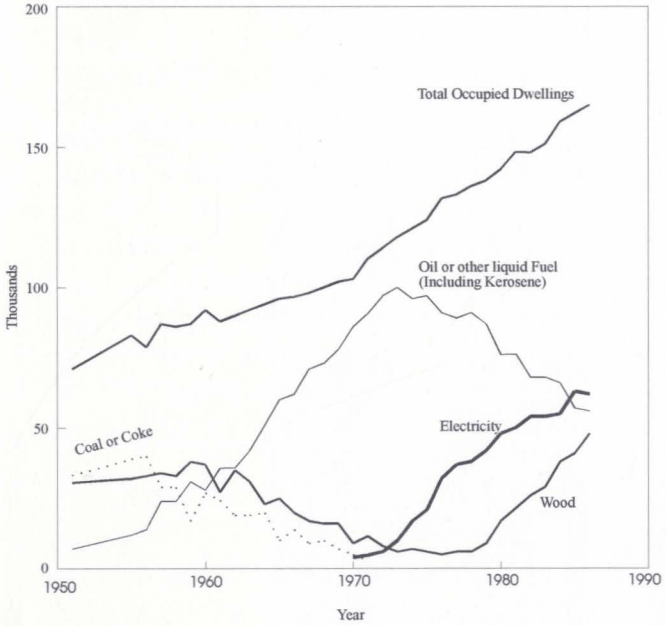

Figure 1.7 Number of occupied dwellings by principal heating fuel in Newfoundland and Labrador between 1951 and 1986. Data from Historical Statistics of Newfoundland and Labrador (1988).

Newfoundland after 1950 (Historical Statistics of Newfoundland and Labrador, 1988). It shows that wood and coal were still the dominant fuel sources as late as the mid 1950's for the province as a whole.

1.8 Thesis Layout

Chapter 2 and associated appendices, document the sampling and geochemical procedures for all analyses. Age calculations derived from ^{210}Pb dating are given in Appendix F.

Lake sediment geochemical results, including lead isotopic data are presented in Chapter 3. Through a series of statistical analyses the lake sediment geochemical data were condensed and related to the main core, QV2 from Quidi Vidi Lake.

Results from all other analyses are presented in Chapter 4, including pollen (all lakes), diatoms (core QV2), charcoal (all lakes), soot (all lakes) and silicate mineralogy (core QV2). In addition, a lake water pH record for core QV2, was determined from diatom data. The pollen data was subjected to cluster analysis, providing an objective stratigraphic zonation.

A discussion of the results is presented in Chapter 5. It focuses on core QV2, with other cores providing supporting evidence for conclusions drawn from this core. The chapter is divided into two parts. The first half discusses anthropogenic

impacts associated with direct soil disturbance, such as farming or urban construction. The second half discusses impacts related to airborne pollutants, such as coal or automobile emissions.

The conclusions and a summary of the present environmental conditions of St. John's and its lakes are covered in Chapter 6.

Chapter 2: Methods

2.1 Lake Core Sampling

Fourteen cores were collected from the ice surface of five lakes in the winter of 1992 (Figs 2.1 and 2.2). Cores were collected from the deeper basins in each lake. A list of all coring sites, their location, water depth and core lengths is given in Appendix A.

2.2 Core Components

Cores were collected using a light-weight, large diameter percussion corer modified from Reasoner (1986). This system provides an effective water-sediment interface collection, and at the same time ample sediment for all analyses. The corer consists of three main parts; the core barrel, core head and a driver (Fig 2.3). Sediment retention was ensured using a basket type core-catcher. The system was operated from the ice surface by means of two lines, a main line attached to the corer and a driver line attached to the driver.

Eight foot (2.4 m) lengths of 10 cm diameter, thin-walled PVC pipe were used for the core barrels. All barrels were thoroughly cleaned and fitted with a catcher (described below).

The core head was made from a one meter length of thick-walled ABS pipe with an internal diameter of 10 cm. Two bolts,

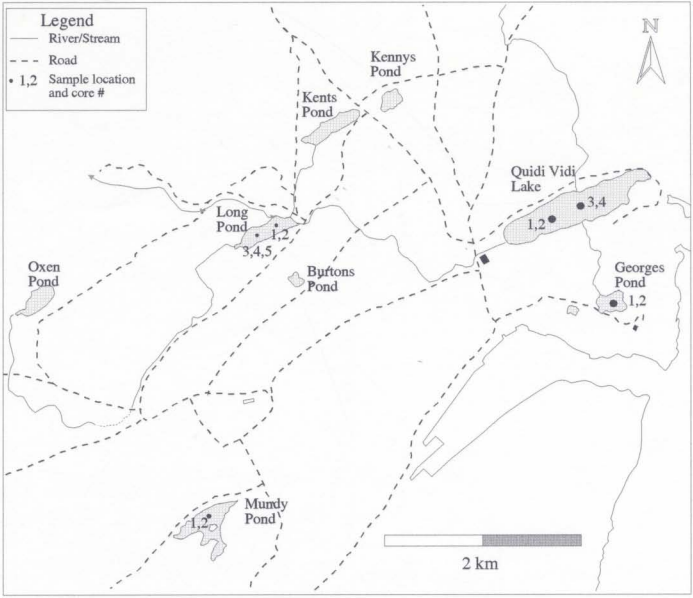

Figure 2.1 Core locations from urban lakes.

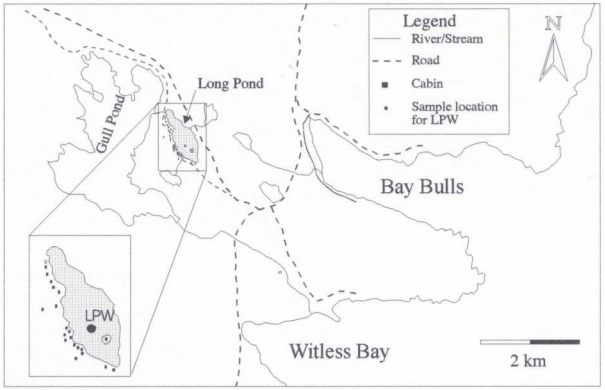

Figure 2.2. Location of core from Long Pond, Witless Bay Line.

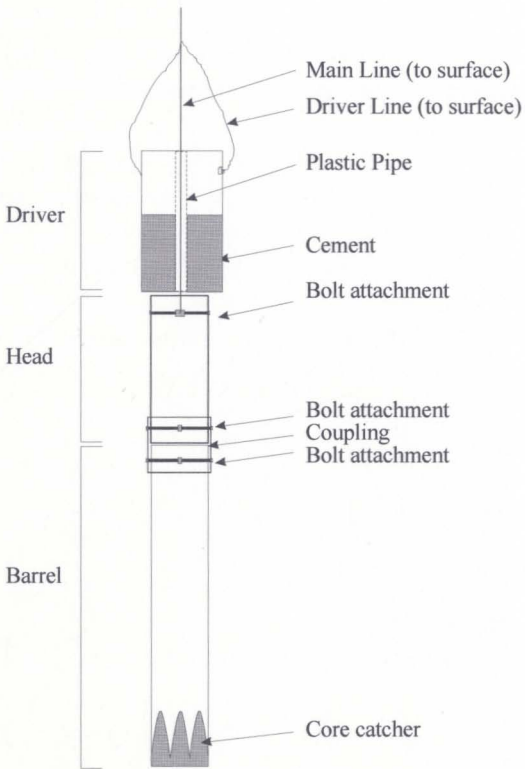

Fig 2.3 Schematic of corer modified from Reasoner (1986).

placed 10 cm from the top of the head at 90° to each other, acted as an attachment for the main line. The base of the head was fitted with an ABS coupling compatible in size to the core barrels. The coupling was glued and bolted to the head. Four holes were drilled at 90° from each other, into the bottom half of the coupling to act as an attachment for the barrels. All barrels were pre-drilled to fit the coupling.

The driver, the percussion device, was made from a 60 cm long, 17 cm diameter ABS pipe. The base of the driver was fitted with a piece of hard flat plastic, with a 3 cm diameter hole at its centre. A 60 cm long plastic pipe (3 cm outside diameter) was placed within the driver and glued to the hole in the hard plastic bottom. For weight, the driver was filled with 30 cm of concrete. The driver line was attached to the driver through two holes drilled near the top of the device.

The basket-type core catcher was fabricated from large tins. These were cut to the proper form, fitted inside at the base of the barrel and rivetted in place. All rivets were flattened to ensure little sediment disturbance. The form of catcher was perfected over a number of coring attempts, the best catcher having seven tapered fingers.

2.3 Coring Operation

Prior to sampling, the barrel was attached to the head and the main line was placed through the driver. After the

sample site was chosen a hole 20 cm in diameter was cut in the ice with an ice auger, and the corer was slowly lowered into the lake in a vertical position, until it reached the bottom. Once the barrel reached the bottom the driver was lowered from the ice surface, along the taut main line to the corer.

The corer was pushed into the sediment, by lifting the driver about 1 metre and allowing it to free-fall, hitting the core head. The main line was kept taut at all times to ensure vertical sediment penetration. Water was able to escape up through the core head and through a series of holes in the core head. After the desired depth was achieved, when the sediment water interface was approximately 1.5 to 2 from the top of the barrel, the driver was pulled to the ice surface and freed from the main line.

The corer and collected sediment column were then retrieved. This was accomplished by maintaining a continuous upward tension on the main line. To prevent core-catcher failure, resulting in loss of sediment, retrieval was completed slowly. Once freed from the lake bed the corer was pulled and raised onto the ice surface. It was kept in a vertical position at all times. The core head was detached and removed.

Water on the sediment column was siphoned off and the top was capped. The bottom 15 cm of the corer was cut off, including the core catcher. Care was taken at this stage to

prevent sediment loss (capping the top first kept the sediment loss through the base minimal, by creating a small vacuum). The bottom was capped and both ends sealed with duct tape. The cores were transported to the Department of Earth Sciences, Memorial University of Newfoundland and placed in cold storage at 4°C. The cores were transported and stored in a vertical position.

2.3.1 Core extrusion

Sediment extrusion was aided by a piston. The piston was constructed of two tapered rubber stoppers, a 30 cm threaded rod, two washers and two nuts. The stoppers, with a 10 cm diameter at their widest end, were placed together, narrow ends abutted. The threaded rod was placed through centered pre-drilled holes of the adjoining stoppers. A washer and a nut were placed at each end. The nuts could be adjusted to change the diameter of the piston to fit the core barrel.

Extrusion was commenced with the core barrel held vertical by first removing the bottom cap, inserting the piston into the base of the barrel followed by removal of the top cap. Water, if present, on top of the sediment column was carefully removed. A piece of centimetre ruled tape was placed inside the barrel at the top to assist sampling. The sediment column was pushed upwards in the barrel, with the aid of small wooden blocks placed under the piston. Once they were in

place, the barrel was pushed towards the floor, raising the sediment column relative to the barrel, until the sediment reached the top.

Measured intervals of sediment were spooned off into cleaned glass sample bottles. Care was taken not to sample smeared material along the edge of the barrel. Sampling was completed in this fashion until the sediment was consolidated enough to extrude into a horizontal trough. Generally 30 cm was spooned off before extrusion into a trough. The trough was made from a 10 cm diameter PVC pipe cut in half along its length.

Extrusion was accomplished by placing the core barrel and its contained sediment horizontally into the trough (Fig 2.4). A threaded rod was then attached to the piston with the back end of the rod placed against an abutment (wall). With the aid of a vice-grip, the barrel was pulled towards the abutment as the sediment extruded into the trough. The column of sediment was split in half with monofilament line, and the top half transferred to another trough. The sediment surface was scraped of any smeared material, and logged. Colour classification was based on the 'Rock-Color Chart' (1984).

2.3.2 Sediment Sampling

The upper 30 to 50 cm of core was sub-sampled at 2 or 3 cm intervals, while the remainder of the core was sampled at

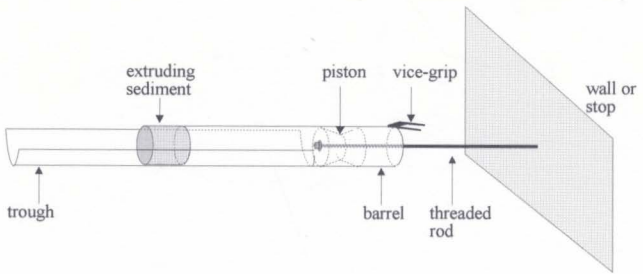

Figure 2.4 Schematic of horizontal sediment extrusion into a trough.

5 cm intervals. Again, care was taken not to sample the smeared sediment at the edges, which was lighter in colour. Samples for water content were collected and measured at this stage. A measured volume of sediment, collected with a cut-off syringe, was placed into clean, pre-weighed and dried crucibles. The wet sample and crucible were weighed, placed in a pre-heated oven at 110°C for 12 to 18 hours, removed to a desiccator, cooled and reweighed. Loss on ignition (LOI) was measured on the dry sediment, by placing 1 g of dried sediment into a clean pre-weighed, pre-dried crucible and combusting it at 500°C for 4 hours, after which it was removed, cooled in a desiccator and reweighed.

Pollen and diatom samples were collected using a 1 cc spoon. The sediment was washed into 100 mL medical bottles with distilled water and kept frozen or at 4°C until use. A conscientious effort was made to collect a sample representative of the whole sample interval. Samples for sediment geochemistry were collected, placed in kraft sediment bags and allowed to air-dry.

2.4 Sample preparation and Geochemical Analysis

After the geochemical sediment samples were dried in an oven at 50°C they were pulverized in an aluminum swing mill to minus 230 mesh (< 63 μm), and placed in plastic vials. At this stage blind duplicates and lab controls were inserted. Blind

duplicates were inserted with one pair for every twenty samples, while quality control standards were inserted prior to digestion at a frequency of one in twenty.

2.4.1 Total and Acid Extractable Analysis

Total element contents were determined at the Geochemical Laboratory of the Newfoundland Department of Mines and Energy by inductively coupled emission spectrometer (ICP-ES) for the elements Al, Ba, Be, Ca, Cd, Ce, Co, Cr, Cu, Dy, Fe, Ga, K, La, Li, Mg, Mn, Na, Nb, Ni, P, Pb, Rb, Sc, Sr, Ti, V, Y and Zn. Analysis of Zr by this method yields partial levels (Finch, 1998). See Appendix B for detailed dissolution procedures.

Total element analysis was also completed by instrumental neutron activation analysis (INAA) on the dry bulk sediment for the elements As, Au, Ba, Br, Ce, Co, Cs, Eu, Fe, Hf, La, Mo, Na, Ni, Rb, Sb, Sc, Se, Sm, Ta, Tb, Th, U, W and Yb. Pre-weighed polyethylene irradiation vials were filled with about 10 grams of sediment, and sent for analysis to Becquerel Laboratories, Ontario.

Acid-extractable concentrations of Cd, Co, Cu, Fe, Mn, Ni, Pb, Zn and (Ag and Mo) were measured at the Geochemical Laboratory of the Newfoundland Department of Mines and Energy by an atomic absorption spectrometer (AAS). Mercury was determined by 'cold vapour' atomic absorption

spectrophotometry by Bondar-Clegg Laboratories Ltd., Ottawa, Ontario. See Appendix B for detailed dissolution procedures and Appendix C for the chemical data.

2.5 Palynomorph and Diatom Preparation and Analysis

Detailed sample preparation procedures for pollen and diatoms are also given in Appendix B. Pollen, spores, diatoms, soot and charcoal were identified using microscopes equipped with interference contrast optics. Pollen and spores were identified at magnifications of 400X and 600X, and diatoms at magnifications of 1000X, under oil immersion.

Counts of pollen and diatoms were accomplished by successive traverses across the slide until a total of 300 pollen grains or diatom valves were identified. *Pediastrum* was also identified and counted with the pollen in the Mundy Pond samples. From the pollen slides, soot and charcoal were tallied simultaneously with the pollen. A cut-off size of $\geq$ 10 µm was used for soot diameters and charcoal lengths. See Appendix D for pollen data and E for diatom data.

Charcoal and soot particles were identified from visual representations and descriptions from Griffin and Goldberg (1981), Renberg and Wik (1984), Wik et al., (1986) and Griffin and Goldberg (1979). Plate I illustrates the character of the charcoal and soot particulates identified in this study. In addition, two other particulates are illustrated in

Plate I, including 'oil droplets' and 'soot A'. These are tentative names since conclusive identification was not achieved. These particulates are not discussed any further; however, for completeness they are included here. Griffin and Goldberg (1983) illustrated a fine-grained soot composed of sub-micron spheres aggregated into irregular chains, which look much like 'soot A'. These were believed to be related to oil fired furnaces. No references were found to identify the tentatively named 'oil droplets', which appear as small light green spheroids that are slightly opaque. Both particulates were identified in the pollen slides.

Pollen and spore taxa were identified from descriptions in Bassett (1978), Kapp (1969), Knut (1989), Moore and Webb (1978) and Moore et al., (1991), and from modern pollen reference collections by Dr. E.T. Burden, Department of Earth Sciences and Dr. J. Macpherson, Department of Geography. Diatom taxa were identified based on descriptions in Barber and Haworth (1981), Camburn et al., (1978, 1984-1986), Cox (1987), Dodd (1987), Foged (1977, 1979, 1981, 1982) Germain (1981), Horace (1981), Koppen (1975), Krammer (1992), Molder and Tynni (1969, 1971, 1972), Patrick and Reimer (1966), Ross (1981), Round (1990a), Tynni (1975, 1976, 1978, 1980), VanLandingham, S. L. (1967 - 1979), Vinyard (1979), Weber (1971), Williams (1985, 1986) and Williams and Round (1986, 1987).

Broken pollen grains, if identifiable, were tallied as half or quarter grains as seen fit. Broken diatom valves, as suggested by Kingston (1986), were tallied if a recognizable feature was present. Quality assurance and control were achieved by standardizing the taxonomic references used for each taxon. This was achieved with the help of Dr. J.C. Kingston, a diatom taxonomic specialist, who examined the diatom set.

2.5.1 Frequency Calculations and pH reconstruction

Since this study examines human impact, pollen percentages were calculated using the total pollen sum (Berglund and Ralska-Jasiewiczowa, 1986). The percentage of each pollen taxon was calculated from;

$$\text{taxon X (\%)} = (GXC)/(TPC)*100\%$$

where;
TPC is total pollen counted and
GXC is grains of taxon X counted

Spore percentages were calculated using;

$$\text{taxon X} = ((GXC)/(TPC + GXC))*100\%$$

Concentrations of charcoal, soot, pollen, and diatoms were calculated using the equation;

$$\text{concentration of X} = ((NXC*ETA)/(ETC*volume))$$

where;

ETC is the exotic spike total counted and
NXC is the number of X counted
ETA is the exotic total added
Volume is in centimetres cubed

A pH reconstruction was performed as a weighted average of the optimal species pH provided in Smol (1992). *Diatoma elongatum* which was abundant in Quidi Vidi Lake was given an optimal pH of 8.45 (Sushil Dixit, per. comm. 1996). Diatoms without a recorded optimal pH were not used in the calculations.

2.6 Common Pb Isotopic Ratios; $^{206}Pb/^{207}Pb$, $^{208}Pb/^{204}Pb$, $^{206}Pb/^{204}Pb$

Common lead isotopic ratios were examined by VG Sector-54 mass spectrometer using a multi-collector assembly. Isotopic measurements were completed by Geotop at Universite du Quebec a Montreal. See Appendix B for detailed sample dissolution procedures for common lead ratios.

2.7 Clay and Mineral Analysis

Both clay (< 2μm) and mineral (> 2μm) sized material were prepared and examined with an X-Ray Diffractometer (XRD). For the clay size material, an oriented smear slide of even thickness was prepared on a glass petrographic slide. The sample was analyzed from 2° to 35° 2θ, with the following XRD settings; 40 Kv, 50 mA, and scanned at 4° 2θ minute^{-1}. Smear

slides of the mineral fraction were made and analyzed from 10° to 60° 2θ at a rate of 10° 2θ minute⁻¹ with the above XRD settings. Clay and mineral identification and peak selection was completed using JCPDS Powder Diffraction index for Minerals software, while peak areas were automatically calculated with the Jade software. See Appendix B for detailed sample preparation procedures.

2.8 Radiometric dates (^{210}Pb, ^{137}Cs and ^{14}C)

Measurements for ^{210}Pb, ^{226}Ra and ^{137}Cs were established by gamma spectrometry by Dr. P. Appleby at the University of Liverpool, UK. ^{137}Cs ^{226}Ra and ^{210}Pb were measured by gamma spectrometry, while ^{210}Po was measured by alpha-spectrometry at Becquerel Labs, Mississauga. See Appendix F for details on age calculations using ^{210}Pb. Radiocarbon (^{14}C) measurements were carried out on dry bulk sediment at the Radiocarbon Dating Laboratory, Geological Survey of Canada, Ottawa.

2.9 Statistical analysis

A univariate analysis identifying the minimum, maximum, mean and standard deviation was carried out on the geochemical data set; results are displayed in Table 2.1. Before any multivariate analysis was carried out, the frequency distributions of the chemical variables were examined through histograms and coefficient of variation. A

Table 2.1 Univariate data, disrtibution (normal or lognormal), F values and variability expressed as a percentage for each element. Note: element symbols are followed by a number representing the analytical method used: 1 represents INAA, 2 is ICP and 3 is AA. Other numbers such as 2A (Cr), 5 (Mo), 6 (Ag) and 18 (Hg) represent special digestions or analytical procedures. Refer to Appendix B for particular procedures. Note, Na, Lu and Th were not log-transformed since the cofficient of variation, which was based on the four Quidi Vidi Lake cores (which were used to generate a PC model), was 0.50, 0.30 and 0.44, respectively. The data presented here shows the variation for the whole data set. Units are in ppm, except for Al, Ca, Fe, K, LOI, Mg and Na which are in percentage, and Au, Hg and P which are in ppb.

Element	min	max	mean	standard deviation	cofficient of variation	Distribution Log (Y/N)	F-Value (%)	Variability (%)
Ag(6)	0.1	1.2	0.27	0.19	0.69	Y	17.54	5.70
Al(2)	1.81	8.2	4.99	1.67	0.33	N	1315.17	0.08
As(1)	1.3	33.1	8.66	5.08	0.59	Y	61.40	1.60
Au(1)	1	49	5.97	8.04	1.35	Y	57.33	1.70
Ba(1)	25	700	272.70	164.97	0.60	Y	42.25	2.40
Ba(2)	55	654	309.54	169.98	0.55	Y	1859.79	0.05
Be(2)	1.2	12.5	3.83	1.52	0.40	N	312.57	0.03
Bi(2)	0.5	6	1.35	0.94	0.70	Y	1.59	62.90
Br(1)	6	167	50.15	31.20	0.62	Y	172.69	0.60
Ca(2)	0.14	1.33	0.32	0.13	0.39	N	352.64	0.30
Cd(2)	0.1	2.8	0.65	0.50	0.77	Y	44.98	2.20
Cd(3)	0.1	2.3	0.55	0.43	0.78	Y	22.55	4.40
Ce(1)	42	295	110.44	41.53	0.38	N	56.88	1.80
Ce(2)	10	297	120.24	42.93	0.36	N	214.70	0.50
Co(1)	1	160	24.07	18.18	0.76	Y	26.23	3.80
Co(2)	3	171	25.37	17.26	0.68	Y	86.31	1.20
Co(3)	1	135	15.14	11.04	0.73	Y	142.79	0.70
Cr(1)	8	1580	37.70	117.33	3.11	Y	5.47	18.30
Cr(2)	1	1619	39.62	114.93	2.90	Y	37.07	2.70
Cr(2a)	6	1509	35.34	107.90	3.05	Y	23.70	4.20
Cs(1)	0.3	7.3	3.45	1.69	0.49	N	50.91	2.00
Cu(2)	10	157	37.34	30.20	0.81	Y	655.26	0.20
Cu(3)	6	121	27.20	22.52	0.83	Y	516.95	0.20
Dy(2)	3.2	19.7	7.86	2.28	0.29	N	141.43	0.70
Eu(1)	0.25	9.2	3.15	1.23	0.39	N	4.51	22.20
Fe(1)	0.7	8.3	3.59	1.91	0.53	Y	139.45	0.70
Fe(2)	0.73	7.46	3.56	1.84	0.52	Y	1823.39	0.06
Fe(3)	0.48	5.99	2.59	1.49	0.58	Y	261.87	0.40
Ga(2)	2	28	13.63	6.68	0.49	N	59.36	1.70
Hf(1)	0.2	6.6	3.04	1.73	0.57	Y	7.50	13.30
Hg(18)	52	2476	298.25	295.36	0.99	Y	46.44	2.20
K(2)	0.08	2.24	0.88	0.69	0.78	Y	4484.76	0.02

cont ...

Element	min	max	mean	standard deviation	cofficient of variation	Distribution Log (Y/N)	F-Value (%)	Variability (%)
La(1)	18	99	41.76	13.09	0.31	N	31.66	3.20
La(2)	22	100	43.13	12.30	0.29	N	38.91	2.60
Li(2)	3.9	56.8	28.29	15.02	0.53	Y	1235.21	0.08
LOI	12.3	53.7	30.86	10.91	0.35	N	536.90	1.90
Lu(1)	0.02	1.5	0.53	0.22	0.41	Y	4.71	21.20
Mg(2)	0.05	0.91	0.35	0.26	0.74	Y	2251.06	0.04
Mn(2)	0.02	3.67	0.17	0.24	1.44	Y	687.30	0.10
Mn(3)	116	28800	1176.98	1935.02	1.64	Y	171.55	0.60
Mo(2)	1	12	4.73	1.98	0.42	N	2.77	36.10
Mo(5)	1	5	2.62	0.73	0.28	N	7.97	12.50
Na(1)	0.09	2	0.74	0.55	0.74	N	123.16	0.80
Na(2)	0.08	1.88	0.70	0.53	0.75	N	2958.28	0.03
Nb(2)	1	19	7.29	4.79	0.66	Y	47.04	2.10
Ni(1)	5	41	6.80	6.08	0.89	Y	3.58	27.90
Ni(2)	5	40	16.41	8.18	0.50	Y	62.12	1.60
Ni(3)	3	22	8.76	4.83	0.55	Y	73.83	1.40
P(2)	818	3232	2007.87	486.51	0.24	N	373.23	0.27
Pb(2)	1	625	129.79	165.64	1.28	Y	203.85	0.50
Pb(3)	3	536	104.87	137.07	1.31	Y	229.64	0.40
Rb(1)	2	110	38.59	29.35	0.76	Y	20.40	4.90
Rb(2)	5	100	37.78	28.93	0.77	Y	82.76	1.20
Sb(1)	0.02	3.6	0.69	0.80	1.15	Y	143.99	0.70
Sc(1)	2.3	17	8.78	3.81	0.43	N	55.88	1.80
Sc(2)	2.6	17.1	9.19	3.93	0.43	N	517.32	0.20
Sm(1)	5	39	11.68	4.09	0.35	N	27.27	3.70
Sr(2)	16	98	45.36	18.85	0.42	N	316.80	0.30
Ta(1)	0.1	1.6	0.60	0.41	0.68	Y	8.98	11.10
Tb(1)	0.69	4.6	1.52	0.50	0.33	N	12.26	8.20
Th(1)	1.5	10.7	5.13	2.54	0.50	Y	110.38	0.90
Th(2)	1	16	4.41	2.85	0.65	Y	1.83	54.60
Ti(2)	21	5037	2387.34	1312.43	0.55	Y	1615.44	0.06
U(1)	0.6	2.7	1.54	0.51	0.33	N	30.11	3.30
V(2)	9	124	52.08	31.39	0.60	N	238.61	0.40
W(1)	1	7.2	1.46	1.18	0.81	Y	26.28	3.80
Y(2)	4	100	42.05	12.21	0.29	N	70.25	1.40
Yb(1)	0.2	10	2.81	1.32	0.47	N	4.68	21.40
Zn(1)	25	1600	245.57	257.01	1.05	Y	8.39	11.90
Zn(2)	21	1210	243.60	200.34	0.82	Y	2388.42	0.04
Zn(3)	17	969	199.60	174.64	0.87	Y	574.98	0.20
Zr(2)	17	164	71.84	38.16	0.53	Y	1.02	98.00

number of elements were determined to be positively skewed based on the coefficient of variation (c.v. > 0.5) and thus were log transformed before further statistical tests were completed.

Analytical control for the geochemical data was attained by calculating F values for each element, using the duplicate samples. The F value compares the variability of the replicated samples to the variability of total data set. Elements that did not show normal distribution were first logged prior to any calculations. The F values were calculated using the formula (from Garrett, 1973);

$$F = \frac{S_D^2}{S_{SA}^2}$$

where;

S_D^2 is total variance determined from all duplicate samples
$S_{SA}2$ is variance of the duplicate pairs

Calculated F values and the percent noise ((100/F)*100%) are displayed in Table 2.1 In summary, in the cases where a particular element was assayed for total concentrations by more than one method, the data with greatest F-value was used, and in the cases where an element was assayed for total and partial digestions, the total concentration data were used.

Elements with high within-pair variance (> 20%) that were determined by only one method, were not used in further statistical analysis.

A cluster analysis was completed, using the SPSS and CONISS program, on both the geochemical and pollen data sets, respectively. These data sets were large and showed much variation. The cluster analysis ensured unbiased analysis of the data. A brief account of the statistical procedures employed on the geochemical and pollen data is presented in Chapters 3 and 4, respectively.

For the pollen and spore data, only taxa that were present in abundance were used in the cluster analysis including *Picea*, *Abies*, *Betula*, *Alnus*, Gramineae, *Rumex*, Polypodiaceae family, *Equisetum*, *Isoetes*, *Sphagnum* and *Lycopodium*.

2.10 Analytical accuracy

Internal controls (D controls) and international standards (LKSD controls) were inserted into the sample set to provide data on relative and absolute accuracy. All controls, their recommended values and ranges obtained in this study are exhibited in Appendix G. For the most part, the absolute accuracy was high, with the exception of several less important elements such as Nb. The relative accuracy was also high, as demonstrated by the D controls.

Chapter 3: Geochemical Results

3.1 Introduction

The large geochemical data set including 14 cores from 5 different lakes made it necessary to reduce the data into an easily interpretable form. This was achieved through a series of statistical procedures executed to identify the main element associations, and to determine whether the main associations make sense with respect to core stratigraphy and historical records of urban change.

3.2 Defining the Major Geochemical Associations

Prior to establishing the geochemical associations, a sub-set of variables was chosen that included only one type of determination for each element (several elements were determined by two or three different techniques - see section 2.9). Elements that showed little variance, such as W, where most samples were below detection limit, were excluded from multi-element procedures. This reduced the data set to 38 elements plus LOI.

To provide a meaningful statistical analysis a data set needs a dimensionality of at least 3 (Garrett, 1993). The dimensionality is computed by division of the number of cases (samples) by the number of variables (elements). In QV2, with 39 variables and 52 cases, the dimensionality is only 1.3,

making any statistical examination meaningless. This problem was solved by combining all four cores from Quidi Vidi Lake, since all four showed similar geochemical profiles. This new data set contained 39 variables and 208 cases, providing a meaningful dimensionality of 5.3.

A principal component (PC) analysis of this data set was computed using SPSS to determine the geochemical associations. Several models were run and a four component model with a varimax rotation was selected. The four component model was chosen for two reasons: the four factors accounted for 93.5% of the variability; and the fifth factor did not contain any unique elements that were not major loadings on one or more of the other four components. The four PCs accounted for 60.2%, 22.2%, 6.8% and 4.3% of the variance in the data set. Table 3.1 shows the element loadings in each PC, using an arbitrary cut off of 0.3.

To test whether these 4 PCs made stratigraphic sense an unsupervised cluster analysis was computed on PC scores from core QV2. The PC scores were computed using the following;

PC1 = 0.967*Ba2 + 0.961*Ni3 + 0.959*lgCu3 + 0.953*V2 - 0.949*lgBr1 + 0.939*U1 + 0.939*Sc2 + 0.939*lgPb3 + 0.938*lgZn2 + 0.934*K2 + 0.930*Mg2 + 0.929*Ga2 + 0.925*Na2 + 0.922*lgSb1 + 0.919*lgRb2 + 0.919*Al2 - 0.917*LOI + 0.916*Th1 + 0.910*Cr2 + 0.904*Sr2 + 0.868*Ti2 + 0.860*Fe2 + 0.856*Zr2 + 0.839*lgAu1 + 0.802*Li2 + 0.798*Cs1 + 0.669*Ca2 + 0.588*As1 - 0.346*Tb1 - 0.370*Sm1 - 0.447*Ce2 + 0.552*lgHg18

PC2 = -0.335*K2 - 0.329*Mg2 - 0.352*Na2 - 0.329*lgRb2 + 0.334*LOI - 0.319*Th1 - 0.345*Sr2 - 0.380*Ti2 -

Table 3.1 Element loadings in each Principal Component, computed from the four Quidi Vidi Lake cores. Percent variance is displayed at the bottoı Note: lg means the data was log transformed before it was used to compute PCs.

Element	Component			
	1	2	3	4
Ba2	0.967			
Ni3	0.961			
lgCu3	0.959			
V2	0.953			
lgBr1	-0.949			
U1	0.939			
lgPb3	0.939			
Sc2	0.939			
lgZn2	0.938			
K2	0.934	-0.335		
Mg2	0.930	-0.329		
Ga2	0.929			
Na2	0.925	-0.352		
lgSb1	0.922			
Al2	0.919			
lgRb2	0.919	-0.329		
LOI	-0.917	0.334		
Th1	0.916	-0.319		
Cr2	0.910			
Sr2	0.904	-0.345		
Ti2	0.868	-0.380		
Fe2	0.860		0.424	
Zr2	0.856	-0.376		
lgAu1	0.839	-0.324		0.347
Li2	0.802			0.437
Cs1	0.798			0.325
Ca2	0.669		-0.594	-0.376
As1	0.588		0.487	0.525
La2		0.955		
Y2		0.954		
Be2		0.933		
Dy2		0.926		
Tb1	-0.346	0.908		
Sm1	-0.370	0.877		
Ce2	-0.447	0.842		
P2		0.809		0.352
lgMn2			0.916	
lgCo3		0.401	0.816	
lgHg18	0.552			0.623
% variance	60.2	22.2	6.8	4.3

0.376*Zr2 - 0.324*lgAu1 + 0.955*La2 + 0.954*Y2 + 0.933*Be2 + 0.926*Dy2 + 0.908*Tb1 + 0.877*Sm1 + 0.842*Ce2 + 0.809*P2 + 0.401*lgCo3

PC3 = 0.424*Fe2 - 0.594*Ca2 + 0.487*As1 + 0.916*lgMn2 + 0.816*lgCo3

PC4 = 0.347*lgAu1 + 0.437*Li2 + 0.325*Cs1 - 0.376*Ca2 + 0.525*As1 + 0.352*P2 + 0.623*lqHq18

The unsupervised cluster analysis on these PC scores does not specify how many clusters are expected or where they are to be found. The results of this analysis showed a stratigraphically coherent model, defining 4 continuous sections of core, showing an empirical concurrence with the visual geochemical stratigraphy. Independent cluster analyses computed on each of the other Quidi Vidi Lake cores showed similar patterns as in QV2. The similarity of these patterns from the other cores suggests the cluster analysis was effective for defining stratigraphy.

Since the cluster analysis proved to be effective, a discriminant function model was developed that could be applied to the whole data set. In this model the grouping variables were the four stratigraphic sections defined by cluster analysis on QV2, and the independent variables were the four PCs computed on all four cores from Quidi Vidi Lake. These PCs were computed using the equations defining PC1, PC2, PC3 and PC4 on all four cores from Quidi Vidi Lake. The discriminant functions developed from the QV2 training set

were then applied to all cores. It is worth noting that in the statistical analysis SPSS only used the first three PCs in the discriminant calculations, since the fourth did not significantly contribute to the discriminant function.

The discriminant function (DF) was calculated by the following:

DF = aPC1 + bPC2 + cPC3 + dPC4;

where;

a, b, c and d are constants.

This discriminant function was tested on the training set from core QV2. In this analysis the discriminant function mis-classified ten out of 54 samples, providing a classification success rate of 81%. All but one of the mis-classified samples occurred at the boundary between sections 3 and 4, which define the natural baseline conditions. The other mis-classified sample occurred at the boundary of sections 1 and 2 (See table 3.2 for the comparison data), which for this study is more important. Since the discriminant functions worked well on the training group, a discriminant analysis was computed on all other cores, enabling a direct comparison to the four groups established in Quidi Vidi Lake.

3.3 Results from Statistical Analysis on Geochemical data

3.3.1 Core QV2; the main variations

Table 3.2 A comparision of the discriminant functions derived from the four Quidi Vidi Lake cores (the predicted group) and core QV2 (the computed group).

core QV2 Sample #	Depth (cm)	Predicted group	Computed group
QV2-002	1	1	1
QV2-004	3	1	1
QV2-006	5	1	1
QV2-008	7	1	1
QV2-010	9	1	1
QV2-012	11	1	1
QV2-014	13	1	1
QV2-016	15	1	1
QV2-018	17	1	1
QV2-020	19	1	1
QV2-022	21	1	1
QV2-024	23	1	1
QV2-027	25.5	1	1
QV2-029	28	1	1
QV2-031	30	1	1
QV2-033	32	1	1
QV2-035	34	2	1
QV2-037	36	2	2
QV2-039	38	2	2
QV2-041	40	1	1
QV2-043	42	2	2
QV2-045	44	2	2
QV2-047	46	2	2
QV2-050	48.5	2	2
QV2-055	52.5	2	2
QV2-060	57.5	2	2
QV2-065	62.5	2	2

core QV2 Sample #	Depth (cm)	Predicted group	Computed group
QV2-070	67.5	3	3
QV2-075	72.5	3	3
QV2-080	77.5	3	3
QV2-085	82.5	3	3
QV2-090	87.5	3	3
QV2-095	92.5	3	3
QV2-100	97.5	3	3
QV2-105	102.5	3	3
QV2-110	107.5	3	3
QV2-115	112.5	3	3
QV2-120	117.5	3	3
QV2-125	122.5	4	3
QV2-130	127.5	4	3
QV2-135	132.5	4	3
QV2-140	137.5	4	3
QV2-145	142.5	4	3
QV2-150	147.5	4	3
QV2-155	152.5	4	3
QV2-160	157.5	4	3
QV2-165	162.5	4	3
QV2-170	167.5	4	4
QV2-175	172.5	4	4
QV2-180	178.5	4	4
QV2-185	182.5	4	4
QV2-190	187.5	4	4
QV2-195	192.5	4	4
QV2-200	197.5	4	4

The cluster analysis that sub-divided the data into four sections is superimposed on the PC profiles in Fig 3.1. Divisions occur at 165, 70 and 29 cm. Sections 4 and 3 occur in the bottom part of the core where the geochemical data showed little change. Section 2 delineates an episode where many elements show gradual concentration increases, and where numerous heavy metals show high concentrations. Section 1, through the top part of the core delineates a period of stable, but high concentrations.

3.3.1.a Principal component 1; core QV2

Principal component 1 includes all the major elements (Al, Ca, Fe, K, Mg and Na), most of the trace elements and LOI with a negative loading. This PC profile shows a uniform decline from the base, through sections 4 and 3, to about 82.5 cm (Fig 3.1). From 82.5 cm the profile shows a rapid increase, through the upper portion of section 3, into section 2. The rate of increase gradually declines upward through section 2 and into section 1, where a small increase is observed through the top 9 cm.

All major elements, except Ca, show increases starting at 82.5 cm. A number of elements including Al, Fe and Mg show continued increases to about 38-40 cm, while Na and K show continued increases to about 32 cm (Fig 3.2). These elements show stable levels through the remaining core, except through

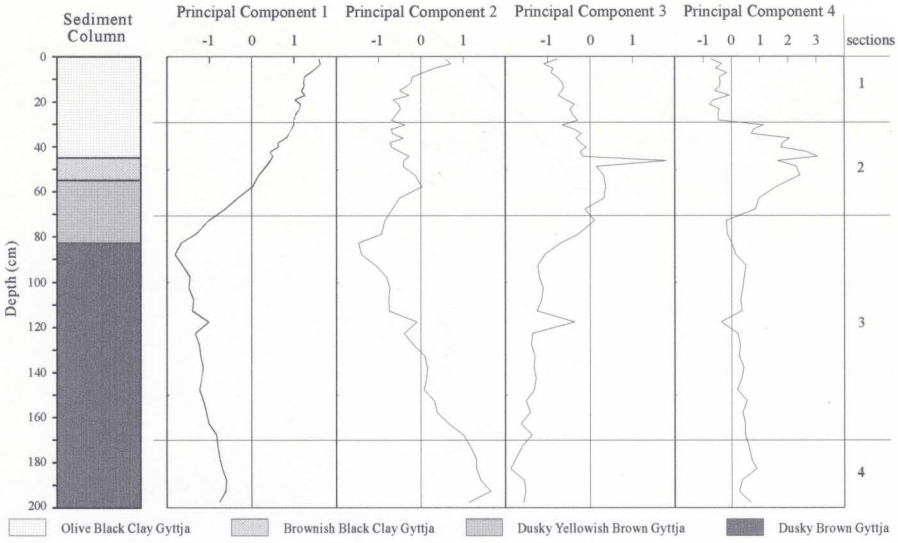

Figure 3.1 Principal component profiles and cluster sections for core QV2.

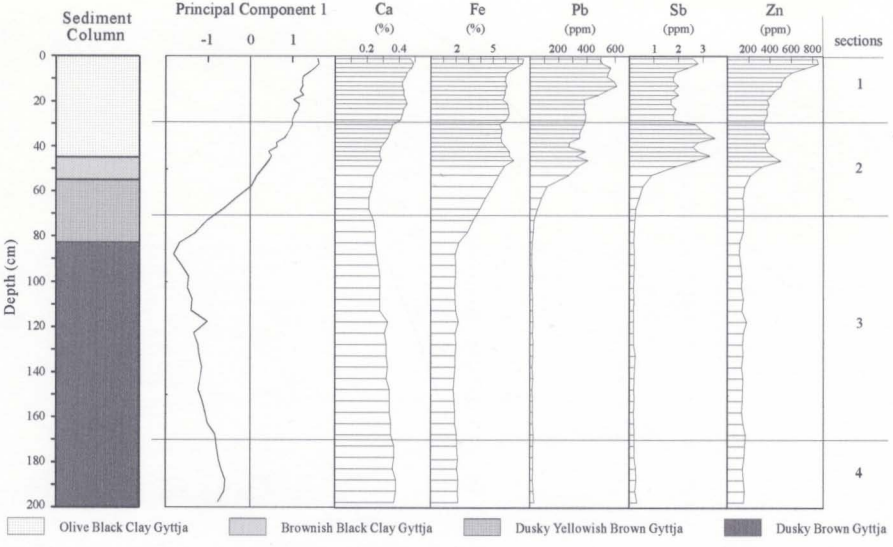

Figure 3.2 Principal component 1 and selected element profiles for core QV2.

the upper 7 cm, where concentrations decline, except for Fe which increases. LOI declines from 82.5 cm to about 21-15 cm, above which it shows a small increase.

The Ca profile, unlike the other major elements, shows no discernible increase until 62.5 cm, coinciding with the interval between sections 3 and 2 (Fig 3.2). Through section 2, to about 29 cm, Ca shows a gradual increase, although at a lesser rate than the other major elements. At 29 cm, the interval between sections 2 and 1, Ca shows a small inflection, above which concentrations are comparatively higher, but show little change.

Through section 2 most metal profiles show an increase; a number of these elements including As, Hg, Fe, Pb, Sb and Zn exhibit spikes in concentration (As, Au and Hg are discussed under PC 4). An inflection in the Sb profile, where the concentration declines sharply, coincides with the boundary between sections 2 and 1. Several metals including Pb and Zn, show continued increases through section 2 and into section 1. Lead shows a sharp increase above 19 cm to peak at 13 cm (613 ppm); above 13 cm it declines gradually. Zinc concentrations remain relatively steady to 19 cm, increase sharply to 9 cm and show a sharp increase to 3 cm, where a concentration of 852 ppm was recorded. A number of other profiles, including Cu, Sb and V increase through the upper 7 - 9 cm.

3.3.1.b Principal component 2; Core QV2

This component is dominated by the rare earth elements. The PC profile mimics the general profile of the rare earth elements, which behave in a similar manner to one another. The PC profile shows a decline through section 4 and into section 3 to 82.5 cm (Fig 3.1). From 82.5 cm the profile increases, continuing into group 2 to about 57.5 cm. Through the remaining portion of section 2 the profile shows a small decline. In section 1 the PC profile shows a small increase to 9 cm, above which it increases sharply to the top of the core.

3.3.1.c Principal component 3; Core QV2

This PC is dominated by Mn and Co, with lesser loadings of As, Ca and Fe. The profile shows a gentle increase through sections 4 and 3, up to 82.5 cm (Fig 3.1). As with PCs 1 and 2, it displays increases starting at 82.5 cm. From 82.5 cm the profile shows an increase to 57.5 cm, above which it declines continually, except for a spike at 46 cm, which reflects a concentration spike in Mn and Co.

Manganese is unique in that it starts to show increases above its stable basal trend at 107.5 cm. Cobalt shows increases starting at 82.5 cm, like most elements, to a high between 62.5 and 52.5 cm. Above 52.5 cm, Co remains steady with lower concentrations through the upper core.

3.3.1.d Principal component 4; Core QV2

Elements which load onto this component include As, Au, Ca, Cs, Li, Hg and P. Of these, only As and Hg have loadings greater than 0.5. Sections 4 and 3, from the core-bottom upwards, show a gentle decline (Fig 3.1). Between sections 3 and 2, at 70 cm, the profile exhibits an abrupt increase. This increase continues into section 2, to about mid-section, above which it declines. Between section 2 and 1, at 30 cm, the profile shows a sharp decline, with little change through section 1.

Although Hg is the most heavily weighted element in this PC, the Au profile shows good agreement with the section divisions at 70 and 29 cm (Fig 3.3). Between 72.5 and 67.5 cm Au shows a sharp increase, from levels below detection limit, while between 30 and 28 cm it declines sharply. Both As and Hg show sharp decreases at the boundary between sections 2 and 1, similar to that observed in the Au profile. Arsenic starts to show increases above the basal section at 82.5 cm, while Hg starts at 57.5 cm.

3.3.2 Discriminant function groupings of cores QV1, 3 and 4

As expected, these cores show stratigraphic similarities to core QV2 (Fig 3.4). Sections 1 and 2 are shallower in QV1, which was sampled adjacent to core QV2. This observation is consistent with individual element profiles which show changes

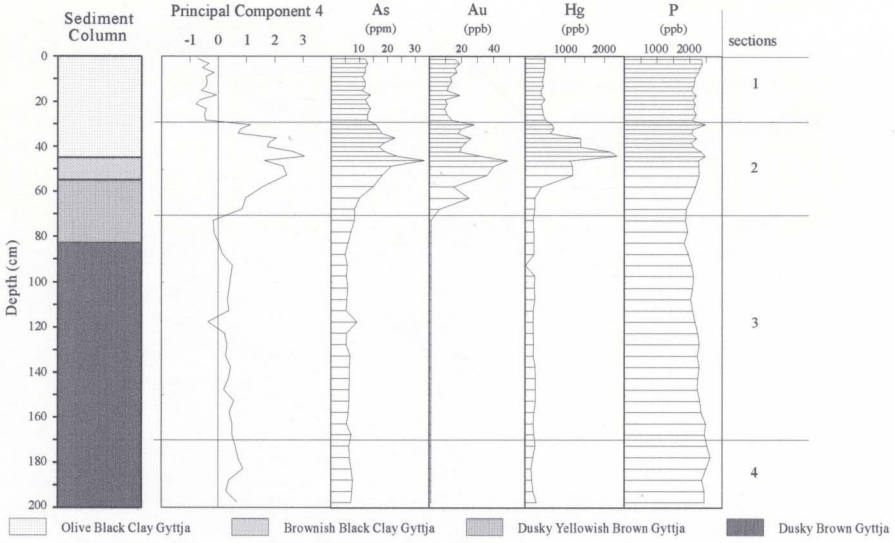

Figure 3.3 Principal component 4 and selected element profiles from core QV2.

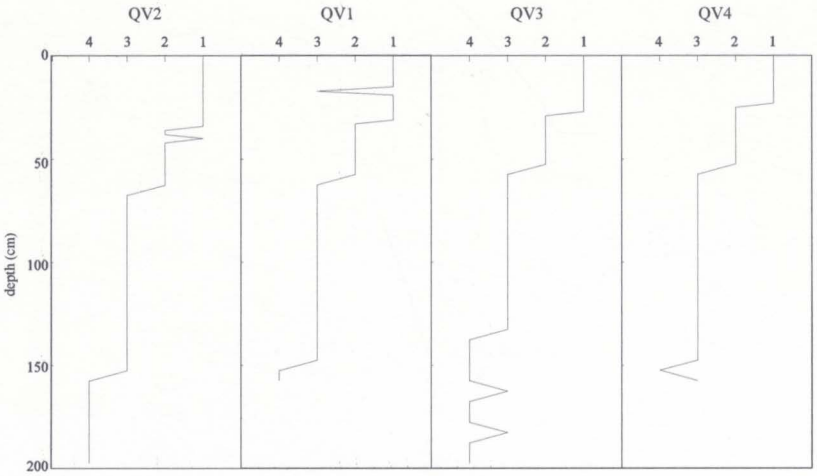

Figure 3.4 Section profiles for Quidi Vidi Lake cores, computed using a discriminant function derived from core QV2.

starting at depths a little shallower than in QV2. Cores QV3 and QV4, both collected at the opposite end of the lake, closely mirror each other and show initial disturbances starting higher in the core than observed in cores QV1 and QV2. Section 4, however, is less well defined in these cores than in core QV2.

3.3.3 Discriminant function groupings of Long Pond cores

The discriminant profiles from this lake behave slightly differently from that shown in core QV2 (Fig 3.5). Only two samples from the five Long Pond cores classify into section 2; one sample from each LP3 and LP4. Sections 3 and 4 dominate the stratigraphic sequence for these cores. Section 1, however, is displayed nicely in all cores, and as in Quidi Vidi Lake corresponds to the clay rich layer at the top of the sediment column.

The absence of section 2 from this lake is not unexpected. In section 2 of core QV2, the lithophilic elements show a gradual increase over a wide interval of core, and a number of heavy metals show a coinciding peak. In Long Pond, the major elements show an abrupt increase over a small interval, between 24 and 18 cm. The heavy metals do not show any discernable peak at depth that could compare to the peak in core QV2. The two samples that are grouped as section 2 in this lake do show slightly higher metal levels.

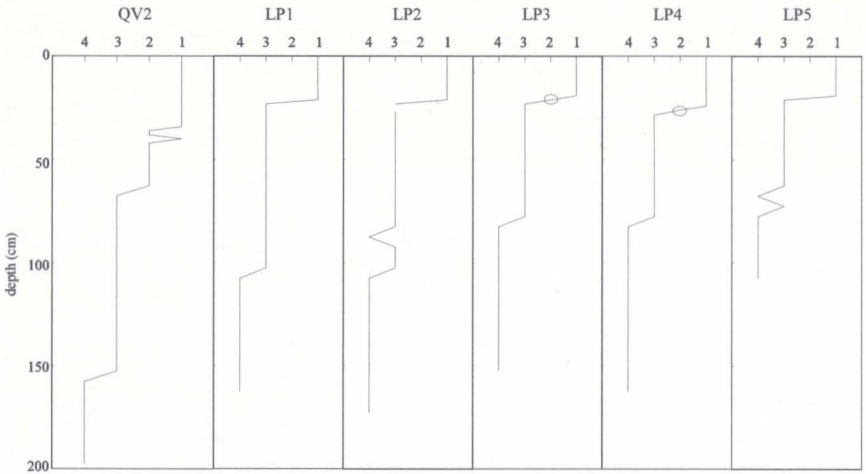

Figure 3.5 Section profiles for Long Pond cores, computed using a discriminant function derived from core QV2. The circles denote samples which classified into section 2.

3.3.4 Discriminant function groupings of Mundy Pond

The discriminant profiles from this lake are dominated by section 3 through the basal portion of core, and section 2 through the upper portion of core (Fig 3.6). Core MP1 does show section 1 through a narrow interval between 5 and 7 cm. The boundary between sections 3 and 2 for these two cores occurs at different depths; 20 cm in MP1 compared to 10 cm in MP2. This difference is consistent with observations during sampling, which suggested the surface sediments of MP2 were lost. This difference in depth is also clearly shown in element profiles, and most notably for Cr (Fig 3.7).

The lack of any significant expression for section 1 is surprising since core MP1 does show high concentrations of the major elements through the upper 20 cm. In addition, the upper 20 cm is a clay rich interval similar to that observed in both Long Pond and Quidi Vidi Lake. A metal peak at depth in section 2, approximately between 23 and 17 cm for As, Au, Hg, Pb and Sb, may correspond to the metal peak in section 2 of core QV2.

Chromium levels in this pond were extremely high and deserve special mention. The Cr level at its peak in MP2 (> 1500 ppm) is 100 fold background levels. No other element in any lake in this study showed an increase of this magnitude.

3.3.5 Discriminant groupings of Georges Pond

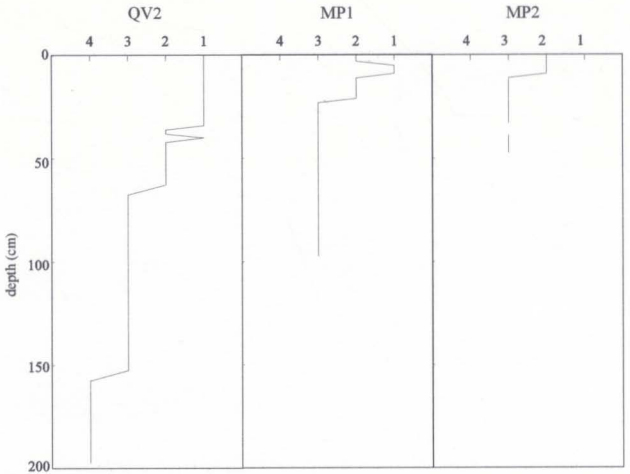

Figure 3.6 Section profiles for Mundy Pond cores, computed using a discriminant function derived from core QV2.

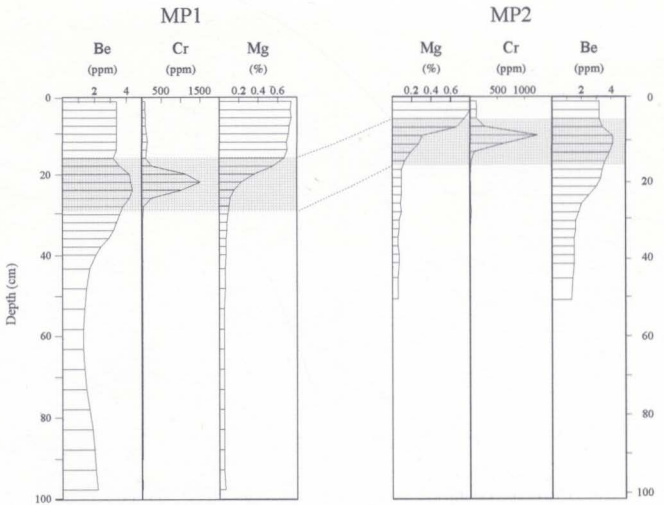

Figure 3.7 Element profiles from cores MP1 and MP2 depicting the prominant Cr peak and the depth contrast of individual features between the cores.

Both cores from this lake classify entirely as section 3, except for a thin interval classifying as section 2 (Fig 3.8). Section 2, near the top of the cores, occurs between 17 and 15 cm in GP1 and between 11 and 9 cm in GP2.

Of the lakes sampled in the local urban area and based on the magnitude of individual element concentration change, Georges Pond shows the least evidence for disturbance. In addition, this lake does not contain the clay rich upper layer that was observed in the other urban lakes. It does, however, as the groupings suggest show an undisturbed lower section and a narrow disturbed upper section of core.

3.3.6 Discriminant groupings of Long Pond, Witless Bay Line

The discriminant analysis of core LPW indicated that the whole core is equivalent to the basal sections of QV2, classifying as either group 3 or 4 (Fig 3.9). This core shows the least amount of change of all the cores collected and thus the discriminant classifications are not surprising.

Although this core is equivalent to the basal sections of core QV2, a number of elements do show subtle increases through the upper part of the core. Slight concentration increases above 9 cm occur for the elements Pb, Sb, K, Mg, Na, Ti and Ba.

3.4 Statistical summary

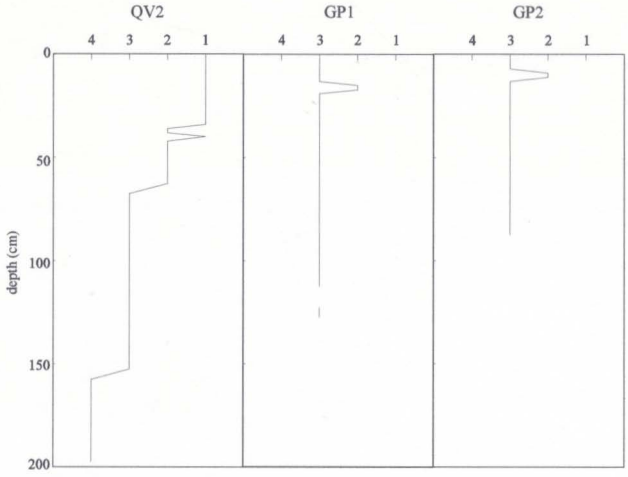

Figure 3.8 Section profiles for Georges Pond cores, computed using a discriminant function derived from core QV2.

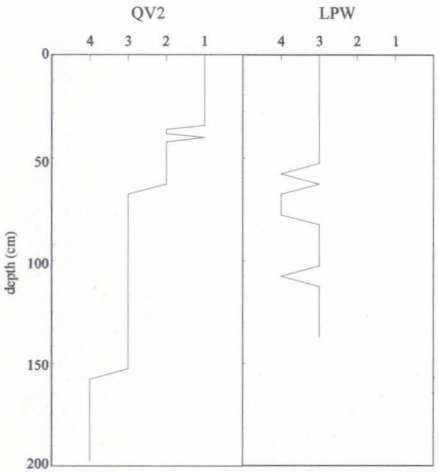

Figure 3.9 Section profile for core LPW, computed using a discriminant function derived from core QV2.

In summary, the statistical procedures employed here allow all the data to be re-classified and compared to changes detailed in Quidi Vidi Lake. The comparison provides a data set, reduced down to sections defined by discriminant function scores. In grouping the data into 4 PCs and calculating discriminant functions, many of the small but potentially important changes recorded from individual element profiles are lost. Therefore, in the discussion (Chapter 5), individual profiles will be used to highlight and characterize some important events.

3.5 Common Lead Isotopic Ratios

3.5.1 Common Lead Isotopic Ratios from Quidi Vidi Lake, core QV2

The common lead isotopic ratio profiles for this core are shown in Figure 3.10. All ratios show a similar trend with a stable basal section, declines through the upper mid-core followed by increases to the top.

The stable basal period between 157.5 and 97.5 cm encompasses the lower three samples. Basal ratios for $^{206}Pb/^{207}Pb$ average 1.1875 and have a narrow range of 0.0025. The other ratios show a similar steady profile through this section. Above this stable interval the $^{206}Pb/^{207}Pb$ profile shows a gradual decline to 34 cm. Between 34 and 29 cm the ratio declines significantly to 1.1319, from 1.1629. The ratio

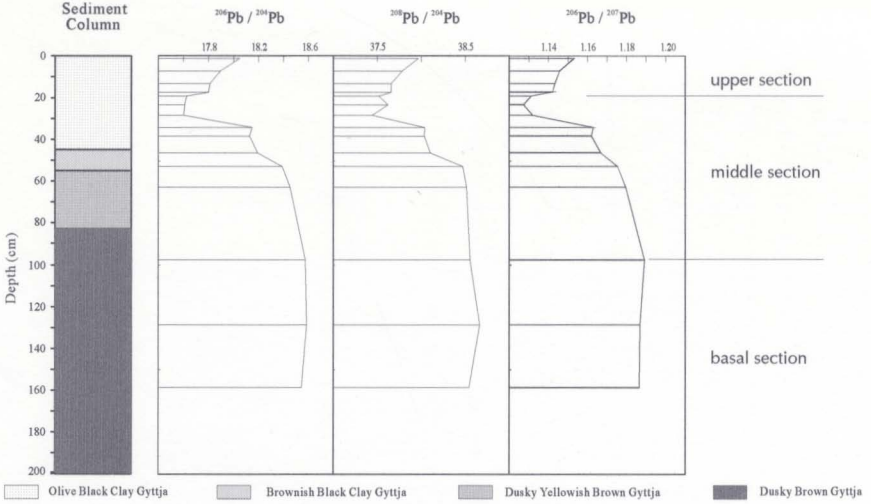

Figure 3.10 Common lead isotopic ratio profiles from core QV2.

remains low to 19 cm, and increases abruptly to 1.1421 at 17 cm. Above 17 cm, through the upper part of the core, the $^{206}Pb/^{207}Pb$ increases gradually to 1.1525 at 1 cm.

3.5.2 Common Lead Isotopic Ratios in Long Pond Witless Bay Line, core LPW

The common lead isotopic ratios versus depth profiles from this core are shown in Figure 3.11. All ratios show a similar trend, with a stable basal section and slight changes through the top. These patterns are similar to that from Quidi Vidi Lake, however, the magnitude of change is much less.

Through the basal three samples, encompassing the section of core between 122.5 and 25 cm, the $^{206}Pb/^{207}Pb$ ratio is uniform. Through this section of core the ratio averages 1.1867 with a narrow range of 0.0011. Above 25 cm, the ratio first shows a decline to 9 cm (1.1822) followed by a slight decrease to 1 cm (1.1815).

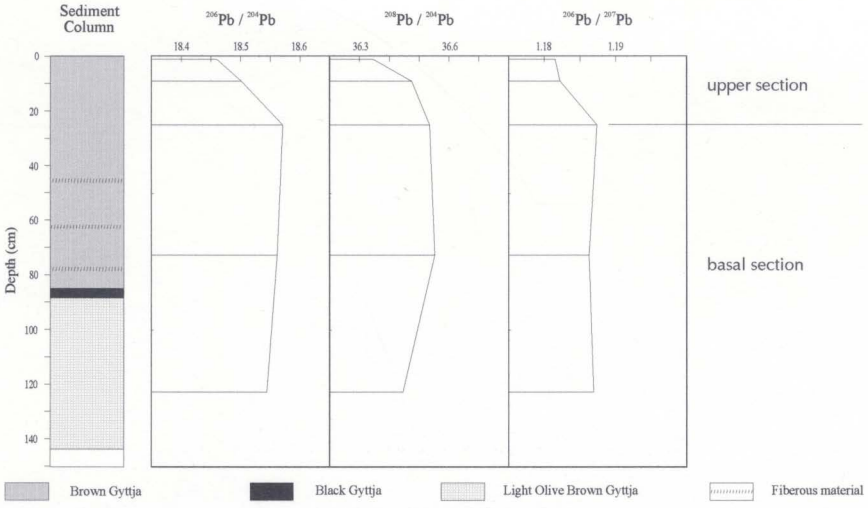

Figure 3.11 Common lead isotopic ratio profiles from core LPW.

Chapter 4: Biological and physical parameters recorded in the lake sediment cores.

4.1 Palynology

Palynomorph profiles from each urban lake show broadly similar patterns of change that can be correlated across the urban area. In sharp contrast is the core LPW (Long Pond, Wiltless Bay Line) which shows few, if any, of the changes seen in the cores from St. John's. The pollen assemblages from each of the sampled lakes are described in this chapter.

4.2 Pollen Zonation

Cluster analysis, using percentage, was used to create a dendrogram for pollen zone selection, thereby eliminating subjective interpretations. For zone selection, established by using the resulting dendrogram, an arbitrary value of 100 for the 'total sum of squares' was selected. In several cases the statistical analysis did not provide separations at locations where a visual analysis would strongly suggest otherwise. This, however, occurred where the dimensionality of the data set suggests the statistical analysis is subject to problems (Garrett, 1993). In these cases a subjective zone separation was imposed on the data. It is worth noting that none of the five pollen data sets satisfy "Garretts rule", where dimensionality of at least 3 is required to provide meaningful

results. The analysis, however, did provide reasonable assemblages based on a visual inspection and thus dendrograms were used to separate the data.

A 'sum of squares' value of 100 did provide a general framework, dividing the data to show broad scale changes. Ranking the changes displayed in the initial tree of the dendrogram to separate zones 1 and 2, it is apparent that zone 1 represents the lower core with little change and zone 2 represents the upper core where significant changes occur.

4.2.1 Urban palynology of St. John's

The pollen and spore profiles from the urban area show distinctive assemblage zones containing subzones characterized by abundances of specific taxa. The lower zone 1 is dominated by tree taxa while zone 2, representing the upper half of the core is dominated by grass and herb taxa. Through this upper zone the demise of tree taxa occurs. Core QV2 is the closest to the heart of the urban development and, as such, contains the most complete record of change.

4.2.2 Pollen assemblage from Quidi Vidi Lake

Zone 1, *Picea-Betula* subzone, below 85 cm is dominated by these taxa, which account for the greatest percentages (Fig 4.1). Minor variations are observed. The interval between 112.5 and 102.5 cm shows elevated *Betula* values and lower

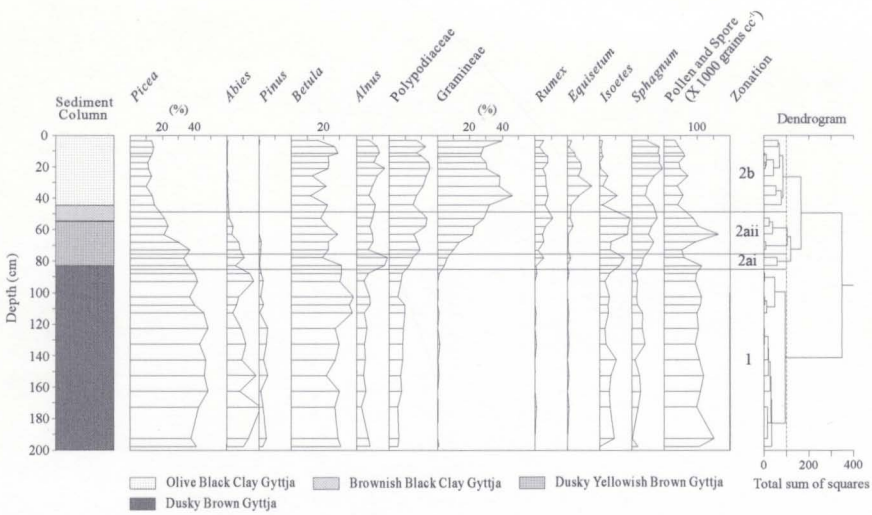

Figure 4.1 Stratigraphic profiles for the most abundant pollen and spore types in QV2.

Picea and *Abies* values. In this zone, and between 142.5 and 132.5 cm, *Isoetes* and *Sphagnum* show a 'reverse' where *Isoetes* declines and *Sphagnum* increases.

Subzone 2ai, the *Alnus*-Gramineae-*Isoetes*-*Rumex* subzone, occurs between 85 and 75 cm. This subzone is dominated by peaks in *Alnus* and *Isoetes*, with the first increases in Gramineae and *Rumex*. Increases in other taxa are also noted including Polypodiaceae and *Sphagnum*. Decreases are observed in the *Pinus* and *Betula* profiles, with *Pinus* declining to very low levels; it is for the most part non-existent above.

Subzone 2aii, the Gramineae-*Isoetes* subzone, extends from 75 to 48 cm. Gramineae increases from 10% to 29% between 72.5 and 52.5 cm. *Isoetes* declines from subzone 2ai, to a low between 72.5 and 67.5 cm (approximately 7%) followed by a plateau between 62.5 and 52.5 cm; where percentages range between 17% and 19%.

Tree taxa through this subzone show notable declines. *Picea* declines from 37% to 22% between 72.5 and 52.5 cm, while *Abies* declines to insignificant amounts. Other taxa including ferns (Polypodiaceae) and wetland plants (*Sphagnum*) increase slightly through this subzone.

Subzone 2b, the Gramineae-*Equisetum* subzone, extends from 49 cm to the top of the core. Gramineae increases from subzone 2b to peak at 38 cm (46%), declines to 13 cm (27%) and increases to 1 cm (40%). *Equisetum* increases abruptly from 44

cm (2%) to peak at 32 cm (15%), and declines above. Other taxa show notable changes through this subzone including *Betula* which shows higher values through the upper 23 cm, and *Isoetes*, which fluctuates as it declines to very low levels at the top.

The pollen and spore counts through this core show general agreement with selected zones/subzones. Counts are constant through zone 1, and show variability as they decline through zone 2. A peak is observed in subzone 2aii at 62.5 cm.

4.2.3 Pollen assemblage from core LP5

Zone 1, below 55 cm, shows stable percentages in all taxa (Fig 4.2). This core shows slightly higher *Betula* percentages and lower *Picea* percentages between 67.5 and 62.5 cm, similar to that observed in core QV2 between 112.5 and 102.5 cm. These intervals from the two different cores, however, may not represent an equivalent time period.

Subzone 2a, the *Alnus*-Gramineae-*Rumex* subzone, extends from 55 to 20 cm and is first marked by increases in these taxa. *Alnus* shows a small increase between zone 1 and subzone 2a, and remains relatively constant through the rest of the core. Gramineae and *Rumex* show the first notable increases at the bottom of this subzone, with measurable amounts (≥ 1%) at 52.5 and 57.5 cm, respectively. Gramineae increases gradually to 21 cm (21%), while *Rumex* shows little change after its

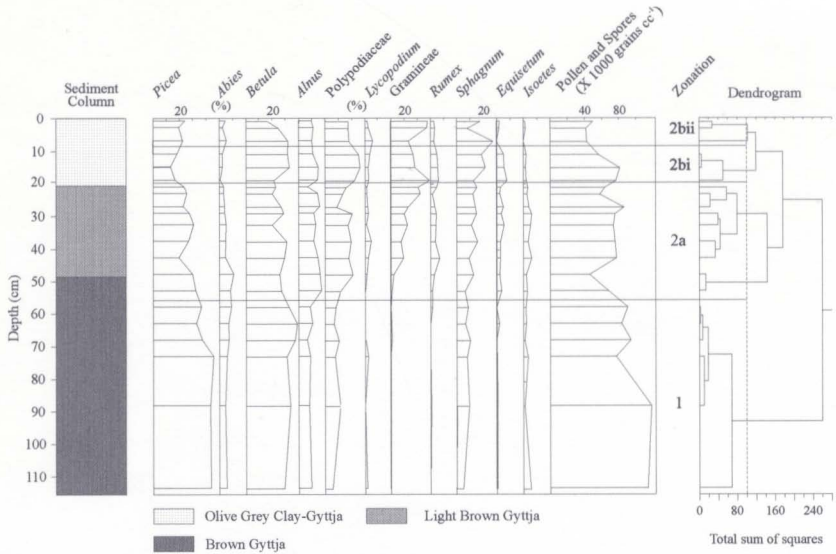

Figure 4.2 Stratigraphic profiles for the most abundant pollen and spore types in core LP5.

initial increase.

Throughout this subzone other taxa show increases, including the following: the Polypodiaceae family, *Sphagnum* and *Equisetum*. *Isoetes*, which shows a small increase compared to levels in zone 1, exhibits slightly higher percentages between 42 and 29 cm (4%-8%). A number of taxa show declines, including *Picea* and *Betula*.

Subzone 2bi, between 20 and 9 cm, the Polypodiaceae-*Equisetum* subzone, is marked by high percentages of these taxa. Polypodiaceae percentages range between 22% and 26%, compared to a range of 6% and 21% in the remainder of the core. *Equisetum* increases from subzone 2a to 8% at 19 cm, followed by a gradual decline to 5% at 11 cm. Other changes through this subzone include; *Betula* increases sharply between 19 and 15 cm, *Sphagnum* shows a continued increase, Gramineae declines by nearly 50%, and *Picea* shows a small, but abrupt decrease between subzones 2a and 2bi.

Subzone 2bii, the Gramineae subzone, through the upper 9 cm, is marked by a sharp increase in Gramineae, doubling between 7 and 3 cm (13% to 27%) and steady to 1 cm. Most other taxa remain constant through this subzone, except *Betula* and *Sphagnum* which show an overall decline.

The pollen and spore concentration curve shows an overall decline upwards. Interesting, the profile shows a large decline in zone 1, between 87.5 cm and 72.5 cm. In zone 2, the

count profile is variable, showing an overall decline upwards.

4.2.4 Pollen and spore assemblage from Georges Pond

The dendrogram for this lake caused much difficulty in interpretation. A major pollen change is observed between 62.5 and 57.5 cm in some of the most abundant taxa (Fig 4.3). However, using a 'total sum of squares' value of 100 for zoning, this widespread change is not distinguished from the bottom stable interval. The dimensionality of this analysis was 2.1, lower than the critical value of 3, meaning any statistical analysis is subject to problems. In light of the dimensionality problem and the sharp change between 62.5 and 57.5 cm, a zone division was placed at 60 cm.

Zone 1, below 60 cm, is divided into two subzones. Subzone 1a, below 120 cm, the *Betula-Alnus-Equisetum* subzone, is defined with high percentages of all three taxa, especially *Equisetum*. Subzone 1b, between 120 and 60 cm, the *Picea-Betula* subzone, shows high levels of these taxa. *Picea* which shows a relatively flat interval between 118.5 and 87.5 cm (46% and 51%), declines to 62.5 cm (31%). *Betula* first declines from subzone 1a to show a gradual overall increase to 60% at 62.5 cm. Although *Alnus* and *Equisetum* decline from subzone 1a, percentages are relatively high at 118.5 and 112.5 cm.

Subzone 2ai, the *Picea-Alnus*-Gramineae subzone extends from 60 to 45 cm. *Picea* shows a sharp increase from subzone

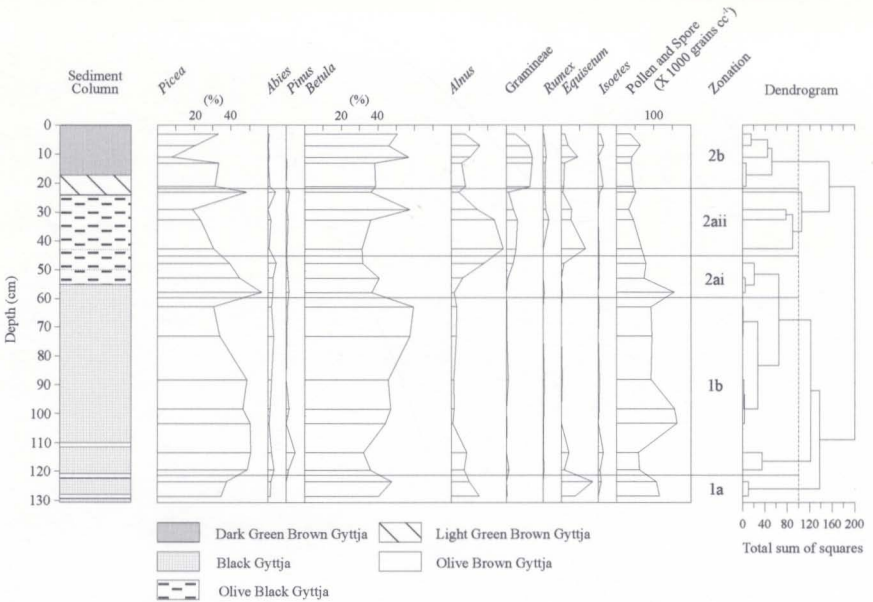

Figure 4.3 Stratigraphic profiles for the most abundant pollen and spore types in core GP1.

1b, doubling between 62.5 and 57.5 cm, above which it declines sharply to 47.5 cm (39%). *Alnus* in this subzone shows an initial increase between 57.5 and 52.5 cm, while Gramineae starts increasing through the next interval between 52.5 and 47.5 cm. *Betula* percentages decline by nearly 50% between subzones 1b and 2ai.

Subzone 2aii, the *Alnus-Equisetum* subzone, extends from 45 to 22 cm. *Alnus* increases from subzone 2ai to peak at 42.5 cm (28%), remains steady to 32.5 cm and declines sharply to 4% at 23 cm. *Equisetum* also increases from subzone 2ai to peak at 42.5 cm (13%), but declines steadily to < 1% at 23 cm. Other taxa show abrupt changes in this subzone. For instance *Picea*, which declines to 29 cm (19%) shows a 2.5 fold increase to 23 cm (48%), while *Betula* exhibits a notable peak at 29 cm (57%). *Rumex*, in this subzone, first occurs at percentages above 1% at 32.5 cm (3%).

Subzone 2b, the Gramineae subzone above 22 cm, is marked by high concentrations of this taxon. Gramineae shows a sharp increase from subzone 2aii, increasing from 1% at 23 cm to 13% at 21 cm. From 21 cm, Gramineae remains steady to 7 cm (12%), but declines to 3 cm. In this subzone a number of taxa show abrupt changes between 13 and 11 cm including; *Betula* which doubles (28% to 56%), *Equisetum* which shows a sharp increase and *Picea* which shows a 75% decline.

Pollen and spore counts through this core show an overall

agreement with the two major zones, zones 1 and 2. With the exception of a high counts in subzone 2b and a peak in subzone 2ai, the count profile is steady through zone 1 and shows declines through zone 2.

4.2.5 Pollen and spore assemblage from Mundy Pond

As with Georges Pond, the dendrogram analysis for this core failed to separate a major change between 42.5 and 37.5 cm (Fig 4.4). Again the dimensionality of the statistical analysis for this pollen assemblage was much less than 3, at 1.0. In light of this low dimensionality and the notable change between 42.5 and 37.5 cm, a zone division was placed at 40 cm. This division correlates with a sharp increase in *Equisetum*, found in disturbed wet areas, forest areas and a pond plant, which may reflect impacts upon the lake or increased disturbed areas, prior to larger changes in the local vegetation.

Zone 1, the *Picea-Betula* subzone, below 40 cm is dominated by these taxa (Fig 4.4). Percentages of *Picea* and *Betula* are high and stable through this zone. *Alnus* and Polypodiaceae show a small increase between the widely spaced samples at 77.5 and 42.5 cm.

Subzone 2ai, the Gramineae-Polypodiaceae-*Equisetum* subzone, occurs between 40 and 25 cm. *Equisetum* shows an increase to peak at 37.5 cm (10%) followed by a decline to the

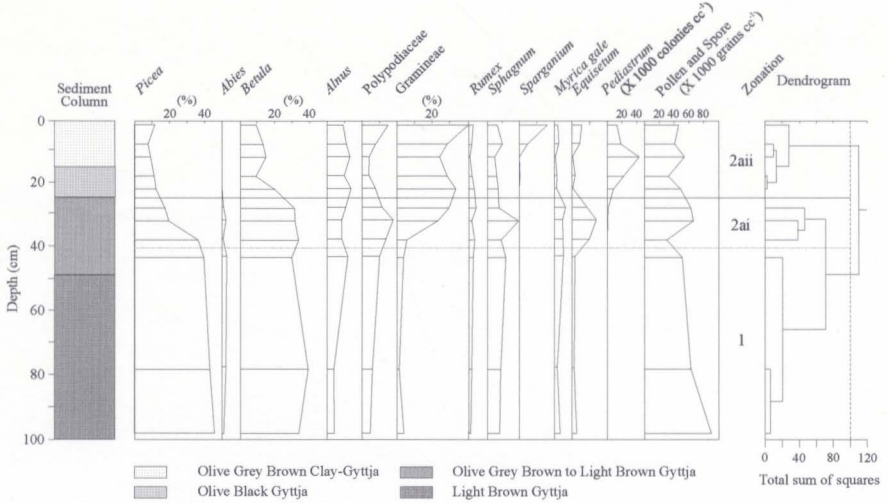

Figure 4.4 Stratigraphic profiles for the most abundant pollen and spore types in core MP1.

top of the subzone. Polypodiaceae shows a similar trend, but with less relative change. Gramineae shows it first discernable increase, above the background, between 37.5 and 32.5 cm. Trees show a decline through this interval, especially *Picea*, while *Alnus* and *Betula* show little change.

Subzone 2aii, the Gramineae-*Alnus* subzone, includes the upper 25 cm. Gramineae shows high percentages through this subzone, while *Alnus*, with percentages ranging between 9% and 14%, exhibits slightly higher percentages than in the subzone below. *Betula* in this subzone shows a sharp drop to 17 cm (10%) with little change above. Through the top 11 cm, Gramineae, Polypodiaceae and *Sphagnum* show notable increases.

Pediastrum colonies, an aquatic alga, shows a notable peak in this subzone. Counts increases from less than 800 colonies cc^{-1} in subzones 1 and 2ai to peak at 43,000 colonies cc^{-1} at 11 cm followed by a decline to 13,000 colonies cc^{-1} at 1 cm. This was the only core to show high levels of this alga. (*Pediastrum* colonies were not used in the cluster analysis and subsequent dendrogram).

Pollen and spore counts in this core show very little overall change. Through zone 2, however, the profile is variable showing slightly higher percentages in subzone 2ai.

4.2.6 Pollen and Spore assemblage from Long Pond Witless Bay Line

The pollen and spore assemblage from this lake showed much less variation than the other urban lakes, which is expected since this lake represents a background or control lake for the study. This assemblage is divided into two zones, a lower stable zone below 29 cm, and an upper zone exhibiting changes (Fig 4.5).

Through zone 1, which is subdivided into 2 subzones, *Picea*, *Betula* and *Isoetes* are the dominant taxa. A spike in the *Betula* percentages at 97.5 cm, corresponds to a low in *Picea* at that depth. In Subzone 1a, *Betula* shows relatively higher percentages, while in subzone 1b, *Isoetes* shows increases to 57.5 cm, followed by a small decline to the top of the subzone. Percentages of *Isoetes* which range between 19% and 28% in this subzone are high compared to all other cores.

Zone 2 is subdivided into 2 subzones. Generally, through these subzones *Isoetes* shows notable increases, as *Picea* shows a sharp decline through subzone 2aii. It should be noted that in Appendix D, count data for *Picea* in the upper 15 cm shows lower counts than *Isoetes*, yet *Picea* shows a higher percentage in the plotted percentage profile. This difference is due to the difference in calculating the percentage of pollen taxa versus spore taxa (see section 2.5.1). *Betula* is variable with lower percentages than in zone 1. Unlike any other core, *Abies* percentages show an initial increase and stable percentages through these subzones. *Alnus* shows a small increase through

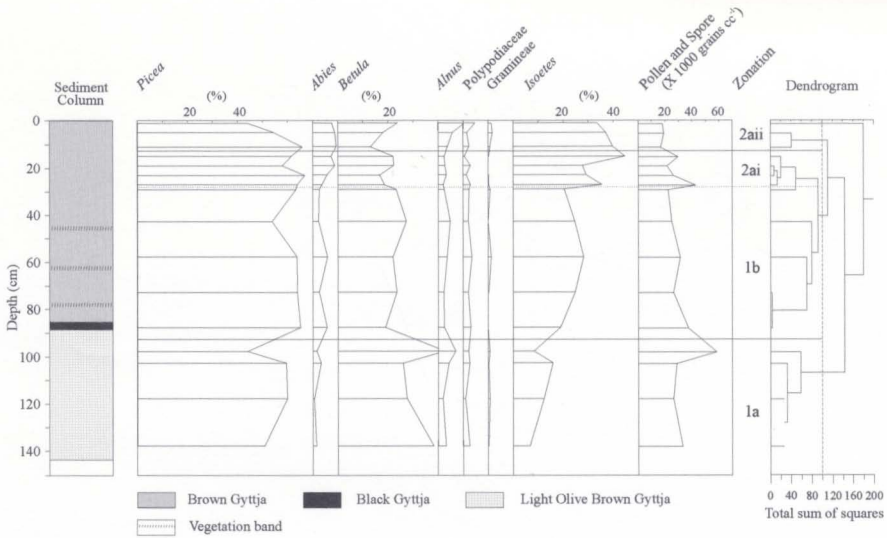

Figure 4.5 Stratigraphic profiles for the most abundant pollen and spore types in core LPW.

subzone 2aii.

The dendrogram analysis suggests a further subzone including only the upper sample. For this reason, and since the upper sample shows a continuation of the trends observed in subzone 2aii, this subzone was left out.

The pollen and spore count profile shows, with the exception of three spikes at 97.5, 27 and 15 cm, an overall gradual decline upwards.

4.3 Results of Diatom analysis from core QV2

Five samples from core QV2 at depths of 167.5, 127.5, 74, 28, and 5 cm were examined for diatoms. In total, more than 130 diatom taxa were encountered throughout the data set.

4.3.1 Individual Taxa

Taxa that contribute to high percentages or notable changes are displayed in Figure 4.6. Though the number of species encountered within core QV2 exceeded 100, five species accounted for the largest fraction and changes observed.

Tabellaria flocculosa str. III sensu, a periphytic diatom (attached in the littoral zone), shows a large continued increase from the basal samples to 74 cm, but declines to very low levels in the upper two samples. *Asterionella formosa*, a planktonic taxon, shows the inverse with low basal percentages and high upper core percentages, exhibiting a large increase

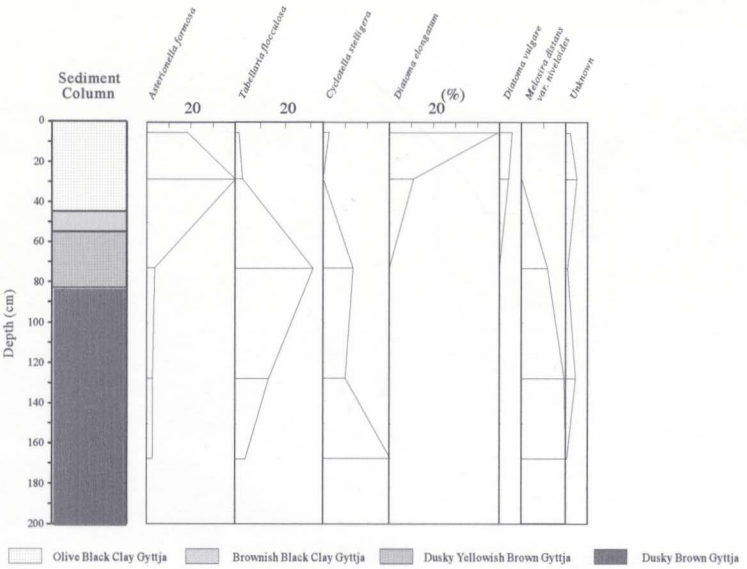

Figure 4.6 Stratigraphic profiles for the most abundant diatom taxa in core QV2. Units are in percentages.

between 74 and 28 cm. *Cyclotella stelligeria*, a planktonic diatom, shows relatively higher percentages in the basal three samples with very low levels through 28 and 5 cm, a pattern which is mimicked by *Melosira distans* var. *niveloides*, a planktonic diatom. This species, however, declines to non-detectable levels in the upper two samples.

Only one *Diatoma* sp. valve was identified from the basal three samples, yet *Diatoma elongatum*, a planktonic diatom, accounts for the largest fraction at 11% and 49.2% in the samples at 28 and 5 cm, respectively.

4.3.2 Morphological and Ecological Changes

An examination of the morphological forms shows a large change in both the Pennales and Centrales (Fig 4.7). The Centrales drop from approximately 26% of the total in the basal two samples to less than 1% in the upper section. The Pennales increase from 70% in the basal two samples to 97% in the upper sample. This change is exhibited in the Pennales:Centrales ratio (C:P) which increases from < 5 in the three basal samples to 29 at 28 cm. Another marked shift occurs between 28 cm and 5 cm where the ratio increases to 107.

The planktonic:benthic (P:B) ratio which displays general ecological changes increases toward the top of the core (see Fig 4.7). The ratio ranges from 0.65 to 2.0 in the bottom four

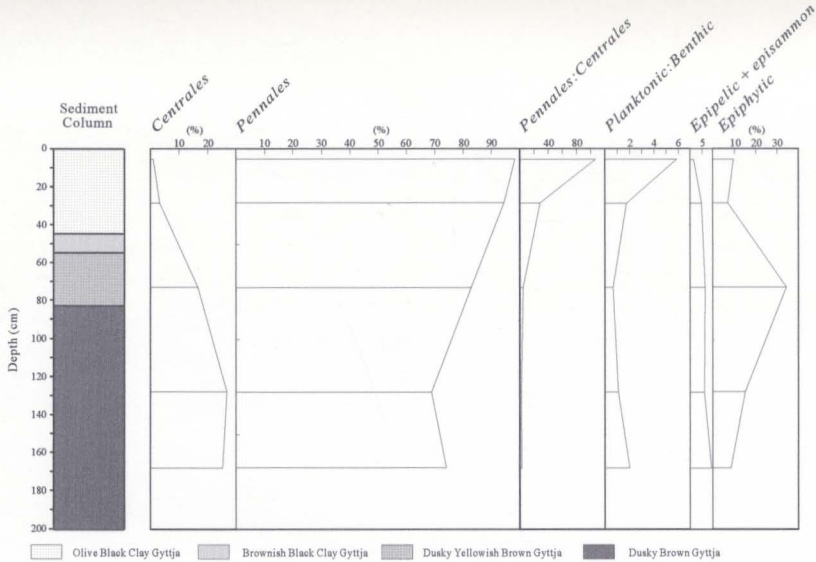

Figure 4.7 Morphological form and ecological characteristics represented by the diatom community in core QV2.

samples and increases to 5.9 at 5 cm. Among the benthic fractions the epiphytes (attached to plants) peak in abundance at 72.5 cm. The epiphytic portion increases steadily from 8% at the base to 34% at 72.5 cm. This is followed by a sharp decline through the upper samples (7% to 10%).

The sum of the epipsammic (attached to sand grains) and the epipelic taxa (attached to mud) declines slightly upward. These forms account for a small percentage of the total valve count throughout the core. The bottom four samples range 5.5% to 9.4% and decrease to 1.5% in the top sample.

4.3.3 pH reconstruction

The diatom community was used to reconstruct the lake water pH through the interval represented in the core. The pH was reconstructed by a weighted average technique, (Birks et al., 1990) using the optimal pH for the individual diatom species as recorded in Dixit et al., (1992). An optimal pH of 8.45 was used for *Diatoma elongatum* (Smol, 1996 pers. comm.).

The reconstructed pH for core QV2 shows lower pH values at the base of the core compared to the top, and a range of 1.6 pH units throughout the core (Figure 4.8). The basal three samples range between 6.47 and 6.28 and are followed by an increase to approximately 7.24 and 7.93 at 28 and 5 cm, respectively.

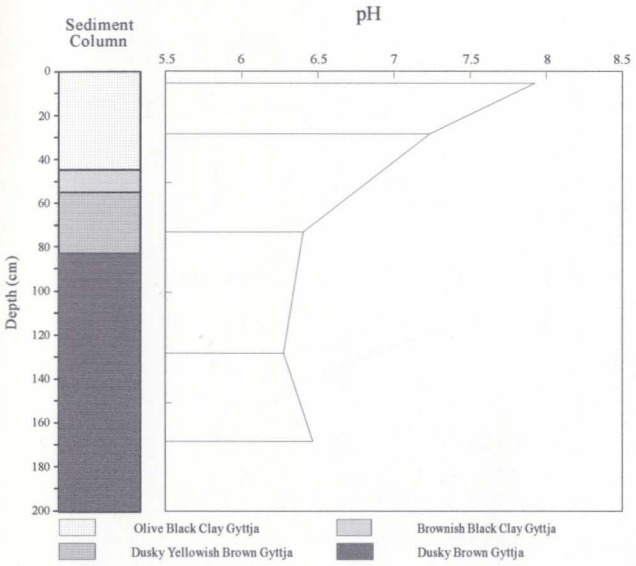

Figure 4.8 Reconstructed lake water pH from diatom analysis of core QV2.

4.4 Charcoal and soot from sediment cores

4.4.1 Charcoal and soot from core QV2

Counts per cubic centimetre versus depth profiles of the these particulates show a basal section with only charcoal present and an upper section where soot particulates are introduced and increase sharply upwards (Fig 4.9).

Charcoal particles are present throughout the core. Below 92.5 cm charcoal was observed in eight of the twelve samples examined. Counts through this section were generally low (> 1000 particles cc^{-1}) except at 132.5 cm (2250 particles cc^{-1}). Above 92.5 cm charcoal is ubiquitous. The interval between 92.5 and 72.5 cm shows low counts (244 and 2283 particles cc^{-1}), but these are on average greater than recorded through the basal section. Between 72.5 and 52.5 cm charcoal counts show a steady increase to 46,830 particles cc^{-1} and are relatively steady to 44 cm. A sharp increase is observed between 44 and 25.5 cm (112,000 particles cc^{-1}), with a peak at 38 cm (117,000 particles cc^{-1}). From 25 cm to the top the profile declines steadily to 15,000 particles cc^{-1}.

Soot particulates first appear at 57.5 cm (1200 particles cc^{-1}) and show a nearly linear increase to 32 cm (4900 particles cc^{-1}). The profile declines to 25.5 cm (2550 particles cc^{-1}) and shows a step-wise increase to 17 cm (16,000 particles cc^{-1}). Soot counts between 25.5 and 23 cm increase 4 fold. Above 17 cm, the soot profile shows a steady decline

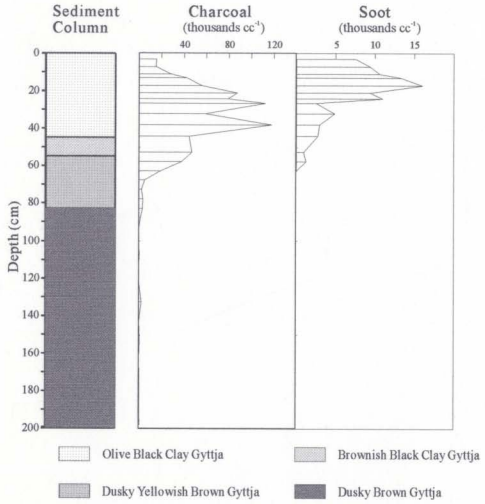

Figure 4.9 Charcoal and soot particle profiles from core QV2.

to 3 cm (7500 particles cc^{-1}).

4.4.2 Charcoal and soot from core LP5

Charcoal and soot profiles from this core show similar trends. Charcoal is present throughout the core, as in Quidi Vidi Lake, and soot first appears at 42.5 cm (Fig 4.10).

Charcoal is present in all samples except two, at 87.5 and 72.5 cm. The basal sample at 112.5 cm shows a high count of 3700 particles cc^{-1}. The profile shows a constant interval between 67.5 cm and 29 cm (ranging between 680 and 2700 particles cc^{-1}). A sharp spike is observed to 21 cm (18,000 particles cc^{-1}). From 21 cm counts decline to 11 cm (9400 particles cc^{-1}) after which they increase to the top of the core again (16,000 particles cc^{-1}).

From the base up, soot first appears at 42.5 cm (1100 particles cc^{-1}). It shows a low between 37.5 and 29 cm (290 - 440 particles cc^{-1}) and increases to 21 cm (1400 particles cc^{-1}). A sharp increase is observed between 21 and 19 cm where counts more than double. Above 19 cm the profile shows a gradual increase to 11 cm (4400 particles cc^{-1}), is relatively stable to 3 cm and spikes up to 1 cm (9240 particles cc^{-1}).

4.4.3 Charcoal and soot from core MP1

Particulates from this core show increases within the upper core as seen in previous ponds. Charcoal is present

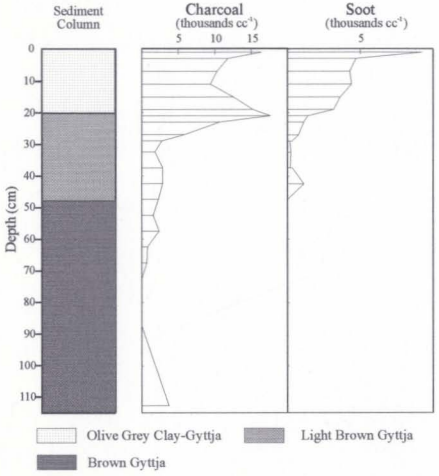

Figure 4.10 Charcoal and soot particle profiles from core LP5.

throughout the core while soot first appear within the upper 21 cm (Fig 4.11).

Charcoal particles show typically lower abundances in the basal section and sharp increases through the top of the core. From the base at 97.5 to 31 cm counts range between 680 and 1650 particles cc^{-1}, and increase to 2700 particles cc^{-1} at 27 cm. A moderate increase between 27 and 21 cm is followed by a sharp increase to a peak at 17 cm (46,000 particles cc^{-1}). The profile shows a decline to 11 cm and an increase above, with levels of 36,000 and 39,000 particles cc^{-1} in the upper two samples.

The soot profile shows a simple trend. The first appearance of this particulate occurs at 21 cm (880 particles cc^{-1}), above which it steadily increases to 7 cm and nearly steady to 1 cm (9000 particles cc^{-1}).

4.4.4 Charcoal and soot from core GP1

Particulates from this core show increases within the upper sediments, peaking near the surface followed by a decline through to the top sample (Fig 4.12).

Charcoal particles are present in all but one sample. Charcoal shows a basal section, between 127.5 and 97.5 cm, with relatively high counts (430 - 2700 particles cc^{-1}). Counts remain low through to 57.5 cm, where a value of 930 particles cc^{-1} was obtained. Above 57.5 cm the profile is erratic

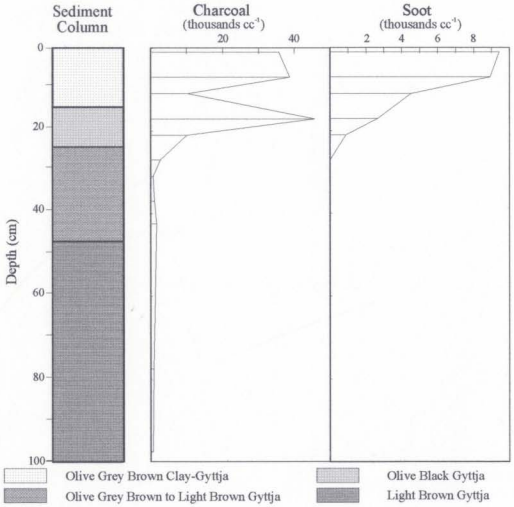

Figure 4.11 Charcoal and soot particle profiles from core MP1.

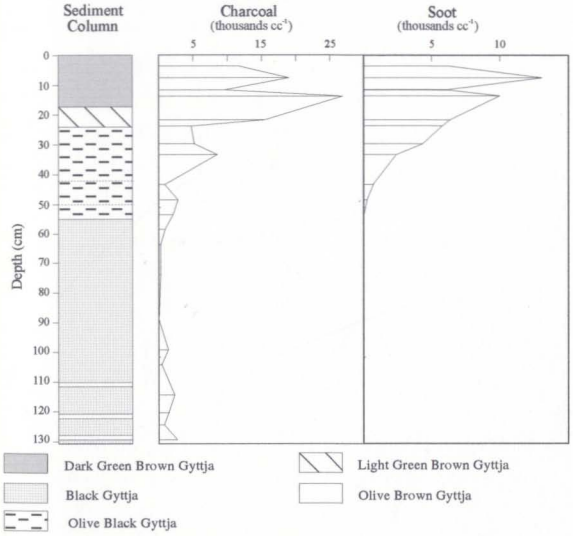

Figure 4.12 Charcoal and soot particle profiles from core GP1.

although an overall increase to 23 cm (4700 particles cc^{-1}) is evident. It increases sharply to 21 cm (16,000 particles cc^{-1}) and further to peak at 13 cm (27,000 particles cc^{-1}). Counts drop to 11 cm and fluctuate in the upper two samples with little overall change.

The soot profile is simple with a steady increase upward, after the initial appearance. Soot first appears at 47.5 cm (230 particles cc^{-1}) and increases steadily to 13 cm (10,000 particles cc^{-1}). From 13 cm the profile is variable showing a peak at 7 cm (13,000 particles cc^{-1}).

4.4.5 Charcoal from core LPW

Charcoal was the only particulate observed in this core. It shows a relative uniform profile throughout, except at 97.5 cm, where the highest count was obtained (7500 particles cc^{-1})(Fig 4.13). Through the remainder of the core charcoal counts range between 250 and 2400 particles cc^{-1} with a small peak at 42.5 cm (1500 particles cc^{-1}). Between 15 and 5 cm counts are consistent, ranging from 1000 to 1500 particles cc^{-1}, followed by an increase to 2400 particles cc^{-1} in the top sample.

4.5 Radiometric dating

4.5.1 ^{14}C from lake cores

A total of five bulk sediment samples from four different

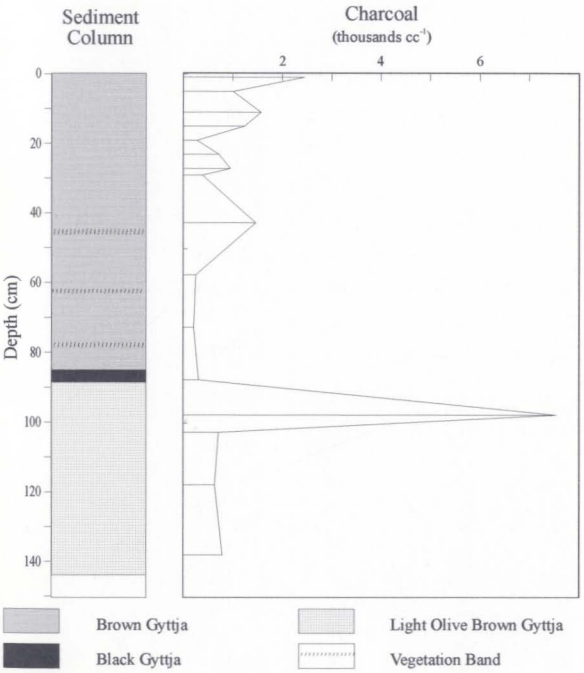

Figure 4.13 Charcoal particle profile from core LPW.

lakes were submitted for ^{14}C analysis. All samples selected come from basal units in the pre-European interval, providing information on the average background sedimentation and influx rates through out the pre-European core. No sample from Mundy Pond was submitted for analysis. ^{14}C data is listed in Table 4.1 below.

Radiocarbon ages were used to calculate the calendar age of the samples using Radiocarbon Calibration Program REV 4.0 (Stuiver and Reimer, 1993)., and the calibration data from Stuiver et al., (1998). Column 5 of table 4.1 shows the calculated calender ages for each sample.

Table 4.1 ^{14}C and calculated dates from QV2, LP5, GP1 and LPW.

Core	interval	^{14}C age	GSC ref. No.	1σ max. cal. age (cal age intercepts) min. cal. age
QV2	185-190 cm	2920 ± 60	GSC-5469	BC: 1256 (1126) 1005
QV2	100-105 cm	1110 ± 70	GSC-5528	AD: 885 (902,917,962) 1015
LP5	110-115 cm	2260 ± 70	GSC-5480	BC: 397 (377,266,264) 204
GP1	115-120 cm	3960 ± 70	GSC-5485	BC: 2568 (2468) 2349
LPW	130-135 cm	5240 ± 90	GSC-5498	BC: 4221 (4039,4018,4000) 3964

4.5.2 ^{137}Cs profile from QV2

^{137}Cs, an artificial radioisotope, was introduced into the Earth's environment as a result of atmospheric nuclear weapons testing (Jaakkola et al., 1983, Pennington et al., 1973). Its use as a dating method stems from its rate of atmospheric

fallout rather than its short half-life of 30 years. Atmospheric fallout of this isotope first occurred in 1954 and peaked in the northern hemisphere in 1963 (Pennington et al., 1973 and Longmore et al., 1983). Negligible amounts of ^{137}Cs were deposited before 1954 (Jaakkola et al., 1983). This pattern of fallout provides two distinct chronological markers at 1954 and 1963.

The ^{137}Cs activity profile for core QV2 shows a distinct trend first appearing at 34 cm and peaking at 25.5 cm (Fig 4.14). These depths of 34 and 25.5 cm have been correlated to 1954 and 1963, respectively.

4.5.3 ^{210}Pb dating from QV2

^{210}Pb with a half life of 22.26 years provides an effective dating technique capable of dating sediments as old as 150 years. It is a naturally occurring radioisotope produced from the decay of ^{238}U through a series of intermediate isotopes to ^{210}Pb.

The dating technique is a result of the disequilibrium between ^{210}Pb and ^{226}Ra, its parent. The disequilibrium arises because of the mobility of ^{222}Rn, a gaseous intermediate isotope with a half life of 3.83 days (Appleby and Oldfield, 1983). The mobility of the gas phase allows it to escape from the soil to the atmosphere where it then decays to ^{210}Pb. ^{210}Pb a solid phase, falls to the land surface or onto lakes where

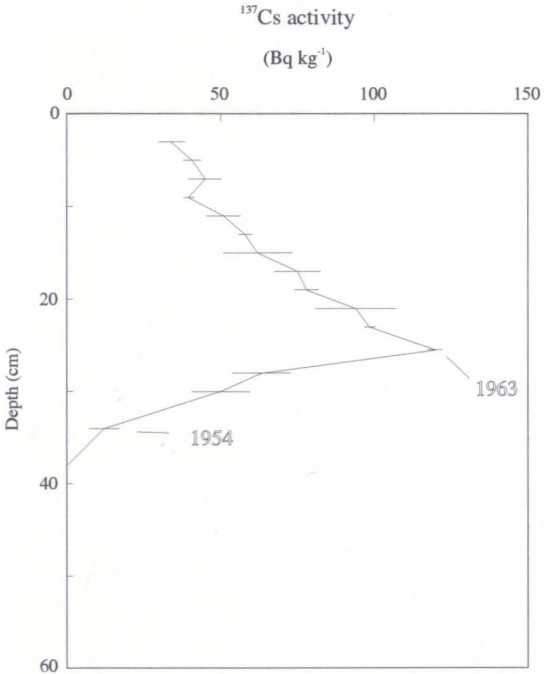

Figure 4.14 ^{137}Cs versus depth profile for core QV2.

it is deposited on the lake bottom.

This 'extra' or 'excess' ^{210}Pb from atmospheric deposition is not in equilibrium with ^{226}Ra already present in the sediment. This excess ^{210}Pb is known as the 'unsupported' fraction, while the portion in radioactive equilibrium with ^{226}Ra in the sediment is known as 'supported' fraction. The unsupported fraction is used to date sediments.

Two models, the CRS (constant rate of supply) and CIC (constant initial concentration) models, have been used for age calculations (Olsson, 1986). The CRS model is the most widely accepted and is based on the assumption of constant atmospheric fallout. This results in a constant amount of unsupported ^{210}Pb per chronological unit, despite fluctuations in dry mass (Appleby and Oldfield, 1978, Appleby et al., 1979). The CIC model applies well in areas with a constant accumulation rate, as it is based on the assumption that a constant amount of unsupported ^{210}Pb falls in one specific area per year.

Total and unsupported fractions of ^{210}Pb versus depth from QV2 are shown in Figures 4.15 and 4.16. The total ^{210}Pb profile is unusual in that the activity declines logarithmically down to 17 cm, but below to 49 cm the profile is relatively constant, at activities just above the ^{226}Ra activity. The profile of sediment dry bulk density (Fig 4.17) shows that the section of the core between 17 and 49 cm is abnormally dense,

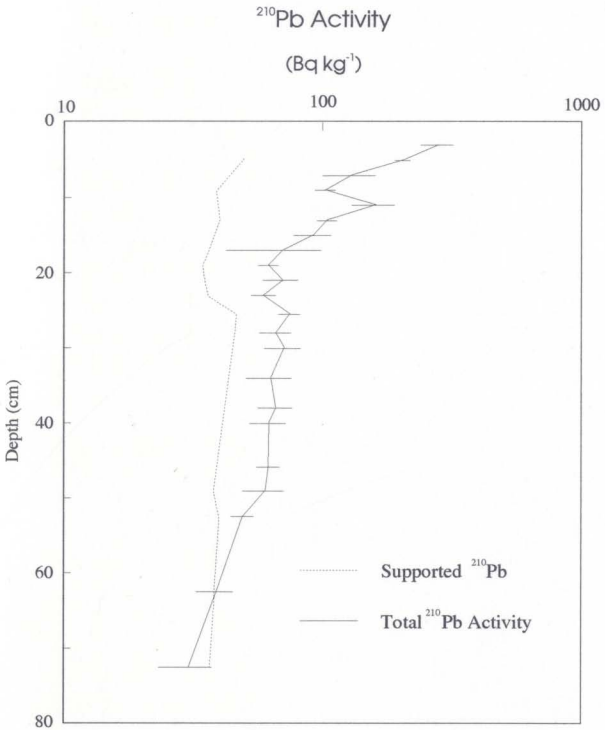

Figure 4.15 Total and supported ^{210}Pb activities versus depth profiles from core QV2.

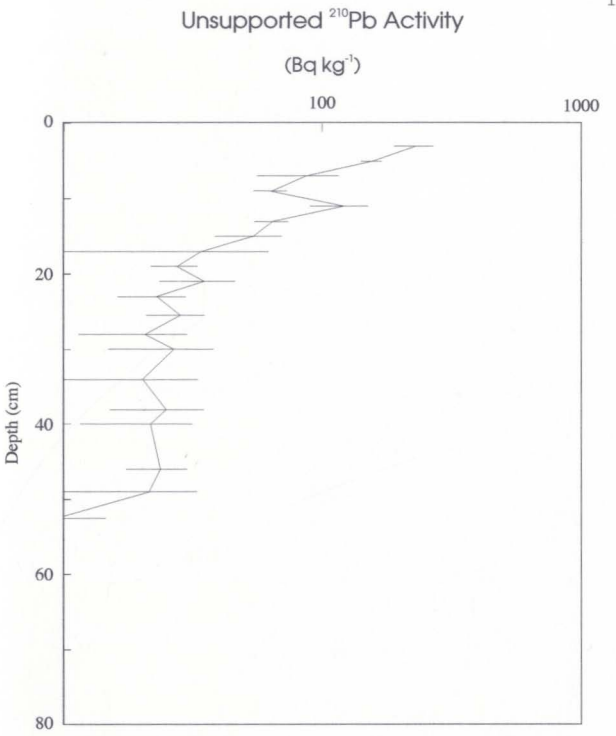

Figure 4.16 The unsupported ^{210}Pb activity versus depth profile from core QV2.

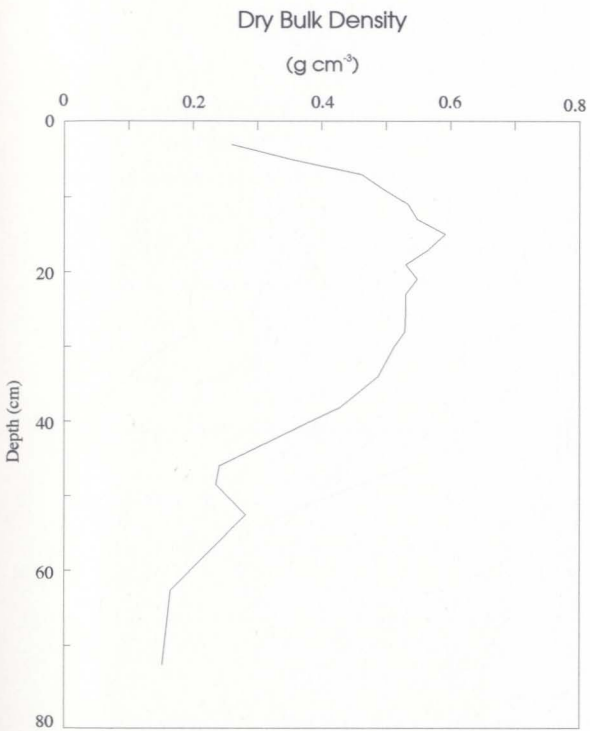

Figure 4.17 Dry bulk density versus depth profile from core QV2.

suggesting changes in sedimentation rates. Below 49 cm, ^{210}Pb declines again and radioactive equilibrium is reached at ca. 55 cm (Report on the Radiometric Dating of Quidi Vidi Lake: Core QV2, By P. Appleby 1994).

The irregular profile of unsupported ^{210}Pb suggests that the CIC model is inappropriate (Appleby and Oldfield, 1978, Appleby and Oldfield, 1983). The CIC model is applicable to lakes where the profile of unsupported ^{210}Pb plotted on a concentration (logarithmic) versus depth profile is linear. Applying the CRS model to date the core, however, conflicts with the two chronostratigraphic ^{137}Cs markers. The ^{137}Cs profile suggests that 1963 and 1954 are at 25.5 and 34 cm depth, respectively, while the CRS model dates these depths at 1941 and 1924, respectively.

The flux of ^{210}Pb also suggests that the CRS model is unlikely to apply in view of the high ^{210}Pb inventory. Up to 1954 the ^{210}Pb atmospheric flux is quite normal calculated at 153 Bq $m^{-2}y^{-1}$, but increases to 317 Bq $m^{-2}y^{-1}$ between 1954 and 1963 after which it increases further to 487 Bq $m^{-2}y^{-1}$. These values in the upper sections are more than double the normal atmospheric flux indicating massive acceleration of sedimentation (Appleby, 1994).

To successfully date this core, the two ^{137}Cs chronostratigraphic markers were used to divide the core into three sections; below 34 cm, 34 to 25.5 cm and above 25.5 cm

depth. This allowed the CRS model to be applied to each section individually, following the procedure discussed in Oldfield and Appleby, 1984. Dates obtained from this method are displayed in Table 4.2. See Appendix F for detailed procedure for calculation of ^{210}Pb dates for QV2.

4.5.4 Radiometric dates from Long Pond, St. John's

4.5.4.a ^{137}Cs from LP5 and LP3

An inadequate number of ^{137}Cs samples was examined from these cores to date the horizons corresponding to 1963 and 1954. The data, however, do show the broad intervals where these dates most likely occur.

Only four samples from LP5 at 32.5, 19, 15 and 9 cm were examined for ^{137}Cs. If this core contains an undisturbed ^{137}Cs profile, then it can be concluded that 19 cm depth is closer in age to 1963 than the upper two samples (Fig 4.18). As well, the interval corresponding to 1954 lies somewhere between 32.5 and 19 cm.

Figure 4.18 shows the ^{137}Cs activity profile for core LP3. Only two samples in this core, at 22 and 20 cm, were examined for ^{137}Cs, both of which contained the isotope. The only inference made from this data is that 22 cm depth is equal or younger than 1954.

4.6 Clay mineralogy from Quidi Vidi Lake, core QV2

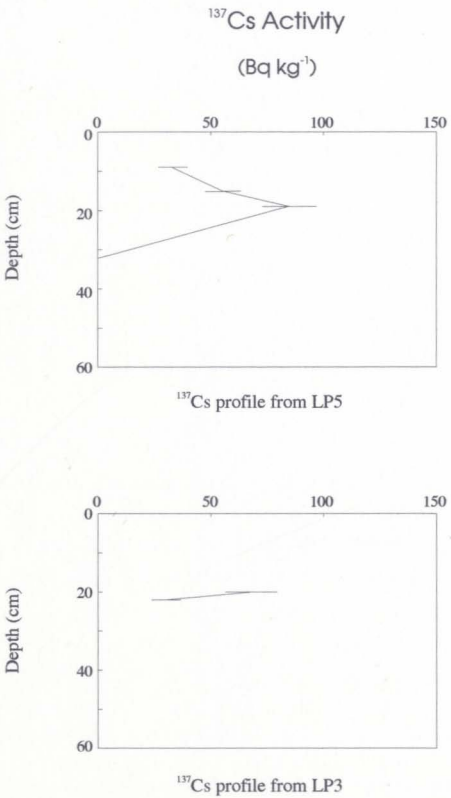

Figure 4.18 The ^{137}Cs activities versus depth profiles from cores LP5 and LP3. ^{137}Cs activities for LP5 at 35 cm were below detectable levels.

Table 4.2 Calculated ages from core QV2, based on ^{210}Pb analysis. See appendix F for age calculation procedures.

Depth (cm)	Date (AD)	Age (yr)	error (yr)
3	1986.9	5.1	1
5	1984.1	7.9	1
7	1981.5	10.5	2
9	1979.5	12.5	2
11	1976.6	15.4	3
13	1973.3	18.7	3
15	1970.8	21.2	3
17	1968.8	23.2	4
19	1967.4	24.6	4
21	1966.0	26	4
23	1964.6	27.4	5
25.5	1963.0	29	5
28	1960.5	31.6	5
30	1958.4	33.6	5
34	1954.0	38	5
38	1943.0	49.3	6
40	1936.3	56.2	7
46	1913.0	80.8	13
48.5	1899.8	95.4	13
52.5	1869.9	132.4	13

Representative diffractograms of the clay mineralogy are shown in Figure 4.19. All diffractograms show a similar profile with eight to ten identifiable peaks. Many of these peaks are second and third order reflections for the same clay mineral. Three prominent peaks at approximately 7.1 Å, 10.0 Å and 14.2 Å (12.5°, 8.8° and 6.2° 2θ peaks, respectively) appear in all samples and possibly represent different clay minerals. A fourth peak at 12.3 Å (7.95° 2θ peak) appears in about half the samples. Results from the scan of the JCPDS Powder Diffraction index for Minerals showed that the clay minerals chlorite, illite, smectite-kaolinite and hydrobiotite were the best possibilities for the identified peaks.

4.6.1 Peak identification for clay minerals

The 7.1 Å reflection is the first-order reflection for kaolinite and second-order reflection for chlorite. Biscaye, 1964, and Moore and Reynolds, 1989, suggest that a close examination of the 24.5° and 25.2° 2θ region can help to determine the clay type present. The enlarged region showed only one peak at a d-spacing of 3.54 Å (25.1°-25.2° 2θ) identifying chlorite as the only phase. Kaolinite, if present in large enough quantities, would show a peak at 3.58 Å (24.9° 2θ).

The 10.0 Å peak is the first-order reflection for illite. The presence of illite is supported by the presence of a

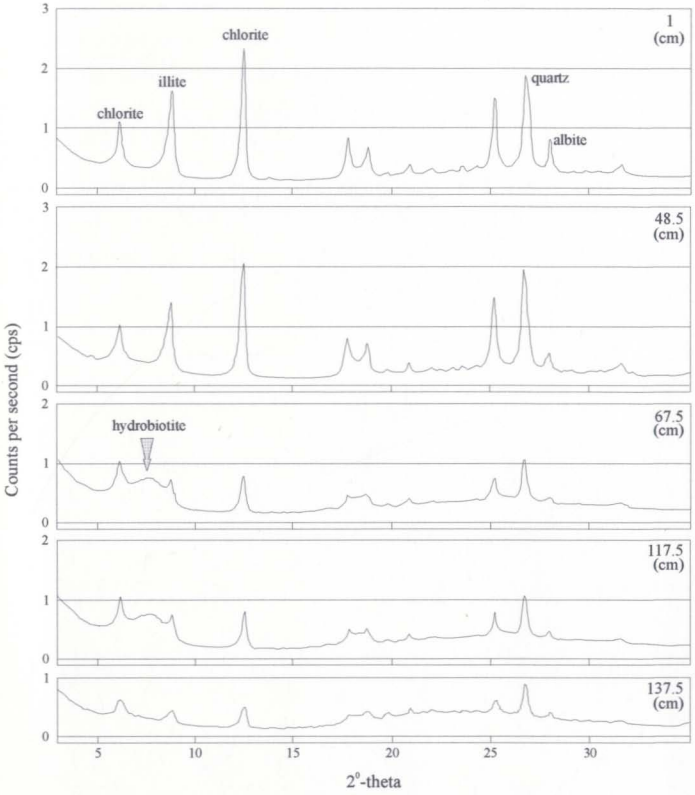

Figure 4.19 Diffractograms for the clay size fraction for selected samples from core QV2. The sample depth for each diffractogram is shown in the upper right hand corner.

strong 5.0 Å peak (17.8 2θ), its second-order reflection. Glauconite, another possibility has no or a very weak 5.0 Å peak (Moore and Reynolds, 1989), suggesting it could be present. The strong peak at 5.0 Å, however, does provide a positive identification of illite.

The 14.2 Å peak corresponds to the first-order reflector of chlorite. Smectite also has reflectors in the 12-15 Å region (Hardy and Tucker, 1988). The reflectors at 6.2° 2θ and 18.8° 2θ (14.2 Å and 4.74 Å) are positive indicators and suggest that chlorite is the main mineral contributing to the 14.2 Å peak. Again, however, smectite minerals maybe present in minor amounts.

The 12.3 Å peak corresponds to hydrobiotite, a mixed-layered structure composed of mica and vermiculite (Brindley, 1981, Moore and Reynolds, 1989). This peak is small and noticeable above background intermittently throughout the core, and thus is not regarded as one of the major phases.

Quartz and albite were also identified in the diffractograms obtained from the clay smears. Their main reflectors occur at 3.34 Å (26.67° 2θ) and 3.20 Å (27.92° 2θ), respectively.

4.6.2 Semi-quantitative analysis of clay mineralogy

Quantitative analysis of x-ray patterns for clay is subject to many problems (Hardy and Tucker, 1988, Moore and

Reynolds, 1989, Brindley, 1981, Biscaye, 1965). The intensity of a peak cannot be used as a direct measure of its abundance because of differences between diffractograms, however, relative comparisons may be made between peak ratios (Biscaye, 1965).

A semi-quantitative approach was taken to observe the relative changes of abundance of the clays throughout the core. For this analysis, Moore and Reynolds (1989) suggest using only the reflectors > 10° 2θ, and the reflectors closest to each other for the different clays. Thus, the reflectors at 5.00 Å for illite and 4.74 Å for chlorite were used. Quartz in the clay size fraction was also examined. The peak at 3.38 Å was used for quartz analysis.

The profile of the ratio of the peak intensity of illite/chlorite shows a general separation of the upper and lower core (Fig 4.20). Ratios between 77.5 cm and the base are less than one, ranging between 0.41 and 0.83, while in the upper portion ratios are greater than one, ranging from 1.16 to 2.23.

Ratios of illite/quartz and chlorite/quartz show different trends (Fig 4.20). Illite/quartz distinguishes the lower and upper core with ratios less than 0.2 below 77.5 cm, ranging from 0.10 to 0.19, and greater than 0.2 above 77.5, ranging from 0.22 to 0.55. For chlorite/quartz the profile is variable throughout with no distinguishable difference.

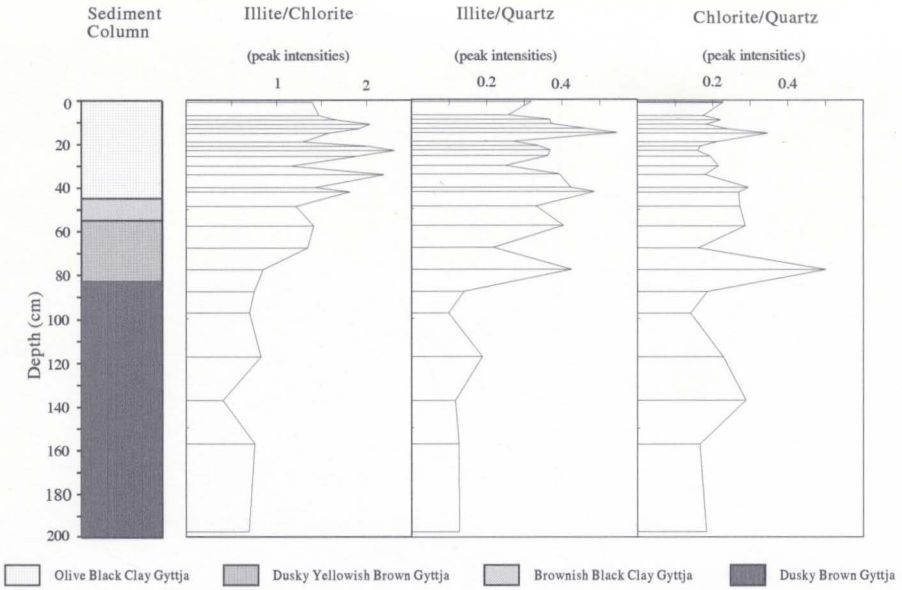

Figure 4.20 Profiles of the ratio of peak intensities versus depth for illite, chlorite and quartz in the < 2um size fraction from core QV2.

4.6.3 Results from > 2 μm fraction

Peak selection and identification with the JCPDS Powder Diffraction index for Minerals showed that quartz and albite were the only distinguishable minerals in the fraction > 2 μm. Both minerals were present in all samples. Figure 4.21 shows three representative diffractograms from the base to the top of core QV2. Intensities for the mineral phases increase up through the core with quartz having the larger intensity in all cases.

A semi-quantitative analysis was performed on the data to observe the relative changes throughout the core. Hardy and Tucker (1988) report that the peak area of a mineral is proportional to its concentration, however, minerals from different crystal systems have different diffracting abilities. No correction factor was applied to the data set since a semi-quantitative approach was taken and only two minerals were observed.

The area under the main peaks for quartz and albite (3.34 Å (26.6° 2θ) and 3.20 Å (27.9° 2θ), respectively) through the core is shown in Figure 4.22. For albite, the area in the basal section, at and below 87.5 cm varies from 13 to 40 cps (counts per second). Between 87.5 and 57.5 cm, cps increase from 13 to 80; above 57.5 cm cps are relatively high varying between 79 and 125. The area under the quartz peak shows a similar trend. At and below 87.5 cm, cps vary between 86 and

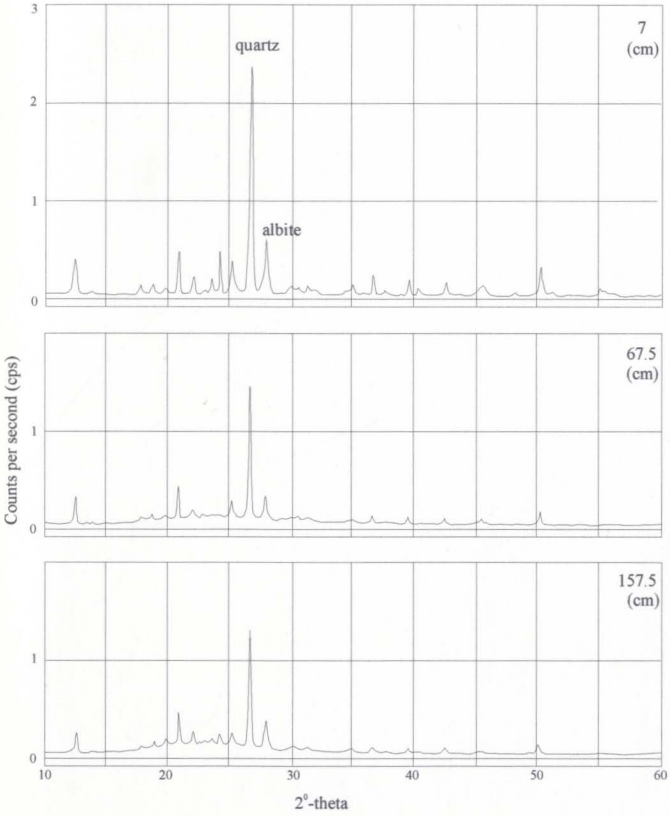

Figure 4.21 Diffractograms for the > 2 um size fraction for selected samples from core QV2. The sample depth for each diffractogram is shown in the upper right hand corner.

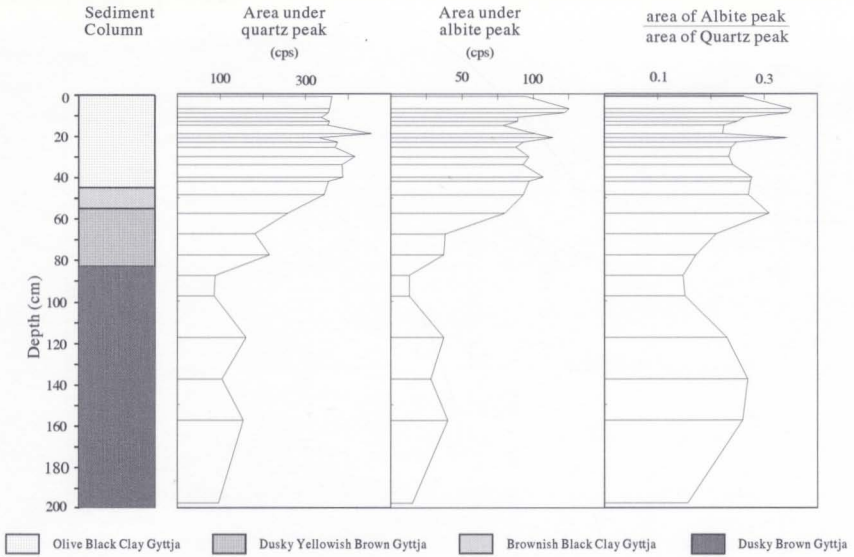

Figure 4.22 Profile of the counts per second versus depth for quartz and albite in the > 2μm size fraction from core QV2.

161, increase from 88 to 250 between 87.5 and 57.5 cm and range between 332 and 455 cps above 57.5 cm.

The ratio of quartz\albite shows somewhat lower values in the basal section compared to higher values in the upper core (Fig 4.22). At 87.5 cm and below the ratio varies between 0.15 and 0.27, increases between 87.5 and 57.5 cm (0.15 - 0.31) and is high and variable above 57.5 cm (ranging between 0.22 and 0.35).

4.7 Sedimentation and Influx Rates

Core QV2 was dated via ^{14}C, ^{137}Cs and ^{210}Pb and therefore its chronology is the most detailed of this study (see section 4.5). These dates and a pollen-inferred date of 1757 at 82.5 cm, which will be discussed later, allow detailed calculations for sedimentation and influx rates. The sedimentation rate is the rate of wet volume sediment deposition per year while the influx rate is the rate of deposition of dry material per unit area per year.

sed rate = (interval thickness in cm)/(years represented by interval)

influx rate = (dry mass per unit area)/(years represented by interval)

Figure 4.23 shows the sedimentation and influx rates calculated for QV2. See Appendix H for influx and wet sedimentation rate data for core QV2, including interpolated

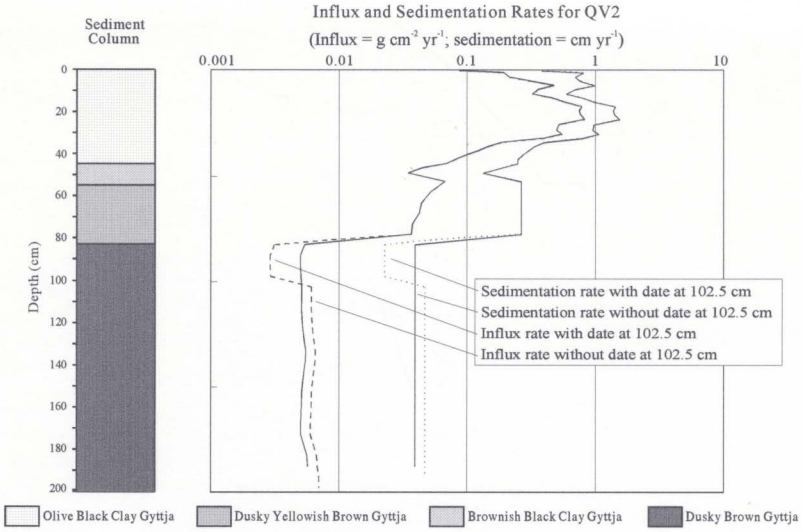

Figure 4.23 Influx and sedimentation rates for core QV2, with and without the date of 917 A.D. at 100-105 cm.

values. Note that rates are calculated from the base upwards and that interpolated dates have been placed at intervals that were not directly dated. Figure 4.23 exhibits four profiles, one set showing sedimentation and influx rates for the entire core and another showing the rates excluding the date at 102.5 cm. The profiles with the date at 100-105 (102.5) cm show a rate drop between 102.5 and 97.5 cm. While possible, this drop is probably not real, since the first human disturbances were determined to be higher in the core.

This decline between 102.5 and 97.5 cm suggests either the date at 102.5 cm, the interpolated date at 82.5 cm or the date at 192.5 cm is incorrect. The date at 82.5 cm is based on an increase in the Gramineae profile suggesting first cultivation around Quidi Vidi Lake. From MacKinnon (1981) the first farm in that area was developed around 1757. This Gramineae change also corresponds to a colour change noted in the stratigraphic column at 83 cm. The other two dates are based on ^{14}C and the dated material may have incorporated old C from the watershed, creating an artificially old date (Olsson, 1986).

It is reasonable to suggest the sedimentation rate from the base to 82.5 cm was probably relatively slow and uniform. When the date at 102.5 cm is dropped the profiles are smoother and probably more realistic. This suggests that the date at 102.5 cm is too old by about 290 years. This, however, is

contingent on the assumption there was no anthropogenic activity in the Quidi Vidi Lake area before 1757, that would have caused increased sediment input. No evidence from any data collected suggests this lake was directly subject to earlier anthropogenic influences.

Figure 4.23 shows a constant influx and sedimentation rate from the base to 82.5 cm (1757) where the rates are 0.005 g $cm^{-2}yr^{-1}$ and 0.036 cm yr^{-1}, respectively. Rates show the first sharp increases between 82.5 and 77.5 cm (1757-1776) increasing by approximately 6.8 fold over the basal rates. Up to 52.5 cm (1870) the influx rate nearly doubles to 0.0672 g cm^{-2} yr^{-1}, while the sedimentation rate remains constant. This difference is the result of a decline in the water content. Water content, which affects the sedimentation rate, declines through this interval.

Between 52.5 and 48.5 cm (1870-1900) both profiles show a sharp decline. The influx and sedimentation rates both drop by half (0.0347 g cm^{-2} yr^{-1} and 0.1340 cm yr^{-1}, respectively). Above 48.5 cm (1900) the profiles can be zoned into a number of different intervals. First, between 48.5 and 30 cm (1900-1958) the profiles show a large relatively uniform increase. The influx rate increases by a factor of 16 to 0.551 g cm^{-2} yr^{-1} while the sedimentation rate increases by a factor of 8 to 1.07 cm yr^{-1}. The influx and sedimentation profiles show a stable period between 30 and 25.5 cm (1958-1963) and a sharp

increase over a narrow interval between 25.5 and 23 cm (1963-1964). At this point the highest influx and sedimentation rates are observed at 0.823 g cm^{-2} yr^{-1} and 1.56 cm yr^{-1}, respectively.

Between 23 and 17 cm (1963-1969) the rates remain relatively constant and decline sharply to 9.0 cm (1979). Above 9 cm, the profiles increase to 7.0 cm (1981) and gradually decline to 3 cm. The influx shows a continued decline to 1 cm (1989), while the sedimentation profile shows a small increase.

Chapter 5: Discussion

5.1 - General Introduction

Sediment cores taken from lakes in St. John's record many types of change in their physical, chemical and fossil content. Each core and each type of record could be interpreted in different ways, which by themselves are ambiguous. Collective use of all data narrows the possible interpretations, and allows a well-constrained reconstruction of the history of environmental change, and its probable causes.

5.2. Presentation of geochemical data

Geochemical data can be displayed in numerous ways including concentration, influx rate and ratioed to a lithophilic element. No one format is best-suited to all data sets, and establishing which format best suits the goals of this study is imperative.

To illustrate the effectiveness of each data format for discerning anthropogenic impacts recorded in the lake sediment cores, selected elements are displayed in Figure 5.1 in different formats. Comparison of elements that represent very different processes and sources, such as Pb and Al, help to show the effectiveness of influx and concentration profiles. The concentration profiles for Pb and Al show two very

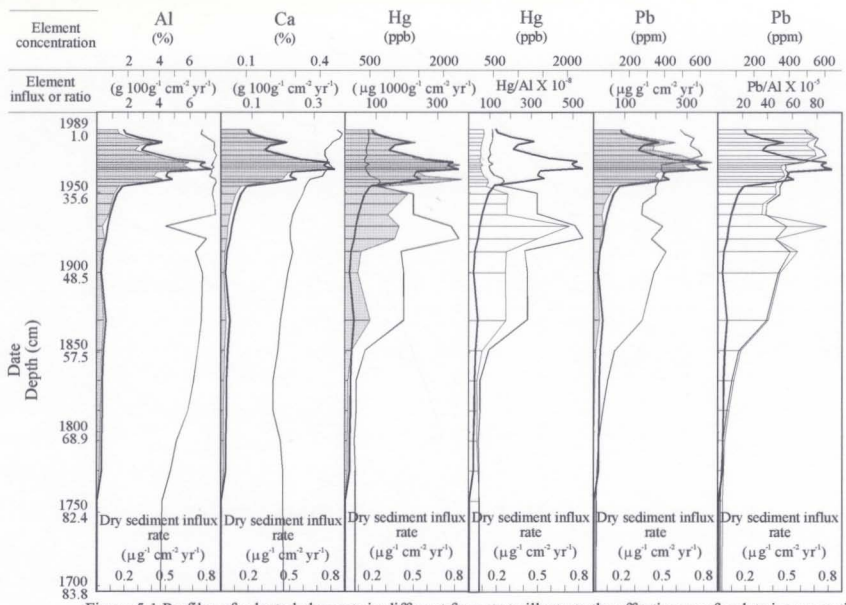

Figure 5.1 Profiles of selected elements in different formats to illustrate the effectiveness for data interpretation. The filled area is element influx, the unfilled area is element ratios, the thick line is sediment influx and the thin line is element concentration.

different trends for the last 250 years. From about 1750, Al shows a gradual doubling to about 1940 when constant levels are reached. Lead, however, shows several intervals of change including 1800 - 1850, 1850 - 1920 and 1963 - 1973, where the concentration profile shows large variations and increases.

In contrast, the influx profiles for both elements show very similar trends, mimicking the dry sediment influx profile. Upon close inspection the large relative changes displayed by the Pb concentration profile are present in the Pb influx profile, however, the relative magnitude of change is small and not easily detected in the influx profile. The dry sediment influx rate shows a very large increase (160 fold) from pre-disturbance levels, and thus when metal influxes are calculated the changes observed in the concentration profile are subdued. Thus, in this study the concentration profiles are more effective for displaying changes than influx profiles.

The dominating effect of variations in the dry sediment influx rate is also observed for elements believed to have a similar source, such as Al and Ca. Aluminum shows a continuous increase from 82.5 to 40 cm, while Ca shows no increase until 57.5 cm. Up to 57.5 cm Ca shows a steady decline from the basal samples. The influx profiles for these elements closely mirror each other, and the apparent difference displayed in the concentration profile is lost. Any interpretation based

solely on the influx profiles would overlook this potentially important difference.

The Hg influx profile displays a relative 'high' between 72.5 and 48.5 cm (1800 - 1900), which is also displayed in the concentration profile. Lead shows a similar high in the concentration profile, but the same feature is not so apparent in the Pb influx profile as in the Hg influx profile. The lack of relative prominence of this feature in the Pb influx profile is due to the larger relative increases of Pb in the upper section of core, which results is an apparent 'dampening' effect.

When ratioed to a lithophilic element such as Al, elements display a trend very similar to the concentration profile. This effect can be seen for both Pb and Hg in Figure 5.1. In both cases the Pb:Al and Hg:Al closely mirror the concentration profile for Pb and Hg, respectively. The spike observed in the ratioed profile is the result of an anomalously low Al concentration at that interval, and may well be spurious as it is not observed in the cores from Quidi Vidi Lake.

The examples above show that the concentration format is the most effective for interpreting change. The concentration profile does not, however, provide the whole picture. The dry sediment influx profile is also important for data interpretation. If, for example, a metal is being supplied at

a constant rate and the sediment influx rate is increasing, the end result is a concentration profile exhibiting a decline. This type of situation could be wrongly interpreted. Where the element is a component of the sediment matter, such as Al, K and Mg for example, increased sedimentation would not cause a 'diluted' concentration profile. Thus, the concentration profiles in conjunction with the dry sediment influx rate are most effective for interpolating anthropogenic impacts.

5.3 Chapter format

Discerning changes recorded in lake sediment is sometimes confusing, since a single element or a suite of elements can have many potential sources. At best, this type of study documents measured variations, that in most cases represent broad scale changes over time, rather than specific events. In an attempt to make this large data set meaningful, and at the same time manageable, this chapter is divided into two. The first half focuses on impacts related directly to physical disturbances of the natural landscape, such as forest cutting and farming. The second half focuses on impacts related to emissions from fossil fuel use, such as Pb from automobiles, which has little to do with landscape disturbances.

5.4 Record of impacts related to watershed soil disturbances

5.4.1 The Earliest Settlers

Discovered in 1497, Newfoundland's earliest history was one of a migratory population, based on a summer fishery. In an attempt to prevent permanent settlement, prior to 1790 houses in St. John's were not allowed to have attached chimneys (O'Neill, 1976). This edict did not, however, succeed in discouraging permanent settlement as the records show St. John's first resident settled in 1605. The migratory fishery declined after 1790, at which time the population of all of Newfoundland started to grow.

Upon examination of all data, it appears that charcoal may provide the first evidence for human disturbance of this area (Fig 5.2). Charcoal is observed in all samples from 87.5 cm (1630) and above, but only intermittently below 87.5 cm. The sample at 87.5 cm, is a composite of material between 90 and 85 cm loosely representing the interval between 1556 and 1690. The ubiquitous presence of charcoal at and above 87.5 cm suggests a constant supply, most likely from the combustion of wood as a fuel.

5.4.2 The dawn of farming

The growth of agriculture and denudation of the forests have been documented in section 1.7.1 of Chapter 1. The earliest farming near Quidi Vidi Lake started in 1757. Its spread continued until 1850 when agriculture was practised

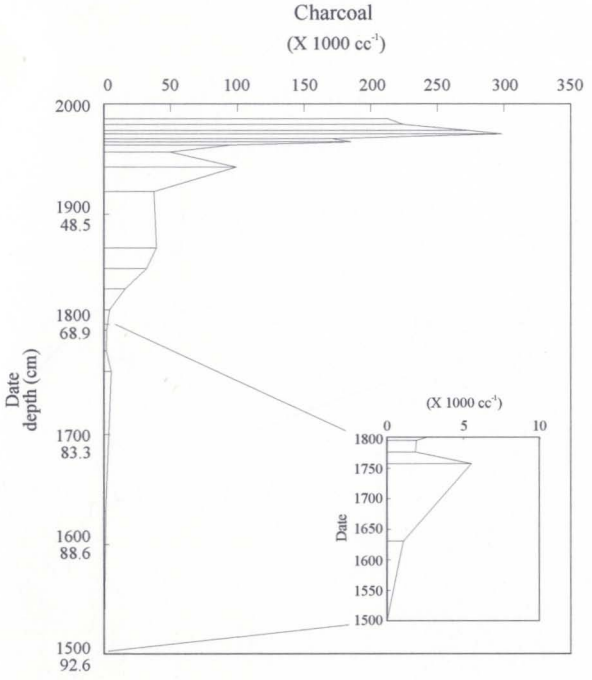

Figure 5.2 Charcoal in core QV2. The inset probably shows the earliest increases related to human use.

throughout the area now covered by the city (see Figure 1.5). Livestock and crop production grew to peak between 1911 and 1921, after which local production declined.

5.4.3 The Farming Era

The first major disturbance in core QV2 occurs at 82.5 cm (1757), where Principal Components (PCs) 1, 2 and 3 show increases from the basal trends. This corresponds to concentration increases in most lithophilic elements (majors), as LOI declines (Fig 5.3). Together with Si, which was not measured, the lithophilic elements and LOI make up a large fraction of the sediment, and thus the changes recorded at 82.5 cm suggests soil disturbance.

Elements such as Al, K, Mg and Na are constituents of most rock-forming and clay minerals. In the > 2 μm sediment fraction of core QV2, albite ($NaAlSi_3O_8$) and quartz (SiO_2) were dominant, while in the < 2μm fraction illite and chlorite ($Mg_{0.7}Al_4(Si_6Al_2)O_{20}(OH)_4$) were dominant. Between 87.5 (1630) and 77.5 cm (1776), XRD count data double for illite, chlorite, quartz and albite; suggesting at that time there was an increase in the quantity of clastic input, compared to the period represented in the basal section (Fig 5.4).

Coincident with changes in the sediment composition are changes in the pollen assemblage as seen in pollen subzone 2ai (Fig 5.5). Increases in Gramineae and corresponding declines

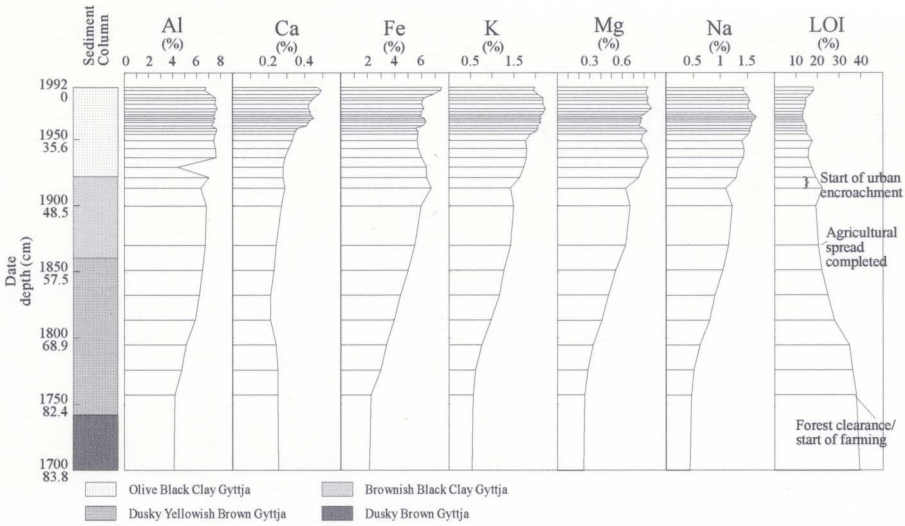

Figure 5.3 Selected lithophilic element concentration profiles (Al, Ca, Fe, K, Mg, Na and LOI) from Principal Component 1, core QV2

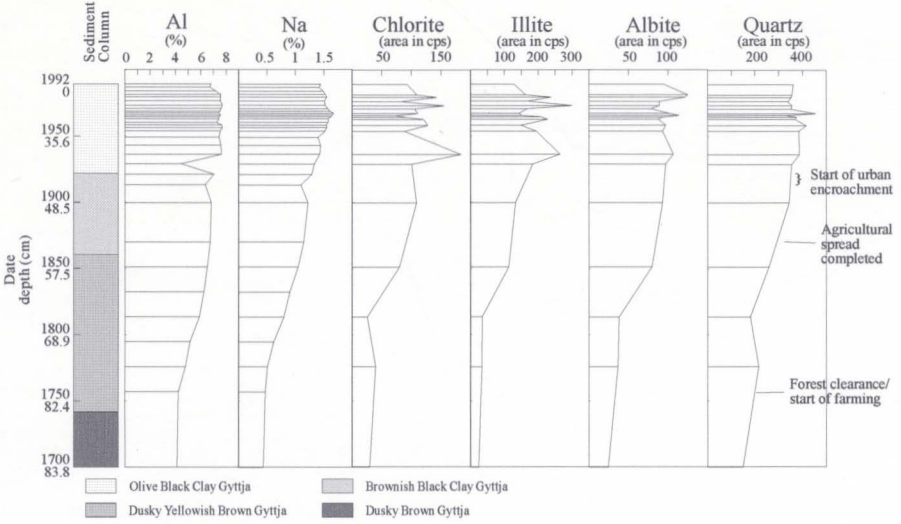

Figure 5.4 Clay and mineral XRD data, Al and Na concentrations from core QV2.

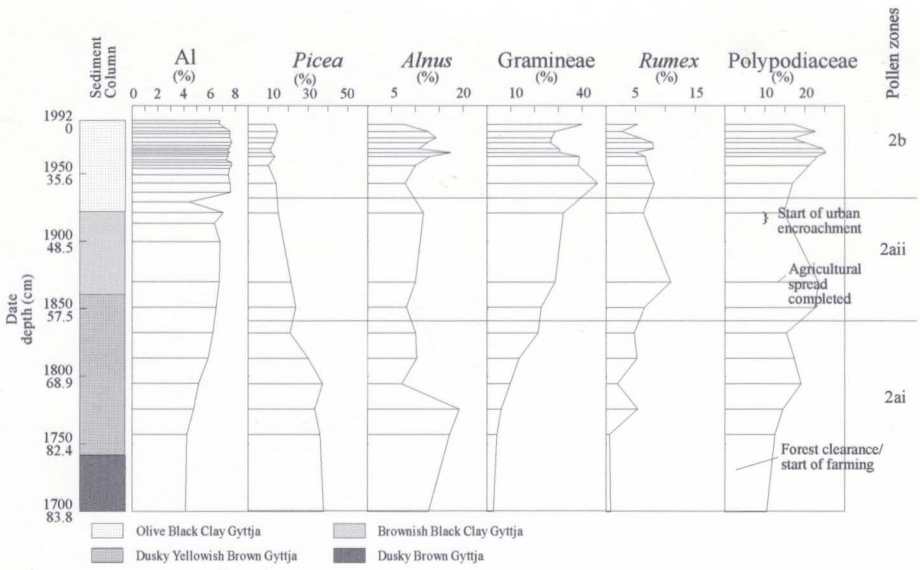

Figure 5.5 Selected pollen percentage profiles and Al concentration profile from core QV2.

of arboreal pollen at about 82.5 cm (1757) indicate opening of the forest canopy. Increases in shrubs (*Alnus*), ferns (Polypodiaceae) and European weeds (*Rumex*) in subzone 2ai provide further evidence for clearing.

Simultaneous changes in vegetation assemblages, lithophilic element concentrations, clay and mineral fractions indicate deforestation and the inception of agriculture near Quidi Vidi Lake. A sediment colour change at 83 cm in core QV2, may mark most closely the first impact of early agriculture. According to MacKinnon (1981) agriculture near Quidi Vidi Lake started around 1757.

5.4.3.i Lithophilic composition of sediment through the main farming era

The lithophilic elements from PC1, including Al, K, Mg, Na, Ti and Fe show increases up to the peak of agricultural production between 46 and 44 cm (1911 - 1921), and beyond in some cases (Fig 5.3). Concentration profiles for Al, Na and Ti show steeper increases during the early part of the farming period, suggesting greater relative impacts on lake sediment chemistry with the earliest soil disturbances. Iron, on the other hand shows a linear increase from 82.5 to 46 cm (1757 - 1913), suggesting its lake sediment concentration was controlled, in part, by other factors.

The Ca concentration profile differs from the other

lithophilic elements through the main farming era. Calcium shows a continued decline up to 62.5 cm (1832), carrying over from the decline recorded in the basal section. Above 62.5 cm Ca increases gradually to 28 cm (1960) (Fig 5.3). The geology and soils in this area contain low levels of carbonate, which might explain some of the concentration profile (Heringa, 1981). The XRD data reconfirm low Ca levels in both the dominant clay and mineral fractions, which are Na-Al-Mg-K based.

The section of core inferred to date between 1757 and 1869 (the oldest ^{210}Pb date) probably does not correctly reflect the nature of early soil disturbances. Initial forest clearance and subsequent farming may have caused an early peak in sediment influx, much as Dearing (1991) illustrated from other studies. Evidence to suggest an early episode of soil erosion into Quidi Vidi Lake might be observed in the pollen and spore count profile and influx profiles for *Picea*, *Betula*, *Alnus* and Gramineae, all of which peak at 62.5 cm (1832) (Fig 5.6). This feature may represent washing of previously deposited pollen in the watershed soils, as a result of intense soil disturbances.

5.4.3.ii Pollen percentages through the upper farming interval

The Gramineae increase and the *Picea* and *Abies* decline through pollen subzone 2aii to 38 cm (1943) points to

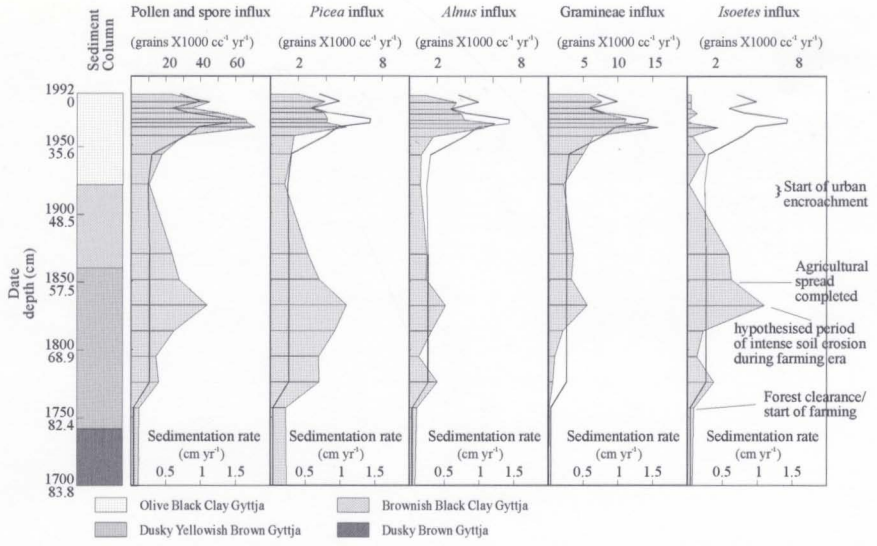

Figure 5.6 Pollen influx profiles showing the influx peak at about 1830. This peak may represent an early intense period of soil erosion. The shaded area is the pollen influx and the line is the sedimentation rate.

continued encroachment of land clearance into forested areas. Neither the Gramineae percentage nor influx profiles correspond to the peak of crop production between 1911 and 1921 (Figs 5.5 and 5.6). The Gramineae increase above 44 cm (1921) may reflect land abandonment and succession of grasses into open areas. This hypothesis supported by data from MacKinnon (1991) who noted that more than 5000 acres of cultivated land was abandoned in St. John's between 1911 and 1935.

5.4.3.iii Clay through upper farming interval

The XRD data shows the four major components increasing up to 40 cm (1935) (Fig 5.4). Above 40 cm the XRD data fluctuate, but do not show any overall change. These observations are consistent with abundances for most of the lithophilic elements of PC1. The lack of change above 1930-1940 suggests that some critical point was reached where, in known periods of more intensive erosion, sediment influx did not alter the relative levels of clay and mineral fractions, or lithophilic element concentrations in the lake sediment.

5.4.3.iv Lacustrine impacts associated with farming (1757-1949)

Lacustrine impacts associated with forest clearance and the establishment of agriculture are inferred from the diatom

and aquatic spore (*Isoetes*) data. The only sample examined for diatoms during the farming era was at 74 cm (1790). It indicated an inferred lake water pH of 6.40, well within the natural background range defined in the two basal samples (6.28 and 6.47) (Fig 5.7). With poor error control and a reconstructed pH based on data from another location, the reconstructed pH values for Quidi Vidi Lake may reflect the direction of change more accurately than the magnitude of change.

All diatom taxa, except *Tabellaria flocculosa*, show little or no change from the base of the core (Fig 4.6). Although the increase of *Tabellaria flocculosa* is a linear projection from the basal two samples, percentages double suggesting a possible anthropogenic influence rather than a natural phenomenon, although this change may be due totally to natural conditions. In as much as the ecological significance of this increase is unknown, work by Kingston et al., (1990) suggests it could represent increased humic acid levels. This situation could arise with increased flushing of organic matter from tree felling and agriculture (Vuorela, 1980). The percentages of Centrales and Pennales, however, do change from the basal section to 74 cm (1790), suggesting that while early farming may not have affected the lake pH, it may have started to affect the composition of the diatom community.

Isoetes, a submerged aquatic plant, is an effective

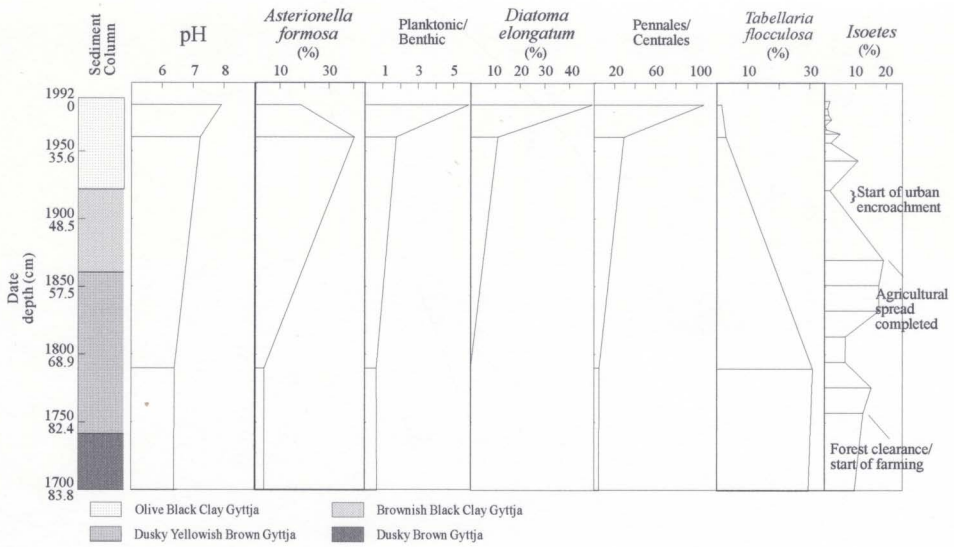

Figure 5.7 Diatom reconstructed pH, selected diatom species, morphological and ecological data and *Isoetes* from core QV2

lacustrine indicator of local human disturbances (Vuorela, 1980). Vuorela showed data from several UK watersheds which suggested that increases of *Isoetes* mark incipient clearance or cultivation. *Isoetes* thrives only within an optimal range of mineral matter accumulation. Intense mineral accumulation, changes in lake water pH or taxa competition can cause a decline in abundance.

In core QV2, *Isoetes* shows high percentage abundance in pollen subzone 2ai, during early forest-agriculture disturbances, but declines between 77.5 and 72.5 cm (1775 - 1794) into subzone 2aii (Figs 4.1 and 5.7). This decline occurs when the diatom-reconstructed lake pH showed no measurable change from pre-European levels, suggesting other reasons for its decline possibly including excess sedimentation or a flora-fauna competition. Flora-fauna competition, for example, may have come in the form of diatom growth on the *Isoetes* plant, causing its decline. Throughout the remaining farming era, *Isoetes* is the only aquatic indicator. Relatively high percentages between 62.5 and 52.5 cm (1832 - 1870) indicate lake conditions were optimal for *Isoetes*. The subsequent decline suggests species stress due to changing conditions.

Although phosphorous in sediment has been used as a tool for measuring the trophic status of lake water, numerous studies have shown it that does not reflect the history of a

lake's trophic state, but rather is closely controlled by Fe, Mn and clay sorption (Bortleson and Lee, 1974, and Brugam, 1978b, Engstrom and Wright, 1984). In QV2, the P concentration profile does not pin-point specific periods of high trophy, even during known times of sewage pollution (see Fig 3.3). The featureless profile suggest P is not applicable for measuring lake trophy in this case, and its sedimentation is probably controlled by other factors.

5.4.4 Suburban/urban development

MacKinnon (1981) noted that rapid urban encroachment upon farmlands began after 1911, as most of the city remained between the harbour and the crest of Freshwater Hill up to 1900 (see Fig 1.2). Significant urban growth started between 1911 and 1921, and gradually declined to around 1945 - 1950. About 1945 the population increased abruptly, suggesting the start of major urban development (see Fig 1.6). City development was faster and more extensive after Confederation (1949) as St. John's became the leading government and services centre.

5.4.4.i Sediment influx through the urban era

The sediment influx through most of the farming era was interpolated (between 1757 - 1870), and thus few changes can be recognized to 52.5 cm (1870) (Fig 5.8). The influx rate is

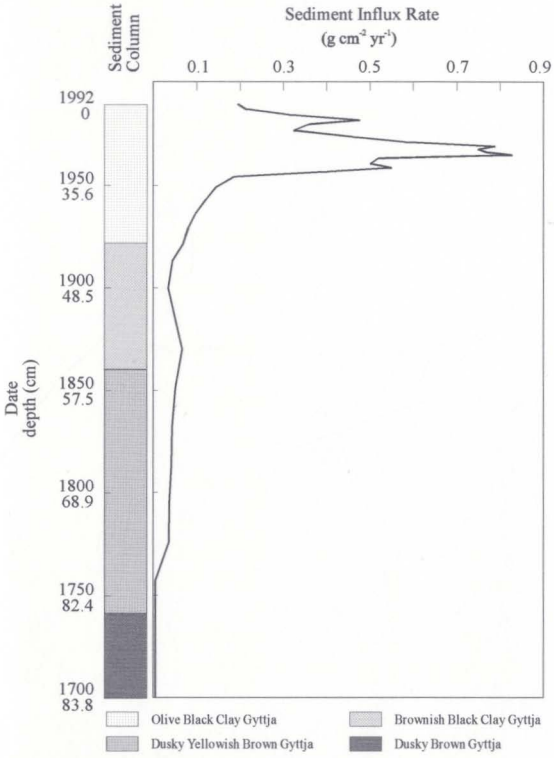

Figure 5.8 Dry sediment influx profile for core QV2.

constant between 52.5 and 46 cm (1870 - 1913), but shows a continuous increase between 46 to 34 cm (1913 - 1954). This increase occurred through urbanization as the city grew steadily, spreading to the Long Pond area. Most of the construction during that time was of a residential type, except Fort Pepperrell, built in 1941, on the north banks of Quidi Vidi Lake. The sediment influx profile, however, shows no discernable impacts related to this large military development.

After Confederation, rapid growth of the city is evident from the sediment influx profile. Between 34 and 32 cm (1954 - 1956) the sediment influx rate doubles. This short interval probably reflects intense residential sub-division development along the Rennies Mill River Valley, above Quidi Vidi Lake. The abrupt dry sediment influx increase indicates the impact was large and possibly unimpeded. Unimpeded erosion would result from the removal of the natural vegetation cover, and construction of roads, parking lots and storm sewers. Storm sewers probably played an important role allowing instantaneous run-off of material to streams and lakes. This, of course, would be most intense during construction, until some point when the urban landscape was transformed into a blanket of concrete, pavement and lawns.

The influx rate remained steady to 25.5 cm (1963), but increased abruptly between 25.5 and 23 cm (1963 - 1965),

implying another period of intense construction. Residential construction rates for the city doubled between 1960 and 1963, and again between 1965 and 1966 (Fig 5.9). Between 23 and 17 cm (1965 - 1969), the influx rate remained very high, and shows the single most intense period of watershed disturbance recorded in Quidi Vidi Lake. Figure 1.2 shows that much of the area north of Quidi Vidi Lake was developed after 1961, during these periods of intense sediment input.

Above 17 cm (1969) the sediment influx rate declines to the top of the core. The decline suggests most of the construction of city infrastructure was completed in this catchment. There is no obvious explanation for a small increase in sedimentation at 7 cm (1982), but it may reflect developments near either Long Pond or Virginia Lake.

5.4.4.ii Chemical profiles through the urban era

Lithophilic elements from PC1 show little concentration change above 38 cm (1943) as farming declined and city development increased. Calcium, K and Na do, however, show continued increases from the farming era to peak between 28 and 15 cm (1960 - 1970), during which time LOI declines to its lowest levels (Fig 5.3). It is unclear why Al, Fe and Mg increase only to about 1940, whereas Ca, K and Na concentrations increase to about 1960-1970. One possibility might lie in the geochemical variability of the watershed

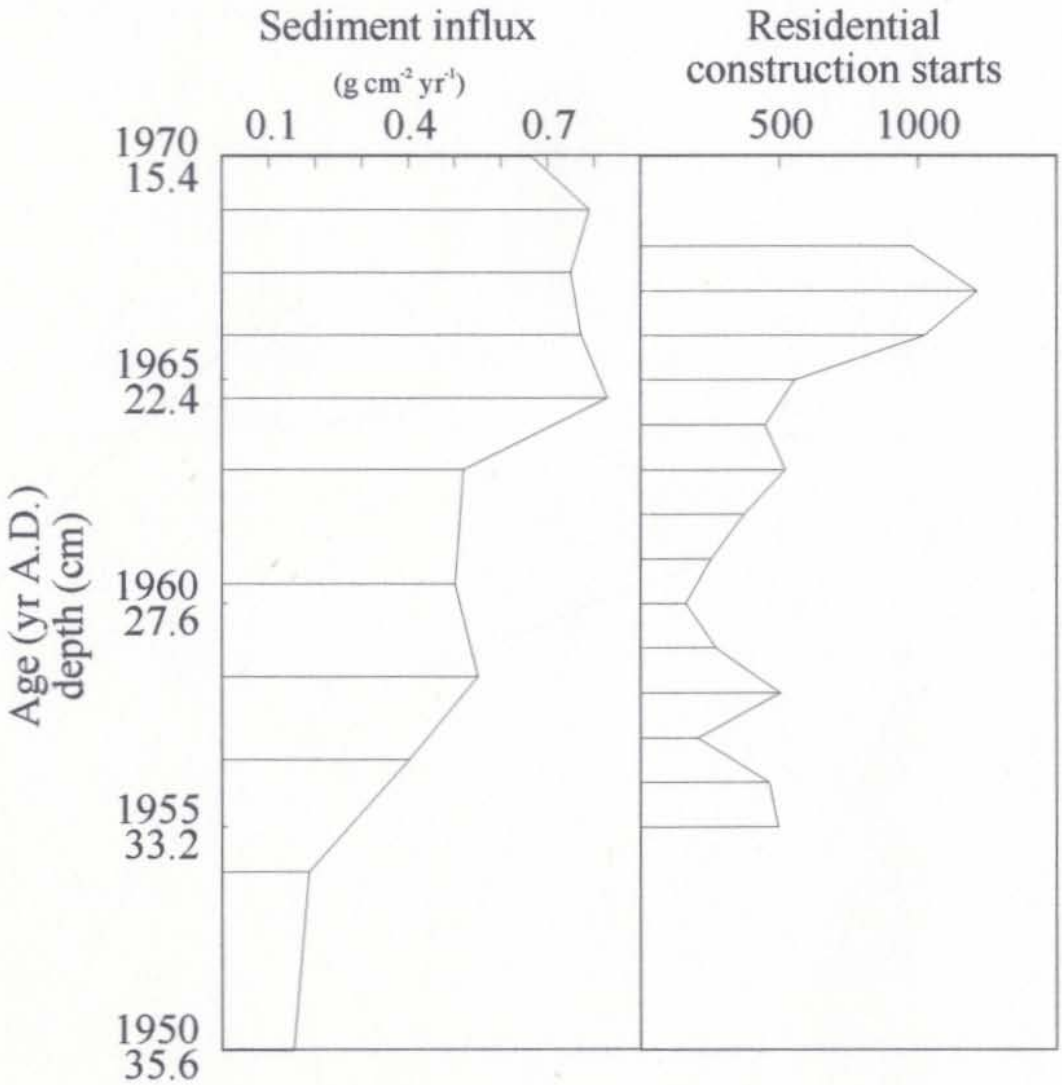

Figure 5.9 Dry sediment influx for core QV2 and residential construction starts in St. John's for the interval between 1950 and 1970. (Source: Newfoundland Statistics of Newfoundland and Labrador, 1981).

soils, which would be selectively disturbed as the city grew. Basal concentration profiles for the urban lakes and Georges Pond show a variety of geochemical signatures from lake to lake, suggesting the soil composition, which is controlled by the underlying bedrock, varies slightly throughout the city (Fig 5.10).

Of the lithophilic elements, Ca deviates the most, exhibiting increases through the sediments deposited during the urban era. Increases observed in the Ca profile, and particularly between 34 and 25.5 cm (1954 - 1963), show a strong empirical relationship to increases in the dry sediment influx (Fig 5.11). This relationship is not observed for the other lithophilic elements. Mackereth (1966) and Bortleson and Lee (1974) suggest Ca concentrations increase during periods of high sedimentation rates, which prevents leaching of $CaCO_3$ from sediments. Their study areas, however, are carbonate rich, unlike the St. John's area.

In core QV2 above 15 cm (1971), where the dry sediment influx declines, Ca shows a continued increase. The other lithophilic elements, except Fe, show little change above 15 cm. As the other lithophilic elements show little change, this Ca increase suggests anthropogenic additions of Ca. One potential source of Ca is liming, which may have come from liming and fertilizer used on the golf course along Virginia River (Bally Hally Golf course), as well as on lawns around

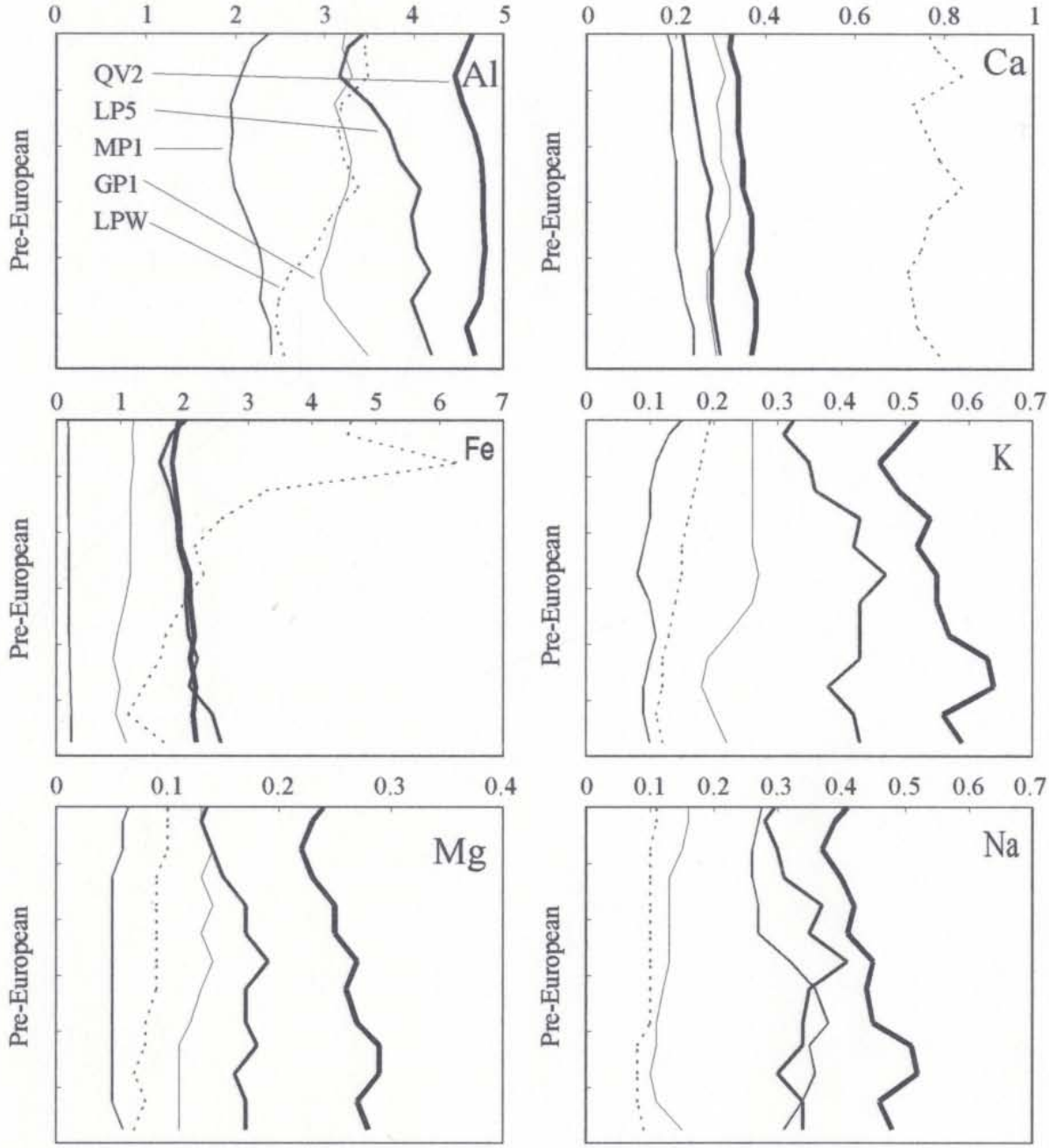

Figure 5.10 Pre-European concentrations of lithophilic elements for the five sampled lakes. All concentrations are in percent.

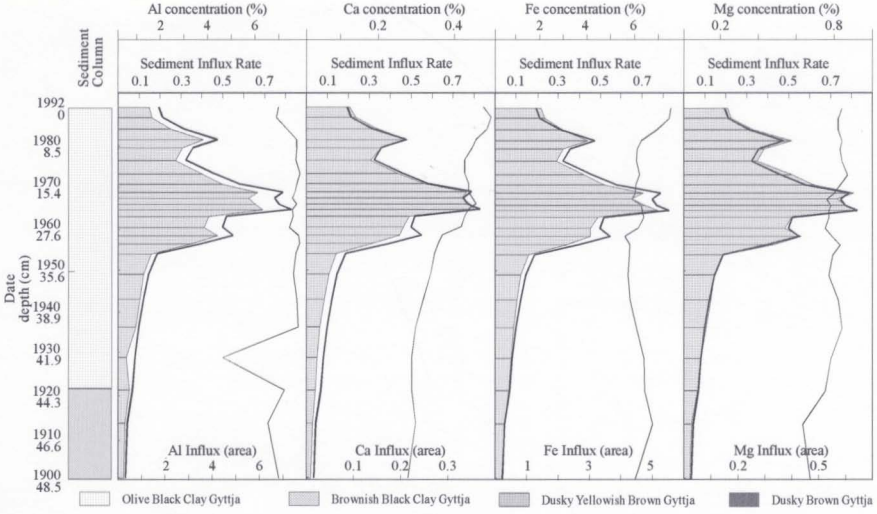

Figure 5.11 Influx and concentration profiles of selected elements and dry sediment influx rate from core QV2. The filled area is the element influx, the thin line is element concentration and the thick line is sediment influx. Sediment influx units are g cm^{-2} yr^{-1} and g $100g^{-1}$ cm^{-2} yr^{-1} for the element influx.

the military base.

Another possible anthropogenic Ca source is concrete. The dissolution of concrete could add Ca to the lake water, some of which may get deposited in the lake sediment. In the last 50 years the amount of concrete in the watershed has increased sharply. Addition of 'exotic' construction material from outside the watershed could also play a role introducing materials selectively enriched in certain elements, such as Ca. However, neither the XRD nor the chemical data identify any obvious 'exotic' construction material.

5.4.4.iii Pollen changes through the urban era

Since most forest cover was removed during the farming era, arboreal pollen percentages are low throughout the urban period. Above the Gramineae peak at 38 cm (1943), Gramineae percentages steadily decline to 13 cm (1973) (Fig 5.5). This decline coincides with the most intensive period of city development, and thus probably reflects city encroachment upon abandoned fields. The slight increase above and after 13 cm (1973) may be result of the establishment of urban lawns and grass along the river channels.

5.4.4.iv Lacustrine Impacts associated with urban sprawl

The increase in the lake water pH observed in Quidi Vidi Lake is one of the most obvious lacustrine impacts of urban

sprawl. The pH increased to 7.2 and 7.9 between 28 and 5 cm (1960 - 1984), respectively (Fig 5.7). No diatom samples were examined in the section of core between 74 and 28 cm (1790 - 1960); thus it is impossible to determine if most of the pH increase occurred before or after urban development. This pH increase over the last 30 years is contrary to trends observed in remote Newfoundland lakes, which show recent acidification (Scruton et al., 1990).

As previously stated, the reconstructed lake water pH for Quidi Vidi probably shows the direction of shift more accurately than actual change. Nevertheless, other pH data from local studies suggest the reconstructed values have some degree of validity. One time pH readings such as 7.36 in Kenny's Pond (Gibson and Haedrich, 1988), 7.2 in Long Pond (O'Connel and Andrews, 1976), 7.4 and 9.4 in Leary's Brook (McCallum, 1981) and 7.65 in Virginia River (Gibson, Unpublished data 1983) span the reconstructed pH range in 1960 and 1984 from Quidi Vidi Lake.

The high pH levels in Leary's Brook may provide evidence for the high reconstructed values at 1960 and 1984. *Diatoma elongatum*, which has high representation in the 1960 and 1980 samples, suggests high Cl^- and pH (8.45) conditions. One-time blooms of this taxa from either winter road salt practices or chemical spills such as ammonia, would result in a high reconstructed pH. By removing *Diatoma elongatum* from the

reconstructing calculations, the 1984 pH for Quidi Vidi becomes 7.1, more consistent with measured water data.

The pH increase in Quidi Vidi Lake implies an alkalinity increase in the lake water. This hypothesis is supported by Blake (1992) who showed that levels of Ca (> 7.8 ppm) and Mg (2.2 ppm) in the urban lake water, are amongst the highest on the northeast Avalon Peninsula. Emissions of potentially acidifying agents within the urban setting, from fossil fuel combustion for example, should lead to lake acidification. There is strong evidence for increase SO_4^{2-} from acid deposition in the urban waterways as highlighted by Blake (1992), who showed SO_4^{2-} levels in the urban lakes at 5 times higher than background. The reconstructed lake water pH values, however, suggest the urban lakes show little effect of high acid deposition, thus pointing to a high buffering capacity. Low metal levels in a limited analysis of brown trout in Leary's and Virginia Brooks (Gibson, unpublished data, 1983, Dept of Fisheries and Oceans) also point to enhanced buffering. A high buffering capacity would make metals less bio-available, despite the higher levels found in sediment. The increase in buffering capacity is probably due to a number of factors. One potential buffering agent, already identified, is concrete, a source for Ca and Mg. Dissolution of Ca and Mg from concrete would cause an increase in carbonate levels in the urban lakes. Most of the concrete

structures in the Quidi Vidi Lake watershed were built after 1949, coincident with the pH changes documented in 1960 and 1984.

The diatom, *Asterionella formosa*, points to another impact of urbanization. *Asterionella formosa*, which peaked at 28 cm (1960), is a marker for increased productivity (Pennington, 1981). Sources include sewage inputs (Brugam, 1978a) and increased P loadings (Dearing and Foster, 1986). Documented and anecdotal evidence indicates Quidi Vidi Lake received raw sewage during the late 1940s and early 1960s (Bland, 1946 and Mr Robert McNealy, pers. comm.) Thus, the 1960 peak probably reflects a period of domestic sewage input, which has since declined.

5.4.5 Farming and urban growth in Mundy Pond and Long Pond

Forest clearance and agricultural impacts observed in Quidi Vidi Lake are also observed at Long Pond and Mundy Pond. These impacts include; increased Gramineae pollen, a decline in tree pollen, increased lithophilic element concentrations and a decline in LOI (see Figs 4.2 and 4.4).

The increased lithophilic element concentration, in association with forest clearance and agriculture in Long Pond and Mundy Pond, is less in magnitude than that observed in Quidi Vidi Lake (see Fig 5.12). This difference may lie in the timing, quantity and location of cultivated lands. The larger

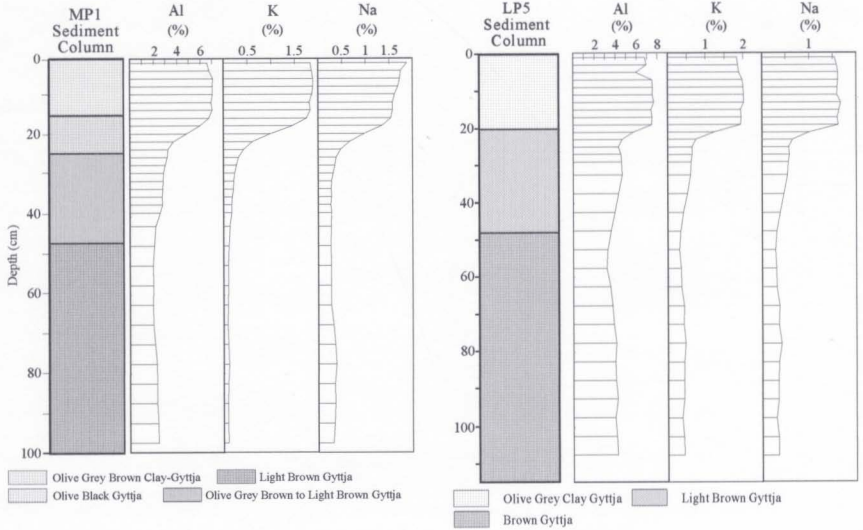

Figure 5.12 Sediment columns and selected concentration profiles from cores MP1 (left) and LP5 (right). The sharp sediment and concentration changes at about 20 cm are probably post-1950.

watershed of Quidi Vidi meant it was susceptible to greater agricultural impacts than the other urban lakes. Most of the farmland affecting Quidi Vidi Lake was upstream from the outset. In the Long Pond and Mundy Pond areas, however, agricultural development occurred much later, and most development was adjacent to or down drainage. Thus, the impacts from farming and forest clearance for these lakes were less in magnitude and occurred much later than that recorded in Quidi Vidi.

Increases in lithophilic elements in Mundy Pond and Long Pond occurring in the upper 25 cm, are associated with sharp sediment changes (see Fig 5.12). Lithophilic element concentrations in Long Pond begin to increase at about 23 cm and continue to about 17 cm; these coincide with a pronounced sediment change at 20 cm. Although ^{137}Cs activities between two different lakes may or may not be directly correlated, using comparative ^{137}Cs activity levels from Quidi Vidi Lake, 19 cm in Long Pond is close to 1963, while 32.5 cm is pre-1954. These dates coincide with a watershed history which tracks urban construction after 1955. Similar increases in Mundy Pond occur between 25 and 15 cm.

5.5 Element signatures of fossil fuel emissions

5.5.1 General introduction

While the watershed soils are the dominant contributor to

the lithophilic element composition of the lake sediment, the same cannot be said for some of the minor elements. Lead, for example, shows a 30-fold increase from basal levels, compared to a 4 or 5-fold increase for the lithophilic elements. Thus, additional sources, processes or activities must have contributed material selectively enriched in certain elements.

By-products from the combustion of fossil fuels seem to be the largest contributor of metals to lake sediment in St. John's. Fossil fuels including coal, gasoline and fuel oil are or were used in manufacturing, transportation and heating. The following section is a short summary of the historical use of fossil fuels, and emissions related to these uses. This will provide an understanding of how these uses relate to the geochemical data.

5.5.2 Emission signatures for fuel use in St. John's

The historical use of fuels can be partially reconstructed from charcoal, soot, heavy metal and lead isotopic profiles. Charcoal particles are probably the first indicators of anthropogenic impact recorded in Quidi Vidi Lake. Thus, up to 1803, the year of the first documented coal import into Newfoundland (Head, 1976), wood was probably the only fuel.

Soot, a by-product of coal combustion, was emitted from manufacturing industries and residential premises. Soot,

sometimes called fly ash or spheroidal particles, is composed of small (generally < 30 μm in this study) opaque spheres that may contain high levels of heavy metals (Block and Dams, 1975; 1976; Davison et al., 1974).

Presumably, coal became an important fuel shortly after its introduction, and with the establishment of industry in the 1840's coal consumption grew immensely. Coal was extensively used for residential heating until oil furnaces became popular in the late 1950s and early 1960s. Atmospheric pollution attributed to coal use was evident through time. A public health commission in 1910 noted the polluted city air was unhealthy for the ill (Zierler and Nustard, 1982). Mr. Robert McNealy (pers. com.) remarked that pollution from coal combustion in the 1950's was so dense at times that it was difficult to see across the harbour from Freshwater Hill, a distance of 2 km.

Use of leaded gasoline in motor vehicles certainly played a major role in the deposition of heavy metals, particularly Pb. Leaded gasoline has been available in Canada since 1926 (Royal Society of Canada, 1986), but according to Mr. Bob Faulkner, it was not widely used until after WWII (Irving Oil Ltd., pers. com. 1993). Leaded gasoline contains a lead isotopic ratio, representative of the lead ore body from which the lead was mined. If the ratio is sufficiently different from the natural ambient ratio, then recognition of exotic

anthropogenic lead deposition is possible. Many times, however, tetraethyl lead producers obtained lead ingots from various suppliers resulting in a mixed gasoline signature. In addition to this, other anthropogenic inputs cause a further mixing making identification of specific sources difficult.

5.5.3 Impacts discerned from heavy metals concentrations

5.5.3.i Impacts discerned form Pb changes

The initial rise of lead that occurs at 82.5 cm (1757) is coincident with the establishment of agriculture around Quidi Vidi Lake (Fig 5.13). This relationship suggests the earliest lead increase was a result of increased Pb deposited from watershed soils, rather than an outside or exotic source.

In an attempt to identify the first excess lead in Quidi Vidi Lake sediment, the following equation was used;

$$Pb_{excess} = totalPb_x - [Al_x / Al_{bkg}] * [Pb_{bkg}]$$

Where;

Pb_{excess} : is the anthropogenic Pb concentration
total Pb_x : is the total Pb concentration at depth X
Al_x : is the concentration of Al at depth X
Al_{bkg} : is the average Al concentration through the basal 100 cm
Pb_{bkg} : is the average Pb concentration through the basal 100 cm

This procedure assumes a uniform natural ratio of Pb to Al in the catchment soils. This is an oversimplification which

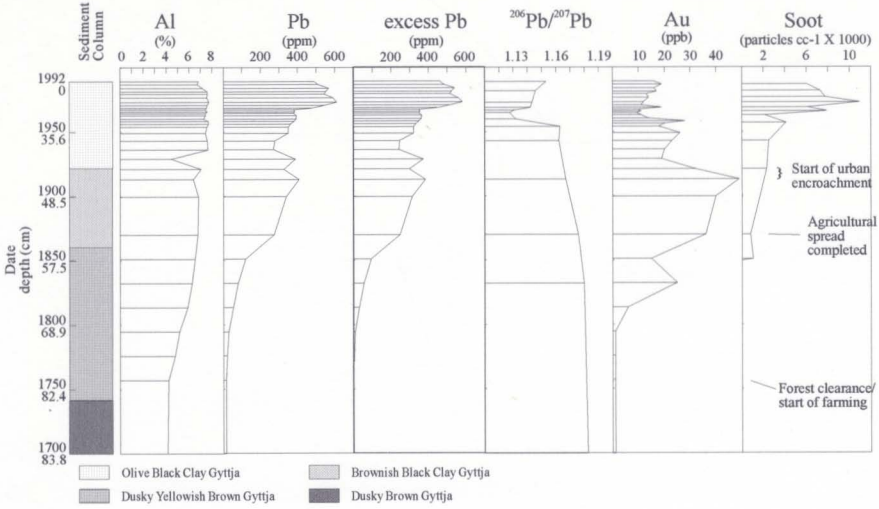

Figure 5.13 Al, Au, Pb, lead isotopic data, excess lead and soot profiles from core QV2.

precludes pin-pointing the exact depth of the first excess lead. The first evidence for excess lead (9 ppm) occurs at 72.5 cm (1795), accounting for 31% of the total lead in that sample (Fig 5.13).

Isotopic ratios from Quidi Vidi Lake and Long Pond, Witless Bay Line, indicate a very uniform natural isotopic ratio for this area. The three basal samples from each lake, all of which are pre-European, show a very small range (1.1863 - 1.1891), averaging 1.1872 and having a standard deviation of 0.0009 (see Fig 3.10 and 3.11). Data from these lakes, located 30 km apart and in similar geology, suggest that changes to the Pb isotopic ratios are effective for evaluating exotic leads in this area.

Lead isotopes provide the first conclusive evidence for exotic lead at 62.5 cm (1832) (no data are available for the interval between about 1100 and 1832). The $^{206}Pb/^{207}Pb$ ratio at 62.5 cm shows a decline from the basal signal defined by the bottom three samples (see Fig 3.10 for the full profile and Fig 5.13 for the profile above 1700). The calculated excess Pb at this depth is approximately 56 ppm (70% of the total lead). Hamilton and Clifton (1979) in a core from Bristol Channel, observed a similar trend, dated between 1850 and 1870, which was attributed to coal combustion associated with the Industrial Revolution. Establishing conclusively that the first exotic lead deposited in Quidi Vidi Lake occurred at

62.5 cm (1832), when there were presumably few settlers in the watershed, suggests the Pb was transported to the lake as airborne pollution. This pollution was probably from coal combustion within the urban core, which then was adjacent to the harbour.

Contemporaneous concentration increases for a suite of elements from PC1 and PC4 including As, Au, Hg, Pb, Sb and Zn, as well as soot, suggest a potentially common source tied to the Pb isotopic shift (Figs 5.13 and 5.14). This metal association has been attributed to coal combustion by other authors, including Block and Dams (1975, 1976) and Davison et al., (1974). Gold is unique in that coal was probably the largest anthropogenic source of this metal in St. John's, if not the only one. Gold in core QV2 first occurs above detectable levels at 67.5 cm (1813). This is in close agreement with the first excess Pb at 72.5 cm (1795), the first isotopically distinctive Pb at 62.5 cm (1832) and records for the first coal shipments to Newfoundland (1803) (Prowse, 1895).

The timing for the first appearance of soot, when there were few people living in the watershed, also suggests an airborne source, originating from coal combustion along the harbour area. It is unclear why no soot particles were observed below 57.5 cm (1851), when presumed by-products from coal combustion began to increase, including heavy metal

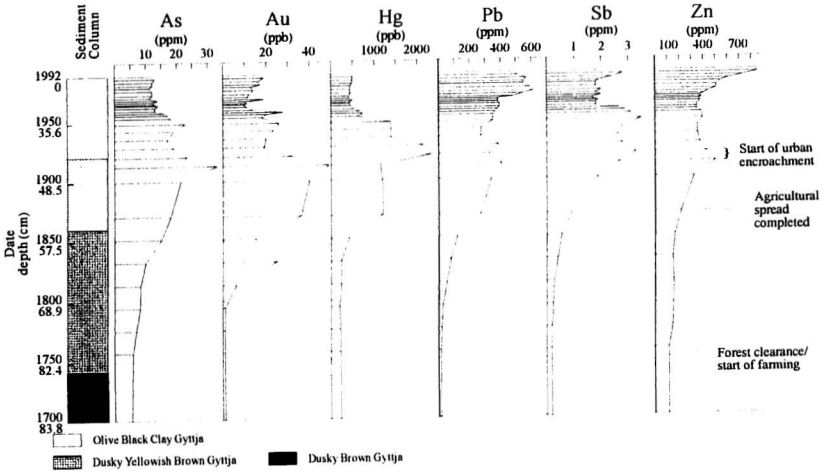

Figure 5.14 As, Au, Hg, Pb, Sb and Zn profiles from core QV2 showing elevated metal levels from coal combustion.

levels (1795) and the first lead isotopic changes (1832). An explanation for the late appearance of soot might be related to the cut-off size of the particles counted or to the concentration in the sediment; in the earliest coal combustion period its concentration may have been too low and particle too small for detection during pollen counts.

Heavy metals linked to coal combustion exhibit increases which start at different depths. The most notable is Zn which shows no discernable increase above background until 52.5 cm (1870), and much later than the other metals (Fig 5.14). Kingston et al., (1990) note that increases of Zn in lake sediment lag behind Pb, partially because of higher background levels damping the relative change from additional inputs. This is similar in Quidi Vidi Lake; the background level of Zn is about 120 ppm compared to Pb which is about 15-20 ppm. Kingston et al., (1990) and Tessier et al., (1989) also suggest the lag in Zn could be related to lower pH levels, inhibiting partitioning of Zn into the sediment from the water.

The 'heavy' metal association thought to be derived from coal emissions, shows increases starting about 62.5 cm (1832) and peaking between 48.5 and 44 cm (1900-1921), in the so called 'coal peak'. The Pb isotopic data at 46 cm (1913) shows continued declines from ratios recorded at 52.5 cm (1870), confirming a greater relative amount of exotic Pb, most likely

from coal emissions. In this 'coal peak' a pronounced shift in heavy metal peaks suggest differing sources for coal. Gold peaks at 48.5 cm (1900) and drops sharply to 46 cm (1913), while Hg increases sharply through the same interval (Fig 5.14). This departure in the Au and Hg profiles may suggest a change to coal which is relatively enriched in Hg.

Although this peak between 1900 and 1921 has been attributed to coal by-product inputs, other sources for these metals are possible. Lead, for example, may be derived from leaded paint, lead pipes or other sources of lead that were more commonly used in the past. Coal combustion and the resultant increased atmospheric acidicity likely caused increased metal leaching thus contributing to increased lead loadings from other sources such as paint, for example. Tanneries, of which there was at least one and possibly two in the Quidi Vidi Lake watershed probably contributed to metal loadings, although it appears that the life-span of these tanneries in this watershed was limited to about 10 to 15 years between 1908 and 1920 (Joy, 1977 and St. John's City Directory, 1908-1909, 1913, 1919). Other industries, household materials, insecticides and fungicides all could have contributed metals to the lake sediment during this time. Most industries, however, were located along the waterfront for all of St. John's history. Most of the population base for St. John's lived outside the Quidi Vidi Lake watershed until

between 1911 and 1921 when settlement started in earnest. In addition, there appears to have been little regard for the environment throughout the history of St. John's. Although these factors alone do not account for all the possible metal sources, it does suggest that they had little influence on the lakes environment during the 1900 - 1920 interval. Other sources for metals cannot be ruled out or eliminated, but there is more evidence to suggest this peak at depth is at least in part related to coal combustion.

The concentrations of As, Au, Hg and to some extent Zn all decline above this 'coal peak', up to approximately 28 cm (1960). This decline is unexpected since coal was extensively used until oil furnaces became popular in late 1950s and early 1960s. The observed decline could be the result of sediment dilution with increased sediment input. The sediment influx between 46 and 36 cm (1913-1949) increases 2.7 fold, and even more sharply to 28 cm (1960), increasing 2.5 fold from the rate at 36 cm (1949).

Above the 'coal peak' Pb and Sb show a decline between 44 and 40 cm (1921 - 1936), similar to the other metals, but unlike the other metals they increase sharply between 38 and 36 cm (1943 - 1949) (Fig 5.14). This increase as other heavy metals decline suggests an additional source for Pb and Sb, and perhaps from sources other than coal. The isotopic data suggests that there were no new sources of lead between 40 and

34 cm (1936 - 1949), unless the isotopic signature was similar to ratios present at that time (Fig 5.13).

Of the metals associated with the coal peak, Pb is the only element that does not decline above 36 cm (1949). Between 38 and 17 cm (1943 - 1969) the combination of dry sediment flux rate, the Pb concentration and Pb isotopic ratios show three periods when the amount of lead entering the lake sediment increased sharply, including 38 - 34 cm (1943-1954), 34 - 25.5 cm (1954-1963) and 19 - 17 cm (1967-1969) (Fig 5.15).

The first interval suggesting a Pb increase occurs between 38 and 34 cm (1943 - 1954), where the concentration of lead remains constant as the dry sedimentation rate increases about 1.5 fold. The sustained concentration suggests a Pb increase to counterbalance dilution by increased sediment. The additional lead may have come from a combination of increased coal combustion and combustion of leaded automobile gasoline, which was first imported into Newfoundland in 1944-1945. The population of St. John's showed an increase after 1945, which is inferred to mean increased coal consumption. Coal combustion probably peaked in the 1950s, just before oil furnaces became popular, and probably was the single biggest source of anthropogenic Pb at that time. The soot profile also increases through this interval, suggesting increased coal consumption. Interpretation based on the soot profile,

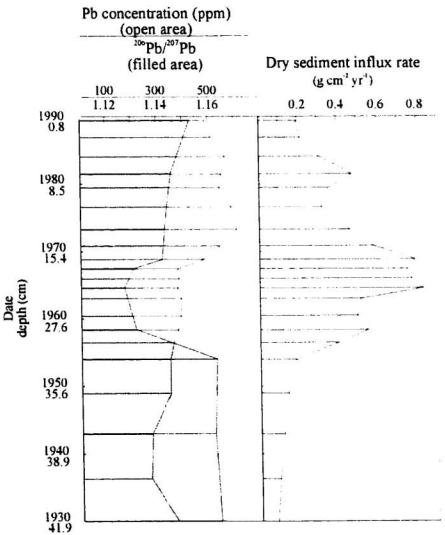

Figure 5.15 Lead concentration, isotope ratio and sediment influx profiles for core QV2 to illustrate changes in lead input and sources between 1930 and 1990.

however, could be misleading, as will discussed later.

The isotopic ratios show no change between 1943 and 1954, suggesting this new exotic lead had a signature close to the average ratio entering the lake at that time (approximately 1.163 in 1954). This ratio is in keeping with the historical leaded gasoline ratios in Canada, which range between 1.14 and 1.16 (Rosman et al., 1994). Although import data shows that gasoline was imported from Canada in 1944-1945 and 1949, it may have originated in the USA, where gasoline had a ratio of 1.149 before 1967 (Ritson et al., 1994). Its not known if the USA military imported their own gasoline for use at Fort Pepperrell.

The second interval of sharp Pb increase occurs between 1954 and 1963. Between 34 and 28 cm (1954 - 1960), the $^{206}Pb/^{207}Pb$ ratio decreases sharply, sediment influx triples and Pb concentration slightly increases. These changes suggest the amount of lead entering the lake increased to counter the effects of sediment dilution, and a new 'exotic' lead, with a lower isotopic ratio was introduced into the watershed.

Given the time during which this sediment was deposited, the most plausible explanation for these changes lies with increased emissions from the combustion of a leaded gasoline with a low isotopic ratio. This is in keeping with historical records that show automobile registration increasing sharply during the mid 1950's, which presumably continued into the

1960s. A calculated 92% of the lead with a $^{206}Pb/^{207}Pb$ ratio of 1.125 was anthropogenic at 28 cm (1960). This low ratio could be explained by a mixture including leaded gasolines with lead ores derived from either Trail, B.C., Canada or Australian (Broken Hill), which have $^{206}Pb/^{207}Pb$ ratios of 1.064 and 1.037, respectively (Hamilton and Clifton, 1979). The decline in $^{206}Pb/^{207}Pb$ could have been dampened by the possible reservoir of lead in the watershed soils that had accumulated from 100 years of coal combustion.

The third period of sharp Pb increases in Quidi Vidi Lake occurs between 19 and 17 cm (1967 - 1969), where the concentration and isotopic ratio show an abrupt increase, while the dry sedimentation influx rate remains constant. The concentration increase may have occurred as a result of increased automobile numbers, resulting in more emissions. The isotopic shift suggests a change in Pb sources, from low ratio ores like Australia or B.C. to higher ratio ores such as Missouri, USA (1.28 - 1.33) (Shirahata et al., 1980) or Bathurst, New Brunswick (1.16) (Cumming and Richards, 1975 and Stanton and Russell, 1959). Both ores are known to have been used as lead sources in gasoline (Macdonald et al., 1991, Shirahata et al., 1980 and Stukas and Wong, 1981).

Above 17 cm (1969) lead concentration levels continue to increase until 13 cm (1973), where a maximum value of 613 ppm was reached (Fig 5.15). The lead peak in 1973 coincides with

the peak of tetra ethyl lead emissions into the Canadian environment (Royal Society of Canada, 1986). Above 13 cm (1973), both the lead influx and concentration profiles show a decline. This is consistent with lead levels in gasoline which declined from 1974 to its eventual phasing out in 1989. The increase in the $^{206}Pb/^{207}Pb$ ratio above 17 cm (1973) probably reflects a decline of contributions from leaded gasoline.

5.5.3.ii Other metals above the coal peak

Chromium, Cu and Zn concentrations increase about 2 fold above 23 cm (1965), while Cd, Fe and Sb show increases above 7 cm (1982) (Fig 5.16). Increases in Cr, Cu and Zn occur immediately after the sediment influx rate declines, suggesting the increase could be partially explained by a decline in sediment dilution. The increases, however, suggest an anthropogenic source, although redox controls such as complexing with Fe oxyhydroxides cannot be ruled out.

Increases for all these elements, except Sb, is a lake-wide feature displayed in all four cores from Quidi Vidi Lake. Similar increases with less magnitude are observed in the surface sediments of Long Pond and Mundy Pond. The preservation of stratigraphy in the shallow Mundy Pond, however, is probably poor since the sediment is susceptible to wave winnowing. These features are not observed in Georges

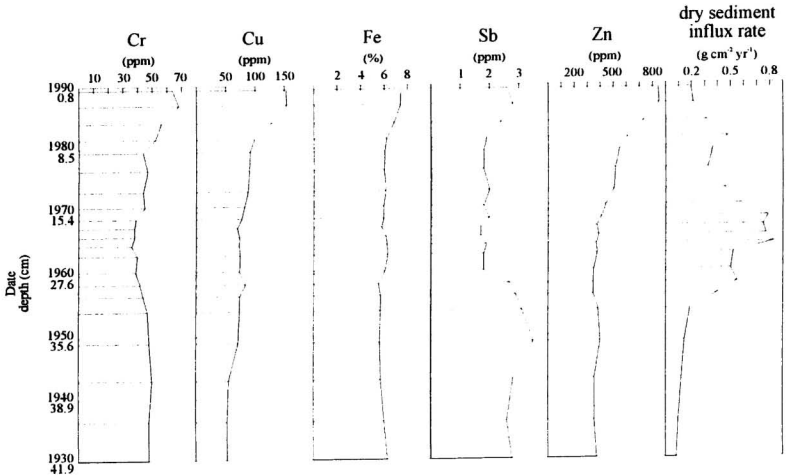

Figure 5.16 Cr, Cu, Fe, Sb and Zn profiles and sediment influx profile from core QV2, showing metal increases in the upper sediments.

Pond, suggesting the source or processes that caused the increases are related to an urban/suburban phenomenon.

5.6 History and spatial distribution of airborne pollution in St. John's

The level of urbanization in the Georges Pond watershed, on Signal Hill, is relatively low compared to the other urban lakes. The site, however, has had 300 years of history including denudation of the forest cover, establishment of fortifications, a hospital, concrete damming of the lake, and recent establishment of an interpretation centre with sufficient roads and parking lots. These features, however, are minor in comparison of the city itself and thus Georges Pond, in a National Historic Park, located adjacent and above the city allows it to identify the potential effects from fallout from fuel emissions. The other urban lakes have a compounding effect of storm sewers which provide an efficient drainage of surface pollution, which swamps atmospheric inputs.

Georges Pond provides evidence to suggest the 'coal peak' and soot increases observed in Quidi Vidi were the result of airborne pollution from coal combustion. The presence of soot in Georges Pond at 47.5 cm supports the hypothesis that coal combustion contributed to airborne pollution early in the history of St. John's. A small metal peak for Au, Hg, Sb and

Pb between 37.5 and 29 cm (Fig 5.17) may correspond to the 'coal peak' in Quidi Vidi Lake.

The lack of a readily discernable heavy metal peak in Long Pond, St. John's suggests the fallout from coal emissions was greatest around the harbour area, and dispersed rapidly outwards (Fig 5.18). The local prevailing westerly wind direction may have contributed to this situation, skewing the deposition pattern by carrying most emissions to the ocean.

The appearance of soot in Long Pond at depth, however, does suggest coal emissions were deposited in that watershed, albeit at lower concentrations than areas closer to the city core. In Mundy Pond, the appearance of soot at 22 cm, corresponds to peaks in heavy metals that are probably related to coal combustion (Fig 5.19). The soot counts are relatively high after 1950 in cores MP1 and LP5. In these cores the abrupt increases in clay content, and increases in lithophilic elements near the top of the core are believed to be post-1950, since clay and lithophilic element increases were most likely associated with soil erosion from urban development that occurred mostly after 1950. Mundy Pond is a little more unique as a portion of this pond was infilled sometime between 1942 and 1950 (Map of the City of St. John's 1942 and 1950), which may have complicated the signature just prior to 1950. In addition, soot counts remain high through upper core sections, suggesting that over the last 40 years there has

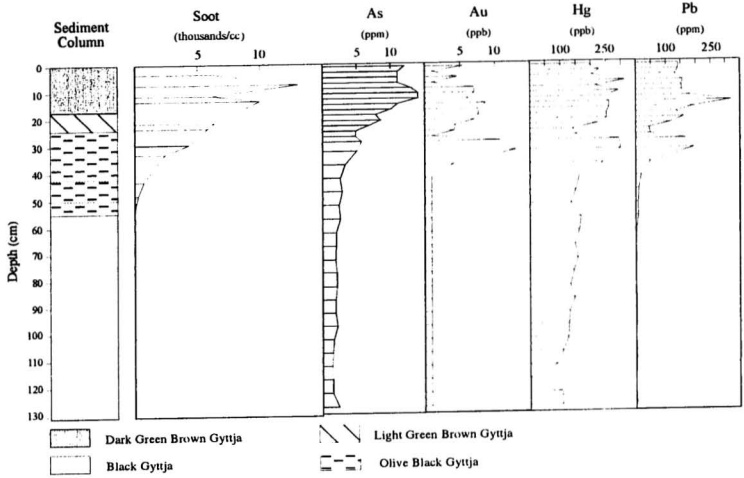

Figure 5.17 Soot, As, Au, Hg and Pb profiles from core GP1 to illustrate the distribution of airborne pollution from coal combustion.

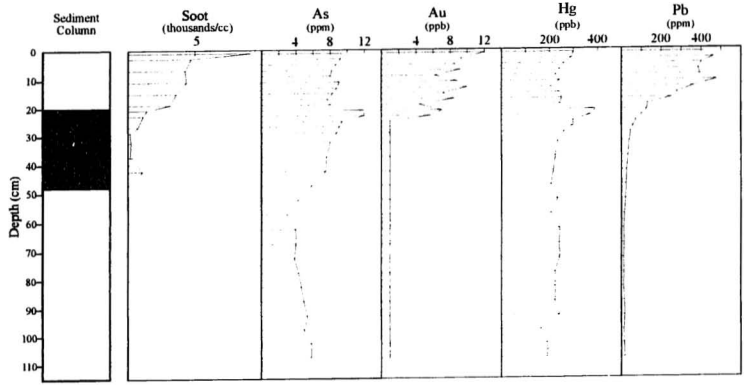

Figure 5.18 Soot and selected metal profiles from core LP5 to illustrate the distribution of airborne pollution from coal combustion.

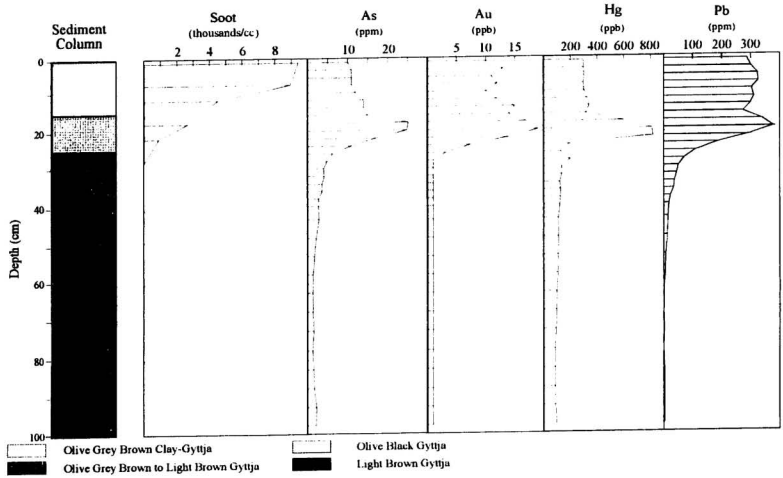

Figure 5.19 Soot, As, Au, Hg and Pb profiles from core MP1 to illustrate the distribution of airborne pollution from coal combustion.

been a constant supply. This supply occurs well after the 1960s when coal combustion, the main contributor of soot, declined to negligible levels.

The sharp rise in soot counts at about 20 cm in LP5, coincides with increases in lithophilic element concentrations, a change in sediment type and a sharp rise in charcoal counts. A similar feature is observed in Mundy Pond, where charcoal and soot increase sharply between 11 and 7 cm. The increase in soot and charcoal at these depths may suggest that there is a reservoir of pollutants related to fossil fuel and wood combustion in the watershed soils of St. John's. Wik and Renberg (1987) found a similar situation in Sweden, where remote areas showed high levels of soot which was the result of centuries of coal combustion. The abruptness of the increases of these particulates in both Long Pond and Mundy Pond suggests intense soil disturbance, and an efficient flushing system aided by storm sewers. Along with the potential reservoir of metals from coal combustion is a reservoir of lead related to leaded gasoline use. With 100 years of coal combustion, 40 years of leaded gasoline use, and continued use of bunker crude by large facilities, the city's soils may have become a large reservoir of potentially toxic metals.

Chapter 6: Summary and Conclusions

Measurement of chemical, physical and biological changes in lake sediment cores from St. John's, has been effective for discerning different periods and magnitudes of anthropogenic influences, and for identifying potential sources. This multi-faceted approach has identified broad-scale impacts associated with agriculture and urban development. Superimposed on these periods of physical disturbances are chemical impacts associated with the use of fossil fuels, namely coal and leaded gasoline.

The earliest disturbances in the sediment column in Quidi Vidi Lake occur at 82.5 cm, when pollen changes suggest forest clearance, probably for agricultural purposes. Historically, agriculture began about 1750-1760 in the Quidi Vidi Lake area and continued to spread, reaching its spatial maximum about 1850. Agricultural production grew and peaked between 1911 and 1921, declining afterwards when urban sprawl started encroaching upon cultivated lands. Compared to most Canadian centres, urban growth in St. John's was modest, except just after Confederation in 1949. Between 1950 and 1970, a large portion of the city was developed and most of the construction occurred in the Quidi Vidi Lake watershed. A large area on the north side of Quidi Vidi Lake was developed in the early 1940's with the war efforts (see Fig 1.2).

Disturbances related to the evolution from a farming community to an urban centre resulted in denudation of the natural vegetation, followed by increased rates of soil erosion. During the agriculture era, sediment influx was stable at about 10 times pre-European rates. From about 1910, when urban sprawl began, sediment influxes increased with greater of erosion. Based on the sediment influx data, erosion rates continued to increase from 1910 to peak between 1950 and 1970, declining afterwards. Impacts associated with soil erosion were recorded in the lake sediment as higher clastic and clay content, and a decline in the organic fraction as measured by loss-on-ignition.

Coincident with periods of city growth that were associated with the physical soil disturbance are emissions of heavy metals and particulates from coal and leaded gasoline combustion. Coal use probably started about 1800 and increased rapidly after 1845 with the establishment of heavy industry. Residential fuel use was also an important contributor since coal was the main heating source until the late 1950s and early 1960s when oil furnaces became popular. Leaded gasoline use started in Newfoundland about 1945. In Canada, and presumably Newfoundland, lead emissions from automobiles peaked in 1973, and declined afterwards with the introduction of low leaded gasoline, followed by its eventual phasing out in 1989.

Pollution from coal combustion contributed metals including As, Au, Hg, Pb, Sb and Zn, and also soot to the local environment. In Quidi Vidi Lake, the first evidence of exotic Pb additions, as recorded in the Pb isotopic ratios, is observed at 62.5 cm (1832). This early 'exotic' lead was probably from coal combustion. It is unlikely that much if any of this lead came from foundries since there were no foundries built until the late 1840s. With the continued population increase and the establishment of industry by the late nineteenth century, coal combustion and the emission of toxic metals increased steadily.

After 1940, the lead concentration and isotopic profiles, in combination with the dry sediment influx profile suggest three periods of increased lead emissions; 1943-1954, 1954-1963 and 1967-1969, which correspond to the sediment intervals in Quidi Vidi Lake core QV2 between 38-34 cm, 34-25.5 cm and 19-17 cm, respectively. The first period was probably related to the introduction of leaded gasoline into St. John's and increased coal emissions. The population rise that occurred after 1945 is inferred to mean increased coal consumption, until oil furnaces became popular. The other two periods likely reflect increased Pb emissions from automobiles. The Pb isotopic data suggest that between 1960 and 1967, automobile gasoline consumed in St. John's probably contained lead from either Broken Hill, Australia or British Columbia,

Canada.

Aquatic impacts from the anthropogenic effects of farming, urban growth and fossil fuel emissions were inferred from the diatom data. Before 1800, the diatom data show little change, indicating the earliest forest and agricultural disturbances had little impact on the aquatic life or the lake water pH. Through the urban era, however, the data show notable impacts. The most obvious is the sharp lake water pH increase at 1960 and 1984, where reconstructed pH values were 7.2 and 7.9, respectively. This compares to 6.4 and 6.7 recorded in the pre-European section of core. Indicator species, including *Asterionella formosa*, suggest the lake was more eutrophic in 1960, while *Diatoma elongatum* may reflect impacts related to winter salting of roads. The combined impacts of the urban setting have also caused a decline in diatom diversity in most recent times.

The high reconstructed pH levels and high SO_4^{2-} in Quidi Vidi Lake suggest it is highly buffered. Considering the large volume of fossil fuel emissions (SO_4^{2-}) within the city, the buffering capacity must be significant. One potential buffering agent is thought to be concrete. The dissolution of concrete adds Ca and Mg to urban waterways causing an increase in their carbonate content, thereby buffering the lakes. The amount of concrete in the watershed has increased significantly since Confederation. The low metal levels in

fish taken from several urban rivers is probably the result of the high buffering capacity in the urban waterways.

The data collected from the sediment cores in combination with historical information, shows the most stressful period for the urban lakes and the urban atmosphere occurred around the 1950s. Lake stress was probably highest in Quidi Vidi Lake between 1950 and 1970, when sediment influx rates were at their peak. Stresses from atmospheric fallout probably peaked with the peak of coal combustion in the 1950s.

High sediment inputs during the 1950s and 1960s resulted from an intense period of residential construction. Soils disturbed from these activities were transported rapidly into lakes. This was aided by pavement and storm sewers that have little storage capacity and allow instantaneous run-off. For comparison, sediment influxes at their peak were 15 fold those recorded in the farming era. Over the last 25 years the sedimentation rate has declined considerably. This was the result of declining construction as the urban landscape was transformed into a blanket of lawns, concrete and pavement.

Storm sewers still play an important role allowing pollutants accumulating on parking lots and roadways to be flushed into the urban waterways. The importance of storm sewers in today's environment can be gathered from data presented by Ault et al., (1970) who noted that most automobile exhaust emissions are deposited within 500 feet of

roads. Since most of the city environment is covered with concrete and pavement, this implies that automobile pollution has a short watershed residence time and is rapidly flushed to the lakes. Automobile pollution not only includes exhaust emissions, but also products of wear from tires and brake pads, and oil spillage.

The high sedimentation rates in the city have had an overwhelming effect on metal influx rates. Most of the toxic elements including As, Hg, Pb and Zn for example, show the greatest period of influx between 1950 and 1970, coinciding with the period of highest sediment influx. Although it seems fortuitous that there were high sediment influxes with the high metal influxes, the rate of metal influx seems be controlled by the rate of sediment influx. This relationship is probably a function of the potentially large metal reservoir in the watershed soils. Although the geologic units in this area contribute to metals, such as Pb from the St. John's shales where lake sediment within this unit show levels about 20 ppm, the proportion of geologic metals to that of anthropogenic levels within the watershed soils is most likely to be very small.

Although several decades have passed since coal use has ended, the continued influx of soot from coal combustion suggests there may be a reservoir of soot and related metals in the watershed soils. This potential metal reservoir is not

only from the 100 years of coal combustion, but also 40 years of leaded gasoline combustion. This relationship suggests the urban lakes will be influenced by previously deposited metals for many centuries to come.

Unlike lake stresses, atmospheric stresses are much more difficult to discern, since lake sediments are not as effective for measuring atmospheric conditions. Based on the historical use of coal, which is believed to be the single biggest air pollutant, the greatest period of atmospheric stress probably occurred in the 1950s when coal consumption was at its peak, just before oil furnaces became abundant.

The recent declines observed for sediment and metal influxes, and metal concentrations suggest lake conditions are improving. In the last 15 years sediment influx has declined by 60%, and by 75% from its highest level in 1965. Although unlikely to occur, based on the rate of sediment influx decline between 1973 and 1989, it would take only 12 years to achieve pre-European sedimentation rates (Fig 6.1). Since metal influxes are controlled by the sediment influx, similar time frames were calculated for the metal influx rates to decline to pre-European levels. As an example, it would take about 9 and 12 years, for Pb and Hg, respectively to decline to pre-European levels. Similar time frames exist for all elements, not only the metals.

Although in theory metal influx rates could decline to

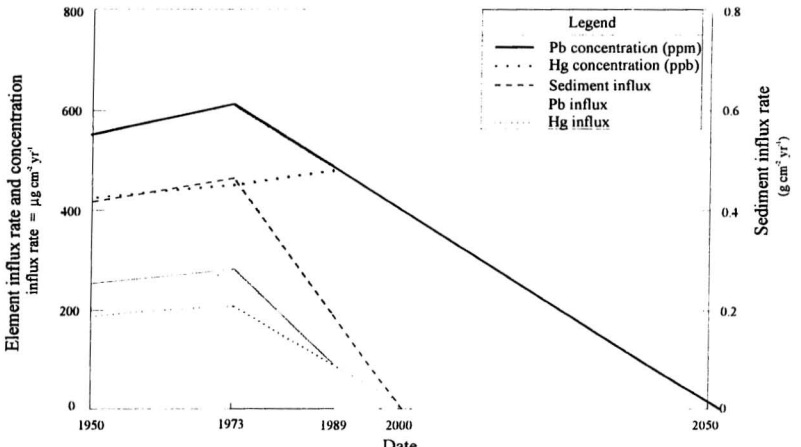

Figure 6.1. Theoretical time projections for the decline of element concentrations and influxes, and sediment influx to pre-1750 levels. Projections are based on the linear decline between 1973 and 1989. The Hg concentration shows no decline between 1973 and 1989 and thus, theoretically, will not return to pre-1750 levels.

pre-European rates in 12 years, the rate of concentration decline portrays a different scenario (Fig 6.1). For example, using the rate of concentration decline through the last 15 years it will take about 60 years for lead to reach pre-European levels. Elements like Hg, which show a small increase in concentration through the last 15 years, suggest pre-European levels are unachievable. This predicament is probably in part explained by the higher concentrations of metals in the watershed soils.

Looking into the future, data collected in this study will allow society to evaluate the past changes and to plan management strategies for future use of the urban waterbodies. All lakes in St. John's have shown recent improvements concerning sediment and metal influxes and metal concentrations. However, to attempt to manage the urban ecosystems, planners must consider not only the present, but also impacts from the past. Impacts related to coal combustion, for example, have possibly created a large reservoir of metals in the watershed soils. This metal accumulation will undoubtably play an important role in the management of the urban waterbodies.

Although the lakes are presently well buffered, immobilizing heavy metals in the sediment, the same conclusion cannot be drawn for the watershed soils. It is unclear how the metals are held in the soils, and how readily they may be

leached could be very important for the future. This argument for high metal content in the soils is just that, and further work is needed to establish the conditions of these soils. If the metals are present, and if the proper conditions exist in the urban soils (high phosphorous) the leachable lead component in the soils can dramatically decline (Berti and Cunningham, 1994). The soils in this area, however, are naturally acidic, and in combination with the high emissions of acidifying agents in the city, these soils may be liberating metals much more readily than lake sediments. Establishing the nature of this reservoir of metals, and its relationship to the lakes is of the utmost importance for determining the degree of influence these potentially toxic metals have on the urban waterways. This body of metals, and its potential impacts could hold the key to the health of the urban lake system. This reservoir and the availability of the metals may also play an important part in the general uptake in the population through the ingestion of soil and dust.

If the lakes become acidified, the metals being carried from the reservoir would undoubtably have a deleterious effect on the lake ecosystem. Lake water acidification could allow much of the lake sediment metal content, which in some cases is high enough to be classified as toxic, to enter the lake water, allowing it to become more bioavailable. Although impacts related to lake acidification are an unknown, further

study of the lake sediment may provide some insight. The section of core between 1800 and 1960 was not examined for diatoms. This section of core covers the most intense period of coal combustion, before the urban landscape was developed. If acidification occurred through that interval, impacts related to lake acidification could be discerned from the diatom data.

The future health of urban waterways will depend in part on conditions that could liberate this reservoir of toxic metals from the watershed soils and lake sediments. Because the watershed reservoir is potentially large, widespread and partially buried under city infrastructure, there is little that can be done to rectify it. Reduction of erosion and sedimentation into urban lakes, by better sedimentation control through storm sewers, is probably the best mechanism for managing this potential accumulation of metals. Another mechanism is maintaining the artificially high pH and buffering capacity, which in its present situation seems to be self sustaining because of the city landscape. In their present state with a neutral pH, declining sediment and metal influxes, and high buffering capacities, these urban lakes are in some sort of equilibrium with the city. Changing just one component in this equilibrium could upset the balance causing more harm than good.

REFERENCES

Adams, F.G. 1988. St. John's - The Last 100 Years. Creative Publishers, St. John's, Newfoundland. 154 pages.

Adams, F.G. 1991. Potpourri of Old St. John's. Creative Publishers, 87 pages.

Anderson, N. and Korsman, T. 1990. Land-use change and lake acidification : Iron Age de-settlement in northern Sweden as a pre-industrial analogue. Phil. Trans. R. Soc. Lond., Vol. B 327, pp. 373-376.

Appleby, P.G. 1994. Report on radiometric dating of Quidi Vidi Lake. Internal consultants report, Department of Mines and Energy, Geological Survey file 001N/10/0616, St. John's.

Appleby, P.G. and Oldfield, F. 1978. The calculation of ^{210}Pb dates assuming a constant rate of supply of unsupported ^{210}Pb to the sediment. Catena, Vol. 5, pp. 1-8.

Appleby, P.G. and Oldfield, F. 1983. The assessment of ^{210}Pb data from sites with varying sediment accumulation rates. Hydrobiologia, Vol 103, pp. 29-35.

Appleby, P.G. and Oldfield, F. 1984. Empirical testing of ^{210}Pb models. *In* Lake sediments and Environmental History, E.Y. Hawarth and J.G. Lund (editors), pp. 93-124. Leicester University Press.

Appleby, P.G., Oldfield, F., Thompson, R., Huttunen, P., and Tolonen, K. 1979. ^{210}Pb dating of annually laminated lake sediments from Finland. Nature, Vol. 280, pp. 53-55.

Appleby, P.G., Nolan, P.J., Gifford, D.W., Godfrey, M.J., Oldfield, F., Anderson, N.J. and Battarbee, R.W. 1986. ^{210}Pb dating by low background gamma counting. Hydrobiologia, Vol. 144, pp. 21-27.

Appleby, P.G., Nolan, P.J., Gifford, D.W., Oldfield, F., Anderson, N.J., and Battarbee R.W. 1986. ^{210}Pb dating by low background gamma counting. Hydrobiologia, Vol. 141, pp. 21-27.

Ault, W.U., Senechal, R.G. and Erlebach, W.E. 1970. Isotopic composition as natural tracer of lead in the environment. Environmental Science and Technology, Vol 4, No. 4, pp. 305-313.

Baker, M., Pitt, J.M, Pitt, R.D.W. 1990. The Illustrated History of Newfoundland Light and Power. Creative Publishers, St. John's, Newfoundland. 340 pages.

Barber, H.G and Haworth, E.Y. 1981. A guide to the morphology of the diatom frustule. Freshwater Biological Association, Scientific Publication, No. 44. 112 pages.

Bassett, I.J. 1978. An atlas of pollen grains and common fungus spores of Canada. Research Branch, Canada Department of Agriculture. 321 pages.

Battarbee, R.W. 1986. Diatom analysis. Chapter 26 in: B.E. Berglund, ed. Handbook of Holocene Palaeoecology and Palaeohydrology. John Wiley and Sons: Chichester. pp. 527-570.

Berge. F, Brodin, Y-W., Cronberg, G., El-Daoushy, F., Hoeg, H.I., Nilssen, J.P., Renberg, I., Rippey, B., Sandoy, S., Timberlid, A. and Wik, M. 1990. Palaeolimnological changes related to acid deposition and land-use in the catchments of two Norwegian soft-water lakes. Phil. Trans, Royal Society of London, Vol. B 327, pp. 385-389.

Berglund, B.E. and Ralska-Jasiewiczowa, M. 1986. Pollen analysis and pollen diagrams. In Handbook of Holocene Palaeoecology and Palaeohydrology, B. E. Berglund (editor). John Wiley and Sons Ltd, Chichester. pp. 455-484.

Berti, W.R. and Cunningham, S.D. 1994. Remediating soil lead with green plants. *In* Trace Substances, Environment and Health. C. Richard Cothern US Environmental Protection Agency, Washington DC, USA (editor). Science Reviews, Northwood. pp. 43-51.

Bieger, T., Hellou, J. and Abrajano Jr., T.A. 1996. Petroleum Biomarkers as Traces of Lubricating Oil Contamination. Marine Pollution Bulletin. Vol. 22, No. 3, pp. 270-274.

Birks, H.J.B., Berge, F., and Boyle, J.F. 1990. A test of the land-sue hypothesis for recent lake acidification by using hill-top lakes in southwest Norway : an extended summary. Phil. Trans. R. Soc. Lond., Vol. B 327, pp. 369-370.

Birks, H.J.B., Line, J.M., Juggins, S., Stevenson, A.C. and terBraak, C.J.F. 1990. Diatoms and pH reconstruction. Phil. Trans. Royal Society of London, Vol. B 327, pp.

263-278.

Biscaye, P.E. 1964. Distinction between kaolinite and chlorite in recent sediments by X-Ray diffraction. American Mineralogist, Vol. 41, pp. 1281-1289.

Biscaye, P.E. 1965. Mineralogy and Sedimentation of Recent Deep-Sea Clay in the Atlantic Ocean and Adjacent Seas and Oceans. Geological Society of American Bulletin, Vol 76, pp. 803-832.

Blake, D.M. 1992. Anthropogenic Impacts on Lakewater Geochemistry in Watersheds in the St. John's Area. B.Sc. honours thesis, Memorial University of Newfoundland. 111 pages.

Bland, J. 1946. Report on the City of St. John's, Newfoundland. *For* The Commission on Town Planning. 24 pages.

Block, C. and Dams, R. 1975. Inorganic composition of Belgian Coals and Coal Ashes. Environmental Science and Technology, Vol. 9, No. 2, pp. 146-150.

Block, C. and Dams, R. 1975. Lead contents of coal, coal ash, and fly ash content. Water, Air, and Soil Pollution, Vol. 5, pp. 207-211.

Block, C. and Dams, R. 1976. Study of fly ash emissions during combustion of coal. Environmental Science and Technology, Vol. 10, No. 10, pp. 1011-1017.

Bloom, N.S. and Crecelius, E.A. 1987. Distribution of silver, mercury, lead, copper and cadmium in central Puget Sound sediments. Marine Chemistry, Vol. 21, pp. 377-390.

Bortleson, G.C. and Lee, F.G. 1974. Phosphorus, iron, manganese distribution in sediment cores of six Wisconsin lakes. Limnol. Oceanogr. Vol. 19, pp. 794-801.

Boutron, C.F. and Gorlach, U. 1990. The occurrence of heavy metals in Antarctic and Greenland ancient ice and recent snow. *In* Metal Speciation in the Environment. (Editors Broekart, J.A.C., Gucer, S. and Adams, F.) Plenum Publishing Corporation, London and New York.

Bradbury, J.P. 1986. Effects of forest fire and other disturbances on wilderness lakes in northeastern Minnesota. II. Paleolimnology. Arch. Hydrobiol., Vol.

106, No. 2, pp. 203-217.

Brindley, G.W. 1981. X-Ray identification (with ancillary techniques) of Clay Minerals. *In* Short Course in Clays and the Resource Geologist, Mineralogical Association of Canada. Ed F.J. Longstaffe, Calgary, May 1981, pp. 22-38, CO-OP Press.

Brinkman, D.W and Dickson, J.R. 1995. Contaminants in used lubricating oils and their fate during distillation/ hydrotreatment re-refining. Environmental Science and Technology, Vol. 29, No. 1, pp. 81-86.

Brugam, R.B. 1978a. Pollen Indicators of land-use change in southern Connecticut. Quaternary Research, Vol 9, pp. 349-362.

Brugam, R.B. 1978b. Human disturbance and the historical development of Linsley Pond. Ecology, Vol. 59, No. 1, pp. 19-36.

Buchanan, R.A. and Houlihan, T. 1987. St. John's Waterways and Wetlands: An environmental policy study, Planning Department, City of St. John's, 80 pages.

Buckley, D.E. and Winters, G.V. 1992. Geochemical characteristics of contaminated surficial sediments in Halifax Harbour: impact of waste discharge. Canadian Journal of Earth Sciences, Vol. 29, No. 12, pp. 2617-2639.

Burden, E.T. 1978. Pollen and Algal assemblages in cored sediments from Gignac Lake and Second Lake (Simcoe Co., Ontario): Relationships with Lacustrine facies, geochemistry and vegetation. M.Sc. thesis, Dept. of Geology, The University of Toronto.

Burden, E.T., McAndrews, J.H. and Norris, G. 1986. Palynology of Indian and European forest clearance and farming in lake sediment cores from Awenda Provincial Park, Ontario. Canadian Journal of Earth Science, Vol. 23, pp. 43-54.

Butler, D.L. 1990. Pollen and geochemical analysis of a sediment core from Branscombes Pond, Mount Pearl, Newfoundland: the anthropogenic record. B.Sc. honours thesis, Memorial University of Newfoundland, 51 pages.

Camburn, K.E. and Kingston, J.C. 1986. The genus *Melosira* from soft-water lakes with special reference to northern

Michigan, Wisconsin, and Minnesota. *In* J.P. Smol, R.W. Battarbee, R.B. Davis and J. Merilainen, editors. Diatoms and lake acidity. Developments in Hydrobiology. W. Junk Publishers, Dordrecht, The Netherlands.

Camburn, K.E., Lowe, R.L. and Stoneburner, D.L. 1978. The Haptobenthic Diatom Flora of Long Branch Creek, South Carolina. Nova Hedwigia, Band XXX. 239 pages.

Camburn, K.E., Kingston, J.C., and Charles, D.F. (eds) 1984-1986. PIRLA (Paleoecological Investigation of Recent Lake Acidification), Diatom Icongraph. PIRLA Unpublished Report Series, Report 3.

Canadian Council of Ministers of the Environment (CCME). 1995. Protocol for the derivation of Canadian Sediment Quality guidelines for the protection of Aquatic Life, Report CCME EPC-98E. Guidelines Division, Environment Canada. 38 pages.

Candow, J.E. 1979. A Structural and Narrative History of Signal Hill National Historic Park and Area to 1945. Parks Canada, Manuscript Report Number 348. 397 pages.

Carignan, J., Gariepy, C., Machado, N. and Rive, N. 1993. Pb isotopic geochemistry of granitoids and gneisses from the lake Archean Pontiac and Abitibi Subprovinces of Canada. Chemical Geology, Vol. 106, pp. 299-316.

Charles, D.F. 1990. Effects of acidic deposition on North American lakes : palaeolimnological evidence from diatoms and chrysophytes. Phil. Trans. R. Soc. Lond, Vol. B 327, pp. 403-412.

Christopher, T.K. 1991. Mapping Anthropogenic effects of urbanization in the St. John's area using inorganic geochemistry of lake sediments. B.Sc. honours thesis, Memorial University of Newfoundland. 105 pages.

Christopher, T.K., Davenport, P.H. and Burden, E.T. 1993. The effect of urban and industrial development on the geochemistry of the watersheds in the St. John's area: preliminary results. Current Research, Newfoundland Dept. of Mines and Energy, Geological Survey Branch, Report 93-1, pp. 419-433.

Chow, T.J. and Earl, J.L. 1972. Lead isotopes in North American coals. Science, Vol. 176, pp. 510-511.

Coish, C. 1983. (compiler and editor). Newfoundland Date book. Lifestyle Books, Grand Falls, NF. 189 pages.

Cook, C.D. 1991. Tales of the Trails; The Newfoundland Railway. Creative Publishers, St. John's, Newfoundland.

Cox, E.J. 1987. Studies on the diatom genus Navicula Bory. VI. The identity, structure and ecology of some freshwater species. Diatom Research, Vol. 2, No. 2, pp. 159-174.

Crecelius, E.A. and Piper, D.Z. 1973. Particulate lead contamination recorded in sedimentary cores from Lake Washington, Seattle. Environmental Science and Technology, Vol. 7, No. 11, pp. 1053-1055.

Cumming G.L. and Richards, J.R. 1975. Ore lead isotope ratios in a continuously changing Earth. Earth and Planetary Science Letters, Vol. 28, pp. 155-171.

Davenport, P.H., Nolan, L.W., Butler, A.J., Wagenbauer, H.A. and Honarvar, P. 1996. The digital geochemical atlas of Newfoundland. Department of Mines and Energy, Geological Survey of Newfoundland, open file NFLD /2607, version 1.2.

Davenport, P.H., Christopher, T.K., Vardy, S. and Nolan, L.W. 1993. Geochemical Mapping in Newfoundland and Labrador: its role in establishing geochemical baselines for the measurement of environmental change. Journal of Geochemical Exploration, Vol. 49, pp. 177-200.

Davis, M.B. 1976. Erosion rates and land-use history in southern Michigan. Environmental Conservation, Vol. 3, No. 2, pp. 139-148.

Davison, W. 1993. Iron and manganese in lakes. Earth Science Reviews, Vol. 34, pp. 119-163.

Davison, R.L, Natusch, D.F.S., Wallace, J.R. and Evans, C.A. 1974. Trace elements in fly ash, dependence of concentration on particle size. Environmental Science and Technology, Vol. 8, No. 13, pp. 1107-1113.

Dean, W.E. and Gorham, E. 1976. Major chemical and mineral components of profundal surface sediments in Minnesota lakes. Limnology and Oceanography, Vol. 21, No. 2, pp. 259-285.

Dearing, J.A. 1991. Lake sediment records of erosional

processes. In J.P. Smith, P.G. Appleby, R.W. Battarbee, J.A. Dearing, R. Flower, E.Y. Haworth, F. Oldfield and P.E. O'Sullivan (editors). Environmental History and Palaeolimnology. Hydrobiologia, Vol. 214, pp. 99-106, 1991.

Dearing, J.A. 1986. Core correlation and total sediment influx. *In* Handbook of Holocene Palaeoecology and Palaeohydrology. Edited by B. E. Bergland, John Wiley and Sons Ltd., Chichester. 869 pages.

Dearing, J.A. and Foster, I.D. 1986. Lake sediment and palaeohydrological studies. *In* Handbook of Holocene Palaeoecology and Palaeohydrology. Editor B. Berglund: pages 67-90. John Wiley and Sons. 869 pages.

Dearing, J.A., Hakansson, H., Liedberg-Jonsson, B., Persson, A., Skansjo, S., Widholm, D. and El-Daoushy., F. 1987. Lake sediment used to quantify the erosional response to land use change in southern Sweden. Oikos, Vol. 50, pp. 60-78.

Dixit, S.S., Smol, J.P., Kingston, J.C. and Charles, D.F. 1992. Diatoms: powerful indicators of environmental change. Environmental Science and Technology, Vol. 26, No. 1, pp. 23-33.

Dodd, J.J. 1987. The illustrated flora of Illinois. Diatoms. Southern Illinois University Press, Carbondale. 478 pages.

Drover, D.H. 1993. Investigation of the sources and movement of contaminants in the Nut Brook Pond Drainage basin. B.Sc. honours thesis, Memorial University of Newfoundland. 149 pages.

Edgington, D.N. and Robbins, J.A. 1976. Records of Lead Deposition in Lake Michigan Sediments since 1800. Environmental Science and Technology, Vol. 10, No. 3. pp. 266-274.

Engstrom, D.R. and Swain, E.B. 1997. Recent declines in atmospheric mercury deposition in the upper midwest. Environmental Science and Technology, Vol. 31, No. 4. pp. 960-967.

Engstrom, D.R. and Wright, H.E. 1984. Chemical stratigraphy of lake sediments as a record of environmental change. *In* Lake Sediments and Environmental History. Edited by E. Y.

Hayworth and J. W. G. Lund. Leicester University Press, pp. 10-67.

Engstrom, D.R, Swain, E.B. and Kingston, J.C. 1985. A palaeolimnological record of human disturbance from Harvey's Lake, Vermont: geochemistry, pigments and diatoms. Freshwater Biology, Vol. 15, pp. 261-288.

Evans, R.D. and Dillon, P.J. 1982. Historical changes in anthropogenic lead fallout in southern Ontario, Canada. Hydrobiologia, Vol. 91, pp. 131-137.

Evans, R.D. and Rigler, F.H. 1980. Calculation of the total anthropogenic lead in the sediments of a rural Ontario lake. Environmental Science and Technology, Vol. 14, No. 2, pp. 216-218.

Environment Canada. 1981. Canadian Climatic Normals, 1951-1980, Temperature and Precipitation, Atlantic Provinces. Atmospheric Environment Services, Ottawa, Canada.

Finch, C.J. 1998. Inductively Coupled Plasma-Emission Spectrometry (ICP-ES) at the Geochemical Laboratory. Current Research, Newfoundland Dept. of Mines and Energy, Geological Survey, Report 98-1, pages 179-193.

Flegal, A.R., Itoh, K., Patterson, C.C. and Wong, C.S. 1986. Vertical profile of lead isotopic compositions in the north-east Pacific. Nature, Vol. 321, pp. 689-690.

Foged, N. 1977. Freshwater diatoms in Ireland. Bibliotheca phycologica. Bd. 34. 221 pages.

Foged, N. 1979. Diatoms in New Zealand, the North Island. Bibliotheca phycologica. Bd. 47. 224 pages.

Foged, N. 1981. Diatoms in Alaska. Bibliotheca phycologica. Bd. 53. 316 pages.

Foged, N. 1982. Diatoms in Bornholm, Denmark. Bibliotheca phycologica. Bd. 59. 174 pages.

Folk, R.L. 1980. Petrology of Sedimentary Rocks. Hemphill Publishing Company, Austin, Texas.

Fortescue, J.A.C. 1986. Geochemical stratigraphy of organic lake sediments from selected lakes north and east of Lake Superior. Ontario Geologic Survey Map 80-757.

Fortescue, J.A.C. and Vida, E.A. 1991 The use of lake sediment cores to map environmental change in Ontario, Canada. In: F. Mrna (Editor), Exploration Geochemistry 1990, Geol. Surv. Czechoslovakia, Prague, pp. 92-107.

Friske, P.W.B. 1995. Effects of limnological variation on element distribution in lake sediments from Tatin Lake, central British Columbia - implications for the use of lake sediment data in exploration and environmental studies. *In* Current Research 1995-E; Geological Survey of Canada. pp. 59-67.

Gaillard, M.-J., Dearing, J.A, El-Daoushy, F., Enell, M., and Kakansson, H. 1991. A multidisciplinary study of the lake Bjaresjosjon (S Sweden): land-use history, soil erosion, lake trophy and lake-level fluctuations during the last 3000 years. In P. Smith, P. G. Appleby, R. W. Battarbee, J. A. Dearing, R. Flower, E. Y. Haworth, F. Oldfield and P. E. O'Sullivan (editors). Environmental History and Palaelimnology. Hydrobiologia, Vol. 214, pp. 107-114.

Garrett R.G. 1973. The determination of sampling and analytical errors in exploration geochemistry-a reply. Economic Geology, Vol. 68, pp. 282-283.

Garrett, R.G. 1993. Another cry from the heart. Explore, No. 81, pp. 9-14.

Gayer, R. and Rickard, D. 1994. Colloform gold in coal from southwest Wales. Geology, Vol. 22, pp. 35-38.

Gearing, J.N., Buckley, D.E. and Smith, J.N. 1991. Hydrocarbon and metal contents in a sediment core from Halifax Harbour: A chronology of contamination. Can. J. Fish. Aquat. Sci., Vol. 48, pp. 2344-2354.

Germain, H. 1981. Flore Des Diatomees eaux douces et sauma tres. Societe Nouvelles Des editions Boubee, Paris. 444 pages.

Gibson, R.J. and Haedrich, R.L. 1988. The Exceptional Growth of Juvenile Atlantic Salmon (*salmo salar*) in the city waters of St. John's, Newfoundland, Canada. Pol. Arch. Hydrobiol., Vol. 35, No. 3-4, pp. 385-407.

Goldberg, E.D., Hodge, V.F., Griffin, J.J. and Koide, M. 1981. Impact of Fossil Fuel Combustion on the Sediments of Lake Michigan. Environmental Science and Technology, Vol. 15, No 4, pp. 466-471.

Goldstein, H.L. and Siegmund, C.W. 1976. Influence of heavy fuel oil combustion and boiler combustion conditions on particulate emissions. Environmental Science and Technology, Vol. 10, No. 12, pp. 1109-1114.

Graney, J.R., Halliday, A.N., Keeler, G.J., Nriagu, J.O., Robbins, J.A. and Norton, S.A. 1995. Isotopic record of lead pollution in lake sediments from the northeastern United States. Geochimica et Cosmochimica Acta, Vol. 59, No. 9, pp. 1715-1728.

Griffin, J.J. and Goldberg, E.D. 1979. Morphologies and Origin of Elemental Carbon in the Environment. Science, Vol. 206, pp. 563-565.

Griffin, J.J. and Goldberg, E.D. 1981. Sphericity as a characteristic of solids from fossil fuel burning in a Lake Michigan sediment. Geochimica et Cosmochimica Acta, Vol. 45, pp. 763-769.

Griffin, J.J. and Goldberg, E.D. 1983. Impact of Fossil Fuels Combustions on Sediments of Lake Michigan, A Reprise. Environmental Science and Technology, Vol. 17, pp. 244-245.

Hallberg, R.O. 1991. Environmental implications of metal distribution in Baltic Sea sediments. Ambio, Vol. 20, No. 7, pp. 309-316.

Hamilton, E.I and Clifton, R.J. 1979. Isotopic abundances of lead in estuarine sediments, Swansea Bay, Bristol Channel. Estuarine and Coastal Marine Science, Vol 8, pp. 271-278.

Hardy, J. and Tucker, M. 1988. X-ray powder diffraction of sediments. *In*: Techniques in Sedimentology, Edited by Maurice Tucker, pp. 191-228.

Head, C.G. 1976. Eighteenth Century Newfoundland. McClelland and Stewart Limited, Toronto, 296 pages.

Heringa, P.K. 1981. Soils of the Avalon Peninsula, Newfoundland. Research Branch, Agriculture Canada, Newfoundland Soil Survey Report No. 3, St. John's, 117 pages.

Historical Statistics of Newfoundland and Labrador. 1981. Volume II(3). Department of Public Works and Services, Government of Newfoundland and Labrador.

Historical Statistics of Newfoundland and Labrador. 1988. Volume II(V). Department of Public Works and Services, Government of Newfoundland and Labrador.

Hopper, J.F. 1991. Regional source discrimination of atmospheric aerosols in Europe using the isotopic composition of lead. Tellus, Vol. 43B, pp. 45-60.

Horace, G. 1981. A guide to the morphology of the Diatom Frustule: with a key to the British freshwater genera. Ambleside, Cumbria: Freshwater Biological Association. 112 pages.

Imboden, D.M. 1974. Phosphorus model of lake eutrophication. Limnology and Oceanography, Vol. 19, No. 2, pp. 297-304.

Jaakkola, T., Tolonen, K., Huttunen, P. and Leskinen, S. 1983. The use of fallout ^{137}Cs and $^{239,240}Pu$ for dating of lake sediments. Hydrobiologia, Vol. 103, pp. 15-19.

Joy, J.L. 1977. The Growth and Development of trades and Manufacturing in St. John's, 1870 - 1910. Master of Arts, Department of History, Memorial University of Newfoundland, 221 pages.

Kapp, R.O. 1969. How to know pollen and spores. Dubusque, Iowa, W.C. Brown Co. 249 pages.

Kerminen, V-M., Makela, T.E., Ojanen, C.H., Hillamo, R.E., Vilhunen, J.K., Rantanen, L., Havers, N., Bohlen, A.V. and Klockow, D., 1997. Characterization of the particulate phase in the exhaust from a diesel car. Environmental Science and Technology, Vol. 31, No. pp. 1883-1889.

King, A.F. 1990. Geology of the St. John's Area. Department of Mines and Energy, Geological Survey of Newfoundland, Report 90-2, 102 pages.

Kingston, J.C. 1986. Diatom Analysis - Basic Protocol. Section 6.1 in: D.F. Charles and D.R. Whitehead, eds. Paleoecological Investigation of Recent Lake Acidification, Methods and Project Description. Electric Power Research Institute, Palo Alto, California. EPRI EA-4906. pp. 6-1 to 6-11.

Kingston, J.C., Cook, R.B., Kreis, R.G., Camburn, K.E., Norton, S.A., Sweets, P.R., Binford, M.W., Mitchell,

M.J., Schindler, S.C., Shane, L.C.K. and King, G.A. 1990. Paleoecological investigation of recent lake acidification in northern Great Lakes states. Journal of Paleolimnology, Vol. 4, pp. 153-201.

Knudson, B.M. 1952. The diatom genus Tabellaria. I. Taxonomy and morphology. Annales Botanica, N.S., Vol 16, pp. 421-440.

Knudson, B.M. 1953. The diatom genus Tabellaria. II. Taxonomy and morphology of the plankton varieties. Annales Botanica, N.S., Vol 17, pp. 131-155.

Knut, F. 1989. Textbook of pollen analysis. Wiley Chichester. 328 pages.

Koppen, J.D. 1975. A morphological and taxonomic consideration of Tabellaria (Bacillariophyceae) from the northcentral United States. Journal of Phycology, Vol 11, pp. 236-244.

Korhola, A. and Blom, T. 1996. Marked early 20th century pollution and the subsequent recovery or Toolo Bay, central Helsinki, as indicated by subfossil diatom assemblage changes. Hydrobiologica, Vol. 324, pp. 169-179.

Korner, H. 1971. Morphlolgied and Taxonomie der Diatomeengattung Asterionella. Nova Hedwigia, Vol 20, pp. 557-724.

Krammer, V.K. 1992. Die Gattung Pinnularia in Bayern. Denkschriften der Regenburgischen Botanischen Gesellschaft, Bd. 52, 308 pages.

Koppen, J.D. 1975. A morphological and taxonomic consideration of *Tabellaria* (Bacillariophyceae) from the north-central United States, Journal of Phycol., Vol. 11, pp. 236-244.

Longmore, M.E., O'Leary, B.M. and Rose, C.W. 1983. Caesium-137 profiles in the sediments of a partial-meromictic lake on Great Sandy Island (Fraser Island) Queensland, Australia. Hydrobiologia, Vol. 103, pp. 21-27.

MacDonald, J.D. 1969. Newfoundland Industrial Tour 1969, Industrial development, Newfoundland. Montreal Board of Trade tour. 60 pages.

Macdonald, R.W., Macdonald, D.M., O'Brien, M.C. and Gobeil, C. 1991. Accumulation of heavy metals (Pb, Zn, Cu, Cd),

carbon and nitrogen in sediments from Strait of Georgia, B.C., Canada. Marine Chemistry, Vol. 34, pp. 109-135.

MacKinnon, R.A. 1981. The Growth of Commercial Agriculture around St. John's, 1800-1935: A Study of Local Trade in Response to Urban Demand. Master of Arts, Department of Geography, Memorial University of Newfoundland, 109 pages.

MacKinnon, R.A. 1991. Farming the rock : The evolution of commercial agriculture around St. John's, Newfoundland, to 1945. Acadiensis, Vol. XX, No. 2, pp. 32-61.

Macpherson, J.B. and MacKinnon, R.A. 1988. Clearance, agriculture and suburbanization: effects on sedimentation in a small Newfoundland lake. In: 26th Congress of the International Geographical Union, Abstracts, Vol 2, Sydney, Australia, 21-26 August, 1988, 355 pages.

MacKereth, F.J.H. 1966. Some chemical observations on post-glacial lake sediments. Phil. Trans. R. Soc., Vol. B 250, pp. 165-213.

Mannion, A.M. 1989. Palaeoecological evidence for environmental change during the last 200 years. I. Biological data. Progress in Physical Geography, Vol. 13, No. 1, pp. 23-46.

Mannion, A.M. 1989. Palaeoecological evidence for environmental change during the last 200 years. II. Chemical data. Progress in Physical Geography, Vol 13, No. 1, pp. 192-215.

Manhes, G., Allegre, C.J., Dupre, B., and Hamelin, B. 1980. Lead isotope study of basic-ultrabasic layered complexes: speculations about the age of the earth and Primitive mantle characteristics. Earth and Planetary Science Letters, Vol. 47, pp. 370 - 382.

Marrie, P.J. 1984. Water Quality Study of: Mundy Pond, Kennys Pond, Long Pond, Kents Pond, Quidi Vidi Lake, Newfoundland Department of Environment, 13 pages.

Mason, R.P., Fitzgerald, W.F. and Morel, M.M. 1994. The biogeochemical cycling of elemental mercury: Anthropogenic influences. Geochimica et Cosmochimica Acta, Vol 58, No. 15, pp. 3191-3198.

Mathewes, R.W. and D'Auria, J.M. 1982. Historic changes in an

urban watershed determined by pollen and geochemical analysis of lake sediment. Canadian Journal of Earth Science, Vol. 19, pp. 2114 - 2125.

McCallum, I.M. 1981. The sources of variation in storm runoff quantity and quality in the partially urbanized Leary's Brook Basin, St. John's, Newfoundland. Masters of Science Thesis, Department of Geography, Memorial University of Newfoundland. 202 pages.

McLead, D. 1991. Magnetic spherules in recent lake sediments. In J.P. Smith, P.G. Appleby, R.W. Battarbee, J.A. Dearing, R. Flower, E.Y. Haworth, F. Oldfield and P.E. O'Sullivan (editors). Environmental History and Palaelimnology. Hydrobiologia, Vol. 214, pp. 91-97.

Meger, S.A. 1986. Polluted precipitation and the geochronology of mercury deposition in lake sediment of northern Minnesota. Water, Air, and Soil Pollution. Vol. 30, pp. 411-419.

Mehra, O.P., and Jackson, M.L. 1960. Iron oxide removal from soils and clays by dithionite-citrate system buffered with sodium bicarbonate, pp. 317-327, *In* Clays and clay minerals, proceedings of the Seventh National Conference, Edited by Swineford, A., London, Pergamon Press, 369 pages.

Molder, K. and Tynni, R. 1969. Uber Finnlands rezente und subfossile Diatomeen, III. Geological Survey of Finland, Bulletin 41, pp. 235-251.

Molder, K. and Tynni, R. 1971. Uber Finnlands rezente und subfossile Diatomeen, V. Geological Survey of Finland, Bulletin 43, pp. 203-220.

Molder, K. and Tynni, R. 1972. Uber Finnlands rezente und subfossile Diatomeen, VI. Geological Survey of Finland, Bulletin 44, pp. 141-159.

Moore, D.M. and Reynolds, R.C. 1989. X-ray diffraction and the identification and analysis of clay minerals. Oxford University Press, 332 pages.

Moore, P.D. and Webb, J. A. 1978. An illustrated guide to pollen analysis. New York, Wiley. 133 pages.

Moore, P.D., Webb, J.A. and Collison, M.E. 1991. Pollen analysis. second edition. Oxford, Blackwell Scientific

Publications. 216 pages.

Moss, B. 1981. The composition and ecology of periphyton communities in freshwaters. II. Inter-relationships between water chemistry, phytoplankton populations and periphyton populations in a shallow lake and associated experimental reservoirs ('lund tubes'). Br. phycol. J., Vol. 16, pp. 59-76.

Newfoundland Customs Returns, For the year 1944-1945.

Newfoundland Statistics Agency. 1992. Interprovincial trade flows of goods, Newfoundland and Labrador 1984-1988. Government of Newfoundland and Labrador. 185 pages.

Norton, S.A. and Kahl, J.S. 1991. Progress in understanding the chemical stratigraphy of metals in lake sediments in relation to acidic precipitation. Hydrobiologia, Vol 91, pp. 77-84.

Nriagu, J.O. and Coker, R.C. 1980. Trace metals in humic and fulvic acids from Lake Ontario sediments. Environmental Science and Technology, Vol. 14, No. 4, pp. 443-446.

O'Connell, M.F. and Andrews, C.W. 1976. Physical and Chemical conditions in Long Pond, St. John's, Newfoundland : A pond receiving both rural and urban runoff. Int. Revue ges. Hydrobiol., Vol. 61, No. 1, pp. 63-87.

O'Hara, S.L., Street-Perrott, F. Alayne and Burt, T.P., 1993. Accelerated soil erosion around a Mexican highland lake caused by prehispanic agriculture. Nature, Vol. 362, pp. 48-51.

O'Mally, V.P., Abrajano, Jr. T.A. and Hellou, J. 1996. Stable Carbon Isotopic Apportionment of Individual Polycyclic Aromatic Hydrocarbons in St. John's Harbour, Newfoundland. Environmental Science and Technology, Vol. 30, No. 2, pp. 634-639.

O'Neill, P. 1976. The Oldest City: The Story of St. John's, Newfoundland. Press Porcepic, 1040 pages.

Oldfield, F. and Appleby, P.G. 1984. Empirical testing of ^{210}Pb dating models. *In*: E.Y. Haworth and J.G. Lund (eds.), Lake Sediments and Environmental History, pp. 93-124. Leicester University Press.

Olsson, I.U. 1986. Radiometric dating. *In* Handbook of Holocene

Palaeoecology and Palaeohydrology. Editor B. Berglund: pp. 273-312. John Wiley and Sons.

Olsson, I.U. 1991. Accuracy and precision in sediment chronology. In J.P. Smith, P.G. Appleby, R.W. Battarbee, J.A. Dearing, R. Flower, E.Y. Haworth, F. Oldfield and P.E. O'Sullivan (editors). Environmental History and Palaelimnology. Hydrobiologia, Vol. 214, pp. 25-34.

Osborne, P.L. and Moss, B. 1977. Paleolimnology and trends in the phosphorous and iron budgets of an old man-made lake, Barton Broad, Norfolk. Freshwater Biology, Vol. 7, pp. 213-233.

Paetzel, M., Schrader, H. and Bjerkli, K. 1994. Do Decreased Trace Metal Concentrations in Surficial Skagerrak Sediments over the last 15-30 Years Indicate Decreased Pollution? Environmental Pollution, Vol. 84, pp. 213-226.

Patey, P.P. 1970. The Changing fortunes of the Long Pond Ecosystem. A brief submitted by the Newfoundland Natural History Society in defense of the preservation of Long Pond Marsh and the present course of Leary's Brook, 28 pages.

Patrick, R. and Reimer, C.W. 1966. The diatoms of the United States. Academy of Natural Sciences of Philadelphia, Monograph 13, Philadelphia, Pennsylvania, USA. 688 pages.

Patrick, S.T., Timberlid, J.A. and Stevenson, A.C. 1990. The significance of land-sue and land-management change in the acidification of lakes in Scotland and Norway : an assessment utilizing documentary sources and pollen analysis. Phil. Trans. R. Soc. Lond., Vol. B 327, pp. 363-367.

Pearson, R.E. (compiler and editor) 1969. Atlas of St.John's, Newfoundland. Dept of Geography, Memorial University of Newfoundland.

Pennington, W. Cambray, R.S. and Fisher, E.M. 1973. Observations on lake sediments using fallout Cs-137 as a tracer. Nature, Vol. 242, pp. 324-326.

Pennington, W. 1981. Records of a lake's life in time: the sediments. Hydrobiologia, Vol. 79, pp. 197-219.

Petit, D., Mennessiner, J.P. and Lamberts, L. 1984. Stable lead isotopes in pond sediments as tracer of past and

present atmospheric lead pollution in Belgium. Atmospheric Environment, Vol 18, No. 6. pp. 1189-1193.

Phillips, G.L., Eminson, D. and Moss, B. 1978. A mechanism to account for macrophyte decline in progressively eutrophicated freshwaters. Aquatic Botany, Vol. 4, pp. 103-126.

Pierson, W.R, Gorse, R.A., Szkarlat, A.C., Brachaczek, W.W., Japar, S.M. and Lee, F.S.C. 1983. Mutagenicity and chemical characteristics of carbonaceous particulate matter from vehicles on the road. Environmental Science Technology, Vol 17, No 1, pp. 31-44.

Project Planning Associates. 1961. City of St. John's, Newfoundland. Urban Renewal Study, 84 pages.

Prowse, D.W. 1895. History of Newfoundland. Macmillan and Company, London, 631 pages.

Qvarfort, U. 1983. The influence of mining on Lake Tisken and Lake Runn. Bull. Geol. Inst. Univ. Uppsala, Vol. 10, pp. 111-130.

Reasoner, W.A. 1986. An inexpensive, lightweight percussion core sampling system. Geographie physique et Quaternaire, Vol. XL, No. 2, pp. 217-219.

Renberg, I., Brodin, Y.W., Gronberg, G., El-Daoushy, F., Oldfield, F., Rippey, B., Sandoy, S., Wallin, J.E. and Wik. 1990. Recent acidification and biological changes in Lilla Oresjon, southwest Sweden, and the atmospheric pollution and land use history. Phil. Trans. R. Soc. Lond., Vol. B 327, pp. 391-396.

Renberg, I. Korsman, T. and Anderson, N.J. 1990. Spruce and surface water acidification : an extended summary. Phil. Trans. R. Soc. Lond., Vol. B 327, pp. 371-372.

Renberg, I. Korsman, T. and Birks, H.J.B. 1993. Prehistoric increases in the pH of acid-sensitive Swedish lakes caused by land-use changes. Nature, Vol. 362, pp. 824-827.

Renberg, I., Person, M.W. and Emteryd, O. 1994. Pre-Industrial atmospheric lead contamination detected in Swedish lake sediments. Nature, Vol. 368, pp. 323-326.

Renberg, I. and Wik M. 1984. Dating recent Lake Sediment by

soot particle counting. Verh. Internat. Verein. Limnol., Vol. 22, pp. 712-718.

Rippey, B. 1990. Sediment chemistry and atmospheric contamination. Phil. Trans. Royal Society of London, Vol B 327, pp. 311-317.

Ritson, P.I., Esser, B.K., Niemeyer, S. and Flegal, A.R. 1994. Lead isotopic determination of historical sources of lead to Lake Erie, North America. Geochimica et Cosmochimica Acta, Vol. 58, No. 15, pp. 3292-3305.

Robertson, B. (prepared for Dr. David Alexander) 1986. Newfoundland Small Industries. A Collection of News Stories, 1886-1990.

Rock-Color Chart. 1984. Geological Survey of America, P.O. Box 9140, Boulder, Colorado, 80301, U.S.A.

Rogers, P.J. and Ogden, J.G. III. 1991. Geochemical background: implications for environmental geochemistry in Nova Scotia, Canada. In F. Mrna (Editor), Exploration Geochemistry 1990. Geol. Surv. Czechoslovakia, Prague, pp. 318-323.

Rogers, P.J., Fortescue, J.A.C. and Ogden, J.G. 1991. Baseline geochemical mapping using lake sediments. *In* F. Mrna (editor), Exploration Geochemistry 1990. Geol. Surv. Czechoslovakia, Prague, pp. 312-317.

Rose, N.L. and Juggins, S. 1994. A spatial relationship between carbonaceous particles in lake sediment and sulphur deposition. Atmospheric Environment, Vol. 28, No. 2, pp. 177-183.

Rosman, K.J.R., Chisholm, W., Boutron, C.F., Candelone, J.P. and Gorlach, U. 1993. Isotopic evidence of for the source of lead in Greenland snows since the late 1960s. Nature, Vol. 362, pp. 333-335.

Rosman, K.J.R., Chisholm, W., Boutron, C.F., Candelone, J.P. and Hong, S. 1994. Isotopic evidence to account for changes in the concentration of lead in Greenland snow between 1960 and 1988. Geochimica et Cosmochimica Acta, Vol. 58, No. 15, pp. 3265-3269.

Ross, R. (editor). 1981. Proceedings of the Sixth Symposium on Recent and Fossil Diatoms. Budapest, Sept. 1-5, 1980. Koenigstein, Science Publishers. 487 pages.

Round, F.E. 1990a. The Diatoms: Biology and Morphology of the genera. Cambridge, Cambridge University Press. 747 pages.

Round, F.E. 1990b. Diatom communities - their response to changes in acidity. Phil. Trans. R. Soc. Lond., Vol. B 327, pp. 243-247.

Royal Society of Canada. 1986. Commission on Lead in the Environment. Lead in the Canadian Environment: science and regulation: Final Report. 374 pages.

Schoeman, F.R. and R.E.M. Archibald. 1976-1980. The diatom flora of Southern Africa. CSIR Special Report WAT 50, National Institute for Water Research. Council for Scientific and Industrial Research, Pretoria, South Africa. Loose leaves in binders.

Scruton, D.A., Elner, J.K. and Ray, S.N. 1990. Fossil diatom inferred reconstruction of the pH history of two acidic, clear water lakes from insular Newfoundland, Canada. *In* J. P. Smith, P. G. Appleby, R. W. Battarbee, J. A. Dearing, R. Flower, E. Y. Haworth, F. Oldfield and P. E. O'Sullivan (editors). Environmental History and Palaelimnology. Hydrobiologia, Vol. 214, pp. 107-114.

Scruton, D.A., Elner, J.K., and Howell, G.D. 1987. Paleolimnological Investigation of Freshwater Lake Sediments in Insular Newfoundland. Part 2: Downcore Diatom Stratigraphies and Historical pH Profiles for Seven Lakes. Canadian Technical Report of Fisheries and Aquatic Sciences No. 1521. Science Branch, Dept. of Fisheries and Oceans, St. John's, Newfoundland. 67 pages.

Shirahata, H., Elias, R.W. and Patterson, C.C. 1980. Chronological variations in concentrations and isotopic compositions of anthropogenic atmospheric lead in sediments of a remote subalpine pond. Geochimica et Cosmochimica Acta, Vol. 44, pp. 149-162.

Shotyk, W., Cheburkin, A.K., Appleby, P.G., Fankhauser, A. and Krammers, I.D. 1996. Two thousand years of atmospheric arsenic, antimony, and lead deposition recorded in an ombrotrophic peat bog profile, Jura Mountains, Switzerland. Earth and Plantery Science Letters, Vol. 145, pp. E1-E7.

Simola, H., Huttunen, P., Ronkko, J., and Uimonen-Simola, P. 1991. Palaeolimnological study of an environmental monitoring area, or, Are there pristine lakes in Finland?

In J. P. Smith, P. G. Appleby, R. W. Battarbee, J. A. Dearing, R. Flower, E. Y. Haworth, F. Oldfield and P. E. O'Sullivan (editors). Environmental History and Palaelimnology. Hydrobiologia 214: pp 187-190.

Smith, N.H. 1962. St. John's, Newfoundland. North Americas Oldest City, E.C. Boone, 59 pages.

Smol, J.P. 1980. Fossil synuracean (Chrysophyceae) Scales in lake sediments: a new group of paleoindicators. Canadian Journal of Botnay. Vol. 58, pp. 458-465.

Smol, J.P. 1981. Problems associated with the use of "species diversity" in paleolimnological studies. Quaternary Research, Vol. 15, pp. 209-212.

Smol, J.P.1983 Paleophycology of a high arctic lake near Cape Herschel, Ellesmere Island. Canadian Journal of Botany, Vol. 61, pp. 2195-2204.

Smol, J.P. 1988. Methods in Quaternary Ecology #1. Freshwater Algae. Geoscience Canada, Vol. 14, No. 4, pp. 208-217.

Smol, J.P. 1992. Paleolimnology: an important tool for effective ecosystem management. Journal of Aquatic Ecosystem Health, Vol. 1, pp. 49-58.

Smol, J.P., Battarbee, R.W., Davis, R.B. and Merilainen, J., 1986, eds. Diatoms and Lake Acidity. Dr. W. Junk Publishers, Dordrecht, 307 pages.

Smol, J.P., Brown, S.R. and McNeely, R.N., 1983. Cultural disturbances and trophic history of a small lake from central Canada. Hydrobiologia, Vol. 103, pp. 125-130.

Stanton, R.L. and Russell, R.D. 1959. Anomalous leads and the emplacement of lead sulphide ores. Economic Geology, Vol. 54, pp. 588-607.

Stokes, P.M. and Yung, Y.K. 1986. Phytoplankton in selected LaCloche (Ontario) lakes, pH 4.2-7.0, with special reference to algae as indicators of chemical characteristics. *In* J.P. Smol, R.W. Battarbee, R.B. Davis, and J. Merilainen (editors), Diatoms and Lake Acidity. Dordrecht: Dr. W. Junk Publishers.

Stuiver, M. and Reimer, P.J., 1993. Extended 14C database and revised CALIB radiocarbon calibration program.

Radiocarbon, vol. 35. Pp. 215-230.

Stuiver, M., Reimer, P.J., Bard, E., Beck, J.W., Burr, G.S., Hughen, K.A., Kromer, B., McCormac, F.G, v. d. Plicht, J., and Spurk, M., 1998a. INTCAL98 Radiocarbon age calibration 24,00 - 0 cal BP. Radiocarbon Vol. 40. pp. 1041-1083.

Stukas, V.J. and Wong, C.S. 1981. Stable lead isotopes as a tracer in coastal waters. Science, Vol 211, pp. 1424-1427.

Sturges, W.T. and Barrie, L.A. 1987. Lead 206/207 isotope ratios in the atmosphere of North America as tracers of US and Canadian emissions. Nature, Vol. 329, pp. 144-146.

Sturges, W.T. and Barrie, L.A. 1989. The use of stable lead 206/207 isotope ratios and elemental compositions to discriminate the origins of lead in aerosols at a rural site in eastern Canada. Atmospheric Environment, Vol 23, No. 8. pp. 1645-1657.

Sugden, C.L., Farmer, J.G. and Mackenzie, A.B. 1991. Lead and $^{206}Pb/^{207}Pb$ profiles in ^{210}Pb-dated ombrotrophic peat cores from Scotland. Heavy Metals in the Environment, Vol. 1, pp. 90-93.

Sugden, C.L., Farmer, J.G. and Mackenzie, A.B. 1991. Isotopic characteristics of lead inputs and behaviour in recent Scottish freshwater Loch sediments. Heavy Metals in the Environment, Vol 1, pp. 511-514.

Sugden, C.L., Farmer, J.G. and Mackenzie, A.B. 1991. Isotopic ratios of lead in contemporary environmental material from Scotland. Environmental Geochemistry and Health, Vol 15, No. 2/3, pp. 59-65.

Sunderland and Simard Town Planning Consultants and Canadian-British engineering Consultants. 1970. Saint John's Master Plan Document Number Five: Flow Systems. In Plan, '91: City of St. John's, Newfoundland. Unpublished draft master plan report (Second Draft), St. John's, 31 pages.

Swaine, D.J. 1990. Trace elements in coal. Butterworths, London.

Tessier, A., Carignan, R., Dubreuil, B. and Rapin, F. 1989. Partitioning of zinc between the water column and the oxic sediments in lakes. Geochimica et Cosmochimica Acta,

Vol. 53, pp. 1511-1522.

The Working Group on Environment (Publisher). 1971. Environment 2001, An Integrated Plan For Utilization The Natural Waters of The Quidi Vidi System in St. John's. 18 pages.

Tynni, von R. 1975. Uber Finnlands rezente undsubfossile Diatomeen, VIII. Geological Survey of Finland, Bulletin 274, 35 pages.

Tynni, von R. 1976. Uber Finnlands rezente undsubfossile Diatomeen, IX. Geological Survey of Finland, Bulletin 284, 37 pages.

Tynni, von R. 1978. Uber Finnlands rezente undsubfossile Diatomeen, X. Geological Survey of Finland, Bulletin 296, 55 pages.

Tynni, von R. 1980. Uber Finnlands rezente undsubfossile Diatomeen, XI. Geological Survey of Finland, Bulletin 312, 93 pages.

VanLandingham, S. L. 1967 - 1979. Catalogue of the fossil and recent genera and species of diatoms and their synonyms. Cramer, Lahre to Vaduz, 4654 pages.

Vardy, S. 1991. The Deglaciation and Early Postglacial Environmental History of south-central Newfoundland: Evidence from the palynostratigraphy of lake sediments. Unpublished M.Sc. thesis, Department of Geography, Memorial University of Newfoundland, 208 pages.

Vinyard, W.C. 1979. Diatoms of North America. Mad River Press, Eureka, California, 119 pages.

Vuorela, I. 1980. Microspores of *Isoetes* as indicators of human settlement in pollen analysis. Memoranda Soc. Fauna Flora Fennica, Vol. 56, pp. 13-19.

Weber, C. I. 1971. A Guide to the Common Diatoms at Water Pollution Surveillance System Stations. U.S. Environmental Protection Agency, 98 pages.

Werner, D. (editor). 1977. The biology of diatoms. Blackwell, Oxford, U.K. 498 pages.

Wesselink, L.G., Meiwes, K-J., Matzner, E. and Stein, A. 1995. Long-term changes in water and soil chemistry in spruce

and beech forests, Solling, Germany. Environmental Science Technology, Vol. 29, No. 1, pp. 51-58.

Wik, M., Renberg, I. and Darley, J. 1986. Sedimentary Records of Carbonaceous particles from fossil fuel combustion. Hydrobiologia, Vol. 143, pp. 387-394.

Wik, M. and Renberg, I. 1987. Distribution in forest soils of carbonaceous particles from fossil fuel combustion. Water, Air and Soil Pollution, Vol. 33, pp. 125-129.

Wik, M. and Renberg, I. 1991a. Recent atmospheric deposition in Sweden of carbonaceous particles from fossil-fuel combustion surveyed using lake sediments. Ambio, Vol. 20, No. 7, pp. 289-292.

Wik, M. and Renberg, I. 1991b. Spheroidal carbonaceous particles as a marker for recent sediment distribution. In J.P. Smith, P.G. Appleby, R.W. Battarbee, J.A. Dearing, R. Flower, E.Y. Haworth, F. Oldfield and P.E. O'Sullivan (editors). Environmental History and Palaelimnology. Hydrobiologia, Vol. 214, pp. 85-90.

Williams, D.M. 1985. Morphology, taxonomy and inter-relationships of the ribbed araphid diatoms from the genera Diatoma and Meridion (Diatomaceae: Bacillariophyta). Bibliotheca Diatomologica, Vol. 8: 228 p. + 27 plates.

Williams, D.M. 1986. Comparative morphology of some species of Synedra Ehrenb. Diatom Research, Vol. 1, pp. 131-152.

Williams, D.M. and Round, F.E. 1986. Revision of the genus Synedra Ehrenb. Diatom Research, Vol. 1, pp. 313-339.

Williams, D.M. and Round, F.E. 1987. Revision of the genus Fragilaria Ehrenb. Diatom Research, Vol 2, pp. 267-288.

Winchester, J.N. and Nifong, G.D. 1971. Water pollution in Lake Michigan by trace elements from pollution aerosol fallout. Water, Air, Science Pollution, Vol. 1, pp. 50-64.

Working Group on Environment. 1971. Report on the activities of the Working Group on Environment in St. John's, Newfoundland, 4 pages.

Zierler, A. and Mustard, C. 1982. Signal Hill, An Illustrated History. Newfoundland Historic Trust Co-Operating

Association, Signal Hill National Historic Park. St. John's, Newfoundland, 47 pages.

Plate 1

Charcoal particle. (scale: X 40)

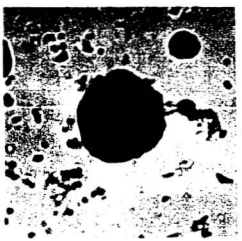

Soot particle. (scale: X 63)

Oil droplet. Another, smaller droplet can be seen in the lower left corner. (Scale X 100)

Soot 'A' particle. (scale: X 40)

Appendix A

Core sites, location, water depth and core lengths.

Core Sample sites					
Lake	Core #	UTM Coordinates Zone 22		Water Depth (m)	Core Length (cm)
		Easting	Northing		
Quidi Vidi Lake	QV1	372670	5270875	12.0	160
	QV2	372680	5270870	12.5	200
	QV3	372850	5270975	8.5	200
	QV4	372860	5270970	9.5	160
Long Pond, St.John's	LP1	369700	5270825	9.5	168
	LP2	369710	5270825	9.5	178
	LP3	369500	5270630	9.0	155
	LP4	369510	5270630	10.0	165
	LP5	369505	5270635	8.5	115
Mundy Pond	MP1	369050	5267725	1.0	103
	MP2	369055	5267725	1.0	51
Georges Pond	GP1	373125	5269950	8.0	130
	GP2	373135	5269950	8.0	90
Long Pond, Witless Bay Line	LPW	360310	5241190	4.5	145

Appendix B: Sample Preparation

For Total and Acid Extractable Elemental Analysis

Sample dissolution for total element contents, was completed by first measuring 2 g of sediment into a glass beaker. The sample was ashed at 600°C for 3 hours, and transferred to a 125 ml teflon beaker where 15 ml of concentrated HF was added followed by a 1:1 mixture of 5 ml of concentrated 50% HCl and 5 ml of $HClO_4$. The sample was mixed and left overnight. The beakers were placed on a hot plate and brought to dryness at 200°C, after which approximately 50 ml of 20% HCl was added and the samples were returned to the hot plate and heated at 100°C until the residue dissolved. The solution was transferred to a 100 ml volumetric flask, cooled and made up to volume with deionized water.

For the acid-extractable analysis, 1 g of sediment was weighed into a glass test tube, 6 ml of 4M HNO_3 - 0.1M HCl were added and left to stand overnight. The samples were stirred, placed in a water bath for two hours at 90°C, stirred again, removed and cooled. The leached solution was then made up to volume with deionized water, mixed and allowed to clear (i.e. particulates allowed to settle).

For mercury determination (via 'cold vapor' atomic absorption spectrophotometry) 0.5 g of dried sediment was dissolved in 20 ml of concentrated HNO_3 and 1 ml of

concentrated HCl in test tube at room temperature for 10 minutes. The test tube was then placed in a water bath at 90°C and allowed to digest for two hours with periodic shaking. After cooling, the solutions were made up to 100 mL with deionized water. The Hg present at that stage was reduced to the elemental state by the addition of 10% weight by volume $SnSO_4$. The Hg vapour was then flushed by a stream of air into an absorption cell mounted in the light path of an atomic absorption spectrophotometer.

Palynomorph and Diatom Preparations

One cubic centimetre sub-samples for pollen were first placed in a plastic test tube and exotic *Lycopodium* spores of known concentration were added. Sample treatment included successive washes in 10% HCl, concentrated HF and concentrated acetic acid. A 9:1 acetic anhydride and concentrated sulphuric acid mixture was added after which it was placed in a warm water bath and stirred for 3 minutes. The sample was washed with concentrated acetic acid and distilled water, stained with Safranin O, stirred, washed and transferred to storage vials. Samples for visual examination were prepared by mounting one or two drops of residue on a slide, allowing it to dry and gluing a cover glass with the bioplastic Elvacite™.

One cubic centimetre sub-samples for diatom preparation were placed in plastic test tubes and treated with successive

acid washes. First, 10% HCl was added, warmed in water bath for 10 minutes and stirred occasionally. Following this 10 ml of 30% H_2O_2 was added and left to react overnight. If residual organics remained the samples were placed in a warm water bath for approximately 4 to 5 hours. The remaining solution was centrifuged and decanted. One part $K_2Cr_2O_7$ solution to two parts concentrated H_2SO_4 was added separately (dichromate before the acid), stirred occasionally and left overnight. Samples were washed, a known concentration of lycopodium spores added, stained with Safranin O and transferred to storage vials.

Prior to visual examination 1 cc of the suspension was placed in a test tube and diluted 10 to 20 times with distilled water. A drop of this solution was placed on a cover slip and allowed to dry. Several drops of the mounting medium, Nafrax™, was placed on a slide and heated on a hot plate. The mounting medium was allowed to bubble after which the cover slip with the diatoms was inverted and placed onto the hot glue. The slide was removed and allowed to cool.

Sample preparation for Common Pb Isotopic Ratios

At Geotop, Universite du Quebec a Montreal common Pb isotopes were determined quantitatively by mass spectrometer. Sample preparation was completed under a controlled atmosphere of a clean room with purified reagents (Manhes et al., 1980).

Sample preparation was modified from Carignan et al. (1993). Five to ten milligrams of sediment were washed in 6N HCl for 12 hours, rinsed with distilled water and allowed to dry. A dilute mixture HF and aqua regia was added and allowed to stand for 30 minutes. The supernatant and residue were recovered and dissolved in HF. Lead was separated from the solution by passing it through anion exchange resin AGI-X8 as described by Manhes et al. (1980).

Clay and Mineral Preparation

Two grams of dried sediment were placed in a 50 mL plastic beaker, filled to 40 mL with distilled water and disaggregated using ultrasonic treatment for approximately three minutes. The samples was transferred to a 100 mL glass beaker, 50 mL of 15% H_2O_2 was added and allowed to react to completeness. The sediment was allowed to settle and the solution decanted. If after several days the sample continued to react it was transferred to test tubes, centrifuged and decanted. Five subsequent treatments with peroxide followed.

Iron was removed from the sample following a procedure modified from Mehra and Jackson (1960). Four mL of 0.6 M sodium citrate followed by 1 mL of 1 M sodium bicarbonate were added to the sample. The sample was placed in a water bath heated to 85°C and one gram of solid sodium dithionite ($Na_2S_2O_4$) was added. The sample was stirred intermittently and

removed after 15 minutes. Approximately 10 drops of saturated $MgCl_2$ solution was added to aid flocculation after which the sample was centrifuged and the solution decanted. Samples were washed with distilled water and placed in an ultracentrifuge for 15 min at 15,000 rpm. This step was repeated twice.

The less than 2 μm size fraction was separated in a column of water using a settling equation from Folk (1980):

$$T = \frac{D}{1500 * A * d^2}$$

where:

T is the settling time in minutes, D is depth of withdrawal in cm, d is particle diameter in mm and A is a constant dependant on viscosity of liquid, the gravitational force and particle density (A=3.57 at 20°C).

The sample was placed in a column of water, agitated and allowed to settle to a depth such that the upper portion of water contained only the clay size fraction (< 2μm) in suspension which was siphoned off. Sediment was allowed to settle out and the water decanted. Saturated $MgCl_2$ solution was added to the clay fraction and washed five subsequent times with distilled water. Saturated $MgCl_2$ was added to aid in clay classification (Moore and Reynolds, 1989). The < 2 μm fraction for all samples was stored in air tight vials until analysis.

Sample preparation for Radiometric dates (^{210} Pb, ^{137}Cs and ^{14}C)

Measurements for ^{210}Pb, ^{226}Ra and ^{137}Cs by Dr. P. Appleby at the University of Liverpool, UK, were made on 1 g of dried sediment using a well-type coaxial low background intrinsic germanium detector fitted with a NaI(Tl) escape suppression shield (Appleby et al., 1986). ^{137}Cs, ^{226}Ra and ^{210}Pb were measured, by Becquerel Labs, Mississauga, on 10 g of sediment by gamma spectrometry for eight hours.

Sample preparation for radiocarbon (^{14}C) dating, completed at the Radiocarbon Dating Laboratory, Geological Survey of Canada, Ottawa was as follows; approximately 25 to 30 g of bulk sample was treated with hot acid and distilled water rinses. Yielded CO_2 was counted for one or two counts of between 2090 and 2600 minutes in a 2-L or 5-L counter. Mixing ratios for the counts were 1.00 for all except one in which the mixing ratio was 1.13.

Appendix C: Lake sediment geochemical data

Core QV1

core QV1 Sample #	Depth (cm)	Ag (6) (ppm)	Al (2) (%)	As (1) (ppm)	Au (1) (ppb)	Ba (1) (ppm)	Ba (2) (ppm)	Be (2) (ppm)	Br (1) (ppm)	Ca (2) (%)
QV1-002	1	0.5	6.82	13.0	20.0	600	601	4.0	20.0	0.51
QV1-004	3	0.5	6.89	12.0	18.0	520	609	3.9	18.0	0.52
QV1-006	5	0.4	6.96	12.0	19.0	530	618	4.1	17.0	0.47
QV1-008	7	0.7	6.92	11.0	16.0	530	618	4.0	16.0	0.49
QV1-010	9	0.8	7.16	12.0	14.0	580	635	3.8	16.0	0.51
QV1-012	11	0.8	7.52	11.0	13.0	540	629	3.6	13.0	0.43
QV1-014	13	0.7	7.58	11.0	17.0	530	640	3.4	13.0	0.42
QV1-016	15	0.6	7.77	11.0	13.0	510	628	3.5	12.0	0.41
QV1-018	17	0.6	7.72	12.0	15.0	600	636	3.3	13.0	0.42
QV1-020	19	0.6	7.70	13.0	12.0	580	635	3.3	13.0	0.42
QV1-022	21	0.6	7.52	13.0	15.0	580	623	3.2	13.0	0.42
QV1-024	23	0.6	7.50	13.0	15.0	570	616	3.1	14.0	0.42
QV1-026	25	0.6	7.59	13.0	14.0	540	613	3.1	14.0	0.43
QV1-028	27	0.5	7.51	13.0	16.0	590	608	3.1	13.0	0.44
QV1-030	29	0.6	7.60	14.0	17.0	550	608	3.0	14.0	0.42
QV1-032	31	0.7	7.51	15.0	21.0	530	602	3.2	15.0	0.37
QV1-034	33	0.7	7.58	19.0	18.0	500	542	3.4	17.0	0.35
QV1-036	35	0.7	7.52	23.2	28.0	490	524	3.7	20.1	0.33
QV1-038	37	0.6	7.56	22.7	26.0	480	497	3.6	21.9	0.33
QV1-040	39	0.7	7.23	23.6	39.0	470	488	3.8	24.5	0.29
QV1-042	41	0.6	6.93	22.5	40.0	400	459	4.1	21.6	0.27
QV1-044	43	0.6	6.89	19.0	49.0	410	444	3.9	25.1	0.25
QV1-046	45	0.6	6.69	22.2	45.0	430	440	4.0	32.9	0.26
QV1-048	47	0.6	6.68	17.0	38.0	410	429	4.2	27.7	0.24
QV1-050	49	0.4	6.73	15.0	18.0	360	429	4.8	26.1	0.24
QV1-055	52.5	0.5	6.58	19.0	14.0	400	409	4.6	30.8	0.25
QV1-060	57.5	0.5	6.19	11.0	10.0	340	371	4.1	32.5	0.22
QV1-065	62.5	0.5	5.49	10.0	4.6	260	309	4.0	40.4	0.24
QV1-070	67.5	0.4	4.25	6.1	<2	220	239	3.5	72.9	0.27
QV1-075	72.5	0.4	5.02	8.9	<2	230	270	4.0	59.0	0.26
QV1-080	77.5	0.4	4.39	6.0	<2	220	241	3.6	70.6	0.28
QV1-085	82.5	0.4	4.55	5.4	3.4	170	247	3.8	62.9	0.28
QV1-090	87.5	0.4	4.56	6.2	<2	210	244	3.9	63.9	0.29
QV1-095	92.5	0.4	4.55	6.0	<2	200	240	4.1	61.5	0.29
QV1-100	97.5	0.4	4.70	6.4	<2	220	259	4.2	59.0	0.29
QV1-105	102.5	0.4	4.77	6.5	<2	200	259	4.3	59.9	0.30
QV1-110	107.5	0.4	4.94	6.2	3.8	210	270	4.6	54.3	0.32
QV1-115	112.5	0.5	4.71	6.1	<2	190	251	4.9	54.1	0.31
QV1-120	117.5	0.5	4.87	7.1	<2	210	261	5.3	56.6	0.32
QV1-125	122.5	0.5	4.72	7.3	<2	210	254	5.4	55.9	0.32
QV1-130	127.5	0.4	4.77	8.1	<2	210	255	5.7	53.9	0.32
QV1-135	132.5	0.4	4.68	6.6	<2	200	255	5.6	48.9	0.32
QV1-140	137.5	0.3	4.65	7.1	<2	220	254	5.7	52.3	0.33
QV1-145	142.5	0.4	4.08	7.4	<2	220	229	5.2	49.8	0.29
QV1-150	147.5	0.4	4.81	6.5	<2	230	271	5.9	49.4	0.33
QV1-155	152.5	0.4	4.87	7.2	<2	210	265	6.2	51.9	0.33
QV1-160	157.5	0.4	4.88	7.3	<2	240	265	6.3	49.6	0.34

Core QV1

Depth (cm)	Cd (2) (ppm)	Cd (3) (ppm)	Ce (1) (ppm)	Ce (2) (ppm)	Co (1) (ppm)	Co (2) (ppm)	Co (3) (ppm)	Cr (1) (ppm)	Cr (2) (ppm)	Cr (2a) (ppm)
1	1.9	1.6	120	119	18.0	23	11	72.0	70	69
3	1.8	1.6	110	118	19.0	22	11	65.0	71	69
5	1.8	1.5	110	121	19.0	22	11	79.0	70	68
7	1.8	1.5	100	122	20.0	22	11	64.0	66	66
9	1.5	1.4	110	119	20.0	22	13	54.0	60	58
11	1.4	1.3	93	117	18.0	22	14	50.0	53	52
13	1.5	1.3	90	110	20.0	21	13	29.0	54	51
15	1.4	1.3	81	113	17.0	22	13	42.0	55	49
17	1.4	1.2	91	112	21.0	21	12	47.0	52	46
19	1.3	1.1	100	112	16.0	21	12	51.0	50	46
21	1.3	1.1	95	108	19.0	21	12	34.0	45	42
23	1.3	1.2	99	104	19.0	20	12	32.0	45	40
25	1.2	1.1	94	100	17.0	20	11	38.0	46	39
27	1.3	1.1	95	99	17.0	20	12	44.0	44	37
29	1.3	1.1	94	95	20.0	20	12	33.0	47	40
31	1.2	1.0	83	99	20.0	22	13	36.0	48	43
33	1.0	0.8	88	100	22.0	23	14	41.0	51	47
35	0.9	0.8	80	101	23.0	26	15	46.0	56	51
37	0.7	0.6	98	101	30.0	28	17	53.0	56	51
39	0.9	0.7	90	99	34.0	31	19	48.0	52	49
41	0.5	0.4	91	101	36.0	37	23	38.0	49	44
43	0.4	0.3	100	108	35.0	29	19	48.0	44	40
45	0.5	0.4	110	112	47.0	41	28	38.0	40	37
47	0.4	0.3	100	10	54.0	48	33	24.0	40	38
49	0.3	0.2	130	134	39.0	36	23	25.0	36	34
52.5	0.3	0.3	140	140	66.0	55	35	40.0	36	33
57.5	0.3	0.2	120	132	49.0	44	27	26.0	31	28
62.5	0.3	0.3	120	138	46.0	46	27	22.0	24	23
67.5	0.4	0.3	110	113	19.0	17	9	32.0	19	17
72.5	0.5	0.4	150	140	41.0	36	22	<15	21	20
77.5	0.5	0.3	130	125	17.0	16	9	23.0	18	17
82.5	0.5	0.3	120	125	16.0	16	9	25.0	18	18
87.5	0.5	0.3	130	134	21.0	18	11	<15	19	18
92.5	0.5	0.4	130	141	18.0	19	12	18.0	24	23
97.5	0.4	0.3	130	138	20.0	19	11	23.0	22	19
102.5	0.4	0.4	140	137	22.0	20	12	41.0	19	17
107.5	0.5	0.4	140	149	20.0	20	12	<15	21	18
112.5	0.6	0.4	130	157	19.0	20	11	20.0	18	16
117.5	0.5	0.4	170	169	22.0	22	12	42.0	18	16
122.5	0.6	0.4	190	173	23.0	21	13	26.0	18	17
127.5	0.7	0.5	200	188	33.0	28	18	17.0	17	17
132.5	0.6	0.5	170	183	24.0	25	14	30.0	18	17
137.5	0.7	0.5	170	178	26.0	24	14	35.0	47	45
142.5	0.6	0.4	180	161	25.0	21	14	<15	26	25
147.5	0.4	0.4	180	186	25.0	23	12	25.0	27	25
152.5	0.8	0.5	190	185	24.0	21	13	19.0	19	17
157.5	0.8	0.5	180	188	24.0	23	14	21.0	29	25

Core QV1

Depth (cm)	Cs (1) (ppm)	Cu (2) (ppm)	Cu (3) (ppm)	Dy (2) (ppm)	Eu (1) (ppm)	Fe (1) (%)	Fe (2) (%)	Fe (3) (%)	Ga (2) (ppm)	Hf (1) (ppm)
1	7.0	157	121	8.2	2.60	8.30	7.31	5.91	23	5.40
3	6.6	151	118	7.9	3.20	7.70	6.97	5.52	23	5.30
5	6.6	151	116	8.7	4.00	7.40	6.94	5.38	24	5.80
7	6.1	147	112	8.3	3.80	7.00	6.86	5.39	24	5.50
9	6.2	118	94	8.0	2.40	6.80	6.37	4.94	23	4.60
11	6.0	95	73	7.6	3.10	5.50	5.92	4.19	26	5.00
13	6.4	87	71	7.1	2.30	5.80	5.85	4.03	26	5.80
15	5.9	93	69	7.2	1.80	5.40	5.88	4.03	24	5.40
17	6.7	84	63	7.0	3.00	6.30	5.73	3.74	25	5.80
19	6.9	80	61	7.0	2.00	6.10	5.66	4.32	26	5.90
21	6.1	79	59	6.8	2.50	5.80	5.48	4.23	25	5.90
23	6.1	77	58	6.7	2.70	5.90	5.42	4.05	24	5.40
25	5.8	75	58	6.7	2.10	5.70	5.38	4.24	22	5.50
27	5.9	73	55	6.5	2.30	5.60	5.35	4.00	24	5.80
29	5.9	74	56	6.2	2.80	5.40	5.37	3.97	22	5.90
31	5.2	77	56	6.3	3.00	5.30	5.40	4.13	23	5.80
33	5.5	73	54	6.4	2.20	5.80	5.51	4.22	25	5.30
35	5.7	70	49	6.7	2.20	6.40	5.82	4.59	24	5.50
37	6.3	56	39	6.7	2.10	7.10	6.17	5.03	24	5.60
39	5.9	57	38	6.7	2.20	7.20	6.37	4.77	24	5.90
41	5.7	44	30	7.2	2.00	6.40	6.33	4.77	23	5.00
43	6.2	38	26	6.8	2.70	5.80	5.45	4.12	22	5.50
45	5.7	39	28	7.1	2.70	5.60	5.16	3.94	21	5.50
47	5.7	35	25	7.3	3.20	6.90	6.53	4.98	22	4.80
49	6.4	35	25	8.6	3.70	6.20	6.10	4.55	22	4.60
52.5	6.5	35	24	8.9	3.80	5.80	5.57	4.19	20	4.50
57.5	6.4	20	14	7.9	3.30	5.30	4.83	3.62	18	3.60
62.5	5.3	17	12	7.9	3.10	4.10	4.08	3.00	15	2.90
67.5	3.6	19	12	6.9	2.90	2.80	2.54	1.79	9	2.60
72.5	4.6	18	13	7.9	5.00	3.80	3.40	2.46	13	3.60
77.5	3.6	17	12	7.2	3.40	2.60	2.36	1.67	11	2.20
82.5	3.7	17	12	7.3	3.30	2.40	2.27	1.59	11	2.70
87.5	4.2	19	13	7.6	3.80	2.20	2.22	1.58	11	2.90
92.5	3.4	19	13	8.0	4.60	2.30	2.18	1.56	10	2.10
97.5	4.5	19	13	8.0	3.80	2.30	2.22	1.63	11	2.90
102.5	4.0	20	14	8.2	4.20	2.40	2.24	1.61	10	1.90
107.5	4.0	21	15	8.6	4.10	2.40	2.32	1.70	11	3.10
112.5	3.8	20	15	9.1	3.30	2.30	2.29	1.66	11	2.10
117.5	4.0	22	16	9.6	3.90	2.70	2.42	1.75	11	3.20
122.5	4.3	20	14	9.7	4.90	2.60	2.27	1.63	10	1.90
127.5	3.7	22	17	10.5	6.00	2.60	2.32	1.58	11	2.70
132.5	3.6	21	15	10.2	5.20	2.20	2.26	1.53	10	2.00
137.5	3.7	22	16	10.1	4.80	2.20	2.27	1.55	9	2.10
142.5	3.6	19	15	9.1	4.90	2.40	2.09	1.58	9	2.20
147.5	4.3	22	16	10.6	4.00	2.40	2.32	1.54	10	2.50
152.5	4.4	24	17	10.8	5.30	2.60	2.36	1.63	10	1.70
157.5	3.8	24	17	10.8	4.30	2.60	2.44	1.66	12	2.10

Core QV1

Depth (cm)	Hg(18) (ppb)	K (2) (%)	La (1) (ppm)	La (2) (ppm)	Li (2) (ppm)	LOI (%)	Lu (1) (ppm)	Mg (2) (%)	Mn (2) (%)	Mn (3) (ppm)
1	403	1.97	68.0	62	41.8	18.3	0.74	0.83	0.14	868
3	379	1.97	63.0	59	42.6	17.3	0.62	0.82	0.13	817
5	407	2.02	63.0	59	42.9	17.2	0.71	0.82	0.12	737
7	389	1.99	60.0	58	43.5	17.0	0.62	0.80	0.12	733
9	389	2.03	54.0	53	44.8	16.1	0.59	0.80	0.12	748
11	395	2.11	46.0	48	46.5	14.6	0.51	0.81	0.12	771
13	389	2.17	45.0	44	48.3	14.1	0.61	0.82	0.12	760
15	372	2.21	39.0	45	46.8	13.8	0.36	0.83	0.12	785
17	371	2.21	44.0	44	47.8	13.5	0.40	0.83	0.12	778
19	377	2.18	47.0	44	47.8	13.3	0.52	0.82	0.14	787
21	350	2.13	43.0	40	46.4	12.8	0.48	0.78	0.14	830
23	373	2.08	42.0	39	45.3	12.9	0.56	0.77	0.14	840
25	358	2.12	41.0	38	45.1	12.8	0.65	0.77	0.15	874
27	368	2.11	41.0	36	44.7	12.6	0.48	0.76	0.15	897
29	428	2.11	40.0	34	45.3	13.4	0.65	0.77	0.15	918
31	595	2.02	36.0	35	49.2	14.7	0.51	0.77	0.15	923
33	726	1.90	37.0	35	53.6	14.7	0.60	0.77	0.15	923
35	1423	1.75	36.0	36	56.1	17.2	0.49	0.76	0.15	954
37	1674	1.78	37.0	35	55.7	16.2	0.54	0.81	0.17	1220
39	1786	1.64	40.0	35	53.4	18.2	0.51	0.73	0.17	1020
41	1340	1.53	40.0	39	52.1	19.1	0.45	0.66	0.17	1050
43	1488	1.49	43.0	40	52.9	19.1	0.38	0.65	0.16	1020
45	1749	1.47	44.0	41	50.3	21.5	0.67	0.64	0.16	1260
47	1321	1.41	46.0	43	49.6	20.1	0.65	0.62	0.26	1920
49	781	1.35	49.0	48	52.2	20.1	0.61	0.57	0.20	1450
52.5	577	1.25	52.0	47	50.4	22.0	0.53	0.51	0.19	1390
57.5	372	1.07	44.0	43	48.2	25.4	0.62	0.43	0.19	1360
62.5	279	0.82	39.0	43	38.9	31.0	0.46	0.34	0.19	1380
67.5	279	0.52	38.0	38	24.6	39.6	0.27	0.23	0.18	1290
72.5	279	0.66	46.0	43	30.8	35.4	0.37	0.29	0.19	1370
77.5	205	0.51	44.0	40	25.6	40.7	0.40	0.23	0.17	1260
82.5	242	0.57	41.0	40	28.4	40.1	0.43	0.25	0.15	965
87.5	255	0.56	45.0	41	29.1	41.2	0.46	0.26	0.14	962
92.5	255	0.53	45.0	44	27.7	41.3	0.55	0.23	0.14	909
97.5	255	0.59	46.0	44	30.2	39.6	0.48	0.26	0.13	862
102.5	255	0.61	46.0	44	30.4	39.2	0.55	0.27	0.13	815
107.5	216	0.66	49.0	48	30.4	38.0	0.55	0.29	0.13	809
112.5	221	0.52	45.0	49	26.4	40.1	0.36	0.23	0.12	789
117.5	225	0.55	55.0	51	28.2	39.1	0.35	0.25	0.12	777
122.5	235	0.50	59.0	53	27.3	40.1	0.51	0.23	0.12	758
127.5	235	0.49	62.0	56	26.5	41.0	0.62	0.22	0.12	795
132.5	255	0.48	55.0	56	26.4	39.9	0.52	0.22	0.12	709
137.5	257	0.48	57.0	55	25.7	40.0	0.63	0.22	0.12	727
142.5	255	0.44	58.0	48	24.3	47.5	0.66	0.20	0.10	707
147.5	270	0.55	58.0	56	30.4	38.6	0.52	0.25	0.11	675
152.5	257	0.54	62.0	58	30.7	39.0	0.58	0.25	0.11	693
157.5	274	0.55	58.0	58	30.2	39.1	0.55	0.25	0.11	726

Core QV1

Depth (cm)	Mo (2) (ppm)	Mo (5) (ppm)	Na (1) (%)	Na (2) (%)	Nb (2) (ppm)	Ni (2) (ppm)	Ni (3) (ppm)	P (2) (ppb)	Pb (2) (ppm)	Pb (3) (ppm)
1	4	3	1.60	1.44	10	31	18	2238	471	395
3	3	3	1.60	1.46	12	31	17	2196	470	386
5	3	3	1.60	1.44	12	31	17	2203	535	401
7	4	3	1.50	1.42	12	31	17	2234	565	447
9	3	3	1.60	1.49	13	30	18	2142	578	455
11	3	2	1.50	1.53	14	29	18	2052	595	502
13	3	2	1.50	1.51	14	30	20	1999	617	536
15	3	2	1.30	1.46	14	29	20	2037	625	532
17	3	2	1.60	1.55	14	29	19	2008	576	482
19	3	2	1.80	1.57	14	28	18	2012	517	423
21	3	2	1.70	1.62	14	27	18	2008	469	395
23	3	2	1.80	1.61	14	28	16	2079	403	334
25	3	2	1.80	1.66	14	27	16	2136	379	308
27	3	2	1.90	1.69	14	27	16	2088	360	291
29	3	<2	1.80	1.63	14	27	16	2102	350	283
31	3	2	1.60	1.56	14	28	17	2189	364	286
33	3	2	1.60	1.54	16	28	17	1982	339	264
35	4	2	1.40	1.40	14	30	17	2161	359	275
37	3	2	1.50	1.42	13	28	16	2163	302	241
39	4	3	1.40	1.29	12	29	16	2285	351	259
41	5	3	1.30	1.21	12	24	14	2328	362	286
43	5	3	1.30	1.20	11	22	12	2418	340	275
45	4	3	1.40	1.19	12	22	14	2376	344	280
47	5	2	1.30	1.13	11	23	14	2007	288	237
49	4	2	1.30	1.11	12	21	12	2247	171	150
52.5	5	3	1.20	1.02	12	20	11	2161	116	89
57.5	5	2	1.00	0.86	10	15	8	1989	73	51
62.5	7	3	0.70	0.67	8	13	7	1871	39	28
67.5	7	2	0.47	0.42	6	14	5	1882	18	12
72.5	6	3	0.67	0.54	6	13	7	1968	22	18
77.5	5	2	0.51	0.41	5	9	5	2008	16	14
82.5	6	2	0.50	0.44	6	9	5	2031	15	13
87.5	7	2	0.52	0.44	6	11	6	2021	19	14
92.5	8	3	0.46	0.41	6	13	6	2107	16	13
97.5	8	3	0.53	0.46	6	11	5	2064	18	14
102.5	8	3	0.56	0.48	6	11	6	2020	15	13
107.5	8	3	0.64	0.56	7	12	6	2000	12	14
112.5	8	3	0.41	0.40	6	11	5	2229	17	14
117.5	6	3	0.53	0.46	6	11	6	2213	18	14
122.5	7	3	0.51	0.40	5	11	6	2136	17	15
127.5	7	3	0.46	0.37	5	12	7	2227	14	17
132.5	5	3	0.41	0.37	5	11	6	2220	17	14
137.5	5	3	0.42	0.36	5	26	5	2187	18	15
142.5	4	3	0.44	0.34	5	15	6	1932	17	16
147.5	4	3	0.48	0.43	6	17	5	2228	18	15
152.5	4	3	0.48	0.41	5	11	6	3232	25	19
157.5	5	3	0.47	0.42	5	15	6	2388	26	20

Core QV1

Depth (cm)	Rb (1) (ppm)	Rb (2) (ppm)	Sb (1) (ppm)	Sc (1) (ppm)	Sc (2) (ppm)	Sm (1) (ppm)	Sr (2) (ppm)	Ta (1) (ppm)	Tb (1) (ppm)	Th (1) (ppm)
1	84.0	79	2.70	14.6	14.5	12.2	78	1.10	1.50	8.9
3	86.0	78	2.50	13.8	14.5	11.5	80	0.83	1.70	8.5
5	90.0	80	2.50	14.0	14.8	11.6	81	1.20	1.60	8.7
7	78.0	80	2.40	13.7	14.8	11.0	79	1.20	1.60	8.5
9	83.0	86	2.10	14.1	15.1	10.5	80	1.20	1.50	8.9
11	80.0	89	1.80	13.0	15.5	9.1	79	1.30	1.30	8.6
13	83.0	91	1.90	13.6	15.9	8.8	78	1.30	1.30	9.1
15	86.0	91	1.80	11.9	15.6	8.2	78	1.20	1.10	8.9
17	98.0	93	2.10	14.0	16.1	9.4	80	1.30	1.30	10.3
19	99.0	97	2.00	15.7	16.3	9.1	81	1.40	1.20	10.2
21	91.0	85	1.90	14.6	15.8	8.6	82	1.20	1.30	10.0
23	95.0	89	2.00	15.1	15.5	8.7	84	1.30	1.30	10.2
25	85.0	83	2.00	14.6	15.6	8.3	84	1.10	1.30	10.0
27	88.0	87	1.90	14.6	15.3	8.5	84	1.30	1.30	10.0
29	95.0	93	2.00	14.1	15.1	8.1	81	1.20	1.20	10.0
31	77.0	92	2.50	13.6	15.8	7.5	79	1.20	1.10	9.2
33	81.0	86	3.10	14.7	16.2	8.1	80	1.00	1.20	9.5
35	78.0	83	3.50	14.0	16.3	8.6	80	1.20	1.40	8.9
37	95.0	83	3.10	15.6	17.1	9.0	72	1.20	1.20	9.3
39	78.0	75	3.20	15.6	16.2	8.6	69	1.10	1.20	8.6
41	70.0	67	1.70	14.6	15.5	9.3	66	0.81	1.40	7.9
43	75.0	66	1.00	14.3	15.1	10.0	56	0.95	1.50	7.6
45	71.0	65	1.00	14.3	14.7	10.3	55	1.00	1.40	7.7
47	66.0	65	0.85	14.4	14.8	10.8	54	0.81	1.50	7.4
49	70.0	64	0.69	14.1	15.0	12.8	53	1.00	1.60	7.5
52.5	64.0	61	0.62	14.4	14.4	13.3	52	1.00	2.00	7.4
57.5	59.0	51	0.36	12.5	13.0	11.7	46	0.72	1.50	6.6
62.5	45.0	38	0.20	9.0	10.8	11.0	42	0.50	1.50	4.7
67.5	25.0	24	0.18	6.9	7.6	10.7	36	0.30	1.50	4.0
72.5	26.0	29	0.21	10.0	9.4	12.0	40	0.40	1.70	4.9
77.5	29.0	23	0.18	7.6	7.6	11.0	36	0.35	1.50	3.8
82.5	35.0	24	0.17	7.6	8.0	10.4	37	0.51	1.50	3.8
87.5	26.0	22	0.18	8.1	8.1	11.3	37	0.59	1.50	4.0
92.5	30.0	25	0.18	7.8	8.1	11.7	36	0.32	1.60	3.6
97.5	28.0	29	0.20	8.4	8.5	11.8	37	0.46	1.60	4.0
102.5	26.0	30	0.19	8.2	8.8	12.1	38	0.38	1.80	4.0
107.5	27.0	30	0.20	8.3	8.9	12.8	43	0.43	1.80	4.6
112.5	23.0	25	0.15	6.8	8.3	12.7	37	0.41	1.70	3.5
117.5	35.0	25	0.19	8.4	8.8	15.7	38	0.28	2.00	4.2
122.5	29.0	22	0.18	9.1	8.5	15.8	36	0.24	2.20	4.2
127.5	28.0	22	0.20	9.1	8.8	16.4	36	0.38	2.30	3.9
132.5	19.0	21	0.20	8.0	8.7	14.6	35	0.35	1.90	3.5
137.5	16.0	20	0.19	8.3	8.5	14.9	35	0.43	2.00	3.7
142.5	25.0	19	0.21	8.5	7.7	15.4	31	0.32	2.10	4.0
147.5	29.0	21	0.17	8.8	9.2	15.8	37	0.50	2.10	4.0
152.5	26.0	24	0.22	8.7	9.0	16.7	36	0.24	2.30	4.0
157.5	25.0	32	0.24	8.6	9.0	16.5	36	0.10	2.20	3.8

Core QV1

Depth (cm)	Ti (2) (ppm)	U (1) (ppm)	V (2) (ppm)	W (1) (ppm)	Y (2) (ppm)	Yb (1) (ppm)	Zn (1) (ppm)	Zn (2) (ppm)	Zn (3) (ppm)	Zr (2) (ppm)
1	3996	2.3	121	5.30	50	3.10	1000.0	833	791	114
3	4097	2.2	120	5.80	49	3.00	950.0	796	720	119
5	4202	2.3	121	5.80	52	3.40	920.0	791	712	124
7	4158	2.3	123	5.60	49	3.30	930.0	801	742	121
9	4230	2.4	119	5.70	45	3.10	770.0	703	615	123
11	4313	2.1	113	5.00	42	2.50	630.0	577	496	126
13	4406	2.3	111	6.30	38	2.60	540.0	507	474	120
15	4309	2.2	113	5.50	39	2.20	500.0	529	469	120
17	4411	2.7	110	4.90	38	2.70	600.0	484	431	131
19	4350	2.4	108	3.50	38	2.70	530.0	450	393	131
21	4414	2.2	105	5.10	37	2.80	450.0	416	380	132
23	4382	2.4	100	2.60	36	2.50	480.0	383	345	126
25	4432	2.5	99	3.40	37	2.40	390.0	363	324	119
27	4417	2.3	98	<2.0	36	2.90	400.0	352	323	119
29	4367	2.3	100	2.40	33	2.50	390.0	343	298	122
31	4418	2.2	99	<2.0	35	2.60	390.0	350	312	130
33	4664	2.2	94	<2.0	35	2.70	430.0	368	317	133
35	4588	2.3	92	<2.0	36	2.30	450.0	406	341	130
37	4546	2.4	92	<2.0	36	2.90	490.0	370	322	131
39	4305	2.3	90	2.10	36	2.70	480.0	430	364	119
41	4072	2.1	82	<2.0	38	2.50	360.0	335	288	119
43	4000	2.1	75	<2.0	40	2.60	320.0	267	228	123
45	3837	2.1	77	<2.0	41	2.80	330.0	271	230	120
47	3880	2.1	78	<2.0	44	2.30	300.0	244	212	117
49	3886	2.2	76	<2.0	50	2.90	270.0	215	175	118
52.5	3750	2.3	71	<2.0	48	3.00	150.0	179	145	118
57.5	3469	2.0	66	<2.0	45	2.90	170.0	162	127	104
62.5	2724	1.6	55	<2.0	44	2.10	180.0	157	119	82
67.5	1803	1.4	37	<2.0	37	1.80	<50	139	103	56
72.5	2237	1.4	45	<2.0	43	2.80	210.0	172	134	70
77.5	1774	1.3	37	<2.0	39	1.60	150.0	135	106	59
82.5	1897	1.3	38	<2.0	39	2.40	100.0	128	99	60
87.5	1855	1.3	38	<2.0	40	2.10	150.0	138	108	60
92.5	1804	1.3	37	<2.0	42	2.00	120.0	128	96	60
97.5	1952	1.3	39	<2.0	43	2.40	170.0	124	96	63
102.5	1938	1.4	38	<2.0	43	2.20	140.0	131	101	64
107.5	2096	1.3	40	<2.0	48	2.70	97.0	139	102	65
112.5	1706	1.3	36	<2.0	49	2.00	99.0	164	128	56
117.5	1821	1.5	39	<2.0	54	2.10	210.0	172	132	63
122.5	1699	1.4	36	<2.0	53	2.80	170.0	150	117	56
127.5	1641	1.4	36	<2.0	56	2.50	180.0	178	147	54
132.5	1620	1.2	36	<2.0	54	2.40	160.0	174	132	54
137.5	1584	1.4	36	<2.0	54	2.70	150.0	162	128	52
142.5	1440	1.3	33	<2.0	48	2.40	140.0	135	120	48
147.5	1760	1.4	40	<2.0	56	2.80	150.0	165	127	59
152.5	1729	1.5	39	<2.0	57	2.70	140.0	163	129	56
157.5	1710	1.4	39	<2.0	58	2.50	100.0	151	125	56

Core QV2

core QV2 Sample #	Depth (cm)	Ag (6) (ppm)	Al (2) (%)	As (1) (ppm)	Au (1) (ppb)	Ba (1) (ppm)	Ba (2) (ppm)	Be (2) (ppm)	Br (1) (ppm)	Ca (2) (%)
QV2-002	1	0.4	6.82	12.0	16.0	590	602	4.0	18.0	0.47
QV2-004	3	0.6	6.73	13.0	19.0	580	594	3.9	17.0	0.49
QV2-006	5	0.7	7.17	12.0	16.0	580	630	3.7	17.0	0.48
QV2-008	7	0.8	7.59	12.0	17.0	610	654	3.5	15.0	0.45
QV2-010	9	0.7	7.59	11.0	13.0	550	640	3.4	14.0	0.44
QV2-012	11	0.7	7.56	12.0	14.0	520	622	3.3	13.0	0.42
QV2-014	13	0.6	7.72	12.0	12.0	550	637	3.3	13.0	0.42
QV2-016	15	0.6	7.60	11.0	11.0	560	628	3.1	12.0	0.43
QV2-018	17	0.5	7.52	14.0	19.0	570	631	3.0	13.0	0.43
QV2-020	19	0.4	7.41	12.0	10.0	510	618	2.9	13.0	0.44
QV2-022	21	0.4	7.58	13.0	11.0	550	632	3.0	13.0	0.45
QV2-024	23	0.4	7.41	14.0	9.5	550	623	2.9	14.0	0.43
QV2-027	25.5	0.4	7.44	13.0	11.0	550	628	2.9	14.0	0.42
QV2-029	28	0.4	7.28	13.0	14.0	520	610	2.9	15.0	0.41
QV2-031	30	1.2	7.67	16.0	28.0	560	628	3.1	16.0	0.36
QV2-033	32	0.8	7.71	17.0	20.0	540	584	3.1	16.0	0.35
QV2-035	34	0.6	7.55	18.0	18.0	510	541	3.4	17.0	0.34
QV2-037	36	0.6	7.45	22.7	26.0	470	575	3.5	21.2	0.33
QV2-039	38	0.5	7.60	19.0	23.0	480	464	3.2	20.0	0.31
QV2-041	40	0.5	7.65	17.0	20.0	430	493	3.3	19.0	0.29
QV2-043	42	0.5	4.45	19.0	19.0	470	486	3.4	22.9	0.28
QV2-045	44	0.6	7.07	23.5	32.0	490	479	3.5	27.6	0.28
QV2-047	46	0.6	6.37	33.1	49.0	430	456	4.0	30.6	0.29
QV2-050	48.5	0.5	6.83	21.3	40.0	390	448	4.0	24.4	0.27
QV2-055	52.5	0.5	6.75	18.0	36.0	390	414	4.2	28.3	0.24
QV2-060	57.5	0.4	6.52	15.0	15.0	350	385	4.5	30.1	0.23
QV2-065	62.5	0.5	6.26	10.0	25.0	290	350	4.0	31.5	0.21
QV2-070	67.5	0.2	5.89	8.3	6.1	250	310	4.0	36.1	0.21
QV2-075	72.5	0.4	5.15	8.2	<2.0	230	271	3.8	50.1	0.24
QV2-080	77.5	<0.2	4.78	7.0	<2.0	200	236	3.8	61.0	0.25
QV2-085	82.5	<0.2	4.23	6.0	<2.0	210	228	3.1	74.7	0.25
QV2-090	87.5	<0.2	4.02	5.0	<2.0	180	215	3.2	77.5	0.26
QV2-095	92.5	<0.2	4.30	5.7	<2.0	210	229	3.5	75.0	0.27
QV2-100	97.5	<0.2	4.53	5.5	<2.0	190	239	3.8	72.2	0.28
QV2-105	102.5	<0.2	4.52	5.8	<2.0	210	234	4.0	70.0	0.28
QV2-110	107.5	<0.2	4.66	5.6	<2.0	220	253	4.0	64.7	0.28
QV2-115	112.5	<0.2	4.59	5.3	<2.0	180	247	4.1	63.2	0.28
QV2-120	117.5	<0.2	4.77	9.2	<2.0	240	251	4.7	57.3	0.33
QV2-125	122.5	<0.2	4.60	5.5	<2.0	190	245	3.9	60.0	0.31
QV2-130	127.5	<0.2	4.66	5.3	<2.0	230	247	4.8	59.6	0.32
QV2-135	132.5	<0.2	4.54	6.8	<2.0	230	240	5.0	63.1	0.32
QV2-140	137.5	<0.2	4.73	6.5	<2.0	220	248	5.1	56.8	0.33
QV2-145	142.5	<0.2	4.59	6.5	<2.0	210	245	5.2	55.7	0.32
QV2-150	147.5	<0.2	4.46	6.3	<2.0	190	236	5.2	57.1	0.34
QV2-155	152.5	<0.2	4.55	6.3	<2.0	180	242	5.4	58.0	0.34
QV2-160	157.5	<0.2	4.68	6.1	<2.0	200	249	5.6	54.1	0.34
QV2-165	162.5	<0.2	4.76	5.5	<2.0	220	247	6.1	55.2	0.35
QV2-170	167.5	<0.2	4.78	7.1	<2.0	220	259	6.4	52.4	0.35
QV2-175	172.5	<0.2	4.78	6.3	<2.0	200	258	6.8	54.1	0.37
QV2-180	178.5	<0.2	4.80	6.5	<2.0	220	258	7.0	54.0	0.37
QV2-185	182.5	<0.2	4.77	7.1	<2.0	220	274	6.8	56.3	0.36
QV2-190	187.5	<0.2	4.75	7.6	<2.0	230	269	7.1	54.3	0.38
QV2-195	192.5	<0.2	4.59	7.4	<2.0	180	256	7.5	52.7	0.38
QV2-200	197.5	<0.2	4.69	7.0	<2.0	220	257	7.0	53.1	0.37

Core QV2

Depth (cm)	Cd (2) (ppm)	Cd (3) (ppm)	Ce (1) (ppm)	Ce (2) (ppm)	Co (1) (ppm)	Co (2) (ppm)	Co (3) (ppm)	Cr (1) (ppm)	Cr (2) (ppm)	Cr (2a) (ppm)
1	2.0	1.5	110	118	22.0	21	13	62.0	68	64
3	1.9	1.5	96	116	20.0	21	13	38.0	72	68
5	1.7	1.3	100	113	20.0	21	14	60.0	60	56
7	1.5	1.2	100	113	21.0	21	13	32.0	53	52
9	1.4	1.2	93	107	23.0	21	13	46.0	49	44
11	1.4	1.2	100	109	19.0	21	13	45.0	50	47
13	1.5	1.2	97	106	17.0	21	13	37.0	49	44
15	1.3	1.1	92	101	18.0	20	12	55.0	51	45
17	1.3	1.1	100	108	19.0	21	11	39.0	45	39
19	1.3	1.0	83	103	14.0	20	11	55.0	43	38
21	1.3	1.1	82	107	14.0	20	12	38.0	43	38
23	1.3	1.1	83	105	18.0	20	11	44.0	43	36
25.5	1.4	1.1	95	106	16.0	20	10	41.0	45	40
28	1.2	1.0	87	104	17.0	21	12	19.0	44	39
30	1.2	1.0	87	99	22.0	23	14	48.0	49	42
32	1.0	0.8	81	94	18.0	21	13	41.0	51	44
34	1.1	0.9	89	96	23.0	25	14	43.0	53	47
36	1.0	0.8	93	100	25.0	26	15	59.0	54	48
38	0.8	0.6	89	94	26.0	25	15	59.0	53	50
40	0.7	0.6	88	99	24.0	26	16	34.0	53	48
42	0.6	0.5	84	102	23.0	26	16	39.0	52	48
44	0.9	0.7	92	98	30.0	30	17	50.0	53	47
46	0.9	0.8	91	91	43.0	42	25	24.0	48	44
48.5	0.5	0.4	92	94	34.0	32	18	46.0	51	48
52.5	0.4	0.3	110	112	48.0	43	28	35.0	41	36
57.5	0.4	0.2	130	133	51.0	48	29	47.0	34	30
62.5	0.4	0.2	110	123	43.0	41	25	28.0	31	27
67.5	0.5	0.2	120	128	29.0	27	15	19.0	28	24
72.5	0.5	0.3	120	128	35.0	33	19	25.0	23	19
77.5	0.5	0.3	120	126	25.0	24	13	16.0	20	17
82.5	0.5	0.2	110	99	15.0	16	9	20.0	18	16
87.5	0.5	0.2	99	99	13.0	13	7	19.0	18	14
92.5	0.5	0.3	110	110	14.0	15	7	25.0	17	14
97.5	0.5	0.3	120	122	15.0	16	8	26.0	23	21
102.5	0.4	0.3	130	126	17.0	17	9	19.0	17	15
107.5	0.5	0.4	120	126	17.0	18	9	28.0	20	18
112.5	0.4	0.4	120	128	15.0	18	9	31.0	17	14
117.5	0.7	0.6	140	156	43.0	41	22	<15	22	19
122.5	0.5	0.4	130	139	16.0	16	9	23.0	17	16
127.5	0.5	0.4	130	149	15.0	17	9	<15	17	15
132.5	0.6	0.5	160	160	18.0	19	10	21.0	22	19
137.5	0.5	0.4	170	161	20.0	17	10	16.0	18	15
142.5	0.5	0.5	160	161	18.0	17	10	<15	16	13
147.5	0.6	0.4	160	161	19.0	17	10	28.0	20	16
152.5	0.5	0.4	170	165	19.0	17	10	24.0	16	14
157.5	0.5	0.5	160	173	20.0	18	11	32.0	19	16
162.5	0.5	0.5	180	176	17.0	17	10	28.0	17	14
167.5	0.6	0.5	180	188	26.0	22	13	30.0	19	15
172.5	0.6	0.5	190	196	18.0	18	11	<15	18	18
178.5	0.6	0.5	190	199	15.0	17	10	<15	18	18
182.5	0.4	0.4	204	190	16.0	15	9	35.0	20	20
187.5	0.5	0.5	204	194	23.0	19	11	26.0	21	18
192.5	0.7	0.5	208	207	20.0	20	11	32.0	18	14
197.5	0.5	0.5	180	185	17.0	18	11	30.0	20	18

Core QV2

Depth (cm)	Cs (1) (ppm)	Cu (2) (ppm)	Cu (3) (ppm)	Dy (2) (ppm)	Eu (1) (ppm)	Fe (1) (%)	Fe (2) (%)	Fe (3) (%)	Ga (2) (ppm)	Hf (1) (ppm)
1	5.9	153	112	8.1	4.40	7.70	7.46	5.81	25	5.80
3	7.0	154	112	8.0	2.10	8.10	7.39	5.99	24	5.10
5	6.3	128	95	7.5	2.90	7.10	6.86	5.15	25	6.40
7	7.3	99	77	6.9	2.50	6.50	6.20	4.59	22	5.00
9	6.6	91	71	6.6	3.00	6.10	6.03	4.21	21	5.20
11	6.3	90	69	6.5	2.40	6.00	6.00	4.16	22	5.10
13	6.4	88	69	6.3	2.70	6.00	6.13	4.19	22	5.40
15	6.5	82	62	5.9	2.30	5.60	5.97	4.46	22	5.50
17	6.7	77	58	6.9	2.40	6.20	5.96	4.26	25	6.50
19	5.7	70	52	6.6	2.60	5.40	5.80	4.06	24	5.40
21	5.2	74	55	7.0	1.90	5.70	6.19	4.49	26	5.10
23	6.4	73	54	6.7	0.25	6.70	6.24	4.52	25	4.70
25.5	5.7	75	55	6.8	2.30	6.60	6.30	4.47	26	5.00
28	5.3	74	53	6.6	2.60	6.00	6.06	4.60	25	5.60
30	5.8	84	60	6.5	1.50	5.70	5.51	4.05	26	4.50
32	5.9	74	54	6.2	2.20	6.00	5.71	4.16	26	5.50
34	5.3	74	50	6.3	3.40	5.90	5.70	3.92	25	5.30
36	6.2	71	50	6.6	1.80	6.10	5.64	4.23	24	5.70
38	5.9	55	38	5.9	2.80	6.20	5.72	4.14	24	6.40
40	5.8	53	37	6.2	2.70	6.40	6.00	4.65	24	5.90
42	5.8	53	38	6.3	2.20	6.60	6.32	4.80	24	4.90
44	6.0	57	38	6.4	2.90	7.40	6.34	4.97	24	5.00
46	4.8	53	37	7.3	3.40	7.50	6.67	5.47	23	4.50
48.5	5.4	43	28	6.7	1.90	6.40	5.94	4.40	22	5.50
52.5	6.0	36	25	7.9	3.30	5.90	5.48	3.99	21	5.20
57.5	6.6	34	22	8.8	4.30	5.40	4.99	3.57	20	4.50
62.5	6.2	24	17	8.1	3.30	4.40	4.40	3.34	19	4.10
67.5	6.6	17	12	7.8	4.30	4.10	3.95	2.68	17	4.00
72.5	5.0	18	13	7.8	2.90	3.40	3.38	2.27	14	2.60
77.5	4.3	17	12	7.4	3.20	3.10	2.96	1.97	12	2.40
82.5	4.0	15	11	6.1	2.40	2.40	2.25	1.50	10	2.40
87.5	3.6	15	11	6.4	2.60	2.20	1.96	1.22	10	2.70
92.5	4.3	18	12	6.9	2.70	2.20	1.99	1.17	10	2.50
97.5	3.9	19	13	7.5	2.90	2.00	1.99	1.26	11	1.90
102.5	4.1	19	13	7.6	3.40	2.00	1.94	1.23	10	2.60
107.5	4.5	20	13	7.6	2.50	2.00	1.96	1.19	10	2.80
112.5	4.4	20	13	7.5	3.20	2.00	1.98	1.23	10	1.80
117.5	3.5	23	15	8.9	4.00	2.20	2.21	1.38	10	2.20
122.5	3.8	26	14	8.0	3.50	1.90	1.95	1.20	10	1.80
127.5	3.7	21	14	8.9	3.80	2.00	2.00	1.24	10	2.40
132.5	3.9	21	15	9.3	4.80	2.30	1.95	1.25	9	1.20
137.5	3.8	20	15	9.4	3.30	2.20	1.96	1.29	11	2.80
142.5	3.9	20	14	9.5	4.40	2.00	1.87	1.22	11	2.70
147.5	3.8	20	15	9.4	3.90	2.00	1.81	1.18	10	2.10
152.5	4.3	21	15	9.8	4.90	2.20	1.86	1.26	11	2.30
157.5	4.0	23	16	9.9	5.10	2.10	1.92	1.35	11	2.10
162.5	4.0	23	17	10.5	5.40	2.10	1.94	1.33	10	2.20
167.5	4.2	24	16	11.5	5.20	2.20	2.08	1.34	11	2.20
172.5	4.1	25	17	11.8	5.20	2.20	2.09	1.39	12	1.80
178.5	4.4	26	18	12.2	5.20	2.20	2.16	1.40	12	2.30
182.5	5.5	25	17	11.7	5.60	2.50	2.09	1.33	12	2.40
187.5	4.9	27	19	12.7	5.50	2.40	2.18	1.44	11	3.30
192.5	4.1	28	19	13.5	6.00	2.20	2.14	1.40	10	2.40
197.5	4.2	26	19	11.6	4.60	2.30	2.19	1.47	11	2.20

Core QV2

Depth (cm)	Hg(18) (ppb)	K (2) (%)	La (1) (ppm)	La (2) (ppm)	Li (2) (ppm)	LOI (%)	Lu (1) (ppm)	Mg (2) (%)	Mn (2) (%)	Mn (3) (ppm)
1	480	1.98	60.0	61	42.8	17.9	0.44	0.84	0.14	828
3	490	1.95	59.0	60	42.3	18.1	0.41	0.82	0.12	787
5	490	2.05	55.0	55	44.5	16.7	0.55	0.82	0.12	760
7	480	2.17	51.0	50	47.0	14.8	0.46	0.84	0.13	793
9	451	2.17	49.0	46	46.9	14.4	0.41	0.83	0.13	801
11	431	2.17	47.0	46	46.9	14.4	0.63	0.84	0.13	817
13	451	2.22	47.0	45	47.2	13.8	0.39	0.87	0.13	829
15	402	2.19	43.0	42	46.6	13.1	0.42	0.83	0.14	882
17	412	2.15	46.0	41	44.7	13.1	0.38	0.80	0.15	932
19	496	2.09	36.0	39	42.2	13.0	0.37	0.76	0.16	979
21	412	2.13	35.0	41	43.6	12.9	0.32	0.78	0.17	1320
23	431	2.09	39.0	39	42.5	13.4	0.20	0.77	0.18	1400
25.5	451	2.12	42.0	40	42.8	13.8	0.60	0.77	0.20	1460
28	519	2.04	38.0	39	43.9	15.0	0.44	0.75	0.17	1330
30	686	2.05	37.0	38	48.2	14.9	0.41	0.79	0.14	918
32	725	2.02	38.0	36	50.7	14.7	0.61	0.83	0.14	892
34	623	1.88	38.0	36	52.6	15.2	0.70	0.79	0.14	861
36	1394	1.77	38.0	38	54.7	17.5	0.60	0.77	0.14	893
38	1394	1.79	36.0	39	54.7	15.8	0.57	0.82	0.14	902
40	1394	1.78	34.0	35	54.8	15.5	0.61	0.84	0.15	949
42	2154	1.73	33.0	35	53.9	17.2	0.55	0.78	0.17	1230
44	2317	1.63	41.0	36	50.9	19.1	0.61	0.75	0.17	1020
46	1140	1.42	41.0	37	46.5	22.2	0.48	0.63	0.83	6620
48.5	1195	1.49	40.0	38	51.4	19.1	0.58	0.67	0.19	1460
52.5	1198	1.42	46.0	42	51.0	20.2	0.74	0.63	0.17	1060
57.5	416	1.27	49.0	46	50.2	21.8	0.70	0.54	0.17	1230
62.5	235	1.16	42.0	40	48.3	24.6	0.65	0.47	0.17	1300
67.5	235	0.97	42.0	41	44.4	27.6	0.55	0.41	0.16	929
72.5	199	0.76	40.0	40	34.8	34.6	0.53	0.33	0.16	1040
77.5	217	0.61	41.0	40	27.6	36.1	0.44	0.28	0.16	986
82.5	217	0.56	36.0	33	26.6	37.8	0.28	0.25	0.14	902
87.5	217	0.49	37.0	35	24.7	41.1	0.40	0.23	0.13	847
92.5	<5	0.55	39.0	37	28.6	41.2	0.39	0.25	0.13	847
97.5	235	0.57	41.0	40	31.1	41.7	0.43	0.26	0.12	785
102.5	226	0.55	43.0	41	30.3	41.8	0.44	0.25	0.12	744
107.5	235	0.61	43.0	44	33.1	40.4	0.50	0.27	0.11	676
112.5	199	0.59	43.0	41	31.4	39.6	0.39	0.27	0.10	657
117.5	199	0.58	49.0	49	30.3	41.3	0.55	0.27	0.12	721
122.5	199	0.54	47.0	47	28.7	40.3	0.55	0.25	0.10	641
127.5	208	0.56	45.0	47	29.5	39.2	0.44	0.26	0.10	646
132.5	199	0.49	50.0	49	27.9	40.9	0.40	0.23	0.10	653
137.5	244	0.54	54.0	50	29.5	39.8	0.53	0.25	0.10	634
142.5	253	0.50	54.0	52	28.6	40.2	0.51	0.23	0.10	607
147.5	253	0.46	53.0	50	26.5	40.7	0.51	0.22	0.10	598
152.5	253	0.49	57.0	53	28.0	40.4	0.45	0.23	0.09	607
157.5	217	0.54	55.0	53	30.3	39.2	0.50	0.25	0.09	629
162.5	199	0.52	58.0	56	30.3	40.1	0.58	0.25	0.09	611
167.5	217	0.55	62.0	60	32.5	40.0	0.71	0.27	0.09	578
172.5	244	0.55	62.0	62	31.7	40.1	0.60	0.26	0.09	586
178.5	187	0.57	58.0	63	32.0	39.8	0.63	0.27	0.09	591
182.5	150	0.63	61.0	61	35.6	38.7	0.47	0.29	0.09	553
187.5	168	0.64	68.0	64	34.2	39.5	0.59	0.29	0.09	595
192.5	187	0.56	69.0	69	32.7	39.3	0.71	0.27	0.09	550
197.5	281	0.59	63.0	61	32.8	39.3	0.65	0.28	0.09	603

Core QV2

Depth (cm)	Mo (2) (ppm)	Mo (5) (ppm)	Na (1) (%)	Na (2) (%)	Nb (2) (ppm)	Ni (2) (ppm)	Ni (3) (ppm)	P (2) (ppb)	Pb (2) (ppm)	Pb (3) (ppm)
1	4	3	1.40	1.44	12	30	18	2363	489	425
3	4	3	1.40	1.42	12	30	18	2386	511	450
5	5	2	1.60	1.49	13	30	18	2325	568	488
7	4	2	1.60	1.52	13	28	18	2265	552	489
9	4	2	1.60	1.55	13	28	17	2171	545	482
11	4	2	1.60	1.51	13	28	18	2141	591	522
13	4	2	1.60	1.52	13	29	18	2122	612	534
15	5	2	1.60	1.57	13	26	17	2054	544	489
17	5	2	1.80	1.61	14	27	16	2199	483	389
19	4	2	1.70	1.67	14	25	15	2104	381	295
21	5	2	1.50	1.65	15	22	15	2162	386	306
23	5	2	1.60	1.62	14	25	16	2110	380	289
25.5	4	2	1.70	1.58	14	26	15	2202	394	299
28	5	2	1.70	1.58	14	26	16	2083	392	314
30	4	2	1.70	1.54	15	27	17	2484	381	296
32	4	2	1.70	1.55	15	27	17	2101	364	291
34	5	2	1.60	1.52	16	28	16	2058	351	267
36	5	2	1.60	1.40	14	28	16	2214	351	276
38	4	2	1.60	1.44	14	28	16	2053	277	229
40	4	2	1.50	1.43	14	27	16	2106	272	228
42	4	2	1.40	1.33	13	26	15	2356	390	237
44	7	2	1.50	1.29	13	27	15	2467	326	249
46	8	3	1.30	1.10	10	27	15	2267	409	326
48.5	8	3	1.40	1.22	12	27	13	2279	340	267
52.5	7	3	1.30	1.15	12	21	13	2292	274	244
57.5	8	3	1.20	1.05	12	18	11	2177	120	82
62.5	8	2	1.00	0.90	10	16	9	2036	80	58
67.5	8	3	0.91	0.80	9	13	7	1899	53	35
72.5	7	3	0.68	0.62	7	15	7	1867	29	21
77.5	8	3	0.57	0.51	6	12	5	1941	22	15
82.5	6	2	0.54	0.47	6	9	5	1825	16	11
87.5	5	2	0.47	0.39	5	9	4	1961	14	10
92.5	6	2	0.50	0.43	6	10	4	2062	13	11
97.5	6	3	0.52	0.46	6	13	5	2118	17	12
102.5	6	3	0.48	0.43	6	11	5	2095	16	12
107.5	6	2	0.54	0.48	6	11	5	2022	17	12
112.5	6	3	0.52	0.46	6	11	5	2088	18	13
117.5	6	3	0.56	0.49	6	22	10	2157	19	14
122.5	5	3	0.45	0.43	4	11	5	2248	18	13
127.5	5	3	0.46	0.45	6	11	6	2284	20	13
132.5	5	3	0.43	0.40	5	13	5	2232	19	14
137.5	5	3	0.50	0.43	5	10	5	2284	15	14
142.5	4	3	0.45	0.39	5	10	6	2243	20	14
147.5	5	3	0.43	0.37	5	11	6	2229	15	14
152.5	5	3	0.47	0.40	5	10	6	2313	17	14
157.5	5	2	0.47	0.42	5	11	6	2336	17	16
162.5	5	3	0.46	0.41	5	10	6	2480	17	16
167.5	5	3	0.50	0.45	5	12	7	2456	23	15
172.5	5	3	0.48	0.44	6	11	6	2529	20	16
178.5	5	3	0.44	0.45	5	11	6	2626	20	17
182.5	5	3	0.57	0.51	5	12	5	2497	20	15
187.5	6	3	0.60	0.52	5	13	7	2368	18	16
192.5	5	3	0.49	0.46	4	12	6	2435	23	17
197.5	5	3	0.52	0.48	5	11	6	2434	27	22

Core QV2

Depth (cm)	Rb (1) (ppm)	Rb (2) (ppm)	Sb (1) (ppm)	Sc (1) (ppm)	Sc (2) (ppm)	Sm (1) (ppm)	Sr (2) (ppm)	Ta (1) (ppm)	Tb (1) (ppm)	Th (1) (ppm)
1	73.0	79	2.60	12.1	14.1	11.3	77	1.00	1.50	8.3
3	84.0	81	2.80	12.1	13.9	11.6	77	0.89	1.70	8.5
5	82.0	88	2.40	13.6	14.5	10.7	77	1.10	1.40	8.7
7	89.0	96	1.90	14.8	15.7	10.0	78	1.20	1.20	10.0
9	90.0	97	1.80	14.4	15.5	9.2	77	1.10	1.30	8.9
11	86.0	95	1.80	14.5	15.4	9.0	75	1.20	1.40	9.1
13	90.0	100	2.00	14.3	15.5	8.8	76	1.20	1.20	9.2
15	88.0	90	1.80	13.8	15.4	8.4	78	1.30	1.30	9.4
17	110.0	88	2.00	15.0	16.1	8.8	85	1.60	1.40	10.7
19	82.0	88	1.70	12.8	15.4	7.7	87	1.00	1.10	9.0
21	85.0	92	1.70	12.3	16.2	7.5	87	1.00	1.10	8.9
23	110.0	90	1.90	13.7	15.5	8.5	85	1.40	1.40	10.2
25.5	90.0	88	1.80	14.7	15.8	8.0	82	1.20	1.10	9.4
28	85.0	87	1.80	13.9	15.7	7.8	82	1.20	1.00	9.2
30	98.0	77	2.70	15.0	16.3	7.7	79	1.00	0.87	10.0
32	93.0	91	2.90	15.7	16.2	7.8	77	1.10	1.10	10.0
34	82.0	81	3.10	14.9	16.2	8.0	79	1.00	1.20	9.3
36	85.0	77	3.50	15.7	16.3	8.4	79	1.10	1.10	8.8
38	78.0	76	2.80	15.9	16.2	8.0	71	1.10	1.10	8.8
40	78.0	72	2.60	15.6	17.0	7.7	69	1.20	1.20	8.4
42	77.0	75	2.80	14.2	16.6	8.0	66	1.10	1.10	8.2
44	74.0	69	3.30	16.2	15.6	8.8	65	1.10	1.30	8.8
46	70.0	61	2.70	14.1	14.3	9.2	64	0.93	1.40	7.7
48.5	67.0	65	1.90	14.9	15.1	9.1	65	1.00	1.30	7.9
52.5	73.0	61	0.91	14.8	14.8	11.1	54	0.87	1.40	7.6
57.5	63.0	58	0.55	14.0	14.0	12.7	51	1.00	1.70	7.2
62.5	63.0	58	0.40	12.5	13.1	10.9	44	0.84	1.60	6.5
67.5	54.0	46	0.26	11.4	12.2	11.3	43	0.86	1.50	6.0
72.5	35.0	33	0.23	9.2	10.2	10.7	41	0.48	1.50	4.9
77.5	34.0	25	0.19	8.0	8.7	11.0	37	0.60	1.50	4.2
82.5	29.0	18	0.18	7.2	7.5	10.0	35	0.43	1.40	4.2
87.5	23.0	19	0.19	6.9	7.1	10.0	34	0.40	1.30	3.4
92.5	28.0	23	0.19	7.4	7.7	10.2	36	0.27	1.50	4.0
97.5	28.0	25	0.18	7.9	8.2	11.0	37	0.29	1.50	3.9
102.5	28.0	20	0.17	7.9	8.1	11.8	36	0.43	1.60	4.1
107.5	26.0	28	0.18	8.4	8.5	11.5	39	0.59	1.50	4.1
112.5	26.0	31	0.17	7.7	8.3	11.2	39	0.35	1.50	3.8
117.5	28.0	23	0.17	8.1	8.7	13.1	42	0.37	1.80	3.9
122.5	26.0	25	0.16	7.7	8.3	12.4	38	0.24	1.70	3.7
127.5	25.0	26	0.17	7.2	8.5	13.1	39	0.35	1.70	3.8
132.5	20.0	21	0.24	7.5	8.3	15.2	37	0.46	2.20	4.0
137.5	27.0	21	0.21	8.2	8.4	14.9	37	0.36	2.10	4.2
142.5	29.0	23	0.20	8.0	8.5	14.8	37	0.43	2.00	3.9
147.5	24.0	23	0.18	7.9	7.9	14.7	36	0.49	2.00	3.7
152.5	24.0	23	0.19	8.6	8.4	15.5	37	0.36	2.10	4.0
157.5	27.0	28	0.17	8.6	8.6	15.1	37	0.45	2.20	4.0
162.5	24.0	25	0.18	8.6	8.8	16.2	37	0.37	2.10	3.9
167.5	27.0	20	0.19	9.1	9.4	17.2	39	0.40	2.30	3.8
172.5	29.0	25	0.19	8.6	9.5	17.4	38	0.10	2.40	3.7
178.5	20.0	23	0.20	8.0	9.8	17.7	39	0.39	2.30	3.9
182.5	32.0	26	0.25	9.2	10.0	19.6	40	0.50	2.80	4.4
187.5	29.0	23	0.27	10.0	10.3	19.8	40	0.41	2.80	4.4
192.5	31.0	23	0.22	9.1	10.3	20.2	39	0.10	2.70	3.9
197.5	27.0	23	0.32	8.9	9.6	18.0	38	0.50	2.40	3.8

Core QV2

Depth (cm)	Ti (2) (ppm)	U (1) (ppm)	V (2) (ppm)	W (1) (ppm)	Y (2) (ppm)	Yb (1) (ppm)	Zn (1) (ppm)	Zn (2) (ppm)	Zn (3) (ppm)	Zr (2) (ppm)
1	4054	2.4	120	5.20	52	2.50	970.0	844	789	120
3	4018	2.4	122	5.90	51	2.20	950.0	852	820	119
5	4207	2.3	124	6.00	47	2.40	860.0	732	697	120
7	4313	2.2	105	6.00	43	2.80	740.0	610	573	124
9	4322	2.2	102	5.70	40	3.10	710.0	546	500	124
11	4283	2.3	102	5.30	39	2.70	540.0	514	473	124
13	4355	2.2	103	7.20	39	2.60	560.0	504	462	128
15	4369	2.3	99	4.40	37	2.50	450.0	443	405	122
17	4456	2.5	115	4.50	38	2.80	490.0	408	352	127
19	4395	2.1	110	2.20	36	2.50	320.0	373	315	120
21	4454	2.2	110	2.20	38	2.50	290.0	389	326	127
23	4310	2.4	110	<2.0	36	1.70	330.0	368	315	120
25.5	4298	2.0	112	3.20	36	3.00	360.0	376	318	121
28	4287	2.2	115	<2.0	36	2.60	370.0	348	309	124
30	4421	2.3	112	<2.0	35	2.60	330.0	347	298	128
32	4582	2.2	107	<2.0	33	2.70	370.0	347	301	129
34	4652	2.2	106	<2.0	35	2.40	400.0	384	320	135
36	4511	2.3	104	<2.0	35	2.30	440.0	397	341	128
38	4575	2.2	91	<2.0	33	2.80	420.0	354	299	126
40	4720	2.1	95	<2.0	34	2.30	400.0	355	316	129
42	4440	2.2	92	<2.0	35	2.10	360.0	375	331	124
44	4215	2.1	89	<2.0	36	2.70	510.0	433	361	120
46	3336	2.0	78	<2.0	37	2.60	530.0	504	443	108
48.5	4005	2.2	80	<2.0	38	2.70	340.0	324	261	116
52.5	3859	2.1	76	<2.0	43	3.00	220.0	215	175	111
57.5	3756	2.0	69	<2.0	47	2.90	130.0	162	127	113
62.5	3506	1.8	68	<2.0	42	2.50	160.0	147	115	104
67.5	3184	1.8	63	<2.0	42	2.50	150.0	154	117	98
72.5	2473	1.4	50	<2.0	42	2.40	130.0	152	120	78
77.5	2060	1.3	43	<2.0	40	1.80	140.0	149	117	66
82.5	1866	1.5	39	<2.0	33	1.20	140.0	117	86	56
87.5	1676	1.1	35	<2.0	35	2.00	56.0	111	83	54
92.5	1824	1.2	37	<2.0	39	1.80	100.0	126	94	60
97.5	1881	1.3	40	<2.0	42	1.70	71.0	137	100	65
102.5	1853	1.3	37	<2.0	42	2.00	78.0	134	101	62
107.5	1972	1.2	40	<2.0	42	2.40	130.0	150	106	65
112.5	1910	1.3	39	<2.0	42	1.80	110.0	136	98	68
117.5	1919	1.4	39	<2.0	49	2.30	120.0	180	138	63
122.5	1784	1.2	38	<2.0	47	2.30	130.0	148	99	60
127.5	1801	1.4	37	<2.0	47	2.10	87.0	143	111	63
132.5	1653	1.4	36	<2.0	49	2.20	130.0	145	112	58
137.5	1731	1.5	38	<2.0	51	2.40	120.0	134	102	65
142.5	1640	1.3	37	<2.0	52	2.30	140.0	145	114	61
147.5	1539	1.2	35	<2.0	51	2.40	110.0	142	111	57
152.5	1597	1.4	36	<2.0	52	2.80	99.0	138	110	62
157.5	1706	1.3	37	<2.0	52	2.70	120.0	131	104	64
162.5	1647	1.3	37	<2.0	56	2.70	150.0	147	120	64
167.5	1772	1.4	41	<2.0	62	3.00	140.0	168	130	68
172.5	1736	1.4	41	<2.0	62	2.80	160.0	162	125	66
178.5	1753	1.4	42	<2.0	64	2.50	110.0	156	122	71
182.5	1859	1.6	43	<2.0	62	3.20	100.0	141	108	72
187.5	1834	1.5	43	<2.0	66	3.70	51.0	148	118	73
192.5	1659	1.5	41	<2.0	72	3.40	100.0	158	124	65
197.5	1736	1.5	42	<2.0	63	2.90	120.0	152	118	64

Core QV3

core QV3 Sample #	Depth (cm)	Ag (6) (ppm)	Al (2) (%)	As (1) (ppm)	Au (1) (ppb)	Ba (1) (ppm)	Ba (2) (ppm)	Be (2) (ppm)	Br (1) (ppm)	Ca (2) (%)	Cd (2) (ppm)	Cd (3) (ppm)	Ce (1) (ppm)
QV3-002	1	0.4	7.07	12.0	19.0	530	612	4.1	17.0	0.47	1.2	1.2	110
QV3-004	3	0.4	7.06	12.0	17.0	510	611	4.1	16.0	0.47	1.4	1.3	110
QV3-006	5	0.7	7.31	9.3	17.0	510	630	4.0	15.0	0.48	1.3	1.2	100
QV3-008	7	0.6	7.62	9.3	14.0	520	626	3.7	13.0	0.46	1.2	1.1	98
QV3-010	9	0.6	7.61	10.0	14.0	570	628	3.7	14.0	0.45	1.2	1.1	100
QV3-012	11	0.5	7.80	11.0	14.0	540	617	3.4	13.0	0.42	1.1	1.1	93
QV3-014	13	0.4	7.90	11.0	12.0	550	607	3.3	13.0	0.41	1.0	1.0	93
QV3-016	15	0.3	7.80	11.0	11.0	490	585	3.3	13.0	0.41	1.0	1.0	93
QV3-018	17	0.2	7.76	12.0	15.0	480	593	3.2	13.0	0.41	1.1	1.1	94
QV3-020	19	0.3	7.59	12.0	24.0	510	583	3.1	13.0	0.41	1.0	1.0	90
QV3-022	21	0.2	7.73	12.0	15.0	500	605	3.2	13.0	0.40	1.2	1.0	87
QV3-024	23	0.2	7.68	13.0	12.0	510	600	3.1	13.0	0.41	1.0	1.0	90
QV3-026	25	0.2	7.72	12.0	16.0	510	597	3.0	13.0	0.41	1.0	1.1	88
QV3-028	27	0.2	7.55	15.0	12.0	500	588	3.1	15.0	0.38	0.9	0.9	86
QV3-030	29	<0.2	7.63	18.0	13.0	530	579	3.1	17.0	0.31	0.6	0.6	87
QV3-032	31	0.2	6.81	24.7	30.0	540	578	3.7	21.7	0.31	0.8	0.8	89
QV3-034	33	0.3	6.87	23.6	41.0	550	648	4.1	21.6	0.29	0.9	0.9	94
QV3-036	35	<0.2	6.31	25.5	33.0	510	609	3.8	19.0	0.29	0.6	0.6	82
QV3-038	37	0.2	6.70	17.0	35.0	450	554	4.1	18.0	0.25	0.4	0.5	94
QV3-040	39	0.2	7.00	15.0	34.0	480	602	4.7	21.6	0.22	0.3	0.3	100
QV3-042	41	<0.2	6.51	15.0	21.0	440	552	4.9	24.1	0.23	0.2	0.4	120
QV3-044	43	0.2	6.71	17.0	13.0	480	553	5.0	24.7	0.21	0.2	0.3	140
QV3-046	45	<0.2	6.69	15.0	8.9	410	534	4.7	23.7	0.22	0.2	0.3	140
QV3-048	47	0.2	6.55	14.0	12.0	380	506	4.4	24.7	0.21	0.3	0.4	130
QV3-050	49	0.3	6.48	18.0	8.8	470	473	4.5	29.3	0.21	0.2	0.3	140
QV3-055	52.5	<0.2	6.03	16.0	6.1	390	431	4.2	30.6	0.20	<0.2	0.3	140
QV3-060	57.5	<0.2	5.26	13.0	<2	350	381	4.1	45.3	0.22	0.4	0.4	150
QV3-065	62.5	<0.2	4.82	9.2	<2	320	353	3.7	50.3	0.23	0.4	0.4	130
QV3-070	67.5	<0.2	4.59	8.5	<2	300	326	3.8	58.4	0.25	0.4	0.5	150
QV3-075	72.5	<0.2	4.57	8.2	<2	290	312	3.9	56.7	0.25	0.4	0.4	150
QV3-080	77.5	<0.2	4.76	7.0	<2	310	326	3.7	50.0	0.25	0.4	0.4	140
QV3-085	82.5	<0.2	4.60	7.5	<2	260	328	3.6	43.3	0.25	0.3	0.3	130
QV3-090	87.5	<0.2	4.67	7.9	<2	250	313	4.0	50.8	0.25	0.4	0.4	150
QV3-095	92.5	<0.2	4.87	8.3	<2	280	336	4.2	44.9	0.25	0.5	0.4	140
QV3-100	97.5	<0.2	4.76	8.3	<2	300	331	4.4	50.6	0.26	0.5	0.5	160
QV3-105	102.5	<0.2	5.07	8.3	<2	330	351	4.7	45.5	0.27	0.5	0.5	160
QV3-110	107.5	<0.2	4.96	9.2	<2	320	340	5.1	46.9	0.26	0.5	0.5	170
QV3-115	112.5	0.2	5.07	8.5	<2	270	343	5.5	42.6	0.26	0.6	0.5	180
QV3-120	117.5	<0.2	4.94	7.5	<2	240	344	5.4	40.5	0.25	0.6	0.5	160
QV3-125	122.5	0.2	5.01	8.8	<2	300	350	5.8	43.0	0.25	0.6	0.5	180
QV3-130	127.5	0.2	4.98	7.9	<2	280	352	6.0	42.6	0.26	0.6	0.6	190
QV3-135	132.5	<0.2	5.04	8.4	<2	290	357	6.3	40.5	0.26	0.6	0.6	180
QV3-140	137.5	<0.2	5.10	8.5	<2	300	363	6.7	42.8	0.26	0.7	0.5	211
QV3-145	142.5	<0.2	5.27	11.0	<2	360	373	7.5	46.5	0.27	0.8	0.6	220
QV3-150	147.5	<0.2	5.27	11.0	<2	320	383	7.8	44.4	0.27	0.7	0.6	228
QV3-155	152.5	<0.2	5.24	11.0	<2	360	390	8.1	46.7	0.27	0.8	0.6	238
QV3-160	157.5	<0.2	5.21	11.0	<2	330	400	8.5	43.9	0.28	0.9	0.6	257
QV3-165	162.5	<0.2	5.20	10.0	<2	360	426	7.5	39.5	0.28	0.7	0.6	226
QV3-170	167.5	<0.2	4.89	11.0	<2	320	402	9.0	43.5	0.29	0.8	0.6	253
QV3-175	172.5	<0.2	4.81	11.0	<2	340	410	9.3	42.1	0.29	0.7	0.6	253
QV3-180	177.5	0.2	4.95	12.0	<2	360	438	10.0	39.4	0.30	0.7	0.6	245
QV3-185	182.5	<0.2	5.14	15.0	<2	310	431	10.2	39.7	0.31	0.9	0.7	253
QV3-190	187.5	0.2	4.90	15.0	<2	350	413	12.5	41.4	0.29	1.0	0.8	245
QV3-195	192.5	<0.2	5.11	18.0	<2	460	454	11.4	49.9	0.29	1.2	0.9	295
QV3-200	197.5	0.2	4.92	15.0	<2	390	384	10.8	52.2	0.28	1.0	0.8	284

Core QV3

Depth (cm)	Ce (2) (ppm)	Co (1) (ppm)	Co (2) (ppm)	Co (3) (ppm)	Cr (1) (ppm)	Cr (2) (ppm)	Cr (2a) (ppm)	Cs (1) (ppm)	Cu (2) (ppm)	Cu (3) (ppm)	Dy (2) (ppm)	Eu (1) (ppm)	Fe (1) (%)
1	118	22.0	26	17	73.0	55	51	5.9	104	72	8.6	2.10	6.30
3	119	24.0	25	17	81.0	57	52	5.6	109	79	8.5	3.60	6.00
5	116	20.0	23	15	51.0	56	52	5.5	110	77	8.3	2.80	5.70
7	94	21.0	22	16	54.0	53	48	6.3	92	70	6.8	2.60	5.40
9	103	20.0	22	15	69.0	54	47	6.7	87	63	7.1	3.20	5.20
11	94	21.0	22	16	59.0	51	46	6.5	77	58	6.3	2.10	5.30
13	103	20.0	22	15	53.0	50	44	6.1	75	58	6.5	1.80	4.90
15	95	18.0	22	14	48.0	49	43	6.0	73	56	6.3	3.20	4.90
17	92	20.0	22	15	60.0	45	39	5.8	74	57	6.2	1.90	4.90
19	85	16.0	21	14	50.0	44	40	5.7	72	54	5.8	3.60	5.00
21	91	18.0	22	14	47.0	48	42	5.8	74	55	6.1	1.50	5.00
23	86	18.0	21	14	72.0	45	41	5.6	70	53	6.0	2.00	5.00
25	80	18.0	21	14	43.0	45	40	5.4	69	53	5.7	1.90	5.00
27	77	21.0	24	15	44.0	47	43	5.5	66	50	5.6	2.10	5.10
29	92	27.0	29	20	56.0	50	46	5.7	53	41	6.1	3.20	5.90
31	87	31.0	35	18	52.0	47	40	5.3	51	35	7.5	2.50	7.90
33	101	37.0	39	20	69.0	50	40	4.9	55	36	7.3	2.30	5.80
35	91	46.0	49	27	47.0	41	37	4.3	44	30	9.9	2.10	6.70
37	88	40.0	42	22	35.0	42	37	5.1	42	28	9.0	2.40	6.70
39	120	42.0	42	23	39.0	42	34	6.0	39	28	9.0	2.50	6.80
41	125	45.0	50	28	37.0	35	31	5.4	37	27	10.1	3.40	7.00
43	148	43.0	43	25	35.0	36	30	6.0	36	27	9.7	3.60	7.20
45	150	63.0	63	38	32.0	30	26	6.6	36	25	9.8	3.80	6.10
47	150	68.0	71	43	42.0	35	30	5.8	30	21	9.4	3.30	6.40
49	154	56.0	59	32	46.0	35	29	5.2	23	16	9.2	2.90	7.40
52.5	151	49.0	55	33	25.0	32	27	4.9	20	14	8.8	3.80	5.90
57.5	155	68.0	74	42	19.0	24	20	3.5	17	12	9.1	3.50	5.80
62.5	143	61.0	65	39	18.0	21	18	3.4	16	13	7.9	3.60	4.40
67.5	156	42.0	45	25	16.0	18	17	2.6	16	12	8.4	3.10	4.20
72.5	162	51.0	55	30	<15	20	17	2.7	17	11	8.4	3.10	4.10
77.5	148	30.0	33	18	<15	20	17	3.0	17	12	8.0	2.80	3.50
82.5	139	39.0	38	21	28.0	20	17	3.8	16	11	7.9	3.70	3.50
87.5	158	41.0	39	22	27.0	19	17	3.8	18	13	8.4	3.40	3.70
92.5	161	47.0	48	28	31.0	19	17	4.1	18	13	8.7	3.20	3.80
97.5	171	53.0	48	28	31.0	19	16	4.2	18	13	8.8	4.10	3.90
102.5	176	47.0	45	26	34.0	19	17	3.8	21	14	9.3	3.90	3.50
107.5	192	81.0	71	43	30.0	21	17	4.0	20	15	10.0	3.90	4.10
112.5	201	57.0	56	32	26.0	20	18	3.6	22	15	10.7	2.40	3.80
117.5	196	37.0	38	24	30.0	19	17	3.5	21	14	10.6	4.10	3.60
122.5	211	63.0	61	34	16.0	19	18	3.8	21	15	11.2	6.00	3.60
127.5	213	37.0	38	22	20.0	17	15	3.2	22	16	11.4	4.40	3.50
132.5	221	37.0	37	20	39.0	20	16	4.2	22	16	11.8	6.10	3.50
137.5	231	41.0	37	21	<15	20	15	4.1	24	16	12.6	5.30	3.80
142.5	246	52.0	52	28	25.0	21	16	4.2	26	17	13.7	5.00	4.00
147.5	252	61.0	56	31	<15	19	15	4.4	26	16	14.0	6.50	4.20
152.5	261	74.0	64	35	28.0	21	13	4.8	28	18	14.5	7.20	4.70
157.5	268	53.0	47	26	40.0	18	12	4.6	27	18	14.7	7.20	4.50
162.5	238	33.0	32	18	19.0	20	14	5.3	27	17	13.4	5.50	3.70
167.5	276	74.0	69	42	30.0	19	12	3.7	28	17	15.8	7.10	4.40
172.5	272	45.0	44	24	26.0	20	13	4.3	28	18	15.9	7.90	4.60
177.5	272	67.0	64	39	35.0	21	14	4.7	30	22	16.5	7.00	5.00
182.5	295	110.0	104	61	32.0	19	12	4.2	35	22	18.8	9.20	6.30
187.5	297	110.0	107	66	28.0	20	14	3.9	39	23	19.7	8.20	4.80
192.5	283	94.0	87	54	<15	22	14	4.4	39	24	19.1	9.20	5.70
197.5	273	65.0	65	37	25.0	21	14	3.6	36	23	17.8	8.30	5.00

Core QV3

Depth (cm)	Fe (2) (%)	Fe (3) (%)	Ga (2) (ppm)	Hf (1) (ppm)	Hg(18) (ppb)	K (2) (%)	La (1) (ppm)	La (2) (ppm)	Li (2) (ppm)	LOI (%)	Lu (1) (ppm)	Mg (2) (%)	Mn (2) (%)
1	6.36	4.74	24	5.10	519	1.93	55.0	58	44.6	17.0	0.63	0.76	0.38
3	6.34	5.01	24	5.60	491	1.96	57.0	59	44.5	16.7	0.64	0.77	0.33
5	6.03	4.33	23	4.70	410	2.03	52.0	57	45.0	15.8	0.76	0.78	0.20
7	5.62	4.24	23	4.30	382	2.16	45.0	41	47.1	14.5	0.52	0.81	0.14
9	5.55	4.02	24	5.30	382	2.19	47.0	45	47.9	14.4	0.62	0.80	0.13
11	5.51	4.14	24	5.90	410	2.23	44.0	39	43.2	13.7	0.60	0.82	0.13
13	5.54	3.98	25	5.60	369	2.22	43.0	41	48.6	13.7	0.61	0.82	0.15
15	5.38	4.27	25	5.10	382	2.16	40.0	36	47.5	13.8	0.53	0.78	0.15
17	5.37	3.99	23	5.30	410	2.13	39.0	35	47.0	13.7	0.60	0.77	0.16
19	5.29	3.82	26	5.20	464	2.13	38.0	30	46.3	13.6	0.57	0.76	0.17
21	5.38	3.94	24	5.30	491	2.14	37.0	35	47.4	13.3	0.67	0.77	0.17
23	5.30	3.90	25	6.30	437	2.11	37.0	30	46.7	13.4	0.50	0.76	0.17
25	5.16	4.02	22	4.70	423	2.14	36.0	30	45.5	13.0	0.67	0.75	0.16
27	5.23	3.90	23	4.50	573	2.04	33.0	29	47.6	14.6	0.46	0.74	0.18
29	5.64	4.45	23	5.70	901	1.84	34.0	32	54.1	14.7	0.56	0.79	0.55
31	7.37	5.95	22	5.10	1324	1.55	38.0	32	47.6	19.0	0.66	0.67	1.92
33	6.05	4.38	23	4.30	1283	1.56	37.0	40	50.1	20.7	0.59	0.65	0.48
35	6.94	5.05	21	4.10	710	1.41	35.0	37	45.3	20.6	0.61	0.60	3.67
37	7.14	5.48	22	4.90	1133	1.48	39.0	35	49.1	18.5	0.67	0.62	2.28
39	7.18	5.43	24	4.30	1256	1.52	42.0	46	53.6	18.6	0.74	0.63	0.53
41	7.12	5.97	22	3.90	723	1.34	42.0	45	49.4	20.4	0.66	0.55	1.53
43	7.20	5.87	22	4.90	560	1.29	48.0	48	52.9	20.7	0.65	0.52	0.40
45	6.49	5.07	22	4.50	464	1.26	46.0	48	50.5	21.4	0.58	0.49	0.39
47	6.54	5.19	22	3.60	464	1.18	44.0	47	49.2	23.9	0.50	0.45	0.47
49	7.11	5.35	21	4.40	355	1.13	42.0	46	48.1	24.3	0.78	0.43	0.33
52.5	6.11	5.04	18	3.90	273	0.97	41.0	44	44.8	27.0	0.68	0.38	0.33
57.5	6.00	4.33	17	3.10	232	0.73	43.0	45	32.1	33.3	0.66	0.30	0.39
62.5	4.42	3.42	13	2.40	218	0.64	40.0	41	27.5	37.6	0.57	0.26	0.36
67.5	4.16	2.99	12	2.30	278	0.52	43.0	45	23.4	41.5	0.61	0.22	0.36
72.5	3.98	2.69	12	2.90	241	0.52	44.0	46	23.5	41.9	0.63	0.22	0.35
77.5	3.70	2.46	12	3.00	231	0.63	40.0	44	28.4	39.7	0.63	0.25	0.32
82.5	3.43	2.31	11	2.30	204	0.65	42.0	42	29.2	42.7	0.38	0.26	0.31
87.5	3.49	2.49	12	2.40	222	0.56	47.0	46	25.4	40.2	0.56	0.23	0.28
92.5	3.51	2.46	12	2.60	222	0.63	46.0	47	28.1	39.6	0.48	0.25	0.27
97.5	3.56	2.45	11	2.20	231	0.56	52.0	49	25.8	41.0	0.50	0.23	0.27
102.5	3.56	2.39	11	2.20	241	0.66	53.0	50	29.3	37.3	0.50	0.27	0.25
107.5	4.04	2.99	12	2.50	222	0.53	56.0	55	26.0	40.1	0.68	0.23	0.27
112.5	4.01	2.78	12	2.10	222	0.53	58.0	58	26.5	39.1	0.67	0.24	0.26
117.5	3.74	2.68	12	2.20	204	0.54	54.0	56	27.2	39.3	0.64	0.24	0.24
122.5	3.62	2.41	13	2.50	241	0.52	60.0	60	26.9	40.3	0.68	0.23	0.24
127.5	3.66	2.53	11	2.40	222	0.50	59.0	62	26.2	40.1	0.71	0.22	0.24
132.5	3.76	2.62	12	2.30	204	0.53	61.0	62	27.5	39.6	0.66	0.24	0.24
137.5	3.87	2.69	12	2.20	222	0.53	64.0	66	28.0	39.2	0.78	0.24	0.24
142.5	3.88	2.66	12	2.60	250	0.52	71.0	72	28.3	40.3	0.83	0.24	0.24
147.5	3.98	2.63	13	2.60	222	0.55	76.0	73	29.8	40.4	1.00	0.25	0.24
152.5	4.47	3.09	13	1.50	222	0.59	82.0	76	30.4	39.3	1.20	0.26	0.24
157.5	4.28	3.07	13	3.00	213	0.61	82.0	77	30.7	39.3	1.10	0.27	0.22
162.5	3.72	2.57	14	3.30	185	0.74	75.0	72	35.5	38.1	0.81	0.31	0.20
167.5	4.31	3.03	12	2.20	204	0.56	85.0	83	28.2	41.1	1.10	0.25	0.22
172.5	4.47	3.09	13	2.70	222	0.56	88.0	84	28.8	41.0	1.00	0.24	0.22
177.5	4.90	3.75	14	2.70	185	0.66	89.0	89	32.3	37.8	1.20	0.28	0.22
182.5	6.65	5.05	15	3.20	213	0.56	95.0	97	28.4	37.9	1.10	0.26	0.30
187.5	4.85	3.36	13	2.10	204	0.55	91.0	100	28.1	37.0	1.00	0.25	0.23
192.5	5.09	3.61	14	2.30	204	0.59	99.0	97	31.9	36.7	1.50	0.27	0.25
197.5	4.55	3.28	14	2.40	204	0.53	95.0	92	27.2	38.1	1.30	0.24	0.23

Core QV3

Depth (cm)	Mn (3) (ppm)	Mo (2) (ppm)	Mo (5) (ppm)	Na (1) (%)	Na (2) (%)	Nb (2) (ppm)	Ni (2) (ppm)	Ni (3) (ppm)	P (2) (ppb)	Pb (2) (ppm)	Pb (3) (ppm)	Rb (1) (ppm)
1	2920	4	2	1.50	1.46	13	28	16	2225	394	333	69.0
3	2630	5	2	1.50	1.48	13	28	16	2277	407	354	72.0
5	1560	5	2	1.50	1.54	13	29	16	2258	456	385	72.0
7	912	5	2	1.40	1.56	14	28	17	2134	465	425	79.0
9	848	5	2	1.40	1.54	14	28	17	2108	478	417	86.0
11	873	4	2	1.50	1.55	14	28	17	1977	444	413	85.0
13	938	5	2	1.50	1.53	16	25	16	2020	424	377	84.0
15	980	5	2	1.50	1.57	16	25	16	1980	386	359	87.0
17	1270	4	2	1.60	1.58	14	25	16	2108	366	330	79.0
19	1410	5	2	1.60	1.62	16	25	15	2090	328	294	81.0
21	1330	4	2	1.50	1.59	14	25	16	2089	342	296	83.0
23	1370	5	2	1.70	1.63	16	27	15	2013	313	277	80.0
25	1050	4	2	1.60	1.64	14	24	15	1975	300	276	76.0
27	1460	5	2	1.50	1.59	14	27	15	1922	290	251	78.0
29	4480	5	2	1.60	1.51	16	25	16	1868	241	212	83.0
31	16000	5	<2	1.40	1.23	12	25	14	2205	316	240	72.0
33	3850	5	2	1.20	1.19	12	30	16	2514	403	301	61.0
35	28800	7	3	1.10	1.11	13	24	14	1737	341	249	56.0
37	18600	5	2	1.10	1.15	13	27	18	1861	326	250	54.0
39	4040	5	2	1.20	1.17	12	23	15	2516	309	237	64.0
41	11300	5	2	1.00	1.05	12	23	14	2380	198	166	54.0
43	3240	6	3	1.00	1.03	10	19	13	2722	121	94	51.0
45	2910	7	3	1.00	1.01	11	20	12	2433	96	67	57.0
47	3700	6	3	0.86	0.91	10	19	12	2404	92	64	56.0
49	2630	6	3	0.86	0.86	8	17	11	2441	80	61	64.0
52.5	2660	8	3	0.84	0.78	8	13	8	2083	53	40	50.0
57.5	2900	11	4	0.66	0.60	7	14	8	1904	36	19	35.0
62.5	2910	8	3	0.59	0.53	5	13	8	1904	18	13	33.0
67.5	3010	9	3	0.48	0.41	4	10	6	2044	16	11	25.0
72.5	2740	9	3	0.46	0.41	5	12	6	2032	16	11	19.0
77.5	2440	9	3	0.54	0.49	6	10	5	1949	16	12	33.0
82.5	2460	8	3	0.57	0.52	6	10	5	1762	18	12	27.0
87.5	2250	9	3	0.48	0.44	5	10	5	2014	14	12	24.0
92.5	2230	9	3	0.50	0.49	6	13	5	1951	16	12	30.0
97.5	2200	9	3	0.50	0.44	5	11	6	2006	16	12	26.0
102.5	1990	8	3	0.59	0.54	6	13	6	2001	21	15	30.0
107.5	2290	9	3	0.47	0.42	5	16	8	2280	20	15	22.0
112.5	2060	8	3	0.43	0.42	5	14	7	2269	20	15	27.0
117.5	1990	7	3	0.44	0.42	5	11	5	2138	16	13	17.0
122.5	1940	7	3	0.44	0.39	3	15	7	2204	22	13	26.0
127.5	2000	6	3	0.43	0.39	3	13	6	2269	22	15	18.0
132.5	1830	6	3	0.44	0.41	4	13	6	2275	20	15	30.0
137.5	1740	6	3	0.44	0.40	4	13	6	2356	20	13	23.0
142.5	1790	6	3	0.43	0.40	4	16	7	2597	26	14	23.0
147.5	1690	6	3	0.48	0.43	5	18	8	2575	24	13	21.0
152.5	1800	5	3	0.55	0.46	4	18	8	2586	25	14	22.0
157.5	1750	5	3	0.55	0.47	4	15	7	2605	27	15	27.0
162.5	1640	4	3	0.70	0.61	5	12	6	2302	23	14	32.0
167.5	1790	5	4	0.50	0.44	4	19	9	2674	28	14	24.0
172.5	1690	4	3	0.51	0.44	4	14	7	2755	26	16	25.0
177.5	1880	5	4	0.60	0.54	5	16	9	2688	27	19	29.0
182.5	2300	7	2	0.49	0.46	<3	21	11	2404	27	18	25.0
187.5	1730	7	5	0.43	0.42	4	24	12	2985	30	16	24.0
192.5	1920	6	4	0.54	0.47	4	22	12	2658	29	15	33.0
197.5	1800	6	4	0.46	0.40	4	20	10	2984	30	16	33.0

Core QV3

Depth (cm)	Rb (2) (ppm)	Sb (1) (ppm)	Sc (1) (ppm)	Sc (2) (ppm)	Sm (1) (ppm)	Sr (2) (ppm)	Ta (1) (ppm)	Tb (1) (ppm)	Th (1) (ppm)	Ti (2) (ppm)	U (1) (ppm)	V (2) (ppm)	W (1) (ppm)
1	75	2.20	13.8	14.6	10.6	78	1.00	1.50	7.8	4167	2.1	106	3.20
3	76	2.10	13.4	14.6	10.8	78	0.93	1.70	7.5	4167	2.1	108	2.60
5	86	1.90	13.2	14.9	10.6	80	1.10	1.50	8.0	4326	2.1	116	3.80
7	91	1.60	12.8	14.6	10.0	73	1.10	1.30	7.9	4421	2.4	114	3.10
9	91	1.70	13.1	15.2	10.6	76	1.30	1.60	8.9	4406	2.4	112	4.50
11	94	1.70	14.0	15.3	9.0	74	1.20	1.40	8.9	4502	2.2	112	3.80
13	98	1.70	14.5	15.8	8.6	73	1.00	1.20	9.0	4561	2.2	107	3.80
15	89	1.60	14.0	15.0	8.2	72	1.10	1.10	8.5	4493	2.2	105	2.40
17	92	1.90	14.1	15.2	8.0	74	1.20	1.20	8.7	4462	2.1	101	2.70
19	92	2.00	14.4	14.5	8.0	72	1.20	1.00	9.1	4501	2.2	100	2.70
21	89	2.00	13.9	15.4	7.7	75	0.92	1.10	8.9	4556	2.2	101	2.20
23	88	2.10	14.2	14.9	7.9	74	0.92	1.20	9.0	4503	2.2	99	<2.0
25	89	1.90	13.8	14.8	7.8	74	0.90	1.20	8.7	4375	2.1	100	<2.0
27	85	2.20	13.0	14.7	7.6	71	1.10	1.10	8.5	4367	2.0	100	<2.0
29	81	2.30	15.3	16.1	7.7	72	1.10	1.30	8.7	4693	2.2	96	<2.0
31	65	2.70	14.7	14.5	8.7	60	0.95	1.30	7.5	3936	2.0	86	<2.0
33	63	2.50	13.4	15.2	8.7	65	0.75	1.30	7.1	3889	2.1	83	<2.0
35	54	1.80	12.6	13.7	8.2	60	1.00	1.10	6.5	3581	1.7	77	<2.0
37	62	1.20	13.0	14.3	9.1	54	0.86	1.20	7.0	3812	1.9	81	<2.0
39	68	0.84	13.7	15.9	10.6	52	0.80	1.50	7.1	3928	2.1	81	<2.0
41	57	0.76	12.3	14.4	11.2	47	0.90	1.30	6.4	3567	1.9	74	<2.0
43	58	0.62	13.2	14.0	12.8	46	0.75	1.90	7.0	3552	2.2	71	<2.0
45	62	0.50	12.7	12.6	12.3	48	0.57	1.60	6.8	3651	2.1	67	<2.0
47	52	0.41	11.4	13.4	11.8	43	0.81	1.70	6.3	3388	2.0	69	<2.0
49	52	0.38	12.4	13.1	15.0	42	1.00	1.90	6.6	3343	2.1	68	<2.0
52.5	45	0.27	11.6	11.8	14.0	40	0.63	1.80	5.9	3032	1.8	62	<2.0
57.5	37	0.21	10.0	9.7	14.0	36	0.46	1.60	4.7	2365	1.5	49	<2.0
62.5	26	0.16	8.7	8.7	12.8	36	0.51	1.40	4.0	2077	1.3	44	<2.0
67.5	20	0.17	8.2	7.8	13.9	34	0.30	1.70	3.7	1732	1.2	38	<2.0
72.5	23	0.17	8.0	7.8	14.0	34	0.42	1.60	3.9	1705	1.2	38	<2.0
77.5	26	0.16	7.8	8.3	12.7	36	0.58	1.50	4.1	1948	1.2	40	<2.0
82.5	26	0.17	8.1	8.3	10.6	37	0.63	1.50	3.6	1933	1.2	41	<2.0
87.5	22	0.19	8.3	7.8	12.3	34	0.48	1.50	4.0	1756	1.3	38	<2.0
92.5	19	0.20	7.9	8.3	12.3	35	0.49	1.60	4.2	1914	1.3	41	<2.0
97.5	28	0.19	8.3	8.0	13.8	34	0.37	2.00	4.1	1723	1.3	38	<2.0
102.5	27	0.23	8.9	8.8	14.0	38	0.50	1.90	4.6	2028	1.5	40	<2.0
107.5	26	0.17	8.7	8.4	15.1	33	0.42	2.00	4.0	1711	1.5	38	<2.0
112.5	24	0.17	8.6	8.8	15.3	33	0.34	1.80	3.9	1760	1.4	39	<2.0
117.5	24	0.17	8.4	8.7	14.8	32	0.49	1.90	3.9	1721	1.3	39	<2.0
122.5	18	0.19	8.6	8.9	16.6	32	0.25	2.20	4.2	1667	1.4	39	<2.0
127.5	27	0.16	8.4	9.1	16.4	31	0.10	2.10	3.8	1635	1.4	39	<2.0
132.5	19	0.16	8.8	9.7	16.9	32	0.39	2.30	3.7	1722	1.4	41	<2.0
137.5	21	0.17	9.1	10.0	18.2	31	0.25	2.40	4.2	1744	1.3	41	<2.0
142.5	23	0.21	9.2	10.6	22.1	31	0.62	3.00	4.4	1721	1.7	43	<2.0
147.5	26	0.17	10.4	10.9	21.6	32	0.54	2.80	4.3	1910	1.6	43	<2.0
152.5	26	0.23	11.7	11.1	22.8	33	0.66	3.10	4.6	1801	1.6	47	<2.0
157.5	31	0.21	11.1	11.1	22.8	34	0.37	3.00	4.6	1795	1.7	46	<2.0
162.5	31	0.23	11.1	11.4	20.6	39	0.37	2.70	4.6	2012	1.8	49	<2.0
167.5	29	0.25	10.5	11.0	23.8	33	0.50	3.20	4.2	1634	1.5	45	<2.0
172.5	27	0.21	10.4	10.9	24.6	33	0.47	3.20	3.9	1623	1.6	45	<2.0
177.5	27	0.23	11.0	11.6	25.5	37	0.38	3.30	4.2	1850	1.9	46	<2.0
182.5	23	0.26	10.7	11.8	27.7	34	0.37	3.70	4.3	1650	1.7	44	<2.0
187.5	26	0.27	10.0	12.2	30.0	32	0.31	3.80	3.9	1560	1.7	44	<2.0
192.5	23	0.36	12.8	12.5	39.0	33	0.40	4.60	5.1	1702	2.3	46	<2.0
197.5	26	0.26	11.8	11.6	34.3	31	0.36	3.70	4.6	1584	1.8	43	<2.0

Core QV3

Depth (cm)	Y (2) (ppm)	Yb (1) (ppm)	Zn (1) (ppm)	Zn (2) (ppm)	Zn (3) (ppm)	Zr (2) (ppm)
1	51	2.90	730.0	679	561	133
3	51	2.90	660.0	717	653	124
5	50	2.70	640.0	751	662	132
7	41	2.40	570.0	676	620	123
9	42	2.70	600.0	654	569	124
11	37	2.30	490.0	491	436	131
13	38	2.80	430.0	449	399	137
15	35	2.90	410.0	416	375	127
17	35	2.50	350.0	393	360	124
19	33	2.50	340.0	372	335	125
21	35	2.80	350.0	372	329	126
23	34	2.70	320.0	350	315	126
25	32	2.30	350.0	342	311	123
27	31	2.70	290.0	331	288	121
29	32	2.70	310.0	302	271	129
31	34	2.80	550.0	484	381	116
33	40	2.40	570.0	570	435	126
35	37	2.30	480.0	417	325	111
37	37	2.60	350.0	334	248	113
39	49	3.00	260.0	282	208	132
41	47	2.80	230.0	231	167	111
43	52	2.70	170.0	207	157	125
45	51	2.70	130.0	196	139	141
47	50	2.60	130.0	200	152	121
49	49	4.50	140.0	202	149	113
52.5	46	5.00	120.0	168	131	106
57.5	47	3.80	210.0	181	131	91
62.5	41	4.40	150.0	158	129	74
67.5	43	4.10	160.0	168	127	62
72.5	44	4.40	190.0	164	115	64
77.5	42	4.30	140.0	156	111	73
82.5	41	2.00	150.0	138	99	75
87.5	46	2.30	180.0	155	111	66
92.5	47	2.20	110.0	155	112	74
97.5	48	2.40	160.0	159	119	67
102.5	50	2.50	170.0	176	126	74
107.5	54	2.60	170.0	187	149	65
112.5	58	2.50	180.0	191	143	68
117.5	56	2.70	150.0	179	140	64
122.5	60	2.70	130.0	186	135	65
127.5	61	2.40	140.0	186	142	63
132.5	63	2.60	150.0	198	144	70
137.5	66	2.70	170.0	201	148	71
142.5	72	3.10	190.0	225	163	69
147.5	74	3.60	170.0	226	166	74
152.5	77	4.10	220.0	239	179	55
157.5	78	4.20	190.0	232	172	55
162.5	72	3.40	160.0	185	138	62
167.5	84	4.00	180.0	213	145	51
172.5	85	4.40	180.0	202	143	49
177.5	87	4.20	100.0	191	145	57
182.5	97	4.80	180.0	234	169	53
187.5	100	3.90	140.0	229	175	52
192.5	98	9.50	340.0	258	192	53
197.5	92	10.00	310.0	251	192	53

Core QV4

core QV4 Sample #	Depth (cm)	Ag (6) (ppm)	Al (2) (%)	As (1) (ppm)	Au (1) (ppb)	Ba (1) (ppm)	Ba (2) (ppm)	Be (2) (ppm)	Br (1) (ppm)	Ca (2) (%)
QV4-002	1	0.6	7.23	10.0	14.0	590	624	4.1	18.0	0.48
QV4-004	3	0.5	7.32	10.0	18.0	590	626	4.1	17.0	0.47
QV4-006	5	0.6	7.42	9.0	17.0	590	616	3.9	15.0	0.47
QV4-008	7	0.6	7.81	10.0	14.0	590	610	3.6	15.0	0.46
QV4-010	9	0.6	7.71	10.0	14.0	590	601	3.5	15.0	0.45
QV4-012	11	0.5	7.94	12.0	14.0	700	590	3.3	17.0	0.45
QV4-014	13	0.4	7.80	11.0	13.0	610	646	3.2	15.0	0.43
QV4-016	15	0.3	7.77	12.0	13.0	590	604	3.1	15.0	0.42
QV4-018	17	0.3	7.74	13.0	13.0	570	591	3.0	15.0	0.42
QV4-020	19	0.2	7.82	13.0	14.0	590	600	3.1	15.0	0.41
QV4-022	21	0.2	7.77	13.0	15.0	620	598	3.1	15.0	0.42
QV4-024	23	0.2	7.72	13.0	13.0	580	592	3.0	16.0	0.44
QV4-026	25	0.3	7.51	18.0	15.0	530	553	3.2	19.0	0.34
QV4-028	27	0.2	7.70	20.0	18.0	550	533	3.3	19.0	0.33
QV4-030	29	<0.2	7.93	17.0	11.0	570	541	3.2	19.0	0.31
QV4-032	31	<0.2	8.20	18.0	11.0	610	516	2.9	17.0	0.30
QV4-034	33	0.3	7.92	18.0	14.0	590	542	3.1	16.0	0.29
QV4-036	35	0.2	7.22	19.0	27.0	580	564	3.9	20.0	0.27
QV4-038	37	0.2	7.03	18.0	29.0	520	547	4.0	21.5	0.26
QV4-040	39	0.2	7.02	17.0	33.0	560	563	4.6	24.6	0.22
QV4-042	41	0.2	6.71	17.0	17.0	540	533	5.1	30.1	0.22
QV4-044	43	<0.2	6.65	18.0	10.0	510	506	5.1	32.2	0.21
QV4-046	45	<0.2	6.59	17.0	9.2	450	487	4.8	27.1	0.22
QV4-048	47	<0.2	6.50	17.0	12.0	500	480	4.7	28.2	0.21
QV4-050	49	0.2	6.46	16.0	11.0	430	462	4.8	32.8	0.21
QV4-055	52.5	<0.2	6.20	15.0	8.5	460	420	4.3	37.1	0.20
QV4-060	57.5	<0.2	5.59	14.0	<2.0	370	370	4.3	44.6	0.22
QV4-065	62.5	<0.2	5.13	12.0	<2.0	340	330	4.1	57.6	0.24
QV4-070	67.5	<0.2	4.41	9.2	<2.0	310	293	3.7	65.3	0.26
QV4-075	72.5	<0.2	4.60	7.7	<2.0	260	288	3.8	65.8	0.27
QV4-080	77.5	<0.2	4.69	6.7	<2.0	260	289	4.0	57.2	0.26
QV4-085	82.5	0.2	4.73	6.5	<2.0	270	303	3.8	56.3	0.26
QV4-090	87.5	<0.2	4.84	7.1	<2.0	300	316	4.0	54.4	0.26
QV4-095	92.5	<0.2	4.68	7.2	<2.0	250	297	4.2	54.9	0.27
QV4-100	97.5	<0.2	4.84	7.0	<2.0	290	310	4.4	54.1	0.28
QV4-105	102.5	<0.2	4.86	7.6	<2.0	330	297	4.5	62.1	0.28
QV4-110	107.5	<0.2	4.98	7.8	<2.0	310	310	4.5	54.7	0.29
QV4-115	112.5	0.2	4.86	8.4	<2.0	290	303	5.0	54.6	0.29
QV4-120	117.5	<0.2	5.11	8.6	<2.0	310	308	5.4	52.4	0.29
QV4-125	122.5	<0.2	4.90	8.1	<2.0	280	304	5.4	51.8	0.28
QV4-130	127.5	0.2	5.03	7.4	<2.0	300	313	5.5	48.2	0.28
QV4-135	132.5	<0.2	4.84	8.3	<2.0	280	298	5.8	51.7	0.29
QV4-140	137.5	<0.2	4.94	8.3	<2.0	300	310	5.9	52.0	0.29
QV4-145	142.5	<0.2	4.97	8.0	<2.0	260	314	6.2	46.9	0.29
QV4-150	147.5	0.2	5.09	8.3	<2.0	290	317	6.7	48.6	0.29
QV4-155	152.5	<0.2	5.12	10.0	<2.0	340	321	6.8	55.9	0.26
QV4-160	157.5	0.2	5.44	10.0	4.9	360	367	5.3	48.4	0.30

Core QV4

Depth (cm)	Cd (2) (ppm)	Cd (3) (ppm)	Ce (1) (ppm)	Ce (2) (ppm)	Co (1) (ppm)	Co (2) (ppm)	Co (3) (ppm)	Cr (1) (ppm)	Cr (2) (ppm)	Cr (2a) (ppm)
1	1.6	1.4	110	123	20.0	22	12	47.0	61	53
3	1.5	1.4	110	121	18.0	22	12	44.0	60	50
5	1.5	1.1	100	119	17.0	23	11	47.0	56	48
7	1.4	1.3	99	116	18.0	21	12	39.0	52	48
9	1.3	1.2	95	112	18.0	23	13	37.0	47	42
11	1.1	1.0	110	106	21.0	23	13	52.0	51	45
13	1.2	1.0	99	112	17.0	21	11	36.0	47	40
15	1.2	1.2	97	110	16.0	20	11	35.0	51	42
17	1.1	1.0	96	104	17.0	20	11	40.0	44	38
19	1.2	1.1	94	106	17.0	21	11	42.0	44	39
21	1.1	1.1	96	104	17.0	20	13	31.0	43	36
23	1.1	0.9	89	103	17.0	20	11	29.0	41	37
25	1.1	0.9	88	100	19.0	23	12	36.0	50	43
27	0.7	0.8	94	95	23.0	27	16	33.0	50	43
29	0.6	0.6	81	94	22.0	27	14	35.0	52	44
31	0.5	0.5	89	91	22.0	26	14	35.0	52	44
33	0.6	0.6	90	96	27.0	29	17	45.0	54	42
35	0.6	0.6	91	107	35.0	40	23	43.0	48	39
37	0.4	0.5	96	105	38.0	42	24	37.0	45	35
39	0.7	0.4	110	124	39.0	43	26	19.0	39	31
41	0.3	0.3	120	139	45.0	46	28	29.0	36	26
43	0.3	0.3	140	141	51.0	48	29	21.0	33	24
45	0.2	0.3	140	145	58.0	59	35	<15	33	23
47	0.4	0.3	140	147	56.0	57	35	26.0	33	23
49	0.4	0.3	130	153	64.0	68	45	16.0	30	23
52.5	0.3	0.3	140	142	58.0	57	34	19.0	27	21
57.5	0.5	0.4	160	148	72.0	67	41	34.0	25	18
62.5	0.5	0.4	160	145	61.0	56	34	<15	22	15
67.5	0.5	0.4	140	136	67.0	68	38	<15	18	13
72.5	0.5	0.4	150	145	28.0	30	16	<15	18	13
77.5	0.5	0.4	130	147	28.0	31	17	23.0	17	13
82.5	0.4	0.3	130	138	31.0	34	20	17.0	18	14
87.5	0.4	0.4	140	140	37.0	40	24	17.0	20	14
92.5	0.5	0.4	140	148	41.0	44	28	18.0	18	13
97.5	0.5	0.4	140	156	35.0	37	20	<15	18	13
102.5	0.6	0.5	160	159	43.0	43	24	21.0	18	13
107.5	0.5	0.5	170	161	45.0	45	27	<15	20	14
112.5	0.6	0.5	180	171	57.0	56	29	<15	16	13
117.5	0.6	0.5	200	185	55.0	55	33	<15	19	14
122.5	0.7	0.5	190	183	51.0	50	29	25.0	18	14
127.5	0.7	0.5	190	187	36.0	35	19	<15	18	14
132.5	0.6	0.5	200	193	56.0	56	32	17.0	17	13
137.5	0.6	0.5	200	192	41.0	39	23	25.0	18	14
142.5	0.6	0.5	200	211	33.0	35	20	25.0	19	15
147.5	0.7	0.6	190	220	31.0	36	22	28.0	22	16
152.5	0.7	0.6	229	220	40.0	37	22	18.0	22	18
157.5	0.6	0.5	180	179	42.0	41	23	16.0	24	20

Core QV4

Depth (cm)	Cs (1) (ppm)	Cu (2) (ppm)	Cu (3) (ppm)	Dy (2) (ppm)	Eu (1) (ppm)	Fe (1) (%)	Fe (2) (%)	Fe (3) (%)	Ga (2) (ppm)	Hf (1) (ppm)
1	5.1	119	82	8.8	3.30	6.30	6.39	4.95	22	5.20
3	5.6	114	82	8.5	2.50	6.10	6.22	4.55	23	5.80
5	5.0	101	67	8.0	2.70	5.30	5.77	4.06	24	5.10
7	5.1	91	68	7.5	2.40	5.40	5.54	4.20	24	5.30
9	5.0	84	61	7.1	2.30	5.50	5.51	4.13	25	4.80
11	6.3	78	53	6.7	1.40	6.30	5.53	3.80	25	6.20
13	5.0	73	53	6.7	2.70	5.40	5.29	3.92	24	6.00
15	4.9	79	56	6.7	1.60	5.50	5.34	4.00	24	5.30
17	4.6	72	49	6.4	2.00	5.10	5.18	3.59	25	5.60
19	4.4	74	50	6.5	1.60	5.30	5.34	3.73	24	5.80
21	4.6	69	51	6.3	2.50	5.20	5.19	3.77	24	5.70
23	4.7	66	44	6.3	1.90	5.00	5.18	3.58	25	5.40
25	4.2	66	46	6.1	1.60	5.20	5.37	3.99	21	5.60
27	5.0	63	42	5.9	2.50	5.60	5.68	4.28	23	5.70
29	5.0	51	33	5.9	1.20	5.80	5.69	3.92	24	5.40
31	5.1	47	32	5.5	1.80	6.00	5.48	3.78	24	6.40
33	5.1	51	36	6.1	2.10	5.80	5.78	4.04	23	5.80
35	4.6	48	32	7.8	2.30	6.60	6.70	4.98	22	5.30
37	4.5	44	29	8.4	2.80	6.90	6.80	5.16	22	4.50
39	4.9	39	27	8.6	3.00	6.70	6.79	5.04	22	4.70
41	5.1	37	25	10.3	3.20	7.10	6.93	5.53	21	5.10
43	5.0	35	24	10.2	3.90	7.70	6.99	5.83	20	4.80
45	5.0	35	24	10.3	3.20	7.20	7.08	5.51	20	4.40
47	5.3	34	23	9.6	3.00	6.30	6.13	4.68	19	4.30
49	5.0	28	21	9.7	3.30	6.30	6.30	5.34	18	4.70
52.5	5.4	19	14	8.8	3.80	6.40	5.52	4.17	17	4.00
57.5	4.5	18	13	8.5	3.60	5.40	4.86	3.83	16	3.20
62.5	3.6	18	12	8.2	3.10	4.80	4.23	3.25	14	3.30
67.5	2.7	17	11	8.0	2.30	3.90	3.63	2.40	12	3.40
72.5	3.0	17	11	8.1	3.50	3.70	3.28	2.23	11	2.50
77.5	2.4	17	12	8.1	3.30	3.20	3.18	2.20	13	2.50
82.5	3.1	17	11	7.8	3.00	3.10	3.07	1.98	13	2.50
87.5	3.6	17	12	7.9	2.80	3.20	3.15	2.17	12	2.50
92.5	3.0	18	12	8.4	3.40	3.00	2.94	2.05	11	2.50
97.5	3.2	21	12	8.7	3.60	3.20	3.04	1.97	14	2.50
102.5	3.7	19	12	8.7	4.00	3.40	2.99	2.01	11	3.10
107.5	3.3	20	13	9.0	3.30	3.20	2.98	2.06	11	3.00
112.5	3.3	20	13	9.5	3.70	3.40	3.14	2.24	10	2.30
117.5	3.0	22	15	10.1	4.40	3.60	3.38	2.33	11	2.20
122.5	3.2	20	13	10.1	4.30	3.40	3.15	2.11	11	2.50
127.5	3.3	21	14	10.2	4.80	3.20	3.09	2.04	11	2.70
132.5	3.2	21	14	10.6	5.10	3.00	2.84	1.89	9	2.00
137.5	3.2	21	14	10.6	5.00	3.30	3.00	1.97	12	2.70
142.5	3.3	24	14	11.4	5.10	3.10	3.06	1.98	11	2.50
147.5	3.3	25	17	12.3	5.30	3.10	3.15	2.13	11	2.30
152.5	3.9	24	16	12.3	5.00	3.80	3.25	2.13	11	2.10
157.5	3.9	29	19	10.1	4.30	4.20	3.87	2.47	14	3.50

Core QV4

Depth (cm)	Hg(18) (ppb)	K (2) (%)	La (1) (ppm)	La (2) (ppm)	Li (2) (ppm)	LOI (%)	Lu (1) (ppm)	Mg (2) (%)	Mn (2) (%)	Mn (3) (ppm)
1	449	2.05	59.0	61	45.4	16.2	1.00	0.82	0.14	794
3	477	2.07	57.0	58	46.2	23.1	0.92	0.81	0.12	780
5	486	2.07	49.0	55	45.4	15.7	0.87	0.80	0.12	699
7	343	2.14	46.0	50	46.2	14.5	0.89	0.82	0.12	758
9	322	2.15	42.0	47	46.5	14.3	0.74	0.83	0.12	778
11	339	2.24	45.0	42	47.8	13.4	0.81	0.84	0.12	756
13	334	2.15	41.0	43	47.8	13.6	0.77	0.80	0.14	840
15	364	2.15	40.0	42	47.5	13.6	0.89	0.81	0.14	848
17	380	2.12	38.0	36	46.4	13.4	0.93	0.78	0.14	831
19	384	2.11	37.0	39	47.6	13.5	0.91	0.79	0.15	880
21	352	2.13	37.0	38	45.9	13.0	0.85	0.78	0.15	933
23	36	2.10	36.0	38	45.7	13.5	0.87	0.76	0.15	947
25	716	1.90	34.0	36	50.0	15.1	0.76	0.75	0.16	1340
27	1057	1.84	34.0	33	53.4	16.0	0.86	0.80	0.18	1530
29	886	1.95	30.0	31	56.1	14.9	0.78	0.85	0.24	1870
31	933	1.97	31.0	30	56.8	12.3	0.86	0.91	0.18	1500
33	819	1.97	35.0	34	55.0	14.2	0.81	0.89	0.46	3760
35	1752	1.71	37.0	39	51.3	18.0	0.88	0.73	1.07	8990
37	1676	1.61	39.0	40	50.4	17.9	0.86	0.70	1.41	11000
39	2476	1.52	42.0	44	52.8	31.9	0.88	0.65	0.50	3840
41	695	1.35	47.0	47	50.7	18.0	1.00	0.56	1.33	10300
43	510	1.28	49.0	47	50.7	20.4	1.00	0.52	0.75	6200
45	465	1.24	46.0	48	50.6	20.6	1.00	0.49	0.83	6500
47	583	1.19	45.0	48	49.7	22.7	0.85	0.47	0.39	3020
49	446	1.14	43.0	49	47.9	24.1	0.74	0.44	0.34	2860
52.5	261	1.06	43.0	44	47.2	25.4	0.78	0.41	0.27	2210
57.5	235	0.63	45.0	43	38.4	31.2	0.82	0.34	0.30	2390
62.5	206	0.70	46.0	43	30.4	34.6	0.82	0.29	0.30	2420
67.5	222	0.52	43.0	41	23.0	40.8	0.68	0.22	0.31	2380
72.5	209	0.54	45.0	43	24.5	41.0	0.83	0.23	0.30	2350
77.5	192	0.57	41.0	43	25.8	40.4	0.67	0.24	0.27	2140
82.5	183	0.63	40.0	41	29.0	40.2	0.69	0.26	0.25	1930
87.5	191	0.66	42.0	43	31.1	39.3	0.74	0.27	0.24	1960
92.5	189	0.57	42.0	45	27.3	40.0	0.68	0.24	0.23	1840
97.5	187	0.61	42.0	46	29.1	39.7	0.67	0.25	0.22	1640
102.5	207	0.57	48.0	48	25.8	40.0	0.63	0.24	0.21	1630
107.5	183	0.64	51.0	49	27.5	37.9	0.74	0.27	0.20	1520
112.5	213	0.53	55.0	49	25.3	40.7	0.79	0.23	0.20	1610
117.5	199	0.57	57.0	55	26.4	40.2	0.81	0.24	0.18	1530
122.5	189	0.51	58.0	54	26.0	39.4	0.81	0.23	0.18	1440
127.5	195	0.55	57.0	55	27.7	39.0	0.89	0.24	0.17	1350
132.5	195	0.49	60.0	58	24.5	41.4	0.88	0.21	0.17	1310
137.5	195	0.53	59.0	57	26.9	39.6	0.85	0.23	0.16	1010
142.5	182	0.54	59.0	59	28.7	39.0	0.84	0.24	0.17	1030
147.5	214	0.53	55.0	63	28.8	39.4	0.71	0.24	0.17	1080
152.5	201	0.55	67.0	64	29.2	39.0	0.91	0.25	0.17	1320
157.5	277	0.80	55.0	54	32.3	35.1	0.90	0.34	0.28	2090

Core QV4

Depth (cm)	Mo (2) (ppm)	Mo (5) (ppm)	Na (1) (%)	Na (2) (%)	Nb (2) (ppm)	Ni (2) (ppm)	Ni (3) (ppm)	P (2) (ppb)	Pb (2) (ppm)	Pb (3) (ppm)
1	4	2	1.60	1.50	12	30	17	2297	430	355
3	4	2	1.60	1.51	13	30	18	2288	449	382
5	4	2	1.50	1.55	13	30	14	2194	495	366
7	3	2	1.50	1.55	13	28	16	2121	499	412
9	4	2	1.40	1.55	14	28	16	2035	496	405
11	4	2	1.60	1.57	14	27	15	1940	455	365
13	4	2	1.60	1.57	14	27	14	1971	382	316
15	4	2	1.60	1.55	14	28	16	2103	392	332
17	4	2	1.60	1.61	14	26	15	2075	348	282
19	4	2	1.60	1.61	14	26	15	2066	344	279
21	4	2	1.70	1.64	14	26	15	2002	313	265
23	4	<2	1.70	1.67	15	26	13	1927	294	234
25	5	2	1.60	1.56	15	27	14	1796	324	258
27	4	2	1.50	1.46	14	28	15	1861	286	238
29	4	2	1.40	1.45	14	27	14	1827	220	184
31	4	2	1.60	1.57	15	26	15	1583	180	161
33	4	2	1.60	1.48	14	28	15	1626	207	184
35	5	2	1.30	1.23	13	29	15	1779	314	247
37	4	2	1.30	1.22	12	27	14	1802	306	245
39	4	2	1.20	1.16	12	26	14	2375	303	237
41	5	2	1.10	1.06	12	24	12	2445	181	154
43	5	3	1.10	1.01	10	20	12	2477	126	98
45	6	3	1.00	1.01	10	19	10	2183	98	70
47	5	3	1.00	0.92	10	18	9	2529	96	71
49	5	3	0.83	0.87	9	19	11	2367	88	68
52.5	5	2	0.92	0.81	9	14	8	2132	60	44
57.5	5	3	0.77	0.66	7	13	7	1973	36	24
62.5	4	2	0.69	0.57	6	13	6	1955	20	15
67.5	5	3	0.49	0.42	6	12	5	1962	17	13
72.5	4	3	0.51	0.43	5	9	4	1989	16	11
77.5	4	2	0.47	0.44	6	9	4	2000	16	12
82.5	5	3	0.53	0.50	6	10	5	1932	19	11
87.5	4	3	0.59	0.53	6	10	6	1920	16	12
92.5	4	3	0.48	0.45	6	10	6	1981	19	12
97.5	4	3	0.46	0.47	6	9	4	1981	20	12
102.5	4	3	0.50	0.43	6	11	5	2089	17	12
107.5	4	3	0.58	0.51	6	12	6	2041	17	12
112.5	6	3	0.48	0.42	4	12	7	2227	17	13
117.5	7	3	0.54	0.45	4	14	7	2308	19	15
122.5	7	3	0.48	0.39	4	12	6	2151	18	13
127.5	7	3	0.48	0.42	4	10	5	2141	18	14
132.5	9	4	0.44	0.37	4	14	7	2172	20	14
137.5	6	3	0.47	0.40	4	11	5	2212	20	14
142.5	6	3	0.46	0.42	4	11	5	2228	18	14
147.5	8	3	0.41	0.40	4	13	6	2332	22	17
152.5	7	3	0.51	0.42	3	13	6	2359	22	17
157.5	6	3	0.72	0.61	7	14	8	2173	77	52

Core QV4

Depth (cm)	Rb (1) (ppm)	Rb (2) (ppm)	Sb (1) (ppm)	Sc (1) (ppm)	Sc (2) (ppm)	Sm (1) (ppm)	Sr (2) (ppm)	Ta (1) (ppm)	Tb (1) (ppm)	Th (1) (ppm)
1	87.0	84	1.90	14.5	15.0	13.8	82	1.30	1.60	8.6
3	85.0	85	1.90	14.6	15.3	13.5	80	1.20	1.60	8.9
5	82.0	89	1.60	13.8	15.5	12.2	81	1.10	1.50	8.2
7	87.0	86	1.50	13.5	15.5	11.7	78	1.40	1.40	8.7
9	88.0	85	1.60	12.9	15.3	11.3	76	1.30	1.50	8.8
11	110.0	99	1.90	15.2	15.8	12.3	75	1.50	1.60	10.7
13	95.0	85	1.60	15.4	15.9	10.6	78	1.30	1.20	10.0
15	92.0	88	1.80	15.2	15.9	10.2	77	1.30	1.20	9.4
17	90.0	83	1.80	15.0	15.6	10.0	79	1.30	1.30	10.0
19	92.0	91	2.00	14.8	16.0	10.0	81	1.30	1.20	9.3
21	100.0	81	1.90	15.3	14.1	10.0	81	1.10	1.40	10.0
23	89.0	86	1.80	14.3	14.1	9.5	82	1.20	1.10	9.2
25	87.0	73	2.70	14.6	14.6	9.3	77	1.30	1.10	9.2
27	87.0	78	2.80	15.4	15.1	9.4	72	1.10	1.20	8.8
29	93.0	87	2.00	15.2	15.9	9.0	66	1.10	1.10	9.0
31	100.0	88	1.80	16.7	16.1	9.3	67	1.40	1.20	10.0
33	100.0	84	1.60	17.0	16.0	9.3	65	1.30	1.20	9.4
35	84.0	66	1.70	15.7	15.1	10.8	62	1.10	1.30	8.2
37	70.0	64	1.40	15.6	14.4	11.2	59	1.00	1.30	8.2
39	72.0	63	0.84	15.0	14.6	13.3	51	1.00	1.70	7.8
41	73.0	56	0.72	14.0	13.8	15.1	49	1.00	1.90	7.7
43	75.0	58	0.65	14.3	13.1	16.0	46	0.81	1.90	7.5
45	60.0	57	0.56	13.1	12.6	15.7	46	0.92	1.80	7.5
47	63.0	54	0.44	13.2	12.7	15.7	45	1.00	1.90	7.1
49	65.0	57	0.41	12.1	12.8	15.2	44	0.81	2.00	7.0
52.5	65.0	52	0.34	12.8	11.9	15.7	43	1.00	1.90	7.0
57.5	49.0	37	0.24	11.4	9.8	14.6	39	0.61	1.70	5.5
62.5	41.0	29	0.23	10.4	8.5	14.7	37	0.54	1.80	4.9
67.5	31.0	22	0.20	8.1	7.2	13.1	35	0.38	1.50	3.9
72.5	31.0	24	0.16	8.4	7.2	13.9	36	0.39	1.60	3.8
77.5	27.0	26	0.17	7.9	7.5	12.6	36	0.38	1.40	3.8
82.5	29.0	28	0.17	8.2	7.8	12.6	38	0.45	1.40	4.0
87.5	34.0	32	0.16	9.1	8.3	13.2	39	0.60	1.50	4.2
92.5	30.0	30	0.17	8.0	7.7	13.5	36	0.44	1.50	4.0
97.5	31.0	29	0.18	7.8	8.2	14.5	38	0.40	1.60	4.1
102.5	26.0	28	0.21	8.4	7.8	17.0	35	0.47	1.80	4.3
107.5	24.0	23	0.17	9.3	8.2	16.4	39	0.38	1.70	4.6
112.5	26.0	24	0.18	9.3	8.0	17.4	35	0.41	2.00	4.3
117.5	27.0	25	0.20	10.0	8.3	18.7	36	0.52	2.20	4.4
122.5	21.0	23	0.18	10.0	8.2	18.7	34	0.35	2.30	4.1
127.5	27.0	30	0.21	10.0	8.6	18.7	34	0.47	2.10	4.3
132.5	27.0	22	0.18	9.3	8.3	19.7	32	0.37	2.40	4.1
137.5	30.0	26	0.21	9.5	8.5	19.7	33	0.56	2.20	4.2
142.5	27.0	23	0.18	9.3	8.7	19.7	33	0.47	2.30	4.0
147.5	27.0	24	0.19	8.6	9.1	20.2	33	0.48	2.30	3.9
152.5	29.0	24	0.22	10.1	9.3	24.8	33	0.56	2.90	4.8
157.5	36.0	33	0.60	11.0	9.8	17.8	42	0.63	2.10	5.3

Core QV4

Depth (cm)	Ti (2) (ppm)	U (1) (ppm)	V (2) (ppm)	W (1) (ppm)	Y (2) (ppm)	Yb (1) (ppm)	Zn (1) (ppm)	Zn (2) (ppm)	Zn (3) (ppm)	Zr (2) (ppm)
1	4237	2.3	115	3.10	52	5.70	1000.0	783	625	109
3	4327	2.4	117	3.80	49	5.90	950.0	771	619	110
5	4210	2.1	114	3.40	46	5.10	860.0	723	536	108
7	4207	2.2	112	3.10	43	4.90	730.0	648	530	107
9	4300	2.3	110	3.50	40	4.50	680.0	587	466	108
11	4352	2.6	109	4.50	37	5.80	630.0	473	357	112
13	4314	2.3	101	2.10	37	4.80	500.0	394	339	112
15	4244	2.1	101	2.90	36	5.80	450.0	398	325	111
17	4235	2.2	99	<2	34	5.80	490.0	369	289	106
19	4338	2.1	101	<2	34	4.80	480.0	375	288	110
21	4328	2.2	100	<2	34	4.80	430.0	348	286	109
23	4337	2.1	100	<2	34	5.20	360.0	339	257	111
25	4439	2.2	96	<2	33	5.00	410.0	356	280	115
27	4532	2.2	97	<2	31	5.30	430.0	368	298	118
29	4716	2.2	102	<2	31	4.30	330.0	304	226	129
31	5037	2.2	104	<2	29	4.70	280.0	249	193	132
33	4684	2.2	103	<2	31	5.30	370.0	299	241	122
35	3993	2.1	91	<2	38	5.20	500.0	384	318	124
37	3934	2.1	87	<2	39	5.30	470.0	346	268	121
39	3872	2.1	83	<2	46	5.90	350.0	287	227	122
41	3571	2.2	76	<2	50	5.70	290.0	230	169	114
43	3458	2.3	71	<2	50	5.90	240.0	213	158	113
45	3436	2.1	67	<2	50	5.10	260.0	199	143	114
47	3409	2.2	70	<2	51	5.70	270.0	204	143	117
49	3339	2.0	70	<2	52	5.00	190.0	192	147	122
52.5	3258	2.1	65	<2	48	5.70	170.0	161	114	112
57.5	2596	1.7	54	<2	45	4.90	190.0	172	125	88
62.5	2193	1.5	47	<2	44	4.80	240.0	175	137	80
67.5	1723	1.2	38	<2	43	3.90	200.0	163	113	61
72.5	1782	1.3	39	<2	43	4.30	200.0	162	115	66
77.5	1816	1.3	40	<2	43	3.90	130.0	141	98	65
82.5	1923	1.2	42	<2	41	3.70	150.0	138	95	72
87.5	2021	1.3	43	<2	43	4.70	160.0	138	103	74
92.5	1838	1.3	40	<2	44	4.30	150.0	142	106	68
97.5	1931	1.3	41	<2	46	4.20	140.0	147	110	71
102.5	1732	1.5	38	<2	47	4.50	130.0	147	107	65
107.5	1924	1.4	40	<2	49	5.30	180.0	151	111	69
112.5	1696	1.4	38	<2	51	5.10	210.0	160	120	68
117.5	1768	1.5	39	<2	55	5.40	210.0	172	123	64
122.5	1668	1.3	39	<2	56	5.50	180.0	159	115	62
127.5	1754	1.4	40	<2	56	5.50	200.0	165	115	66
132.5	1587	1.4	38	<2	58	5.40	190.0	181	131	60
137.5	1650	1.4	39	<2	57	5.70	150.0	157	116	63
142.5	1735	1.4	39	<2	60	5.50	180.0	184	137	52
147.5	1752	1.3	42	<2	65	5.10	150.0	180	138	54
152.5	1770	1.6	42	<2	65	6.20	180.0	186	143	54
157.5	2329	1.6	52	<2	52	5.80	260.0	228	163	67

Core LP1

core LP1 Sample #	Depth (cm)	Ag (6) (ppm)	Al (2) (%)	As (1) (ppm)	Au (1) (ppb)	Ba (1) (ppm)	Ba (2) (ppm)	Be (2) (ppm)	Br (1) (ppm)	Ca (2) (%)
LP1-002	1	0.7	6.97	10.0	11.0	460	507	3.9	24.2	1.33
LP1-004	3	0.6	7.22	8.9	10.0	460	516	3.8	22.1	0.58
LP1-006	5	0.5	7.27	11.0	10.0	520	520	3.8	23.1	0.44
LP1-008	7	0.5	7.40	10.0	8.1	460	539	3.7	20.0	0.40
LP1-010	9	0.6	7.30	9.1	7.2	480	544	3.7	18.0	0.41
LP1-012	11	1.0	7.34	9.3	10.0	490	529	3.8	19.0	0.41
LP1-014	13	1.2	7.38	10.0	8.0	490	550	4.0	19.0	0.42
LP1-016	15	0.7	7.42	10.0	7.6	450	528	3.6	18.0	0.42
LP1-018	17	0.4	7.34	9.0	7.0	440	485	3.6	17.0	0.41
LP1-020	19	0.4	7.26	8.7	5.0	460	486	3.6	17.0	0.41
LP1-022	21	0.3	6.91	10.0	5.4	390	440	3.7	20.0	0.40
LP1-024	23	0.4	5.45	13.0	8.9	280	333	4.2	31.6	0.36
LP1-026	25	0.4	4.98	14.0	8.4	270	284	4.3	36.3	0.36
LP1-028	27	0.4	4.63	14.0	4.3	220	258	4.1	36.2	0.36
LP1-030	29	0.4	4.57	12.0	3.4	190	246	4.1	35.9	0.37
LP1-033	31.5	0.4	4.45	10.0	6.3	190	237	4.1	38.1	0.35
LP1-036	34.5	0.4	4.57	11.0	4.1	170	229	4.3	37.7	0.34
LP1-040	38	0.4	4.65	9.5	3.6	170	211	4.4	39.8	0.33
LP1-045	42.5	0.4	4.61	9.0	<2	160	207	4.5	39.5	0.31
LP1-050	47.5	0.4	4.33	8.6	<2	160	192	3.9	42.9	0.29
LP1-055	52.5	0.3	4.12	8.1	<2	150	176	3.8	42.8	0.28
LP1-060	57.5	0.3	3.65	8.0	<2	150	142	3.9	54.3	0.24
LP1-065	62.5	0.3	3.47	4.9	<2	100	142	3.1	65.7	0.26
LP1-070	67.5	0.3	3.36	4.1	<2	170	149	2.8	68.2	0.26
LP1-075	72.5	0.3	2.88	2.9	<2	130	141	2.3	84.2	0.24
LP1-080	77.5	0.3	3.39	3.2	<2	140	159	2.5	77.5	0.28
LP1-085	82.5	0.3	3.69	2.9	<2	150	183	2.6	66.9	0.29
LP1-090	87.5	0.2	3.78	4.0	<2	170	202	2.7	53.5	0.35
LP1-095	92.5	0.2	3.93	4.7	<2	170	212	2.7	52.9	0.36
LP1-100	97.5	0.3	4.02	4.8	<2	180	203	2.9	57.8	0.37
LP1-105	102.5	0.3	4.02	4.6	<2	170	191	3.1	65.0	0.33
LP1-110	107.5	0.4	4.00	2.8	<2	140	186	3.4	59.9	0.32
LP1-115	112.5	0.3	4.05	3.0	<2	140	186	3.7	56.5	0.32
LP1-120	117.5	0.4	4.10	3.4	<2	130	185	4.0	61.8	0.32
LP1-125	122.5	0.3	4.24	3.8	<2	200	199	4.2	59.0	0.35
LP1-130	127.5	0.3	4.12	4.2	<2	140	194	4.4	61.3	0.36
LP1-135	132.5	0.3	3.91	3.3	<2	170	181	4.4	60.3	0.33
LP1-140	137.5	0.4	4.15	3.6	<2	170	200	4.8	64.0	0.37
LP1-145	142.5	0.4	3.97	4.0	<2	140	173	5.4	62.0	0.33
LP1-150	147.5	0.4	3.83	3.2	<2	130	165	5.7	59.8	0.31
LP1-155	152.5	0.4	3.89	3.3	<2	130	293	6.1	54.9	0.32
LP1-160	157.5	0.4	3.79	3.5	<2	160	184	6.4	61.0	0.34
LP1-165	162.5	0.3	3.73	3.8	<2	160	202	6.5	55.3	0.37

Core LP1

Depth (cm)	Cd (2) (ppm)	Cd (3) (ppm)	Ce (1) (ppm)	Ce (2) (ppm)	Co (1) (ppm)	Co (2) (ppm)	Co (3) (ppm)	Cr (1) (ppm)	Cr (2) (ppm)	Cr (2a) (ppm)
1	1.5	1.4	130	143	23.0	24	13	70.0	55	49
3	1.4	1.3	120	146	25.0	25	14	47.0	53	47
5	1.2	1.1	140	150	24.0	23	14	25.0	40	33
7	1.4	1.1	120	149	21.0	23	13	38.0	46	42
9	1.5	1.2	130	147	21.0	23	13	44.0	35	31
11	1.6	1.4	130	129	23.0	21	12	29.0	41	36
13	1.7	1.5	130	134	23.0	22	13	55.0	39	35
15	1.5	1.3	120	110	19.0	21	12	37.0	34	31
17	0.6	0.6	120	127	21.0	23	13	29.0	34	29
19	0.5	0.5	110	150	23.0	23	14	25.0	34	31
21	0.6	0.5	110	127	28.0	27	16	30.0	31	27
23	0.7	0.6	100	124	35.0	36	21	18.0	24	22
25	0.6	0.4	120	124	49.0	41	25	<15	23	18
27	0.4	0.4	130	132	50.0	46	27	<15	20	15
29	0.4	0.4	130	142	55.0	50	31	<15	19	14
31.5	0.3	0.3	140	139	46.0	41	26	<15	19	13
34.5	0.3	0.3	140	150	51.0	46	28	<15	19	14
38	0.3	0.3	150	167	54.0	48	30	<15	17	13
42.5	0.3	0.3	150	168	45.0	38	22	<15	16	13
47.5	0.3	0.3	140	158	47.0	49	28	<15	16	12
52.5	0.2	0.3	130	148	39.0	38	23	<15	15	12
57.5	0.2	0.3	140	149	44.0	38	23	21.0	11	10
62.5	0.3	0.2	120	132	17.0	18	11	<15	11	10
67.5	0.2	0.3	100	110	12.0	12	7	<15	11	10
72.5	0.2	0.3	77	81	4.5	8	5	<15	11	9
77.5	0.2	0.2	83	87	9.1	8	5	<15	12	10
82.5	0.2	0.3	86	88	9.1	10	6	19.0	13	12
87.5	0.2	0.3	96	93	9.3	11	6	<15	11	8
92.5	0.2	0.3	100	97	11.0	11	6	<15	11	9
97.5	0.3	0.3	110	108	12.0	12	7	<15	12	9
102.5	0.3	0.3	110	111	11.0	12	7	<15	14	11
107.5	0.3	0.2	97	121	7.7	11	7	<15	14	13
112.5	0.3	0.2	110	130	8.7	11	6	22.0	11	9
117.5	0.4	0.3	140	139	12.0	11	6	19.0	13	13
122.5	0.4	0.3	140	144	11.0	12	6	<15	15	13
127.5	0.3	0.3	140	139	10.0	11	6	19.0	13	12
132.5	0.3	0.3	140	141	10.0	10	6	16.0	14	12
137.5	0.3	0.4	150	145	9.3	11	6	41.0	15	13
142.5	0.5	0.3	150	155	11.0	10	6	17.0	13	12
147.5	0.5	0.3	140	148	9.0	9	6	<15	12	12
152.5	0.3	0.3	130	153	8.6	10	5	30.0	14	12
157.5	0.5	0.3	160	154	7.8	9	5	22.0	22	20
162.5	0.3	0.4	150	150	6.4	9	5	24.0	11	12

Core LP1

Depth (cm)	Cs (1) (ppm)	Cu (2) (ppm)	Cu (3) (ppm)	Dy (2) (ppm)	Eu (1) (ppm)	Fe (1) (%)	Fe (2) (%)	Fe (3) (%)	Ga (2) (ppm)	Hf (1) (ppm)
1	5.3	102	83	8.5	1.80	6.20	5.54	4.00	21	5.70
3	5.9	90	75	8.3	2.40	5.60	5.32	3.83	21	6.00
5	6.2	89	70	8.5	3.80	6.20	5.17	3.65	24	6.10
7	5.4	81	60	8.0	2.70	5.30	5.15	3.49	23	6.50
9	5.3	73	56	8.2	3.10	5.30	5.02	3.44	23	6.00
11	5.5	70	54	7.7	3.40	4.90	4.83	3.42	22	5.80
13	4.8	72	53	7.8	2.60	5.00	4.91	3.45	22	5.80
15	5.3	66	52	7.0	2.60	4.90	4.94	3.38	23	5.30
17	5.3	64	49	7.7	2.40	5.10	5.16	3.49	23	6.00
19	5.4	93	70	8.3	2.80	5.10	5.19	3.58	24	6.60
21	4.7	44	33	7.6	2.30	5.40	5.30	3.93	22	5.40
23	4.0	84	55	8.1	4.20	5.80	5.73	4.32	18	4.50
25	3.9	26	19	8.3	4.50	6.00	5.39	3.98	15	3.60
27	3.8	23	16	8.7	2.80	4.80	4.63	3.17	15	3.80
29	3.9	22	16	9.0	3.90	4.50	4.40	3.09	14	2.80
31.5	3.7	19	14	8.9	3.80	4.30	4.07	3.04	13	3.40
34.5	3.2	19	14	9.4	4.00	4.30	4.20	2.98	12	2.70
38	3.0	18	14	10.1	4.50	3.70	3.57	2.62	12	3.00
42.5	3.2	16	12	10.2	4.90	3.40	3.34	2.30	12	3.40
47.5	2.8	15	11	9.3	3.90	3.30	3.24	2.31	11	1.90
52.5	2.5	14	11	8.9	4.50	3.20	3.17	2.22	10	2.00
57.5	2.4	15	10	8.9	3.50	2.70	2.61	1.87	8	1.10
62.5	2.0	14	10	7.7	3.20	2.30	2.31	1.57	8	1.60
67.5	2.2	15	11	6.6	2.10	1.90	1.89	1.24	8	1.70
72.5	1.7	15	11	5.3	2.80	1.50	1.47	0.90	7	1.50
77.5	2.1	15	11	5.6	2.80	1.70	1.52	0.99	7	1.70
82.5	2.7	16	12	5.6	3.10	1.70	1.60	1.02	8	1.90
87.5	2.6	15	11	5.8	2.60	1.90	1.68	1.02	9	2.40
92.5	2.7	15	11	5.7	2.20	1.90	1.73	1.09	9	2.20
97.5	2.4	17	11	6.4	2.80	1.80	1.67	1.04	8	2.10
102.5	2.3	17	12	7.0	3.40	1.70	1.64	1.07	9	1.80
107.5	2.3	18	14	7.6	3.70	1.60	1.62	1.11	8	2.50
112.5	2.4	19	14	8.2	3.90	1.60	1.64	1.08	8	2.30
117.5	2.8	19	14	8.6	4.30	1.70	1.58	0.99	8	2.90
122.5	3.3	19	15	8.9	5.00	1.80	1.62	1.09	8	2.00
127.5	3.2	19	17	9.0	4.10	1.80	1.54	0.92	8	1.80
132.5	2.8	19	14	9.0	4.50	1.60	1.45	0.96	7	1.90
137.5	3.2	20	14	9.5	5.00	1.70	1.52	0.93	8	3.00
142.5	2.3	20	15	10.6	5.60	1.50	1.42	0.92	7	2.50
147.5	2.2	23	17	10.6	5.00	1.40	1.41	0.91	7	1.60
152.5	2.9	24	17	11.3	4.70	1.40	1.42	0.92	8	2.30
157.5	2.8	24	17	11.5	4.80	1.60	1.38	0.82	7	1.90
162.5	3.6	23	16	11.0	5.20	1.60	1.40	0.85	7	2.40

Core LP1

Depth (cm)	Hg(18) (ppb)	K (2) (%)	La (1) (ppm)	La (2) (ppm)	Li (2) (ppm)	LOI (%)	Lu (1) (ppm)	Mg (2) (%)	Mn (2) (%)	Mn (3) (ppm)
1	230	1.83	61.0	58	45.8	18.3	0.65	0.72	0.17	1320
3	218	1.92	54.0	57	47.9	17.5	0.69	0.71	0.17	989
5	224	1.94	60.0	60	49.3	16.3	0.57	0.71	0.16	968
7	236	2.00	56.0	60	47.8	17.0	0.61	0.69	0.17	993
9	234	1.97	55.0	56	46.2	15.9	0.74	0.69	0.18	1040
11	251	1.90	54.0	48	46.4	16.9	0.71	0.67	0.17	1010
13	248	1.90	54.0	48	46.8	16.7	0.65	0.68	0.17	1010
15	251	1.93	48.0	37	48.4	15.3	0.63	0.66	0.17	991
17	249	1.91	47.0	43	50.1	14.2	0.66	0.65	0.17	945
19	233	1.88	47.0	51	50.3	14.5	0.72	0.64	0.16	961
21	286	1.71	45.0	44	46.6	17.6	0.53	0.58	0.17	1280
23	401	1.14	39.0	42	34.2	26.9	0.54	0.37	0.19	1410
25	369	0.93	47.0	43	30.6	29.7	0.59	0.31	0.18	1340
27	337	0.79	46.0	45	28.8	32.2	0.67	0.26	0.17	1240
29	302	0.73	46.0	47	27.5	32.9	0.64	0.25	0.18	1330
31.5	279	0.69	47.0	46	27.6	32.8	0.62	0.23	0.17	1300
34.5	249	0.66	47.0	47	28.7	33.2	0.57	0.23	0.17	1250
38	207	0.60	50.0	50	26.3	32.7	0.70	0.21	0.16	1320
42.5	208	0.58	49.0	49	26.1	33.1	0.59	0.20	0.16	1010
47.5	205	0.51	45.0	46	23.9	35.1	0.61	0.18	0.16	955
52.5	182	0.46	42.0	43	22.0	35.8	0.44	0.17	0.15	923
57.5	169	0.34	43.0	44	16.7	35.1	0.48	0.13	0.14	822
62.5	189	0.34	40.0	41	16.2	39.7	0.46	0.13	0.14	813
67.5	186	0.35	36.0	36	17.3	41.0	0.35	0.13	0.13	791
72.5	198	0.32	30.0	30	15.1	40.6	0.20	0.13	0.10	707
77.5	184	0.39	32.0	31	18.3	44.1	0.21	0.15	0.10	726
82.5	179	0.50	34.0	32	22.3	44.2	0.31	0.19	0.10	718
87.5	152	0.56	36.0	32	21.8	52.9	0.41	0.22	0.11	773
92.5	127	0.56	35.0	33	23.2	52.7	0.41	0.22	0.11	797
97.5	152	0.52	38.0	35	22.8	52.1	0.31	0.21	0.10	730
102.5	169	0.47	37.0	39	22.1	46.0	0.31	0.19	0.10	649
107.5	202	0.48	35.0	42	22.5	42.2	0.25	0.19	0.09	606
112.5	191	0.49	41.0	45	22.7	40.6	0.47	0.20	0.09	575
117.5	202	0.46	51.0	48	23.0	41.3	0.45	0.19	0.09	535
122.5	179	0.48	54.0	49	24.8	44.5	0.52	0.20	0.09	592
127.5	188	0.45	53.0	45	23.6	45.5	0.40	0.18	0.09	545
132.5	178	0.42	51.0	49	22.2	41.5	0.51	0.18	0.09	510
137.5	180	0.48	57.0	51	23.6	44.2	0.57	0.20	0.09	539
142.5	184	0.38	59.0	58	20.7	41.0	0.55	0.16	0.08	493
147.5	179	0.38	55.0	56	19.4	37.4	0.52	0.16	0.08	452
152.5	182	0.43	52.0	60	21.7	37.3	0.44	0.17	0.08	477
157.5	173	0.43	59.0	65	22.5	39.5	0.50	0.18	0.08	471
162.5	136	0.50	62.0	58	24.1	40.8	0.63	0.20	0.08	515

Core LP1

Depth (cm)	Mo (2) (ppm)	Mo (5) (ppm)	Na (1) (%)	Na (2) (%)	Nb (2) (ppm)	Ni (2) (ppm)	Ni (3) (ppm)	P (2) (ppb)	Pb (2) (ppm)	Pb (3) (ppm)
1	3	3	1.70	1.48	14	24	15	2151	421	315
3	3	3	1.50	1.54	16	24	15	2037	426	331
5	3	3	1.70	1.56	17	25	14	2003	412	324
7	3	3	1.60	1.53	16	25	14	2206	510	386
9	3	3	1.70	1.58	17	23	13	2471	445	341
11	3	3	1.60	1.51	17	22	13	2882	354	285
13	3	3	1.70	1.53	17	23	13	3134	321	256
15	3	3	1.60	1.54	17	21	12	2937	214	189
17	3	2	1.60	1.54	17	20	11	2244	125	96
19	2	3	1.60	1.55	16	18	11	2091	121	97
21	3	3	1.40	1.38	16	18	11	2049	126	96
23	4	4	0.91	0.92	10	15	9	2139	153	110
25	4	4	0.87	0.76	7	13	7	2030	121	85
27	4	5	0.73	0.66	7	11	6	1823	120	79
29	4	4	0.66	0.63	6	10	6	1815	83	57
31.5	4	4	0.65	0.59	7	11	6	1705	79	56
34.5	4	4	0.59	0.56	7	10	5	1769	53	36
38	4	4	0.56	0.52	6	11	5	1629	35	24
42.5	4	4	0.54	0.50	6	10	5	1596	28	20
47.5	4	4	0.46	0.45	5	10	5	1652	28	18
52.5	4	4	0.41	0.42	5	8	4	1620	20	16
57.5	4	4	0.30	0.31	4	8	4	1546	20	16
62.5	3	3	0.32	0.29	4	7	3	1731	18	12
67.5	3	3	0.31	0.30	4	7	3	1793	18	11
72.5	2	3	0.28	0.27	4	5	3	1922	4	6
77.5	3	3	0.36	0.35	4	6	3	2092	5	7
82.5	3	3	0.48	0.44	5	5	3	1948	7	7
87.5	3	4	0.63	0.52	5	7	3	1762	9	6
92.5	4	4	0.61	0.52	5	6	4	1706	8	7
97.5	4	4	0.54	0.48	5	7	3	1840	8	8
102.5	4	4	0.39	0.41	5	7	4	2069	10	9
107.5	3	3	0.34	0.40	5	7	4	2315	9	8
112.5	3	3	0.38	0.41	6	7	4	2417	10	9
117.5	3	4	0.40	0.37	5	7	4	2478	8	9
122.5	4	4	0.46	0.41	5	7	4	2394	9	8
127.5	3	4	0.41	0.38	5	7	4	2467	9	8
132.5	3	4	0.37	0.34	5	7	4	2428	8	8
137.5	3	3	0.46	0.40	5	7	4	2580	7	9
142.5	3	4	0.33	0.30	5	7	4	2804	8	8
147.5	3	3	0.31	0.29	3	7	4	2925	7	8
152.5	3	3	0.31	0.34	5	7	4	2885	12	8
157.5	4	4	0.37	0.35	5	13	4	2859	10	8
162.5	3	4	0.49	0.43	5	7	4	2459	9	9

Core LP1

Depth (cm)	Rb (1) (ppm)	Rb (2) (ppm)	Sb (1) (ppm)	Sc (1) (ppm)	Sc (2) (ppm)	Sm (1) (ppm)	Sr (2) (ppm)	Ta (1) (ppm)	Tb (1) (ppm)	Th (1) (ppm)
1	81.0	79	1.50	13.5	14.0	11.9	98	1.20	1.70	8.7
3	75.0	86	1.30	12.4	14.6	11.5	79	1.30	1.60	8.6
5	92.0	81	1.40	13.8	14.9	13.6	77	1.50	1.90	10.0
7	83.0	87	1.30	13.9	15.0	11.3	77	1.40	1.50	9.3
9	77.0	86	1.20	14.0	15.2	11.0	79	1.30	1.50	9.2
11	86.0	85	1.20	13.7	14.5	11.2	72	1.20	1.60	9.1
13	77.0	82	1.20	13.8	14.7	11.2	75	1.20	1.60	9.2
15	79.0	87	1.10	13.5	14.1	10.6	73	1.30	1.30	8.9
17	76.0	84	1.00	13.7	14.8	10.8	76	1.10	1.40	9.3
19	78.0	84	1.00	13.3	15.6	10.8	81	1.30	1.40	8.9
21	72.0	75	1.10	12.5	13.9	10.6	71	1.20	1.40	8.0
23	42.0	46	1.10	9.0	10.7	10.7	54	0.78	1.60	6.0
25	40.0	40	0.84	10.0	9.5	12.2	49	0.61	1.90	5.7
27	38.0	38	0.56	8.7	9.0	12.8	47	0.69	1.70	5.2
29	33.0	30	0.41	8.1	8.7	13.1	47	0.57	1.90	4.7
31.5	28.0	24	0.36	8.1	8.3	13.3	44	0.52	1.90	4.7
34.5	26.0	32	0.30	7.8	8.3	13.5	43	0.40	1.80	4.5
38	26.0	27	0.24	7.8	8.3	14.8	41	0.43	2.10	4.5
42.5	25.0	28	0.21	7.6	8.2	14.8	39	0.50	2.10	4.4
47.5	27.0	25	0.17	6.8	7.7	13.2	36	0.40	1.90	4.0
52.5	20.0	19	0.15	6.1	7.1	12.1	33	0.35	1.60	3.6
57.5	19.0	13	0.18	5.2	6.3	13.3	27	0.34	1.80	3.4
62.5	18.0	13	0.16	5.4	5.7	11.0	29	0.32	1.60	3.0
67.5	15.0	14	0.15	4.9	5.3	9.4	30	0.23	1.40	2.8
72.5	11.0	13	0.11	4.2	4.6	7.7	27	0.30	1.10	2.5
77.5	17.0	15	0.14	5.0	4.9	8.4	32	0.10	1.20	2.8
82.5	18.0	20	0.13	5.7	5.6	8.3	35	0.43	1.20	3.1
87.5	17.0	19	0.16	6.4	5.9	8.4	43	0.44	1.20	3.3
92.5	23.0	22	0.14	6.3	6.1	8.1	44	0.40	1.10	3.4
97.5	20.0	23	0.14	6.2	6.2	9.0	43	0.51	1.40	3.5
102.5	22.0	23	0.15	5.3	6.1	10.3	37	0.24	1.40	3.4
107.5	20.0	18	0.12	4.7	6.3	10.0	36	0.23	1.40	2.9
112.5	18.0	19	0.13	5.3	6.6	10.9	36	0.31	1.50	3.1
117.5	22.0	23	0.16	6.2	6.5	13.3	34	0.35	1.60	3.5
122.5	19.0	21	0.14	6.9	6.8	13.8	37	0.22	1.80	3.7
127.5	12.0	19	0.18	6.7	6.6	13.4	36	0.38	2.00	3.4
132.5	10.0	21	0.12	6.2	6.3	13.8	33	0.27	1.80	3.1
137.5	19.0	19	0.15	6.9	6.8	15.0	37	0.35	2.00	3.6
142.5	17.0	18	0.18	6.4	6.4	16.5	31	0.26	2.20	3.1
147.5	18.0	14	0.15	5.4	6.4	16.2	29	0.39	2.00	2.9
152.5	13.0	17	0.16	5.3	6.8	16.6	32	0.29	2.30	3.0
157.5	23.0	18	0.21	5.8	7.0	18.7	35	0.46	2.40	3.2
162.5	24.0	17	0.18	6.6	7.0	17.4	39	0.37	2.30	3.3

Core LP1

Depth (cm)	Ti (2) (ppm)	U (1) (ppm)	V (2) (ppm)	W (1) (ppm)	Y (2) (ppm)	Yb (1) (ppm)	Zn (1) (ppm)	Zn (2) (ppm)	Zn (3) (ppm)	Zr (2) (ppm)
1	4160	2.2	100	4.20	45	2.90	660.0	547	449	122
3	4308	2.3	103	4.60	45	2.90	520.0	515	445	125
5	4308	2.6	94	3.80	47	2.80	590.0	462	392	131
7	4336	2.3	91	4.50	46	2.90	510.0	466	375	126
9	4526	2.4	84	4.50	46	3.00	480.0	429	357	130
11	4520	2.5	80	4.30	42	3.20	480.0	463	397	138
13	4549	2.4	81	3.70	42	3.10	510.0	502	413	134
15	4564	2.2	79	2.50	38	2.90	420.0	402	329	131
17	4456	2.2	72	<2	41	2.80	250.0	258	209	133
19	4395	2.3	71	<2	45	2.70	280.0	252	207	131
21	4007	2.1	63	<2	41	2.90	240.0	248	201	126
23	2815	1.7	50	<2	43	2.30	270.0	273	221	90
25	2428	1.7	41	<2	45	2.70	240.0	226	178	75
27	2165	1.6	38	<2	47	2.50	180.0	200	152	70
29	2104	1.5	37	<2	49	2.50	160.0	198	152	65
31.5	1999	1.5	35	<2	48	2.60	140.0	135	108	60
34.5	1974	1.5	35	<2	49	2.50	140.0	137	98	59
38	1839	1.6	33	<2	51	2.80	81.0	119	98	59
42.5	1841	1.6	32	<2	51	2.60	66.0	112	87	60
47.5	1695	1.3	31	<2	49	2.30	88.0	121	97	55
52.5	1550	1.2	28	<2	46	2.30	120.0	114	91	47
57.5	1212	1.3	23	<2	48	2.60	130.0	107	85	37
62.5	1218	1.1	23	<2	41	2.00	69.0	93	72	36
67.5	1241	1.1	22	<2	34	1.50	<50	90	71	36
72.5	1085	0.9	18	<2	27	1.00	<50	70	54	31
77.5	1222	1.0	20	<2	29	1.30	53.0	69	54	35
82.5	1449	1.1	25	<2	30	1.80	63.0	75	56	43
87.5	1464	1.2	25	<2	31	2.10	84.0	90	69	44
92.5	1604	1.2	26	<2	31	1.80	98.0	88	72	45
97.5	1546	1.2	25	<2	34	2.20	<50	90	70	44
102.5	1489	1.3	26	<2	36	1.70	<50	94	72	44
107.5	1500	1.1	25	<2	40	1.20	<50	73	58	45
112.5	1508	1.1	25	<2	42	1.70	<50	83	62	45
117.5	1383	1.3	25	<2	44	2.00	54.0	90	67	43
122.5	1447	1.3	27	<2	45	2.50	54.0	82	59	44
127.5	1384	1.2	26	<2	45	2.40	78.0	94	68	41
132.5	1310	1.2	24	<2	47	2.20	110.0	92	70	41
137.5	1414	1.3	26	<2	50	2.10	75.0	88	66	45
142.5	1229	1.3	24	<2	55	2.50	68.0	102	75	39
147.5	1183	1.1	23	<2	55	2.20	<50	87	67	37
152.5	1289	1.3	24	<2	58	2.20	<50	82	64	41
157.5	1257	1.3	24	<2	59	2.60	81.0	77	56	41
162.5	1322	1.4	25	<2	58	2.80	61.0	76	57	43

Core LP2

core LP2 Sample #	Depth (cm)	Ag (6) (ppm)	Al (2) (%)	As (1) (ppm)	Au (1) (ppb)	Ba (1) (ppm)	Ba (2) (ppm)	Be (2) (ppm)	Br (1) (ppm)	Ca (2) (%)
LP2-002	1	0.5	6.79	10.0	13.0	470	490	4.1	27.1	0.44
LP2-004	3	0.7	6.94	10.0	13.0	450	501	4.0	25.3	0.43
LP2-006	5	0.5	7.34	8.9	14.0	450	483	3.7	22.1	0.41
LP2-008	7	0.4	7.55	8.3	7.5	450	500	3.8	19.0	0.39
LP2-010	9	0.5	7.60	9.0	8.1	460	520	3.7	19.0	0.38
LP2-012	11	0.6	7.53	8.9	7.8	470	519	3.6	17.0	0.41
LP2-014	13	0.9	7.41	8.4	9.1	460	512	3.8	18.0	0.38
LP2-016	15	1.1	7.42	9.3	11.0	470	541	3.8	18.0	0.39
LP2-018	17	0.6	7.56	10.0	7.4	500	518	3.7	18.0	0.39
LP2-020	19	0.3	7.40	10.0	8.0	450	471	3.7	18.0	0.37
LP2-022	21	0.4	7.05	9.3	7.4	420	434	3.8	20.0	0.33
LP2-024	23	0.5	5.30	14.0	9.3	260	314	4.4	32.8	0.25
LP2-026	25	0.5	5.04	11.0	7.2	220	277	4.4	33.7	0.23
LP2-028	27	0.4	4.76	11.0	4.4	200	257	4.2	34.4	0.23
LP2-030	29	0.4	4.50	11.0	3.5	190	240	4.2	35.9	0.22
LP2-032	31	0.4	4.34	10.0	3.3	200	228	4.2	37.1	0.22
LP2-034	33	0.4	4.54	11.0	3.9	210	230	4.4	38.1	0.21
LP2-036	35	0.4	4.50	10.0	<2	130	218	4.4	39.3	0.21
LP2-038	37	0.4	4.56	10.0	<2	180	216	4.5	41.1	0.20
LP2-040	39	0.4	4.51	11.0	<2	190	204	4.4	45.3	0.21
LP2-045	42.5	0.4	4.61	10.0	3.1	170	213	4.4	41.6	0.22
LP2-050	47.5	0.4	4.38	8.6	3.0	180	195	4.4	40.0	0.19
LP2-055	52.5	0.4	4.31	8.6	<2	170	199	3.8	46.9	0.20
LP2-060	57.5	0.3	3.93	7.3	<2	130	168	3.8	42.5	0.20
LP2-065	62.5	0.3	3.55	7.1	<2	100	144	3.5	61.5	0.20
LP2-070	67.5	0.3	3.43	5.1	<2	150	153	3.1	67.5	0.22
LP2-075	72.5	0.4	2.85	3.0	<2	79	135	2.4	77.0	0.21
LP2-080	77.5	0.3	3.29	3.0	<2	140	169	2.5	69.0	0.26
LP2-085	82.5	0.3	3.61	3.1	<2	140	186	2.6	70.1	0.26
LP2-090	87.5	0.2	5.63	4.5	<2	230	318	4.0	56.7	0.49
LP2-095	92.5	0.2	4.00	4.5	<2	190	227	2.6	54.8	0.35
LP2-100	97.5	0.3	4.01	5.1	<2	170	213	2.9	57.5	0.36
LP2-105	102.5	0.3	3.96	4.8	<2	150	197	3.2	64.6	0.33
LP2-110	107.5	0.3	3.92	3.4	<2	160	185	3.4	73.7	0.31
LP2-115	112.5	0.3	4.14	3.7	<2	160	197	3.7	63.4	0.32
LP2-120	117.5	0.4	4.16	3.6	<2	150	198	4.1	61.8	0.32
LP2-125	127.5	0.3	4.30	3.7	<2	150	207	4.2	56.3	0.34
LP2-130	127.5	0.3	4.19	3.9	<2	170	200	4.3	58.3	0.35
LP2-135	132.5	0.3	4.10	3.3	<2	140	194	4.6	59.0	0.34
LP2-140	137.5	0.4	4.14	3.7	<2	160	207	4.8	63.2	0.36
LP2-145	142.5	0.4	4.08	3.8	<2	160	183	5.4	62.5	0.34
LP2-150	147.5	0.3	3.84	3.5	3.1	140	168	6.1	60.0	0.31
LP2-155	152.5	0.4	3.84	4.0	<2	140	172	6.8	58.0	0.33
LP2-160	157.5	0.3	3.89	3.4	<2	160	201	6.8	53.0	0.36
LP2-165	162.5	0.3	3.71	3.7	<2	180	213	6.9	47.5	0.39
LP2-170	167.5	0.3	3.64	4.0	<2	160	202	6.5	52.9	0.36
LP2-175	172.5	0.3	3.29	4.1	<2	160	176	6.5	52.0	0.38

Core LP2

Depth (cm)	Cd (2) (ppm)	Cd (3) (ppm)	Ce (1) (ppm)	Ce (2) (ppm)	Co (1) (ppm)	Co (2) (ppm)	Co (3) (ppm)	Cr (1) (ppm)	Cr (2) (ppm)	Cr (2a) (ppm)
1	1.8	1.5	140	145	24.0	24	13	58.0	63	58
3	1.7	1.4	140	151	24.0	23	13	61.0	57	57
5	1.3	1.1	140	129	23.0	22	13	51.0	47	46
7	1.2	0.9	130	137	22.0	22	12	39.0	46	44
9	1.3	1.2	120	133	24.0	23	13	42.0	48	46
11	1.3	1.0	120	129	20.0	21	12	40.0	41	37
13	1.4	1.1	120	134	22.0	22	12	32.0	40	33
15	1.6	1.3	110	130	22.0	23	13	27.0	39	33
17	1.0	0.8	110	118	22.0	24	14	32.0	36	31
19	0.5	0.4	120	122	23.0	23	13	<15	34	29
21	0.5	0.4	120	127	25.0	26	15	17.0	30	27
23	0.7	0.5	120	125	42.0	41	23	<15	28	25
25	0.6	0.4	120	127	37.0	35	20	17.0	23	20
27	0.5	0.3	120	135	48.0	43	27	<15	21	18
29	0.4	0.3	130	141	51.0	46	28	<15	18	16
31	0.4	0.3	130	146	51.0	48	30	<15	18	15
33	0.4	0.3	130	157	55.0	51	32	18.0	16	16
35	0.3	0.2	140	160	45.0	46	27	<15	17	16
37	0.3	0.2	140	164	47.0	47	29	17.0	17	15
39	0.4	0.3	170	163	54.0	49	30	<15	16	15
42.5	0.3	0.3	150	162	48.0	44	27	17.0	16	15
47.5	0.3	0.2	150	163	50.0	46	28	<15	15	12
52.5	0.4	0.3	150	158	61.0	55	34	<15	15	15
57.5	0.3	0.4	130	147	44.0	44	26	<15	14	13
62.5	0.4	0.3	140	150	56.0	49	29	<15	12	11
67.5	0.3	0.2	110	122	17.0	17	9	<15	12	11
72.5	0.2	0.2	75	89	8.7	10	6	<15	10	10
77.5	0.3	0.2	79	91	7.9	10	6	<15	11	11
82.5	0.3	0.2	79	93	9.1	11	6	<15	15	12
87.5	0.5	0.2	100	140	13.0	17	6	16.0	18	15
92.5	0.2	0.2	98	100	12.0	12	7	29.0	11	13
97.5	0.2	0.3	110	110	13.0	12	7	<15	13	12
102.5	0.3	0.3	120	117	12.0	12	7	20.0	14	12
107.5	0.2	0.2	120	124	11.0	11	7	<15	15	13
112.5	0.3	0.3	120	132	11.0	11	7	<15	15	14
117.5	0.3	0.3	130	140	8.4	12	7	35.0	16	14
127.5	0.3	0.3	130	145	11.0	12	6	<15	16	14
127.5	0.4	0.4	140	147	9.3	12	7	23.0	15	14
132.5	0.3	0.4	120	145	9.5	12	6	35.0	15	13
137.5	0.3	0.2	140	146	10.0	12	6	<15	16	14
142.5	0.4	0.3	150	157	10.0	10	6	33.0	14	13
147.5	0.4	0.4	140	156	8.1	10	6	<15	16	13
152.5	0.5	0.5	150	164	10.0	12	6	22.0	13	13
157.5	0.5	0.4	130	157	8.2	10	6	26.0	13	13
162.5	0.3	0.3	140	150	9.4	10	6	<15	15	14
167.5	0.5	0.4	130	141	8.0	9	5	34.0	13	13
172.5	0.6	0.5	120	142	8.4	9	4	<15	13	12

Core LP2

Depth (cm)	Cs (1) (ppm)	Cu (2) (ppm)	Cu (3) (ppm)	Dy (2) (ppm)	Eu (1) (ppm)	Fe (1) (%)	Fe (2) (%)	Fe (3) (%)	Ga (2) (ppm)	Hf (1) (ppm)
1	5.5	123	100	8.5	3.70	6.80	5.95	4.22	23	5.50
3	5.5	117	96	8.1	3.00	6.00	5.54	4.08	25	6.20
5	6.3	85	75	7.5	3.60	5.40	4.98	3.65	24	5.80
7	6.7	73	61	7.7	3.30	5.20	4.73	3.32	22	6.60
9	5.8	75	64	7.6	3.40	5.10	4.91	3.63	22	5.90
11	5.4	66	57	7.1	2.90	4.90	4.70	3.62	22	6.20
13	5.4	65	53	7.4	2.60	4.70	4.67	3.31	21	5.90
15	4.8	67	54	7.5	2.00	4.80	4.73	3.34	21	5.00
17	5.5	60	51	7.1	3.50	5.30	4.76	3.39	22	6.00
19	5.6	43	34	7.6	3.00	5.60	4.85	3.46	22	6.50
21	5.2	41	32	7.4	2.70	5.40	5.12	3.64	20	5.60
23	4.1	30	22	7.9	2.50	6.10	5.76	4.25	15	3.40
25	3.7	24	17	8.1	2.60	5.00	4.91	3.80	16	3.20
27	3.8	21	16	8.6	3.90	4.60	4.53	3.46	14	3.50
29	3.4	20	15	8.7	4.20	4.30	4.25	3.09	13	2.60
31	3.2	19	14	8.9	3.40	3.80	4.02	2.85	13	3.00
33	3.2	19	15	9.5	3.90	3.80	3.85	2.72	13	2.30
35	3.0	18	14	9.6	4.50	3.80	3.93	2.75	13	2.60
37	3.1	19	14	9.8	4.60	3.70	3.63	2.52	12	3.00
39	4.0	19	14	9.8	4.10	3.90	3.26	2.27	11	2.40
42.5	3.2	18	14	9.8	4.10	3.50	3.18	2.20	11	2.40
47.5	3.0	16	12	9.9	4.30	3.10	3.18	2.26	10	3.10
52.5	3.1	15	12	9.0	3.80	3.30	3.23	2.34	11	1.90
57.5	2.3	14	10	8.8	3.60	2.80	2.96	2.03	10	1.80
62.5	1.9	14	11	8.4	3.60	2.70	2.63	1.80	8	1.80
67.5	2.1	14	10	7.6	3.10	2.20	2.21	1.42	6	1.80
72.5	1.7	13	10	5.9	2.20	1.50	1.61	1.02	5	1.30
77.5	1.9	14	11	5.7	1.90	1.50	1.67	1.02	6	1.20
82.5	2.5	16	12	6.2	2.20	1.70	1.71	1.01	6	1.80
87.5	2.9	21	11	8.7	2.30	2.30	2.68	1.00	13	2.60
92.5	2.9	14	11	6.1	3.10	2.10	1.86	1.08	8	2.90
97.5	3.1	15	11	6.6	3.30	2.00	1.80	1.04	8	2.70
102.5	2.8	16	12	7.2	3.40	1.80	1.68	1.04	6	2.10
107.5	2.4	17	14	7.9	4.40	1.70	1.63	1.09	8	3.00
112.5	2.6	18	14	8.3	3.70	1.70	1.72	1.11	8	2.40
117.5	2.7	19	15	8.7	4.00	1.70	1.68	1.09	8	2.30
127.5	2.6	18	13	8.9	3.80	1.70	1.67	1.06	9	2.00
127.5	3.0	18	14	10.1	4.20	1.70	1.59	1.03	8	2.40
132.5	3.0	19	14	9.1	4.20	1.50	1.57	1.02	6	2.00
137.5	3.2	19	14	9.4	4.10	1.70	1.59	0.97	6	1.90
142.5	3.2	20	15	10.6	5.30	1.70	1.50	0.98	5	1.70
147.5	2.5	21	16	10.8	3.80	1.50	1.47	0.95	5	1.70
152.5	2.5	22	17	11.8	6.10	1.40	1.44	0.92	5	1.80
157.5	2.8	22	16	11.3	5.50	1.40	1.45	0.86	7	1.60
162.5	3.2	21	16	11.1	5.70	1.50	1.47	0.90	7	1.70
167.5	3.0	22	16	10.8	5.60	1.30	1.38	0.83	6	2.00
172.5	2.5	23	19	10.8	4.10	1.20	1.25	0.74	5	1.50

Core LP2

Depth (cm)	Hg(18) (ppb)	K (2) (%)	La (1) (ppm)	La (2) (ppm)	Li (2) (ppm)	LOI (%)	Lu (1) (ppm)	Mg (2) (%)	Mn (2) (%)	Mn (3) (ppm)
1	297	1.78	68.0	60	45.0	20.1	0.70	0.73	0.17	1020
3	273	1.82	67.0	59	45.5	18.9	0.63	0.71	0.15	919
5	220	1.93	60.0	50	50.6	16.3	0.71	0.72	0.14	883
7	224	1.99	61.0	53	50.8	14.9	0.74	0.73	0.14	849
9	262	2.01	57.0	52	49.1	15.4	0.60	0.74	0.15	915
11	238	2.02	56.0	49	46.9	14.0	0.58	0.73	0.14	887
13	237	1.90	52.0	48	47.3	15.7	0.68	0.69	0.15	918
15	260	1.87	49.0	47	47.6	15.9	0.54	0.68	0.16	1020
17	253	1.95	46.0	41	49.2	14.5	0.58	0.68	0.16	1000
19	244	1.88	50.0	43	50.3	13.6	0.53	0.66	0.15	936
21	278	1.72	47.0	43	48.1	16.5	0.74	0.61	0.16	979
23	589	1.03	43.0	42	31.9	28.8	0.57	0.36	0.19	1400
25	NA	0.90	43.0	43	31.1	30.1	0.60	0.31	0.17	1040
27	324	0.78	46.0	44	29.6	31.7	0.60	0.27	0.17	1070
29	280	0.67	47.0	45	27.8	33.4	0.66	0.25	0.17	1050
31	277	0.61	45.0	45	26.8	33.4	0.55	0.23	0.17	1020
33	251	0.61	48.0	49	28.0	33.2	0.54	0.23	0.17	1010
35	233	0.58	45.0	48	26.7	33.5	0.61	0.22	0.16	982
37	213	0.56	45.0	50	26.2	32.5	0.38	0.22	0.16	981
39	222	0.53	51.0	49	24.8	34.0	0.49	0.21	0.15	940
42.5	208	0.56	51.0	48	25.8	35.3	0.73	0.22	0.16	1020
47.5	200	0.48	48.0	48	24.0	33.7	0.56	0.19	0.17	1040
52.5	205	0.48	47.0	47	22.8	36.2	0.53	0.19	0.17	1300
57.5	176	0.39	42.0	42	20.2	35.1	0.54	0.15	0.15	899
62.5	178	0.29	45.0	42	15.3	39.9	0.42	0.12	0.15	879
67.5	175	0.32	40.0	39	18.0	41.9	0.38	0.13	0.14	847
72.5	172	0.25	29.0	31	13.4	40.8	0.40	0.11	0.13	726
77.5	165	0.36	30.0	32	18.4	47.1	0.30	0.15	0.13	801
82.5	164	0.45	29.0	33	21.8	43.0	0.25	0.18	0.12	705
87.5	127	0.83	35.0	48	33.0	31.5	0.33	0.32	0.19	803
92.5	116	0.57	35.0	33	24.4	51.8	0.37	0.22	0.13	810
97.5	135	0.50	38.0	27	22.4	53.7	0.30	0.20	0.13	763
102.5	143	0.45	43.0	39	21.7	50.0	0.38	0.18	0.12	691
107.5	170	0.42	45.0	44	21.7	43.5	0.43	0.17	0.11	619
112.5	167	0.50	45.0	46	23.9	40.4	0.47	0.20	0.10	589
117.5	177	0.48	49.0	49	23.6	41.9	0.51	0.20	0.09	565
127.5	154	0.48	47.0	49	24.7	44.1	0.48	0.20	0.10	575
127.5	162	0.44	49.0	49	23.8	45.2	0.43	0.18	0.09	574
132.5	156	0.43	45.0	50	23.4	43.7	0.30	0.18	0.09	540
137.5	166	0.48	51.0	52	24.2	44.1	0.50	0.20	0.09	531
142.5	174	0.39	60.0	57	21.1	41.6	0.48	0.17	0.09	505
147.5	178	0.38	60.0	59	19.2	37.6	0.62	0.16	0.08	460
152.5	174	0.39	62.0	65	19.3	38.8	0.65	0.16	0.08	483
157.5	157	0.49	59.0	61	23.9	40.3	0.65	0.20	0.08	513
162.5	115	0.52	60.0	60	25.6	42.1	0.73	0.21	0.09	548
167.5	116	0.50	57.0	58	25.2	39.7	0.70	0.21	0.08	506
172.5	123	0.40	55.0	59	21.1	45.2	0.68	0.17	0.08	554

Core LP2

Depth (cm)	Mo (2) (ppm)	Mo (5) (ppm)	Na (1) (%)	Na (2) (%)	Nb (2) (ppm)	Ni (2) (ppm)	Ni (3) (ppm)	P (2) (ppb)	Pb (2) (ppm)	Pb (3) (ppm)
1	4	3	1.70	1.43	14	30	15	2293	414	326
3	4	3	1.80	1.47	14	30	16	2164	459	363
5	4	3	1.80	1.55	17	25	17	1939	390	317
7	4	3	1.90	1.56	17	24	15	1843	410	330
9	4	3	1.70	1.53	16	25	15	2092	530	443
11	3	2	1.80	1.63	17	22	14	2157	434	373
13	3	2	1.60	1.53	16	22	13	2648	342	269
15	3	2	1.60	1.50	16	22	13	3101	301	246
17	4	2	1.50	1.53	16	21	12	2815	194	178
19	3	2	1.70	1.54	16	19	11	2195	116	91
21	4	3	1.60	1.39	15	19	11	1929	114	87
23	5	4	0.92	0.83	8	17	8	2164	165	143
25	4	4	0.80	0.76	7	12	7	2067	127	85
27	5	4	0.71	0.68	6	11	6	1891	90	65
29	4	4	0.66	0.61	6	10	5	1809	77	49
31	5	4	0.59	0.56	5	10	5	1785	60	39
33	5	4	0.56	0.55	5	10	5	1885	50	35
35	5	4	0.53	0.52	5	9	5	1804	43	30
37	5	4	0.50	0.51	5	10	5	1715	34	25
39	6	4	0.52	0.47	5	11	5	1664	33	24
42.5	5	4	0.57	0.52	6	11	5	1620	28	22
47.5	5	4	0.45	0.43	5	8	4	1636	26	19
52.5	4	3	0.48	0.42	5	8	4	1744	24	20
57.5	4	4	0.36	0.36	3	8	4	1596	22	17
62.5	5	4	0.30	0.27	2	8	4	1729	21	15
67.5	4	3	0.32	0.28	2	5	3	1764	18	12
72.5	4	3	0.22	0.22	2	5	4	1835	15	8
77.5	4	3	0.32	0.32	4	6	3	1961	10	7
82.5	4	3	0.38	0.40	4	6	3	2000	9	7
87.5	6	4	0.65	0.78	7	9	3	2447	15	6
92.5	4	4	0.65	0.53	5	6	3	1636	11	7
97.5	5	4	0.52	0.47	3	7	3	1847	9	8
102.5	4	4	0.46	0.40	4	6	3	1983	10	8
107.5	4	3	0.38	0.36	4	6	3	2306	10	8
112.5	3	3	0.44	0.43	5	8	4	2311	12	8
117.5	4	3	0.41	0.39	4	7	4	2488	11	9
127.5	4	3	0.42	0.40	4	7	4	2402	12	9
127.5	4	3	0.42	0.38	4	6	4	2347	10	8
132.5	4	4	0.35	0.36	4	7	3	2512	7	8
137.5	3	3	0.41	0.39	4	7	4	2570	11	8
142.5	3	3	0.37	0.31	2	7	4	2871	11	8
147.5	3	4	0.32	0.30	2	7	4	2979	10	9
152.5	3	4	0.33	0.31	2	7	4	3122	10	9
157.5	3	4	0.43	0.41	4	7	4	2800	11	9
162.5	3	4	0.48	0.46	2	8	4	2334	10	8
167 5	3	3	0.46	0.43	4	8	4	2389	9	8
172.5	3	4	0.33	0.35	2	8	4	2357	11	9

Core LP2

Depth (cm)	Rb (1) (ppm)	Rb (2) (ppm)	Sb (1) (ppm)	Sc (1) (ppm)	Sc (2) (ppm)	Sm (1) (ppm)	Sr (2) (ppm)	Ta (1) (ppm)	Tb (1) (ppm)	Th (1) (ppm)
1	81.0	73	2.00	14.2	12.0	12.7	74	1.30	1.70	8.7
3	76.0	77	1.80	14.3	12.3	12.7	76	1.30	1.80	9.1
5	86.0	81	1.40	14.2	12.5	12.4	70	1.30	1.70	9.4
7	87.0	80	1.20	14.8	13.1	12.5	72	1.40	1.70	10.1
9	85.0	81	1.30	14.2	13.3	11.1	72	1.50	1.60	10.0
11	88.0	82	1.30	13.8	12.9	11.0	73	1.40	1.50	10.0
13	78.0	75	1.20	13.4	12.9	11.1	70	1.50	1.60	9.3
15	76.0	81	1.10	12.9	13.1	10.6	72	1.20	1.60	9.0
17	85.0	76	1.10	12.7	12.9	10.8	58	1.30	1.60	9.2
19	85.0	76	1.10	13.6	12.7	12.0	68	1.40	1.70	10.0
21	80.0	75	1.10	13.2	12.4	11.0	63	1.30	1.50	8.7
23	50.0	42	1.30	10.0	9.1	10.8	42	0.82	1.60	5.5
25	41.0	37	0.79	8.6	9.3	11.3	38	0.69	1.70	5.2
27	37.0	37	0.49	8.3	8.8	12.3	37	0.53	1.70	4.9
29	32.0	31	0.34	7.8	8.3	12.8	34	0.55	1.90	4.5
31	28.0	30	0.33	7.3	8.1	12.6	33	0.41	1.80	4.3
33	33.0	29	0.29	7.3	8.3	13.8	32	0.44	2.00	4.5
35	29.0	26	0.27	7.0	8.0	13.3	31	0.43	1.70	4.0
37	26.0	23	0.26	6.5	8.0	14.5	31	0.55	2.10	4.4
39	26.0	24	0.28	7.1	7.6	16.6	30	0.48	2.40	4.7
42.5	22.0	27	0.26	7.7	7.8	15.1	32	0.51	2.10	4.4
47.5	23.0	18	0.18	6.9	7.4	14.3	29	0.58	2.00	4.0
52.5	21.0	20	0.19	7.1	7.3	13.3	30	0.30	1.80	4.3
57.5	14.0	20	0.15	5.9	6.6	11.9	27	0.36	1.60	3.2
62.5	17.0	18	0.12	5.5	5.7	12.2	25	0.10	1.60	3.3
67.5	15.0	13	0.15	5.2	5.6	10.6	28	0.10	1.50	3.1
72.5	15.0	12	0.11	3.7	4.5	7.9	25	0.28	1.00	2.2
77.5	11.0	15	0.11	4.4	5.2	7.6	32	0.10	1.10	2.6
82.5	21.0	19	0.13	4.6	5.9	8.3	34	0.39	1.10	3.0
87.5	27.0	34	0.16	6.5	9.4	8.8	66	0.37	1.20	3.9
92.5	26.0	22	0.14	6.6	6.5	8.2	47	0.41	1.20	3.8
97.5	23.0	24	0.15	6.0	6.3	8.9	45	0.27	1.30	3.4
102.5	25.0	18	0.16	6.1	6.4	10.5	40	0.39	1.40	3.6
107.5	23.0	15	0.16	5.8	6.2	11.6	36	0.31	1.70	3.3
112.5	21.0	24	0.14	6.2	6.9	12.0	38	0.39	1.70	3.5
117.5	21.0	16	0.13	6.1	6.8	13.2	36	0.37	1.60	3.5
127.5	23.0	17	0.16	6.2	6.8	12.6	39	0.31	1.60	3.5
127.5	21.0	19	0.14	6.3	6.6	13.1	37	0.33	1.70	3.3
132.5	20.0	19	0.13	5.2	6.5	12.9	36	0.39	1.80	2.9
137.5	28.0	19	0.13	6.1	6.8	14.7	37	0.32	2.00	3.5
142.5	18.0	20	0.15	6.6	6.6	16.7	33	0.34	2.20	3.3
147.5	16.0	16	0.17	6.1	6.4	16.5	30	0.23	2.20	2.8
152.5	20.0	17	0.18	5.9	6.6	17.5	31	0.22	2.40	2.9
157.5	15.0	17	0.15	6.4	7.0	16.4	37	0.40	2.20	3.1
162.5	18.0	21	0.21	6.4	7.2	15.9	41	0.50	2.20	3.0
167.5	17.0	17	0.24	6.3	6.9	15.8	37	0.35	2.00	2.9
172.5	15.0	14	0.19	5.3	6.4	15.1	35	0.10	1.90	2.4

Core LP2

Depth (cm)	Ti (2) (ppm)	U (1) (ppm)	V (2) (ppm)	W (1) (ppm)	Y (2) (ppm)	Yb (1) (ppm)	Zn (1) (ppm)	Zn (2) (ppm)	Zn (3) (ppm)	Zr (2) (ppm)
1	4184	2.4	102	4.00	30	2.90	750.0	610	502	118
3	4283	2.4	110	5.70	46	3.10	720.0	588	499	122
5	4529	2.3	99	4.10	42	3.20	530.0	453	400	130
7	4423	2.5	90	4.20	44	3.20	500.0	378	321	136
9	4441	2.3	92	5.60	44	3.00	510.0	425	373	133
11	4611	2.4	84	5.10	42	2.90	420.0	355	321	137
13	4457	2.4	80	3.80	43	2.60	400.0	395	327	136
15	4477	2.3	81	2.90	43	2.60	480.0	462	387	137
17	4547	2.4	77	<2	40	2.80	350.0	338	295	138
19	4394	2.6	70	<2	40	2.90	260.0	221	177	127
21	4030	2.1	64	<2	41	3.10	230.0	219	179	125
23	2577	1.7	48	<2	44	2.40	230.0	260	211	78
25	2325	1.6	40	<2	45	2.30	210.0	220	178	75
27	2166	1.6	36	<2	46	2.50	160.0	193	159	62
29	2001	1.4	34	<2	46	2.30	130.0	164	125	56
31	1912	1.5	32	<2	46	2.40	90.0	147	114	55
33	1941	1.5	33	<2	49	2.50	92.0	157	132	56
35	1838	1.6	32	<2	49	2.60	58.0	147	122	49
37	1801	1.5	30	<2	51	2.50	73.0	152	125	49
39	1825	1.6	29	<2	50	2.20	140.0	176	148	49
42.5	1964	1.7	30	<2	50	2.80	120.0	124	92	53
47.5	1755	1.4	28	<2	52	2.50	88.0	131	108	48
52.5	1787	1.5	29	<2	47	2.50	99.0	143	120	49
57.5	1530	1.1	26	<2	46	2.10	68.0	113	82	41
62.5	1270	1.2	22	<2	45	2.20	120.0	122	90	34
67.5	1280	1.1	22	<2	39	2.00	67.0	99	71	36
72.5	1042	0.8	18	<2	30	1.30	51.0	70	49	29
77.5	1301	0.9	21	<2	30	1.20	<50	82	56	35
82.5	1496	1.0	25	<2	31	1.40	<50	82	55	44
87.5	2334	1.2	40	<2	45	1.70	97.0	154	73	66
92.5	1739	1.2	26	<2	31	1.80	140.0	107	75	51
97.5	1616	1.2	27	<2	35	1.80	73.0	104	71	47
102.5	1518	1.2	25	<2	37	2.00	86.0	92	62	46
107.5	1461	1.2	24	<2	39	1.60	88.0	78	57	46
112.5	1661	1.3	26	<2	43	1.90	<50	91	66	50
117.5	1498	1.3	25	<2	45	2.10	55.0	98	70	49
127.5	1532	1.2	26	<2	45	2.20	75.0	90	64	48
127.5	1419	1.2	25	<2	45	2.10	63.0	96	69	43
132.5	1415	1.2	25	<2	48	1.70	<50	78	55	43
137.5	1481	1.4	26	<2	49	2.40	<50	101	69	47
142.5	1245	1.3	24	<2	57	2.80	75.0	102	76	41
147.5	1178	1.1	23	<2	57	2.40	61.0	104	76	38
152.5	1162	1.1	23	<2	62	2.60	84.0	127	94	38
157.5	1332	1.3	24	<2	61	2.30	60.0	81	58	43
162.5	1358	1.2	25	<2	58	3.00	<50	88	62	41
167.5	1273	1.3	23	<2	57	2.60	82.0	82	58	41
172.5	1047	1.1	21	<2	58	2.30	<50	100	78	33

Core LP3

core LP3 Sample #	Depth (cm)	Ag (6) (ppm)	Al (2) (%)	As (1) (ppm)	Au (1) (ppb)	Ba (1) (ppm)	Ba (2) (ppm)	Be (2) (ppm)	Br (1) (ppm)	Ca (2) (%)
LP3-004	3	0.5	6.86	9.1	10.0	470	497	4.1	24.5	0.40
LP3-006	5	0.3	7.36	8.4	8.6	480	503	3.9	24.6	0.38
LP3-008	7	0.3	7.51	8.2	8.6	480	509	3.8	21.8	0.38
LP3-010	9	0.2	7.52	8.4	9.0	530	517	3.7	19.0	0.38
LP3-012	11	0.6	7.41	8.6	7.8	540	524	3.8	18.0	0.38
LP3-014	13	0.5	7.42	8.5	5.3	490	518	3.7	17.0	0.39
LP3-016	15	0.5	7.49	10.0	7.9	580	552	3.9	19.0	0.39
LP3-018	17	<0.2	7.33	8.0	5.4	450	481	3.8	17.0	0.35
LP3-020	19	<0.2	7.14	8.2	4.6	400	449	3.8	19.0	0.34
LP3-022	21	0.2	5.67	11.0	9.0	310	347	4.2	32.1	0.27
LP3-024	23	<0.2	4.99	12.0	8.0	280	290	4.4	38.6	0.23
LP3-030	27	<0.2	4.61	11.0	3.5	240	252	4.4	37.9	0.21
LP3-035	32.5	<0.2	4.35	6.0	5.4	190	230	4.2	37.8	0.21
LP3-040	37.5	<0.2	4.21	9.2	3.8	180	216	4.2	41.8	0.20
LP3-045	42.5	<0.2	4.42	8.9	<2	190	209	4.3	41.1	0.20
LP3-050	47.5	<0.2	4.48	7.7	<2	180	207	4.3	39.6	0.20
LP3-055	52.5	<0.2	4.09	7.4	<2	150	184	3.8	45.8	0.20
LP3-060	57.5	<0.2	3.70	6.3	<2	140	153	3.7	48.2	0.19
LP3-065	62.5	<0.2	3.34	5.7	2.8	120	139	3.2	67.7	0.21
LP3-070	67.5	<0.2	3.17	3.9	<2	140	139	2.9	74.2	0.21
LP3-075	72.5	<0.2	2.65	2.6	<2	110	131	2.4	80.6	0.22
LP3-080	77.5	<0.2	3.17	3.0	<2	150	159	2.6	81.1	0.23
LP3-085	82.5	<0.2	3.47	2.9	<2	140	176	3.0	76.3	0.25
LP3-090	87.5	0.2	3.54	2.9	<2	170	171	2.9	72.2	0.26
LP3-095	92.5	0.2	3.68	3.8	<2	130	174	3.4	67.4	0.28
LP3-100	97.5	0.2	3.86	3.2	<2	140	195	3.6	65.5	0.28
LP3-105	102.5	0.2	3.90	3.5	<2	130	191	4.0	60.4	0.28
LP3-110	107.5	0.2	3.85	3.4	<2	170	185	4.3	60.1	0.29
LP3-115	112.5	0.2	3.72	3.3	<2	140	176	4.5	63.7	0.29
LP3-120	117.5	0.2	3.81	3.4	<2	170	191	4.7	59.9	0.30
LP3-125	122.5	0.2	3.78	3.5	<2	170	185	5.2	62.8	0.31
LP3-130	127.5	0.2	3.83	3.4	<2	130	181	6.1	55.3	0.30
LP3-135	132.5	0.2	3.70	4.1	<2	150	171	6.7	59.4	0.29
LP3-140	137.5	0.2	3.49	3.3	3.1	150	172	6.7	55.6	0.29
LP3-145	142.5	0.2	3.44	3.1	<2	160	178	6.8	54.2	0.30
LP3-150	147.5	0.2	3.13	3.7	<2	110	154	7.3	49.6	0.27
LP3-155	152.5	0.2	3.01	3.5	3.1	130	148	7.5	48.6	0.27

Core LP3

Depth (cm)	Cd (2) (ppm)	Cd (3) (ppm)	Ce (1) (ppm)	Ce (2) (ppm)	Co (1) (ppm)	Co (2) (ppm)	Co (3) (ppm)	Cr (1) (ppm)	Cr (2) (ppm)	Cr (2a) (ppm)
3	2.0	1.7	130	132	20.0	22	14	65.0	63	58
5	1.4	1.2	130	128	19.0	22	14	41.0	46	43
7	1.6	1.4	130	114	18.0	22	14	41.0	53	43
9	1.4	1.2	130	119	17.0	20	13	50.0	46	40
11	1.4	1.2	130	117	19.0	21	14	41.0	63	60
13	1.4	1.2	120	120	17.0	20	13	21.0	87	82
15	1.3	1.1	130	121	20.0	24	14	20.0	35	30
17	0.6	0.6	110	119	17.0	22	14	23.0	67	65
19	0.4	0.5	110	123	18.0	23	14	16.0	31	25
21	0.8	0.6	120	124	28.0	30	18	21.0	31	26
23	0.8	0.6	120	126	26.0	28	17	17.0	22	19
27	0.6	0.5	120	130	33.0	34	20	<15	20	16
32.5	0.4	0.4	120	137	34.0	40	25	<15	17	13
37.5	0.4	0.3	130	142	35.0	39	23	18.0	15	13
42.5	0.4	0.3	140	153	35.0	39	24	<15	16	13
47.5	0.3	0.3	140	158	31.0	37	22	<15	18	13
52.5	0.3	0.3	130	150	31.0	36	21	<15	14	12
57.5	0.3	0.2	120	141	25.0	30	19	<15	13	11
62.5	0.4	0.3	120	132	18.0	20	13	<15	12	8
67.5	0.3	0.3	110	115	9.4	11	7	<15	11	7
72.5	0.3	0.2	69	83	5.5	7	5	<15	9	6
77.5	0.3	0.2	84	93	7.7	7	5	<15	12	8
82.5	0.3	0.2	93	105	5.8	10	6	<15	13	9
87.5	0.4	0.3	100	105	6.4	8	5	<15	11	8
92.5	0.4	0.3	110	129	10.0	12	8	17.0	13	9
97.5	0.3	0.3	110	123	6.8	10	5	<15	12	10
102.5	0.4	0.3	110	135	8.9	10	6	<15	15	10
107.5	0.4	0.3	110	143	7.6	10	6	<15	14	10
112.5	0.4	0.3	110	144	9.1	10	6	17.0	11	9
117.5	0.4	0.3	120	146	7.9	11	6	<15	12	10
122.5	0.4	0.3	130	150	8.3	10	6	<15	13	10
127.5	0.6	0.4	130	164	7.7	11	6	19.0	13	8
132.5	0.5	0.4	140	167	9.2	11	6	21.0	13	9
137.5	0.5	0.4	130	158	8.3	10	6	25.0	11	8
142.5	0.5	0.4	120	154	7.1	10	5	<15	13	9
147.5	0.5	0.4	110	150	11.0	13	8	<15	12	8
152.5	0.5	0.4	110	148	9.2	12	7	17.0	12	9

Core LP3

Depth (cm)	Cs (1) (ppm)	Cu (2) (ppm)	Cu (3) (ppm)	Dy (2) (ppm)	Eu (1) (ppm)	Fe (1) (%)	Fe (2) (%)	Fe (3) (%)	Ga (2) (ppm)	Hf (1) (ppm)
3	4.4	131	97	8.1	3.10	5.80	5.48	4.35	23	6.00
5	5.4	86	63	7.6	3.10	5.10	4.88	3.81	23	6.40
7	5.0	82	62	7.8	3.30	4.80	4.86	3.72	24	6.20
9	4.5	69	52	7.5	3.20	4.80	4.67	3.49	23	6.00
11	4.3	63	46	7.7	2.40	4.60	4.65	3.43	23	5.80
13	4.5	64	47	7.9	2.60	4.60	4.62	3.57	24	6.00
15	4.4	64	43	7.8	2.90	4.90	5.11	3.54	23	6.20
17	4.2	45	31	7.7	2.20	4.60	4.82	3.63	22	5.90
19	4.2	41	30	7.8	2.50	4.60	4.76	3.66	21	5.80
21	3.3	35	24	8.0	2.50	5.20	4.98	3.74	18	4.20
23	2.9	30	20	8.3	3.50	4.90	4.72	3.52	16	3.90
27	2.6	24	16	8.7	3.90	4.10	4.34	2.91	13	2.70
32.5	2.4	21	14	9.1	3.30	3.40	3.71	2.57	12	2.50
37.5	2.6	19	13	9.1	3.70	3.40	3.56	2.43	12	2.80
42.5	2.6	18	13	9.6	4.10	3.30	3.39	2.37	13	2.80
47.5	2.7	18	12	9.8	3.50	3.00	3.21	2.12	12	2.40
52.5	2.1	15	11	9.1	3.60	2.80	3.01	2.05	10	2.70
57.5	2.1	21	10	8.6	3.80	2.50	2.77	1.89	9	2.20
62.5	2.0	13	10	7.9	3.30	2.20	2.21	1.40	8	2.00
67.5	1.8	13	10	7.3	2.70	1.80	1.78	1.08	6	1.40
72.5	1.0	13	10	5.5	2.80	1.20	1.38	0.85	5	1.50
77.5	1.6	15	11	5.9	2.70	1.50	1.51	1.06	6	1.80
82.5	1.8	16	12	6.8	2.40	1.50	1.69	1.06	8	2.30
87.5	1.6	16	12	6.7	2.80	1.50	1.64	0.99	9	2.30
92.5	1.8	17	12	7.9	2.60	1.50	1.61	0.99	8	2.10
97.5	2.1	19	14	7.8	3.30	1.60	1.68	1.00	9	2.40
102.5	2.1	19	14	8.6	2.50	1.60	1.68	1.06	8	2.20
107.5	1.9	19	14	8.7	3.10	1.50	1.64	1.04	7	2.40
112.5	1.9	19	14	9.0	2.40	1.30	1.58	1.05	5	1.20
117.5	2.2	19	13	9.3	3.60	1.50	1.69	1.01	9	2.40
122.5	2.3	21	15	9.9	5.10	1.40	1.67	1.05	7	2.00
127.5	1.6	21	15	10.7	3.70	1.60	1.90	1.19	7	1.50
132.5	1.8	25	17	11.4	5.00	1.50	1.79	1.15	6	1.30
137.5	2.1	23	17	11.3	4.00	1.20	1.57	0.98	6	2.00
142.5	1.9	23	17	11.5	4.80	1.40	1.55	0.94	7	2.30
147.5	1.3	23	16	11.4	3.60	1.40	1.72	1.09	6	1.00
152.5	1.7	24	17	11.9	3.30	1.20	1.58	0.98	7	0.70

Core LP3

Depth (cm)	Hg(18) (ppb)	K (2) (%)	La (1) (ppm)	La (2) (ppm)	Li (2) (ppm)	LOI (%)	Lu (1) (ppm)	Mg (2) (%)	Mn (2) (%)	Mn (3) (ppm)
3	268	1.78	59.0	57	45.4	22.2	1.00	0.71	0.13	868
5	228	1.90	56.0	50	51.0	16.3	1.00	0.71	0.13	877
7	243	1.89	53.0	45	48.9	16.4	0.89	0.72	0.14	926
9	233	1.92	52.0	47	48.1	14.5	0.86	0.72	0.14	872
11	230	1.87	48.0	43	47.8	14.5	0.90	0.71	0.15	991
13	210	1.90	48.0	45	48.1	14.1	0.85	0.68	0.15	944
15	250	1.95	49.0	43	50.8	14.5	0.95	0.71	0.16	1010
17	221	1.83	42.0	43	50.6	13.4	0.79	0.64	0.15	884
19	219	1.76	39.0	43	49.8	14.6	0.64	0.63	0.15	872
21	346	1.22	41.0	43	37.5	24.5	0.78	0.43	0.17	947
23	409	0.94	42.0	44	31.5	28.7	0.72	0.32	0.17	965
27	348	0.76	42.0	45	28.3	30.8	0.68	0.27	0.17	913
32.5	317	0.64	41.0	46	27.0	33.0	0.66	0.22	0.16	949
37.5	246	0.57	42.0	45	26.2	33.1	0.72	0.21	0.16	972
42.5	223	0.55	43.0	48	26.3	32.0	0.62	0.21	0.16	970
47.5	203	0.54	41.0	48	26.8	32.6	0.66	0.21	0.16	960
52.5	190	0.45	39.0	44	23.0	35.2	0.61	0.18	0.16	929
57.5	176	0.34	35.0	42	19.2	34.8	0.50	0.15	0.14	854
62.5	163	0.28	34.0	40	15.7	40.5	0.36	0.13	0.14	824
67.5	178	0.28	34.0	37	15.6	40.2	0.45	0.12	0.12	741
72.5	180	0.25	25.0	30	12.9	40.5	0.33	0.11	0.10	697
77.5	190	0.33	29.0	33	17.6	40.4	0.34	0.14	0.10	696
82.5	184	0.37	32.0	39	20.1	40.7	0.44	0.16	0.11	698
87.5	184	0.38	35.0	37	19.9	40.2	0.46	0.16	0.10	634
92.5	180	0.36	38.0	45	19.6	41.4	0.40	0.15	0.10	630
97.5	184	0.44	38.0	44	23.4	39.1	0.45	0.18	0.09	596
102.5	190	0.43	41.0	51	23.2	39.4	0.50	0.18	0.09	573
107.5	199	0.39	40.0	50	20.9	38.8	0.55	0.16	0.09	578
112.5	188	0.35	40.0	56	19.8	39.9	0.43	0.15	0.09	542
117.5	178	0.39	44.0	53	22.2	39.7	0.46	0.17	0.09	516
122.5	190	0.36	47.0	56	21.5	39.8	0.57	0.16	0.09	531
127.5	180	0.36	47.0	63	20.6	38.7	0.55	0.16	0.09	503
132.5	178	0.34	53.0	63	18.8	36.2	0.72	0.15	0.08	487
137.5	180	0.34	50.0	62	19.4	36.0	0.60	0.15	0.08	473
142.5	163	0.37	52.0	64	20.6	35.8	0.69	0.16	0.08	475
147.5	146	0.29	49.0	62	17.0	34.6	0.52	0.13	0.08	467
152.5	158	0.28	45.0	63	16.2	34.1	0.60	0.12	0.08	456

Core LP3

Depth (cm)	Mo (2) (ppm)	Mo (5) (ppm)	Na (1) (%)	Na (2) (%)	Nb (2) (ppm)	Ni (2) (ppm)	Ni (3) (ppm)	P (2) (ppb)	Pb (2) (ppm)	Pb (3) (ppm)
3	6	3	1.70	1.45	15	29	15	2231	479	368
5	5	3	1.70	1.48	16	24	13	1984	399	306
7	4	3	1.60	1.46	17	27	14	2106	485	387
9	5	3	1.80	1.54	17	23	13	2188	463	364
11	4	2	1.70	1.51	17	31	13	2803	312	262
13	4	2	1.70	1.56	17	40	13	2516	342	295
15	4	2	1.70	1.56	18	22	12	3140	262	200
17	4	2	1.60	1.49	18	39	10	2355	138	99
19	3	2	1.40	1.41	17	19	10	1917	114	86
21	4	3	1.10	0.99	10	19	8	2075	171	121
23	4	3	0.86	0.75	8	14	7	2026	153	104
27	6	3	0.70	0.63	7	13	5	1914	114	74
32.5	6	4	0.61	0.54	6	12	5	1765	84	53
37.5	6	4	0.53	0.49	6	11	4	1733	54	37
42.5	6	4	0.50	0.47	6	10	5	1665	38	27
47.5	6	3	0.48	0.47	6	9	4	1587	30	20
52.5	6	3	0.41	0.39	5	9	4	1634	24	17
57.5	6	3	0.30	0.31	3	8	4	1560	21	16
62.5	5	3	0.26	0.26	2	7	3	1658	17	12
67.5	5	3	0.26	0.24	3	6	3	1789	15	11
72.5	4	3	0.22	0.21	2	6	3	1887	8	7
77.5	5	3	0.28	0.27	3	6	3	2233	6	6
82.5	5	3	0.33	0.31	4	6	3	2437	8	7
87.5	6	3	0.33	0.31	5	7	3	2392	7	7
92.5	6	3	0.31	0.29	3	9	4	2411	7	8
97.5	6	3	0.37	0.36	5	7	3	2432	8	7
102.5	6	3	0.35	0.33	3	7	4	2548	6	8
107.5	6	3	0.29	0.29	3	8	6	2628	9	8
112.5	5	3	0.24	0.26	3	7	6	2693	6	8
117.5	5	3	0.30	0.30	3	8	3	2622	6	8
122.5	5	3	0.28	0.27	3	7	4	2789	7	9
127.5	6	3	0.27	0.27	3	8	3	2918	8	9
132.5	6	4	0.28	0.25	3	8	4	3131	10	10
137.5	6	3	0.26	0.25	3	7	3	3044	8	9
142.5	7	4	0.27	0.27	2	8	4	2900	11	9
147.5	6	4	0.21	0.22	2	9	4	2815	10	11
152.5	6	3	0.19	0.20	1	8	4	2801	15	11

Core LP3

Depth (cm)	Rb (1) (ppm)	Rb (2) (ppm)	Sb (1) (ppm)	Sc (1) (ppm)	Sc (2) (ppm)	Sm (1) (ppm)	Sr (2) (ppm)	Ta (1) (ppm)	Tb (1) (ppm)	Th (1) (ppm)
3	81.0	78	1.70	13.7	12.6	13.9	73	1.10	1.80	8.7
5	90.0	86	1.20	14.8	12.9	14.0	69	1.30	1.60	10.0
7	88.0	86	1.20	14.1	13.2	13.2	66	1.40	1.50	9.1
9	95.0	87	1.20	14.9	13.4	13.0	70	1.60	1.60	10.0
11	85.0	82	1.00	14.5	13.4	12.7	69	1.40	1.60	9.2
13	83.0	84	1.10	13.5	13.6	12.4	72	1.50	1.40	9.3
15	86.0	80	1.10	14.9	14.2	13.0	72	1.50	1.50	10.0
17	79.0	79	0.86	13.1	13.7	12.0	69	1.40	1.50	8.4
19	80.0	77	0.95	11.7	13.1	12.0	67	1.30	1.40	8.4
21	61.0	49	1.30	11.2	10.4	12.3	49	0.94	1.60	6.6
23	47.0	43	0.90	9.4	9.0	13.1	40	0.75	1.70	5.5
27	39.0	33	0.54	8.2	8.2	13.6	34	0.53	1.80	4.8
32.5	29.0	30	0.35	7.3	7.7	13.5	33	0.50	1.60	4.1
37.5	26.0	25	0.28	7.6	7.4	15.0	31	0.60	1.90	4.3
42.5	31.0	24	0.21	7.3	7.5	15.7	31	0.54	1.90	4.2
47.5	20.0	24	0.21	7.1	7.5	15.5	32	0.44	1.90	4.2
52.5	22.0	24	0.15	6.1	6.7	14.2	29	0.32	1.80	3.9
57.5	16.0	17	0.13	5.4	5.9	13.4	26	0.42	1.70	3.2
62.5	12.0	12	0.16	4.9	5.1	13.1	25	0.28	1.60	2.9
67.5	14.0	15	0.10	4.8	4.7	11.5	25	0.23	1.40	2.8
72.5	5.4	11	0.08	3.6	3.8	8.8	24	0.37	1.10	2.3
77.5	17.0	13	0.10	4.5	4.4	10.0	28	0.10	1.10	2.6
82.5	19.0	13	0.10	4.8	4.9	11.0	31	0.27	1.30	2.9
87.5	18.0	15	0.13	5.2	5.1	11.9	31	0.25	1.40	2.9
92.5	16.0	15	0.11	5.1	5.2	13.0	32	0.27	1.40	2.9
97.5	26.0	18	0.12	5.5	5.7	13.2	34	0.46	1.50	3.2
102.5	17.0	19	0.14	5.5	5.9	14.3	33	0.43	1.50	3.2
107.5	16.0	8	0.13	5.1	5.7	15.2	31	0.34	1.80	3.0
112.5	18.0	16	0.14	4.4	5.4	16.7	30	0.45	1.70	2.9
117.5	26.0	19	0.11	5.5	5.8	16.9	32	0.23	1.90	3.1
122.5	18.0	14	0.15	5.4	5.8	18.0	31	0.26	2.10	2.9
127.5	15.0	16	0.11	5.3	6.1	18.0	30	0.34	2.00	2.8
132.5	15.0	14	0.16	5.5	5.9	20.5	29	0.10	2.30	3.0
137.5	11.0	15	0.15	5.0	5.8	19.7	28	0.34	2.20	2.6
142.5	14.0	14	0.16	5.3	5.9	19.8	30	0.34	2.20	2.5
147.5	17.0	12	0.15	4.7	5.6	18.9	25	0.10	2.30	2.4
152.5	11.0	14	0.16	4.4	5.6	18.4	26	0.23	2.10	2.1

Core LP3

Depth (cm)	Ti (2) (ppm)	U (1) (ppm)	V (2) (ppm)	W (1) (ppm)	Y (2) (ppm)	Yb (1) (ppm)	Zn (1) (ppm)	Zn (2) (ppm)	Zn (3) (ppm)	Zr (2) (ppm)
3	4317	2.3	109	4.20	47	5.50	750.0	602	523	125
5	4401	2.3	98	3.80	43	6.00	660.0	448	385	139
7	4433	2.1	97	3.50	41	5.90	580.0	455	393	134
9	4575	2.2	88	3.80	41	6.10	530.0	372	310	140
11	4644	2.2	81	3.90	41	5.60	500.0	401	338	144
13	4686	2.3	83	3.10	41	5.50	440.0	376	324	147
15	4734	2.4	84	2.40	42	5.50	500.0	431	355	147
17	4454	2.1	72	<2	42	5.10	330.0	297	251	137
19	4277	2.1	67	<2	42	4.60	260.0	216	191	143
21	3025	1.8	55	<2	42	5.10	290.0	227	188	105
23	2464	1.6	46	<2	44	5.30	220.0	207	174	83
27	2188	1.4	39	<2	46	4.80	190.0	159	124	67
32.5	1984	1.1	35	<2	46	3.60	120.0	119	96	62
37.5	1839	1.3	33	<2	49	4.30	100.0	100	84	60
42.5	1837	1.4	27	<2	52	4.20	<50	94	84	60
47.5	1851	1.4	33	<2	52	4.60	76.0	89	70	60
52.5	1642	1.3	30	<2	48	3.90	<50	92	76	51
57.5	1364	1.0	25	<2	47	2.80	<50	79	68	45
62.5	1188	1.1	23	<2	42	2.60	<50	75	63	40
67.5	1143	0.9	20	<2	38	2.90	59.0	57	47	38
72.5	960	0.8	17	<2	29	2.00	<50	44	40	31
77.5	1201	0.9	20	<2	31	1.80	<50	44	36	42
82.5	1357	1.0	23	<2	34	2.10	<50	47	38	42
87.5	1320	1.0	23	<2	35	3.10	64.0	45	42	46
92.5	1266	1.1	23	<2	40	2.90	<50	70	55	44
97.5	1444	1.1	25	<2	40	3.30	<50	54	39	51
102.5	1378	1.1	25	<2	43	3.30	<50	58	41	50
107.5	1221	1.2	24	<2	47	2.70	<50	62	46	44
112.5	1130	1.2	22	<2	50	2.30	<50	53	38	41
117.5	1236	1.2	24	<2	51	3.50	<50	59	42	46
122.5	1180	1.2	24	<2	54	3.60	<50	62	47	43
127.5	1153	1.0	25	<2	59	4.20	<50	77	59	45
132.5	1081	1.1	24	<2	61	3.90	55.0	77	61	41
137.5	1050	1.1	23	<2	60	3.80	<50	62	51	39
142.5	1073	1.1	23	<2	61	4.50	<50	52	38	42
147.5	914	1.1	21	<2	60	3.80	<50	69	55	35
152.5	899	0.9	18	<2	61	3.60	<50	80	64	36

core LP4 Sample #	Depth (cm)	Ag (6) (ppm)	Al (2) (%)	As (1) (ppm)	Au (1) (ppb)	Ba (1) (ppm)	Ba (2) (ppm)	Be (2) (ppm)	Br (1) (ppm)	Ca (2) (%)
LP4-004	2	0.3	6.67	9.0	11.0	430	498	4.2	23.9	0.41
LP4-006	5	0.7	6.94	8.9	11.0	480	495	4.0	22.5	0.40
LP4-008	7	0.2	7.32	7.7	8.1	440	490	3.9	20.1	0.38
LP4-010	9	0.3	7.50	7.5	5.7	480	476	3.9	19.0	0.36
LP4-013	11.5	0.3	7.50	8.6	7.5	480	506	3.8	19.0	0.37
LP4-015	14	0.3	7.43	7.9	5.7	480	499	3.7	17.0	0.39
LP4-017	16	0.8	7.46	7.9	7.6	460	535	4.0	16.0	0.38
LP4-019	18	0.3	7.64	8.5	6.1	520	524	3.7	17.0	0.38
LP4-021	20	<0.2	7.44	7.6	3.9	450	473	3.8	15.0	0.35
LP4-023	22	<0.2	7.32	7.2	4.7	400	434	3.8	16.0	0.34
LP4-025	24	<0.2	7.12	7.4	3.8	350	432	3.8	17.0	0.33
LP4-027	26	0.2	5.66	12.0	8.1	320	351	4.2	29.7	0.27
LP4-030	28.5	0.2	5.01	11.0	10.0	240	293	4.3	34.3	0.22
LP4-035	32.5	0.2	4.50	10.0	3.1	230	241	4.4	37.1	0.19
LP4-040	37.5	0.2	4.19	8.2	<2	180	220	4.2	38.8	0.19
LP4-045	42.5	<0.2	4.34	8.4	3.4	190	209	4.3	39.9	0.19
LP4-050	47.5	0.2	4.39	7.9	<2	170	200	4.3	40.7	0.19
LP4-055	52.5	0.2	4.12	6.9	<2	140	182	3.9	41.5	0.19
LP4-060	57.5	<0.2	3.57	5.7	<2	100	148	3.6	47.2	0.18
LP4-065	62.5	<0.2	3.27	4.4	<2	100	136	3.1	58.8	0.20
LP4-070	67.5	0.2	3.06	3.1	<2	92	139	2.8	69.8	0.21
LP4-075	72.5	0.2	2.71	2.5	<2	120	143	2.4	82.6	0.21
LP4-080	77.5	0.2	3.15	3.0	<2	110	158	2.7	78.9	0.23
LP4-085	82.5	0.2	3.52	3.1	<2	100	179	3.0	73.7	0.24
LP4-090	87.5	0.3	3.48	3.1	<2	120	174	3.1	66.4	0.25
LP4-095	87.5	0.3	3.67	3.4	<2	140	184	3.3	68.9	0.27
LP4-100	97.5	0.3	3.82	2.6	<2	160	195	3.8	63.1	0.28
LP4-105	102.5	0.3	3.77	3.3	4.1	180	187	4.0	59.2	0.28
LP4-110	107.5	0.3	3.85	3.3	<2	160	190	4.3	56.1	0.29
LP4-115	112.5	0.3	3.78	2.9	<2	150	179	4.6	55.6	0.28
LP4-120	117.5	0.2	3.70	3.0	<2	170	183	4.7	55.1	0.30
LP4-125	122.5	0.3	3.84	3.4	<2	150	189	5.0	62.4	0.30
LP4-130	127.5	0.2	3.69	3.2	<2	150	178	5.5	59.0	0.30
LP4-135	132.5	0.3	3.68	3.4	<2	160	171	6.4	59.7	0.29
LP4-140	137.5	0.2	3.55	3.2	<2	150	171	6.6	56.0	0.28
LP4-145	142.5	0.2	3.39	2.8	<2	130	172	7.1	54.7	0.30
LP4-150	147.5	0.2	2.99	3.2	<2	100	150	8.1	48.0	0.27
LP4-155	152.5	0.2	2.91	3.6	<2	130	140	8.3	46.1	0.26
LP4-160	157.5	0.2	2.72	2.7	<2	100	136	6.6	52.4	0.27
LP4-165	162.5	0.2	2.91	2.8	<2	130	134	7.2	53.4	0.30

Depth (cm)	Cd (2) (ppm)	Cd (3) (ppm)	Ce (1) (ppm)	Ce (2) (ppm)	Co (1) (ppm)	Co (2) (ppm)	Co (3) (ppm)	Cr (1) (ppm)	Cr (2) (ppm)	Cr (2a) (ppm)
2	2.2	1.8	110	139	14.0	21	12	63.0	68	63
5	1.8	1.5	110	123	17.0	22	13	57.0	62	55
7	1.3	1.2	110	125	15.0	21	13	53.0	47	41
9	1.1	1.0	110	115	17.0	21	14	46.0	46	37
11.5	1.4	1.2	110	109	16.0	20	12	37.0	47	35
14	1.3	1.1	110	114	15.0	19	12	35.0	36	26
16	1.4	1.3	110	148	17.0	22	13	42.0	41	28
18	1.0	0.9	110	88	16.0	21	14	36.0	37	25
20	0.6	0.5	100	106	16.0	21	13	28.0	33	23
22	0.4	0.4	100	100	16.0	22	14	<15	31	24
24	0.4	0.4	92	104	18.0	25	15	20.0	32	21
26	0.8	0.7	89	125	26.0	32	20	21.0	27	18
28.5	0.7	0.5	97	125	23.0	30	17	20.0	45	32
32.5	0.5	0.4	110	138	31.0	39	22	22.0	18	11
37.5	0.5	0.3	120	143	35.0	40	23	<15	16	10
42.5	0.3	0.3	130	150	33.0	41	22	<15	16	10
47.5	0.4	0.2	130	157	32.0	38	22	<15	16	10
52.5	0.4	0.3	120	150	29.0	41	23	25.0	13	9
57.5	0.4	0.3	110	139	22.0	31	17	16.0	11	8
62.5	0.3	0.3	100	138	14.0	18	11	<15	11	7
67.5	0.3	0.2	83	115	8.5	15	7	<15	11	6
72.5	0.2	0.2	58	83	4.8	9	5	19.0	11	6
77.5	0.3	0.2	75	99	7.8	10	6	<15	11	7
82.5	0.3	0.2	85	108	8.2	11	6	26.0	14	9
87.5	0.3	0.3	92	117	8.3	11	6	<15	12	9
87.5	0.3	0.2	100	123	8.9	11	6	<15	14	9
97.5	0.3	0.2	110	127	6.8	11	6	<15	12	9
102.5	0.3	0.3	120	134	9.4	11	6	25.0	15	10
107.5	0.4	0.3	120	143	8.1	11	6	<15	14	10
112.5	0.4	0.3	120	148	3.8	11	6	17.0	13	9
117.5	0.4	0.3	110	145	7.7	10	6	<15	14	9
122.5	0.4	0.3	120	153	7.4	11	6	26.0	14	10
127.5	0.4	0.4	130	156	7.3	11	6	23.0	13	9
132.5	0.4	0.4	130	158	8.1	10	6	<15	13	9
137.5	0.4	0.4	130	156	7.0	10	5	21.0	13	9
142.5	0.5	0.4	120	157	6.1	9	5	20.0	12	9
147.5	0.5	0.4	120	157	10.0	12	7	16.0	10	8
152.5	0.5	0.4	120	152	7.7	11	7	25.0	10	8
157.5	0.5	0.4	96	128	4.9	8	4	17.0	10	8
162.5	0.6	0.4	96	126	5.3	8	4	18.0	10	7

Depth (cm)	Cs (1) (ppm)	Cu (2) (ppm)	Cu (3) (ppm)	Dy (2) (ppm)	Eu (1) (ppm)	Fe (1) (%)	Fe (2) (%)	Fe (3) (%)	Ga (2) (ppm)	Hf (1) (ppm)
2	4.0	149	106	8.3	3.80	5.70	6.11	4.83	22	4.40
5	4.3	120	86	7.7	2.10	4.90	5.37	4.23	21	5.40
7	4.9	83	59	7.6	2.50	4.50	4.77	3.61	22	5.70
9	5.0	78	57	7.0	3.10	4.40	4.73	3.74	22	5.50
11.5	4.3	74	54	6.8	2.20	4.40	4.77	3.59	23	5.20
14	4.1	63	46	7.0	2.60	4.10	4.50	3.48	23	5.80
16	4.0	64	45	7.0	1.90	4.20	4.70	3.51	23	5.50
18	4.2	54	37	6.3	1.80	4.30	4.81	3.57	23	5.50
20	4.3	45	32	7.0	2.90	4.20	4.75	3.63	22	5.60
22	4.0	41	30	6.7	2.00	4.00	4.67	3.42	23	5.50
24	4.0	39	28	7.0	2.90	4.00	4.69	3.31	22	4.70
26	3.5	35	25	7.5	1.60	4.30	4.74	3.47	17	3.80
28.5	2.7	28	20	8.0	2.00	4.10	4.56	3.10	15	3.40
32.5	2.9	33	15	8.9	2.90	3.40	4.02	2.58	13	2.70
37.5	2.8	20	13	9.2	3.50	3.20	3.57	2.29	11	2.50
42.5	2.7	18	13	9.7	3.00	2.90	3.30	2.21	10	2.80
47.5	2.2	17	12	9.8	3.20	2.80	3.11	2.05	11	2.50
52.5	2.1	15	11	9.3	2.90	2.40	2.94	1.97	10	2.30
57.5	1.7	14	10	8.5	2.50	2.10	2.48	1.66	7	1.40
62.5	1.5	12	10	7.8	1.70	1.80	2.10	1.33	7	1.40
67.5	1.1	22	10	6.9	2.30	1.60	1.76	1.09	7	1.10
72.5	1.2	12	10	5.4	1.50	1.20	1.41	0.86	6	1.30
77.5	1.3	13	10	6.2	2.10	1.40	1.56	0.93	7	1.50
82.5	1.9	15	11	6.8	3.30	1.50	1.67	1.01	9	1.50
87.5	1.7	16	11	7.4	3.00	1.40	1.63	0.97	8	1.70
87.5	1.6	18	12	7.7	3.10	1.50	1.63	1.01	9	1.50
97.5	1.8	19	13	7.8	3.20	1.50	1.70	1.06	9	1.40
102.5	1.9	18	13	8.2	2.90	1.40	1.65	1.02	8	2.80
107.5	1.8	19	13	8.9	2.70	1.40	1.62	1.00	8	1.80
112.5	2.0	19	13	9.3	4.00	1.30	1.56	0.96	8	2.30
117.5	1.4	19	13	9.3	4.90	1.40	1.54	0.93	9	2.00
122.5	2.0	19	13	10.0	3.00	1.50	1.60	0.99	8	2.10
127.5	2.1	20	14	10.4	4.10	1.60	1.58	0.97	8	1.70
132.5	1.7	22	16	11.0	5.00	1.50	1.69	1.11	7	2.00
137.5	1.6	23	16	11.5	3.80	1.40	1.51	0.94	7	1.40
142.5	1.9	24	16	12.3	4.70	1.20	1.40	0.86	8	1.60
147.5	1.7	23	16	13.0	4.10	1.40	1.57	1.04	7	1.00
152.5	1.7	25	17	13.0	4.50	1.20	1.55	1.00	7	1.40
157.5	1.2	23	16	11.0	3.60	0.92	1.11	0.70	5	1.00
162.5	1.4	26	17	11.6	3.90	0.95	1.14	0.75	4	1.20

Depth (cm)	Hg(18) (ppb)	K (2) (%)	La (1) (ppm)	La (2) (ppm)	Li (2) (ppm)	LOI (%)	Lu (1) (ppm)	Mg (2) (%)	Mn (2) (%)	Mn (3) (ppm)
2	287	1.79	50.0	62	43.4	19.6	0.69	0.72	0.14	807
5	287	1.81	45.0	50	45.6	17.7	0.63	0.70	0.13	793
7	216	1.91	45.0	49	49.7	15.8	0.76	0.70	0.12	772
9	204	1.95	48.0	45	51.1	15.1	0.81	0.73	0.13	807
11.5	227	1.92	46.0	43	48.8	15.3	0.88	0.71	0.13	790
14	220	1.87	45.0	43	46.8	13.3	0.85	0.68	0.13	837
16	244	1.84	42.0	40	47.9	15.1	0.75	0.69	0.15	1030
18	244	1.89	41.0	29	50.1	13.4	0.81	0.68	0.15	1030
20	234	1.87	39.0	37	51.8	12.5	0.79	0.66	0.14	941
22	234	1.80	37.0	36	51.7	13.0	0.80	0.64	0.14	911
24	225	1.74	34.0	35	49.0	15.0	0.66	0.62	0.14	918
26	379	1.20	34.0	43	36.8	24.4	0.74	0.43	0.16	1020
28.5	396	0.95	35.0	43	31.4	28.1	0.57	0.34	0.16	987
32.5	313	0.69	38.0	45	28.1	31.1	0.63	0.25	0.16	1010
37.5	272	0.58	39.0	46	26.2	32.6	0.56	0.22	0.16	1030
42.5	218	0.54	41.0	46	27.1	31.9	0.60	0.21	0.16	955
47.5	214	0.51	41.0	46	26.7	32.5	0.70	0.20	0.17	997
52.5	212	0.44	34.0	44	24.0	34.7	0.53	0.18	0.16	946
57.5	173	0.33	32.0	40	18.7	35.3	0.46	0.14	0.14	863
62.5	129	0.27	31.0	40	15.1	40.1	0.43	0.13	0.14	821
67.5	181	0.27	26.0	36	14.8	39.9	0.42	0.12	0.12	782
72.5	177	0.27	21.0	29	14.7	39.3	0.29	0.13	0.11	692
77.5	186	0.32	27.0	34	17.5	40.2	0.39	0.14	0.11	681
82.5	192	0.39	32.0	37	20.8	40.2	0.38	0.17	0.11	699
87.5	184	0.37	33.0	39	19.9	40.4	0.46	0.17	0.11	654
87.5	200	0.40	37.0	41	21.0	40.0	0.54	0.17	0.10	634
97.5	181	0.44	37.0	44	22.7	38.3	0.40	0.19	0.10	614
102.5	190	0.40	40.0	46	21.8	39.7	0.57	0.17	0.10	590
107.5	192	0.40	41.0	49	22.4	40.0	0.43	0.17	0.09	569
112.5	190	0.36	42.0	51	21.5	39.7	0.49	0.16	0.09	528
117.5	177	0.36	37.0	51	21.5	40.0	0.47	0.16	0.09	527
122.5	184	0.39	42.0	53	22.8	40.0	0.51	0.17	0.09	531
127.5	171	0.35	47.0	56	21.0	39.2	0.51	0.15	0.09	503
132.5	184	0.35	51.0	58	19.9	36.9	0.59	0.15	0.08	478
137.5	177	0.35	50.0	60	20.2	35.7	0.72	0.15	0.08	450
142.5	175	0.34	50.0	69	20.0	36.8	0.65	0.15	0.08	463
147.5	149	0.28	51.0	71	16.5	34.7	0.51	0.12	0.07	442
152.5	186	0.25	49.0	70	15.6	33.9	0.74	0.12	0.07	416
157.5	153	0.25	45.0	59	15.3	34.5	0.50	0.11	0.07	409
162.5	167	0.26	44.0	61	16.0	34.8	0.54	0.12	0.07	407

Depth (cm)	Mo (2) (ppm)	Mo (5) (ppm)	Na (1) (%)	Na (2) (%)	Nb (2) (ppm)	Ni (2) (ppm)	Ni (3) (ppm)	P (2) (ppb)	Pb (2) (ppm)	Pb (3) (ppm)
2	5	4	1.30	1.40	13	30	15	2433	458	360
5	5	3	1.30	1.48	15	29	14	2114	513	390
7	5	3	1.40	1.49	16	25	13	1915	388	310
9	7	3	1.40	1.47	16	25	13	1890	391	318
11.5	6	3	1.50	1.47	16	24	13	2092	524	429
14	7	2	1.60	1.54	19	21	12	2431	342	290
16	6	2	1.50	1.46	17	24	12	3208	307	247
18	5	<2	1.50	1.48	17	21	11	3186	197	162
20	6	2	1.50	1.49	17	19	11	2373	122	101
22	6	<2	1.40	1.43	17	19	10	1930	97	77
24	5	2	1.20	1.36	15	19	10	1847	105	81
26	8	2	0.89	0.95	12	19	10	2094	180	125
28.5	10	3	0.77	0.75	9	26	7	1987	152	104
32.5	9	3	0.58	0.57	7	12	5	1816	99	69
37.5	10	2	0.50	0.48	6	11	5	1721	74	53
42.5	10	3	0.47	0.47	5	10	4	1706	36	29
47.5	10	3	0.47	0.44	5	9	3	1610	28	20
52.5	8	3	0.37	0.38	5	9	4	1652	27	19
57.5	10	3	0.29	0.29	3	8	4	1569	20	17
62.5	9	2	0.23	0.24	3	7	3	1659	14	13
67.5	8	2	0.22	0.23	3	6	3	1810	14	12
72.5	8	2	0.20	0.23	3	6	3	1978	6	6
77.5	7	2	0.27	0.27	3	7	3	2286	6	7
82.5	8	2	0.34	0.33	4	8	3	2421	7	8
87.5	8	2	0.33	0.32	4	7	4	2329	9	8
87.5	9	3	0.36	0.33	4	8	4	2368	10	9
97.5	8	3	0.39	0.37	6	7	4	2361	8	8
102.5	5	3	0.35	0.32	5	7	4	2502	8	9
107.5	9	3	0.36	0.33	5	7	4	2609	11	9
112.5	7	3	0.31	0.28	3	7	4	2705	4	8
117.5	7	3	0.30	0.29	5	7	3	2606	10	8
122.5	6	3	0.30	0.31	5	7	4	2719	9	8
127.5	6	3	0.28	0.27	5	7	4	2876	8	8
132.5	6	2	0.29	0.27	3	7	4	3110	8	9
137.5	6	2	0.29	0.27	3	7	4	3115	9	9
142.5	5	3	0.27	0.26	3	8	4	3070	16	9
147.5	6	3	0.23	0.22	2	8	5	2965	13	9
152.5	6	3	0.19	0.20	2	7	5	3038	13	9
157.5	5	3	0.18	0.18	2	5	4	2644	14	8
162.5	5	3	0.22	0.22	2	6	5	2911	11	8

Depth (cm)	Rb (1) (ppm)	Rb (2) (ppm)	Sb (1) (ppm)	Sc (1) (ppm)	Sc (2) (ppm)	Sm (1) (ppm)	Sr (2) (ppm)	Ta (1) (ppm)	Tb (1) (ppm)	Th (1) (ppm)
2	74.0	75	1.80	10.8	12.6	13.0	75	1.20	1.60	7.7
5	72.0	84	1.50	10.8	12.5	13.3	70	1.30	1.50	8.4
7	76.0	82	1.10	12.2	13.2	12.8	70	1.40	1.40	8.4
9	84.0	90	1.00	12.7	12.8	13.5	61	1.40	1.60	8.8
11.5	83.0	94	1.20	12.9	13.3	12.2	67	1.40	1.50	8.6
14	84.0	89	1.10	13.1	12.6	12.3	67	1.50	1.50	9.2
16	78.0	88	1.00	12.5	13.5	11.9	67	1.30	1.40	8.5
18	75.0	93	0.91	13.4	13.1	11.9	62	1.30	1.40	8.9
20	77.0	85	0.77	12.1	13.5	11.6	66	1.30	1.40	8.7
22	75.0	86	0.75	11.8	13.0	11.5	60	1.30	1.50	8.0
24	63.0	81	0.79	10.6	12.5	11.0	60	1.10	1.30	7.6
26	55.0	53	1.10	8.7	10.4	11.8	49	0.92	1.60	6.2
28.5	44.0	45	0.94	8.3	9.2	12.2	40	0.61	1.40	5.2
32.5	32.0	35	0.46	7.2	8.2	14.0	34	0.70	1.50	4.4
37.5	28.0	28	0.29	6.8	7.6	14.6	32	0.50	1.70	3.9
42.5	25.0	26	0.23	7.1	7.3	15.6	31	0.57	1.90	4.2
47.5	21.0	22	0.20	6.8	7.1	16.1	31	0.44	2.00	4.2
52.5	17.0	17	0.16	5.8	6.8	13.5	29	0.32	1.60	3.5
57.5	13.0	15	0.13	4.9	5.7	12.7	26	0.10	1.60	2.9
62.5	12.0	13	0.10	4.3	5.1	11.3	25	0.23	1.30	2.5
67.5	2.0	12	0.10	3.5	4.7	10.4	26	0.10	1.20	2.5
72.5	9.4	9	0.09	2.8	4.0	8.9	25	0.38	1.00	2.4
77.5	13.0	10	0.13	4.0	4.6	10.2	28	0.21	1.10	2.5
82.5	14.0	19	0.13	4.9	5.3	11.0	31	0.36	1.30	2.7
87.5	14.0	15	0.14	4.9	5.3	11.4	31	0.39	1.30	2.9
87.5	17.0	19	0.14	5.5	5.4	12.7	31	0.38	1.40	3.1
97.5	17.0	18	0.13	5.5	5.7	12.7	35	0.46	1.40	3.1
102.5	23.0	12	0.13	5.4	5.5	13.8	32	0.44	1.60	3.1
107.5	16.0	21	0.11	5.5	5.7	14.1	32	0.24	1.40	3.0
112.5	13.0	18	0.11	5.3	5.6	14.7	30	0.34	1.70	2.7
117.5	18.0	19	0.14	5.2	5.6	14.3	31	0.21	1.70	2.8
122.5	19.0	16	0.12	5.0	5.9	17.1	32	0.32	1.80	3.2
127.5	8.7	17	0.14	5.3	5.7	17.8	30	0.45	2.00	2.8
132.5	14.0	15	0.11	5.4	5.9	18.9	28	0.37	2.20	2.8
137.5	14.0	13	0.16	5.4	5.9	19.2	28	0.23	2.00	2.5
142.5	10.0	12	0.14	4.9	5.9	18.9	29	0.10	2.20	2.3
147.5	5.6	8	0.12	4.6	5.7	19.6	26	0.10	2.30	2.0
152.5	5.4	14	0.14	4.6	5.5	19.3	24	0.10	2.30	1.9
157.5	7.7	9	0.12	4.0	4.8	16.9	24	0.25	1.80	1.8
162.5	8.4	7	0.10	4.0	4.8	17.8	25	0.35	1.90	1.6

Depth (cm)	Ti (2) (ppm)	U (1) (ppm)	V (2) (ppm)	W (1) (ppm)	Y (2) (ppm)	Yb (1) (ppm)	Zn (1) (ppm)	Zn (2) (ppm)	Zn (3) (ppm)	Zr (2) (ppm)
2	4193	2.0	112	3.80	49	5.30	680.0	643	552	129
5	4450	2.2	113	4.60	44	3.40	650.0	580	491	131
7	4424	2.1	97	2.60	42	4.60	460.0	432	357	133
9	4307	2.1	93	3.00	39	4.60	420.0	399	343	136
11.5	4416	2.2	93	4.10	38	5.10	450.0	400	339	126
14	4699	2.4	82	3.20	38	5.20	450.0	364	310	140
16	4609	2.3	83	3.30	39	4.80	510.0	467	391	139
18	4685	2.2	82	<2	33	5.20	380.0	368	303	140
20	4464	2.1	74	<2	37	5.20	250.0	260	227	133
22	4461	2.1	72	<2	36	4.50	260.0	223	192	143
24	4120	1.8	68	<2	36	3.80	230.0	228	195	126
26	3022	1.6	55	<2	43	3.80	280.0	297	252	106
28.5	2511	1.6	46	<2	45	4.00	230.0	239	192	89
32.5	21	1.4	38	<2	49	4.20	220.0	205	168	73
37.5	1860	1.3	34	<2	49	3.70	170.0	154	123	66
42.5	1860	1.4	33	<2	50	4.60	160.0	152	121	68
47.5	1813	1.4	32	<2	50	4.60	130.0	133	103	66
52.5	1639	1.1	31	<2	48	3.80	69.0	137	117	59
57.5	1309	0.9	25	<2	45	2.70	130.0	125	107	48
62.5	1161	0.9	22	<2	41	2.50	95.0	135	104	42
67.5	1118	0.9	20	<2	36	2.00	69.0	99	77	40
72.5	1061	0.9	18	<2	28	1.50	<50	78	61	37
77.5	1185	0.9	20	<2	32	2.50	68.0	100	78	43
82.5	1401	1.0	24	<2	35	2.40	68.0	91	69	52
87.5	1331	1.0	23	<2	38	3.00	100.0	92	71	47
87.5	1378	1.0	24	<2	39	3.00	<50	91	71	51
97.5	1473	1.0	25	<2	43	3.10	68.0	85	62	55
102.5	1306	1.0	24	<2	46	3.20	84.0	87	66	50
107.5	1321	1.0	24	<2	48	3.00	56.0	114	88	49
112.5	1204	1.0	22	<2	50	3.40	60.0	97	74	45
117.5	1221	1.0	23	<2	50	2.60	<50	77	57	47
122.5	1271	1.2	24	<2	54	2.90	74.0	107	84	50
127.5	1161	1.1	23	<2	57	3.90	84.0	90	71	44
132.5	1128	1.2	24	<2	60	3.60	99.0	133	109	46
137.5	1122	1.0	23	<2	62	3.80	<50	81	60	45
142.5	1060	1.1	20	<2	63	4.40	68.0	78	60	44
147.5	873	0.9	18	<2	66	4.30	68.0	115	96	36
152.5	804	1.0	17	<2	66	4.00	77.0	107	89	35
157.5	791	0.9	16	<2	56	3.40	<50	70	54	33
162.5	807	0.8	17	<2	58	3.30	55.0	92	72	32

Core LP5

core LP5 Sample #	Depth (cm)	Ag (6) (ppm)	Al (2) (%)	As (1) (ppm)	Au (1) (ppb)	Ba (1) (ppm)	Ba (2) (ppm)	Be (2) (ppm)	Br (1) (ppm)	Ca (2) (%)
LP5-002	1.0	<0.2	6.84	9.3	12.0	460	494	4.3	24.4	0.45
LP5-004	3.0	0.4	6.97	9.2	9.4	420	495	4.1	22.7	0.45
LP5-006	5.0	0.3	6.00	8.7	8.5	440	484	3.9	21.6	0.43
LP5-008	7.0	<0.2	7.52	8.2	9.2	440	493	3.8	21.0	0.41
LP5-010	9.0	<0.2	7.58	8.0	6.2	440	494	3.9	19.0	0.39
LP5-012	11.0	<0.2	7.55	9.1	8.9	510	506	3.8	20.0	0.40
LP5-014	13.0	0.2	7.68	8.8	10.0	530	501	3.7	17.0	0.42
LP5-016	15.0	0.3	7.43	8.3	7.2	450	504	3.7	16.0	0.41
LP5-018	17.0	0.5	7.53	7.7	8.5	450	519	3.9	15.0	0.39
LP5-020	19.0	<0.2	7.48	8.1	4.4	430	471	3.7	15.0	0.38
LP5-022	21.0	<0.2	5.69	12.0	7.1	270	328	4.3	27.1	0.28
LP5-024	23.0	<0.2	4.65	12.0	5.8	200	246	4.4	33.5	0.23
LP5-026	25.0	<0.2	4.30	9.4	<2	160	224	4.1	32.5	0.23
LP5-028	27.0	<0.2	4.54	9.1	<2	160	228	4.2	34.7	0.23
LP5-030	29.0	<0.2	4.58	8.8	<2	190	219	4.3	38.5	0.22
LP5-035	32.5	<0.2	4.65	8.0	<2	150	210	4.3	36.7	0.22
LP5-040	37.5	<0.2	4.33	7.6	<2	160	192	3.8	43.7	0.22
LP5-045	42.5	<0.2	3.93	7.5	<2	130	161	3.7	46.5	0.20
LP5-050	47.5	<0.2	3.60	5.9	<2	130	146	3.4	61.5	0.21
LP5-055	52.5	<0.2	3.26	4.3	<2	98	143	2.8	68.8	0.22
LP5-060	57.5	<0.2	3.17	3.0	<2	120	158	2.6	73.0	0.23
LP5-065	62.5	<0.2	3.51	4.0	<2	110	166	3.1	72.1	0.24
LP5-070	67.5	<0.2	3.73	4.0	<2	150	184	3.3	66.2	0.25
LP5-075	72.5	<0.2	3.84	3.9	<2	130	186	3.6	62.2	0.26
LP5-080	77.5	<0.2	4.07	4.4	<2	150	201	3.9	58.4	0.28
LP5-085	82.5	<0.2	3.98	4.7	<2	160	193	4.2	53.9	0.27
LP5-090	87.5	<0.2	4.04	5.0	<2	160	197	4.5	57.5	0.28
LP5-095	92.5	<0.2	4.18	5.4	<2	130	203	4.9	53.1	0.28
LP5-100	97.5	<0.2	3.98	5.0	<2	130	193	4.9	55.8	0.28
LP5-105	102.5	<0.2	4.09	5.9	<2	150	203	5.3	52.5	0.29
LP5-110	107.5	<0.2	4.20	5.8	<2	160	209	5.8	6.0	0.30

Core LP5

Depth (cm)	Cd (2) (ppm)	Cd (3) (ppm)	Ce (1) (ppm)	Ce (2) (ppm)	Co (1) (ppm)	Co (2) (ppm)	Co (3) (ppm)	Cr (1) (ppm)	Cr (2) (ppm)	Cr (2a) (ppm)
1.0	2.0	1.7	140	141	21.0	21	13	65.0	66	69
3.0	1.9	1.6	140	136	19.0	21	13	77.0	67	54
5.0	1.4	1.2	140	134	24.0	22	14	58.0	53	44
7.0	1.3	1.1	130	133	20.0	22	14	52.0	46	40
9.0	1.2	1.1	130	138	19.0	22	14	54.0	41	39
11.0	1.2	1.1	130	133	20.0	21	13	37.0	47	47
13.0	1.1	1.1	120	119	17.0	20	13	45.0	38	37
15.0	1.1	1.0	120	127	20.0	21	14	52.0	39	34
17.0	1.2	1.0	110	131	19.0	22	13	32.0	37	34
19.0	0.5	0.5	120	121	20.0	22	13	44.0	33	30
21.0	0.5	0.4	110	124	33.0	34	19	<15	28	23
23.0	0.3	0.3	120	138	39.0	41	24	31.0	20	17
25.0	0.2	0.3	120	143	39.0	44	24	34.0	19	15
27.0	0.2	0.3	130	153	39.0	44	24	18.0	18	16
29.0	0.2	0.3	140	156	39.0	41	23	18.0	18	13
32.5	0.2	0.3	140	161	35.0	38	21	38.0	17	13
37.5	0.2	0.3	130	153	36.0	39	22	<15	17	12
42.5	0.2	0.3	130	145	37.0	36	21	24.0	15	10
47.5	0.2	<0.2	130	138	22.0	23	13	21.0	15	10
52.5	0.2	0.2	100	115	10.0	12	7	25.0	13	8
57.5	0.2	0.2	80	94	8.4	10	6	21.0	11	8
62.5	0.2	0.2	100	108	7.5	12	6	16.0	13	9
67.5	0.2	0.3	110	115	12.0	13	7	25.0	16	11
72.5	0.3	0.3	120	128	9.2	13	7	<15	16	11
77.5	0.3	0.3	120	133	8.8	14	8	19.0	15	12
82.5	0.3	0.3	130	147	12.0	15	8	<15	16	12
87.5	0.3	0.4	150	156	13.0	15	8	<15	16	12
92.5	0.3	0.3	160	167	17.0	17	10	22.0	18	13
97.5	0.4	0.3	150	161	14.0	16	9	<15	16	14
102.5	0.4	0.4	160	168	14.0	17	11	33.0	15	12
107.5	0.3	0.4	170	182	17.0	18	12	16.0	17	12

Core LP5

Depth (cm)	Cs (1) (ppm)	Cu (2) (ppm)	Cu (3) (ppm)	Dy (2) (ppm)	Eu (1) (ppm)	Fe (1) (%)	Fe (2) (%)	Fe (3) (%)	Ga (2) (ppm)	Hf (1) (ppm)
1.0	5.4	145	103	8.0	4.70	6.40	5.77	4.45	22	6.10
3.0	5.5	132	99	8.0	3.80	5.60	5.44	4.24	28	5.30
5.0	5.0	100	75	7.5	2.90	5.30	4.80	3.55	20	6.20
7.0	6.0	82	64	7.5	2.70	5.00	4.65	3.52	20	6.50
9.0	5.9	77	60	7.7	3.20	4.60	4.60	3.39	20	5.30
11.0	6.0	72	55	7.4	3.20	5.20	4.61	3.44	20	6.40
13.0	5.8	64	50	7.0	1.70	4.60	4.48	3.43	20	5.80
15.0	5.0	59	44	7.3	2.90	4.80	4.46	3.32	20	5.70
17.0	4.9	59	41	7.3	2.80	4.40	4.60	3.26	20	5.60
19.0	5.3	45	32	7.3	2.80	4.70	4.78	3.31	20	6.30
21.0	4.0	31	21	7.8	2.80	5.10	5.39	4.01	16	3.80
23.0	3.3	24	16	9.0	3.60	4.40	4.75	3.23	15	2.20
25.0	3.0	19	14	9.2	3.80	3.40	3.93	2.54	13	2.80
27.0	2.7	19	14	9.6	3.20	3.30	3.90	2.56	13	2.50
29.0	3.6	19	13	9.8	4.30	3.70	3.57	2.36	12	2.60
32.5	3.0	18	12	10.1	2.90	2.90	3.13	2.01	12	2.40
37.5	3.1	17	11	9.3	2.70	2.80	2.96	1.86	11	2.10
42.5	2.6	15	10	8.9	3.90	2.60	2.68	1.79	10	2.10
47.5	2.2	15	10	8.2	2.50	2.10	2.27	1.47	9	2.40
52.5	2.0	16	11	7.0	3.50	1.80	1.79	1.15	9	1.70
57.5	1.8	17	11	6.1	2.70	1.50	1.62	1.01	8	1.80
62.5	1.7	17	11	6.7	3.30	1.60	1.78	1.12	8	1.90
67.5	2.5	18	13	7.2	3.10	1.80	1.88	1.21	9	1.90
72.5	2.2	18	13	7.9	3.60	1.80	1.91	1.21	9	1.80
77.5	2.3	21	15	8.2	3.40	2.00	2.03	1.36	10	2.20
82.5	2.1	20	14	9.0	3.60	1.90	2.02	1.37	9	2.10
87.5	2.5	21	14	9.3	5.00	2.20	2.07	1.33	10	1.90
92.5	2.8	21	14	9.8	4.40	2.10	2.21	1.36	9	2.00
97.5	2.5	20	14	9.8	4.30	2.10	2.08	1.33	8	2.00
102.5	2.5	21	15	10.2	4.20	2.40	2.45	1.60	10	2.10
107.5	3.1	23	17	11.2	4.90	2.40	2.58	1.73	10	1.50

Core LP5

Depth (cm)	Hg(18) (ppb)	K (2) (%)	La (1) (ppm)	La (2) (ppm)	Li (2) (ppm)	LOI (%)	Lu (1) (ppm)	Mg (2) (%)	Mn (2) (%)	Mn (3) (ppm)
1.0	299	1.84	68.0	61	43.8	19.7	0.66	0.78	0.14	879
3.0	290	1.86	64.0	58	45.7	18.6	0.61	0.75	0.15	975
5.0	262	1.89	60.0	55	47.3	16.5	0.65	0.74	0.13	866
7.0	243	1.98	58.0	52	49.2	16.0	0.65	0.72	0.13	881
9.0	224	2.01	55.0	55	48.9	15.7	0.56	0.72	0.13	876
11.0	243	2.02	53.0	52	48.1	15.3	0.55	0.73	0.13	870
13.0	206	2.02	50.0	45	47.2	13.8	0.63	0.72	0.13	898
15.0	243	1.93	51.0	47	47.4	14.2	0.64	0.69	0.13	948
17.0	252	1.95	46.0	47	49.4	14.2	0.70	0.70	0.14	962
19.0	243	1.93	46.0	42	50.7	13.4	0.73	0.67	0.14	892
21.0	393	1.23	41.0	42	36.3	25.0	0.54	0.43	0.16	984
23.0	374	0.75	44.0	47	27.3	31.2	0.61	0.26	0.17	980
25.0	299	0.65	40.0	47	25.8	32.5	0.61	0.23	0.16	943
27.0	299	0.65	43.0	50	27.3	33.0	0.62	0.23	0.17	947
29.0	262	0.62	45.0	50	26.7	32.2	0.53	0.22	0.16	923
32.5	234	0.60	42.0	50	26.5	32.4	0.39	0.22	0.16	883
37.5	224	0.52	40.0	46	24.5	34.8	0.40	0.19	0.16	891
42.5	215	0.41	41.0	44	20.4	34.7	0.58	0.16	0.15	836
47.5	206	0.34	42.0	43	17.1	38.9	0.50	0.14	0.14	763
52.5	234	0.31	37.0	37	15.9	40.3	0.34	0.13	0.12	744
57.5	206	0.35	29.0	34	16.4	39.6	0.34	0.14	0.11	705
62.5	243	0.36	35.0	38	17.6	41.0	0.35	0.15	0.11	702
67.5	242	0.43	39.0	40	20.6	40.0	0.38	0.17	0.11	715
72.5	243	0.42	41.0	45	20.0	40.4	0.38	0.17	0.11	672
77.5	224	0.47	43.0	47	22.5	39.1	0.40	0.19	0.11	707
82.5	224	0.43	42.0	53	21.0	40.0	0.46	0.17	0.11	658
87.5	224	0.43	50.0	54	21.9	39.6	0.30	0.17	0.11	632
92.5	243	0.43	54.0	58	21.9	39.4	0.46	0.18	0.11	604
97.5	164	0.38	54.0	56	20.0	39.9	0.48	0.16	0.10	607
102.5	191	0.42	56.0	59	21.6	40.0	0.60	0.17	0.11	659
107.5	191	0.43	59.0	69	21.6	40.5	0.56	0.17	0.11	674

Core LP5

Depth (cm)	Mo (2) (ppm)	Mo (5) (ppm)	Na (1) (%)	Na (2) (%)	Nb (2) (ppm)	Ni (2) (ppm)	Ni (3) (ppm)	P (2) (ppb)	Pb (2) (ppm)	Pb (3) (ppm)
1.0	6	3	1.80	1.54	14	29	16	2312	414	357
3.0	6	3	1.70	1.58	16	29	18	2239	464	404
5.0	6	3	1.70	1.61	16	27	15	1943	401	348
7.0	6	2	1.70	1.61	17	24	15	1889	388	350
9.0	6	2	1.60	1.60	16	24	15	1886	395	350
11.0	6	2	1.60	1.59	16	29	15	1970	480	426
13.0	5	2	1.60	1.67	19	22	14	2162	365	346
15.0	6	2	1.70	1.63	17	21	14	2457	285	262
17.0	5	2	1.60	1.60	17	22	13	2779	251	226
19.0	5	2	1.60	1.62	17	19	12	2253	130	101
21.0	7	3	1.00	1.00	10	15	9	2029	128	91
23.0	7	3	0.67	0.65	8	12	6	1891	103	69
25.0	6	3	0.53	0.57	7	11	5	1748	74	44
27.0	7	3	0.54	0.58	7	12	5	1793	59	38
29.0	7	3	0.57	0.55	7	11	5	1716	46	28
32.5	6	3	0.50	0.54	7	11	4	1631	38	22
37.5	6	3	0.43	0.46	7	10	4	1648	31	19
42.5	6	3	0.40	0.38	6	8	4	1594	25	17
47.5	5	2	0.33	0.31	5	8	3	1683	21	14
52.5	5	2	0.28	0.28	4	6	3	1784	20	12
57.5	5	2	0.29	0.30	4	7	3	2061	14	9
62.5	5	3	0.31	0.31	4	6	3	2308	11	8
67.5	5	3	0.37	0.37	6	7	3	2333	12	10
72.5	5	3	0.35	0.35	4	8	3	2229	11	9
77.5	6	3	0.40	0.41	6	8	3	2325	13	9
82.5	5	2	0.33	0.35	4	8	3	2394	11	10
87.5	6	3	0.34	0.34	4	8	4	2427	16	11
92.5	5	3	0.35	0.34	4	8	3	2477	17	10
97.5	5	3	0.31	0.30	4	8	3	2473	12	10
102.5	5	3	0.34	0.34	3	6	3	2472	14	11
107.5	7	4	0.35	0.34	3	6	3	2622	17	13

Core LP5

Depth (cm)	Rb (1) (ppm)	Rb (2) (ppm)	Sb (1) (ppm)	Sc (1) (ppm)	Sc (2) (ppm)	Sm (1) (ppm)	Sr (2) (ppm)	Ta (1) (ppm)	Tb (1) (ppm)	Th (1) (ppm)
1.0	77.0	72	2.00	13.6	13.2	12.4	75	1.30	1.60	8.8
3.0	69.0	76	1.80	13.7	13.5	12.0	75	1.20	1.60	8.5
5.0	78.0	77	1.40	13.7	13.7	12.0	75	1.40	1.60	8.7
7.0	83.0	77	1.20	13.6	13.9	11.7	71	1.30	1.40	9.3
9.0	78.0	81	1.20	13.0	14.3	11.6	71	1.30	1.60	8.9
11.0	78.0	77	1.40	13.2	14.3	11.8	73	1.40	1.80	10.0
13.0	87.0	82	1.30	12.7	14.1	11.9	73	1.60	1.90	10.2
15.0	68.0	76	1.10	13.6	14.2	11.2	73	1.40	1.50	10.0
17.0	74.0	79	1.00	12.9	14.8	10.4	74	1.30	1.50	8.6
19.0	78.0	81	0.92	13.4	14.3	10.7	70	1.30	1.50	8.8
21.0	52.0	52	0.93	10.0	10.7	10.4	47	0.84	1.50	5.9
23.0	35.0	31	0.59	7.7	9.0	12.1	36	0.78	1.70	4.7
25.0	32.0	25	0.32	6.6	8.5	11.7	33	0.53	1.50	4.0
27.0	25.0	25	0.31	6.9	8.8	12.4	35	0.48	1.80	4.0
29.0	26.0	26	0.27	7.5	8.6	13.8	33	0.56	2.00	4.3
32.5	24.0	21	0.25	6.6	8.5	13.7	33	0.50	1.80	4.0
37.5	27.0	20	0.24	6.2	7.8	13.0	31	0.60	1.80	4.2
42.5	20.0	16	0.19	6.0	7.0	12.4	28	0.41	1.80	3.5
47.5	15.0	11	0.15	5.0	6.0	11.5	26	0.41	1.50	3.1
52.5	20.0	8	0.13	4.8	5.1	10.0	26	0.10	1.30	3.0
57.5	14.0	9	0.10	4.0	4.9	8.0	28	0.27	1.10	2.4
62.5	15.0	14	0.13	4.9	5.2	10.0	29	0.21	1.40	2.6
67.5	24.0	14	0.14	5.5	5.9	10.7	31	0.54	1.40	3.2
72.5	20.0	19	0.14	5.2	5.9	11.1	31	0.29	1.60	3.1
77.5	22.0	16	0.18	5.8	6.6	11.7	34	0.38	1.70	3.1
82.5	20.0	16	0.15	5.2	6.3	12.6	31	0.33	1.60	3.0
87.5	21.0	16	0.16	5.5	6.6	14.7	31	0.47	2.00	3.4
92.5	18.0	17	0.16	5.8	6.7	14.9	31	0.54	2.00	3.4
97.5	16.0	15	0.16	5.8	6.3	15.1	29	0.35	2.00	3.0
102.5	18.0	18	0.18	6.2	6.6	15.4	31	0.27	1.90	3.4
107.5	14.0	17	0.15	6.0	7.1	16.0	31	0.31	2.00	3.2

Core LP5

Depth (cm)	Ti (2) (ppm)	U (1) (ppm)	V (2) (ppm)	W (1) (ppm)	Y (2) (ppm)	Yb (1) (ppm)	Zn (1) (ppm)	Zn (2) (ppm)	Zn (3) (ppm)	Zr (2) (ppm)
1.0	4124	2.2	105	5.50	49	3.10	720.0	648	572	128
3.0	4412	2.1	104	5.00	47	3.10	690.0	641	574	132
5.0	4391	2.2	97	3.70	46	2.90	530.0	525	447	136
7.0	4343	2.3	92	3.80	45	2.90	510.0	458	408	131
9.0	4299	2.2	90	4.00	47	3.00	490.0	424	376	164
11.0	4393	2.6	88	4.50	45	3.00	420.0	407	360	159
13.0	4660	2.6	80	4.40	41	2.80	330.0	366	331	141
15.0	4620	2.5	77	4.70	42	2.70	360.0	366	330	145
17.0	4646	2.4	78	2.40	42	2.80	400.0	418	367	149
19.0	4512	2.2	70	<2	40	2.80	300.0	268	224	146
21.0	2912	1.6	51	<2	43	2.30	190.0	241	196	115
23.0	2175	1.4	38	<2	49	2.40	170.0	215	165	77
25.0	1965	1.4	35	<2	49	1.90	130.0	179	129	65
27.0	2060	1.4	36	<2	50	2.20	96.0	161	118	68
29.0	1984	1.5	35	<2	51	2.60	91.0	161	116	64
32.5	1956	1.5	33	<2	51	1.90	70.0	119	86	66
37.5	1791	1.4	32	<2	48	2.10	<50	124	89	59
42.5	1488	1.3	25	<2	48	2.10	120.0	111	81	52
47.5	1286	1.1	24	<2	43	1.70	60.0	118	85	41
52.5	1161	1.0	22	<2	36	1.10	<50	98	70	37
57.5	1182	0.9	20	<2	32	1.70	<50	88	63	40
62.5	1242	1.0	23	<2	36	1.20	78.0	96	69	41
67.5	1409	1.2	25	<2	38	2.00	<50	94	71	49
72.5	1372	1.1	25	<2	42	2.00	56.0	96	70	49
77.5	1568	1.3	27	<2	43	1.70	56.0	94	72	54
82.5	1335	1.1	25	<2	47	1.60	<50	93	71	51
87.5	1326	1.3	26	<2	49	1.50	66.0	102	77	51
92.5	1332	1.2	26	<2	52	2.20	57.0	109	79	51
97.5	1203	1.1	24	<2	52	2.00	<50	96	72	47
102.5	1283	1.4	26	<2	57	2.20	<50	114	82	50
107.5	1325	1.2	27	<2	62	2.20	<50	118	87	53

Core MP1

core MP1 Sample #	Depth (cm)	Ag (6) (ppm)	Al (2) (%)	As (1) (ppm)	Au (1) (ppb)	Ba (1) (ppm)	Ba (2) (ppm)	Be (2) (ppm)	Br (1) (ppm)	Ca (2) (%)
MP1-002	1	<0.2	6.60	10.0	12.0	500	498	3.4	38.6	0.48
MP1-004	3	<0.2	6.77	11.0	13.0	510	500	3.4	36.0	0.47
MP1-006	5	<0.2	7.07	11.0	11.0	520	527	3.4	33.1	0.45
MP1-008	7	<0.2	7.05	11.0	12.0	490	522	3.4	29.7	0.44
MP1-010	9	<0.2	7.06	12.0	10.0	460	521	3.4	25.1	0.42
MP1-012	11	<0.2	6.93	14.0	12.0	460	520	3.4	21.9	0.40
MP1-014	13	<0.2	7.02	14.0	15.0	500	530	3.4	19.0	0.39
MP1-016	15	<0.2	6.72	15.0	14.0	510	514	3.2	20.4	0.38
MP1-018	17	0.2	5.98	25.2	17.0	460	470	3.6	25.0	0.35
MP1-020	19	0.3	4.82	24.7	19.0	360	378	4.2	46.0	0.32
MP1-022	21	0.2	3.67	17.0	14.0	240	269	4.3	50.9	0.25
MP1-024	23	<0.2	3.23	11.0	7.4	170	209	4.4	43.2	0.19
MP1-026	25	<0.2	3.18	6.3	3.2	150	171	4.2	37.1	0.16
MP1-028	27	<0.2	3.00	4.8	<2	130	159	3.8	39.2	0.16
MP1-030	29	<0.2	2.85	4.0	<2	130	147	3.6	45.4	0.15
MP1-032	31	<0.2	2.81	4.1	<2	120	234	3.4	49.6	0.15
MP1-034	33	<0.2	2.80	3.6	<2	120	126	3.2	48.3	0.14
MP1-036	35	<0.2	2.73	3.6	<2	110	120	2.9	55.2	0.16
MP1-038	37	<0.2	2.76	2.7	<2	83	116	2.4	66.4	0.17
MP1-040	39	<0.2	2.55	2.7	<2	92	116	2.1	72.3	0.17
MP1-045	42.5	<0.2	2.19	2.8	<2	77	109	1.7	84.8	0.19
MP1-050	47.5	<0.2	2.06	2.1	<2	98	107	1.5	90.0	0.19
MP1-055	52.5	<0.2	1.95	1.7	<2	95	103	1.4	96.3	0.19
MP1-060	57.5	<0.2	1.97	1.4	<2	96	101	1.3	89.0	0.19
MP1-065	62.5	<0.2	1.94	1.3	<2	98	104	1.3	98.1	0.20
MP1-070	67.5	<0.2	1.99	1.4	<2	120	105	1.4	96.7	0.20
MP1-075	72.5	<0.2	2.12	1.5	<2	140	111	1.5	102.0	0.20
MP1-080	77.5	<0.2	2.27	1.3	<2	110	110	1.7	94.8	0.20
MP1-085	82.5	<0.2	2.31	1.5	<2	110	118	1.9	103.0	0.21
MP1-090	87.5	<0.2	2.28	1.7	<2	120	114	2.0	92.2	0.22
MP1-095	92.5	<0.2	2.40	2.2	<2	110	118	2.1	102.0	0.24
MP1-100	97.5	<0.2	2.41	2.1	<2	94	114	2.2	97.2	0.24

Core MP1

Depth (cm)	Cd (2) (ppm)	Cd (3) (ppm)	Ce (1) (ppm)	Ce (2) (ppm)	Co (1) (ppm)	Co (2) (ppm)	Co (3) (ppm)	Cr (1) (ppm)	Cr (2) (ppm)	Cr (2a) (ppm)
1	2.8	2.2	92	97	21.0	23	12	53.0	83	76
3	2.6	2.3	100	90	19.0	23	13	75.0	83	80
5	2.4	1.9	100	104	19.0	22	12	81.0	90	84
7	2.2	1.8	99	98	21.0	23	12	81.0	93	88
9	2.0	1.7	99	98	21.0	24	13	120.0	114	108
11	2.2	1.7	98	103	21.0	24	13	130.0	145	142
13	2.0	1.6	92	98	21.0	24	13	100.0	123	121
15	2.2	1.8	86	99	24.0	27	17	62.0	106	100
17	2.5	2.1	80	42	33.0	36	24	280.0	278	248
19	1.7	1.3	90	96	42.0	45	26	1320.0	1172	1139
21	1.0	0.8	95	104	47.0	50	30	1580.0	1619	1509
23	0.5	0.4	100	113	49.0	52	30	1080.0	1137	1030
25	0.2	0.2	100	118	26.0	27	16	235.0	276	246
27	0.2	0.2	91	116	13.0	15	9	37.0	41	37
29	0.2	0.2	87	110	7.8	9	6	21.0	26	22
31	0.3	0.2	94	106	7.1	9	5	<15	20	17
33	0.2	0.2	80	104	6.4	9	6	<15	18	15
35	0.2	0.2	80	99	7.9	10	6	<15	20	17
37	0.2	<0.2	76	95	7.8	9	5	<15	14	13
39	0.2	<0.2	83	86	7.6	9	6	21.0	15	11
42.5	<0.2	<0.2	65	76	5.5	8	5	<15	15	13
47.5	0.2	<0.2	63	70	4.8	6	4	<15	15	12
52.5	<0.2	<0.2	56	63	4.9	5	4	<15	14	11
57.5	<0.2	<0.2	51	61	3.2	5	3	<15	12	9
62.5	<0.2	<0.2	53	61	3.9	4	3	<15	17	13
67.5	0.2	<0.2	55	64	2.4	4	3	<15	17	14
72.5	<0.2	0.2	57	67	2.8	4	3	18.0	14	11
77.5	0.2	<0.2	64	74	3.2	5	3	<15	20	17
82.5	0.2	0.2	72	75	3.3	4	3	18.0	17	14
87.5	0.2	<0.2	67	77	3.7	5	3	<15	16	13
92.5	0.2	0.2	79	90	4.8	6	3	16.0	9	7
97.5	0.3	0.2	78	84	3.7	6	3	<15	17	14

Core MP1

Depth (cm)	Cs (1) (ppm)	Cu (2) (ppm)	Cu (3) (ppm)	Dy (2) (ppm)	Eu (1) (ppm)	Fe (1) (%)	Fe (2) (%)	Fe (3) (%)	Ga (2) (ppm)	Hf (1) (ppm)
1	4.4	129	84	7.4	2.90	7.00	6.91	5.04	22	4.80
3	4.3	117	83	7.0	1.90	6.40	6.50	5.17	23	5.40
5	4.5	107	69	7.5	3.00	5.90	6.02	4.10	23	5.80
7	4.2	99	62	7.1	2.20	5.50	5.80	4.10	23	5.20
9	4.1	88	57	6.9	2.40	5.50	5.64	4.09	22	5.20
11	4.2	87	59	6.9	2.30	5.50	5.70	4.41	22	5.10
13	3.8	86	55	6.9	2.10	5.60	5.80	4.16	21	5.00
15	3.6	86	57	6.6	1.70	5.80	5.92	4.27	21	4.20
17	3.7	96	63	6.3	1.70	7.20	6.81	5.17	20	5.10
19	2.8	89	55	6.6	2.40	5.60	5.38	3.61	19	3.50
21	2.1	63	39	7.5	3.00	3.70	3.91	2.68	15	2.70
23	1.5	42	25	8.0	3.00	3.10	3.38	2.28	12	1.60
25	1.2	26	16	8.5	3.20	2.40	2.82	1.95	11	1.40
27	1.3	19	12	8.3	2.80	1.70	2.04	1.32	8	1.50
29	1.1	16	10	7.8	2.80	1.40	1.60	1.06	7	1.40
31	1.1	13	9	7.5	3.10	1.40	1.51	0.96	7	1.20
33	1.1	12	9	7.5	2.30	1.20	1.46	0.96	8	0.78
35	0.9	12	8	6.9	2.20	1.40	1.48	0.94	7	1.30
37	1.1	11	7	6.2	1.40	1.30	1.44	0.91	8	1.20
39	0.8	11	7	5.9	1.50	1.30	1.37	0.90	7	1.20
42.5	0.6	11	7	5.1	1.70	1.10	1.18	0.77	7	0.20
47.5	0.5	11	7	4.8	0.93	1.00	1.05	0.62	7	0.61
52.5	0.8	10	7	4.4	1.30	1.00	0.90	0.58	3	0.72
57.5	0.6	10	6	4.1	2.10	0.86	0.82	0.55	5	0.81
62.5	0.3	10	7	4.1	1.70	0.72	0.76	0.52	4	0.68
67.5	0.3	10	6	4.1	1.50	0.70	0.73	0.50	4	0.90
72.5	0.5	10	7	4.4	1.90	0.84	0.76	0.51	4	0.20
77.5	0.8	11	7	4.7	1.40	0.81	0.80	0.54	4	0.59
82.5	0.4	12	8	4.8	2.10	0.78	0.74	0.50	4	0.20
87.5	0.4	11	7	5.0	2.10	0.74	0.73	0.48	4	1.00
92.5	0.4	15	8	5.4	1.70	0.75	0.81	0.50	4	0.94
97.5	0.5	12	8	5.3	2.10	0.82	0.79	0.54	4	0.66

Core MP1

Depth (cm)	Hg(18) (ppb)	K (2) (%)	La (1) (ppm)	La (2) (ppm)	Li (2) (ppm)	LOI (%)	Lu (1) (ppm)	Mg (2) (%)	Mn (2) (%)	Mn (3) (ppm)
1	295	1.83	50.0	46	42.0	18.3	0.79	0.74	0.16	857
3	299	1.86	48.0	40	43.9	16.5	0.73	0.73	0.14	844
5	303	1.89	46.0	46	45.9	15.1	0.88	0.74	0.14	733
7	297	1.89	43.0	41	45.8	14.6	0.88	0.72	0.14	716
9	303	1.87	41.0	39	45.3	14.8	0.83	0.71	0.14	766
11	325	1.81	41.0	40	44.3	15.9	0.84	0.69	0.14	805
13	340	1.83	39.0	37	44.9	15.5	0.78	0.70	0.15	822
15	318	1.75	35.0	41	42.1	16.8	0.65	0.67	0.18	1060
17	600	1.46	35.0	37	37.5	22.8	0.71	0.55	0.16	1040
19	810	0.99	37.0	41	29.6	28.8	0.68	0.36	0.27	2460
21	819	0.61	37.0	43	20.8	27.5	0.62	0.23	0.11	687
23	193	0.42	38.0	43	15.7	26.0	0.54	0.15	0.10	600
25	128	0.31	36.0	44	13.1	24.9	0.50	0.11	0.09	581
27	200	0.27	33.0	42	11.8	27.4	0.46	0.10	0.08	509
29	134	0.23	31.0	40	11.0	29.0	0.41	0.09	0.09	539
31	134	0.21	32.0	37	10.3	28.3	0.39	0.08	0.08	493
33	119	0.20	28.0	36	9.6	27.8	0.46	0.08	0.07	456
35	128	0.18	26.0	34	9.2	30.3	0.34	0.07	0.08	476
37	124	0.17	28.0	33	9.1	32.2	0.30	0.07	0.08	486
39	119	0.17	26.0	31	8.5	34.2	0.28	0.07	0.08	538
42.5	108	0.13	24.0	28	6.2	38.1	0.28	0.06	0.08	528
47.5	110	0.11	22.0	26	5.4	39.1	0.23	0.06	0.07	470
52.5	108	0.10	21.0	24	5.0	39.0	0.20	0.05	0.07	436
57.5	106	0.10	20.0	24	4.3	39.3	0.27	0.05	0.06	385
62.5	100	0.09	19.0	24	4.1	41.8	0.16	0.05	0.05	349
67.5	96	0.08	20.0	25	3.9	42.1	0.20	0.05	0.05	343
72.5	91	0.10	21.0	26	4.4	41.4	0.28	0.05	0.05	356
77.5	87	0.11	22.0	29	4.4	40.4	0.25	0.05	0.05	306
82.5	87	0.10	25.0	30	4.9	40.2	0.29	0.05	0.05	278
87.5	87	0.09	26.0	30	4.8	39.3	0.20	0.05	0.03	243
92.5	89	0.09	29.0	32	5.2	39.7	0.26	0.05	0.03	215
97.5	96	0.10	27.0	32	5.0	39.5	0.30	0.06	0.03	206

Core MP1

Depth (cm)	Mo (2) (ppm)	Mo (5) (ppm)	Na (1) (%)	Na (2) (%)	Nb (2) (ppm)	Ni (2) (ppm)	Ni (3) (ppm)	P (2) (ppb)	Pb (2) (ppm)	Pb (3) (ppm)
1	7	3	2.00	1.88	9	32	16	1720	287	220
3	8	3	1.80	1.75	10	32	17	1573	301	248
5	8	3	1.80	1.73	12	31	17	1618	324	248
7	7	2	1.70	1.69	12	30	17	1619	325	247
9	7	2	1.60	1.62	12	30	17	1691	303	241
11	9	3	1.60	1.58	10	32	18	1858	311	243
13	11	2	1.60	1.58	10	33	17	1830	299	238
15	9	3	1.40	1.54	11	35	18	1829	274	225
17	12	4	1.40	1.36	10	39	22	2116	339	274
19	11	4	1.10	0.98	8	33	15	2283	379	283
21	12	4	0.69	0.67	6	22	10	1812	293	227
23	10	3	0.46	0.47	6	16	7	1470	188	158
25	10	2	0.34	0.38	2	12	6	1264	111	82
27	7	2	0.32	0.35	4	11	5	1226	71	53
29	8	2	0.28	0.31	3	10	4	1183	51	38
31	7	2	0.28	0.28	4	12	4	1181	45	35
33	6	2	0.26	0.27	4	10	4	1204	37	30
35	6	2	0.26	0.28	3	8	3	1243	34	25
37	6	2	0.26	0.26	4	8	3	1216	23	18
39	5	2	0.29	0.28	3	8	4	1122	18	16
42.5	4	2	0.27	0.27	3	10	4	1003	15	12
47.5	4	2	0.27	0.26	3	10	3	979	13	9
52.5	3	<2	0.30	0.27	3	10	3	925	7	7
57.5	3	<2	0.26	0.27	2	7	4	885	6	5
62.5	5	<2	0.26	0.27	2	10	4	857	<2	4
67.5	3	2	0.29	0.32	2	10	4	842	<2	4
72.5	5	2	0.34	0.36	2	8	5	856	3	4
77.5	4	2	0.33	0.38	2	11	4	851	<2	5
82.5	3	2	0.37	0.35	2	11	5	878	3	5
87.5	4	2	0.36	0.36	2	10	4	887	3	4
92.5	3	2	0.37	0.34	2	11	5	953	3	4
97.5	3	2	0.30	0.31	2	11	5	985	3	4

Core MP1

Depth (cm)	Rb (1) (ppm)	Rb (2) (ppm)	Sb (1) (ppm)	Sc (1) (ppm)	Sc (2) (ppm)	Sm (1) (ppm)	Sr (2) (ppm)	Ta (1) (ppm)	Tb (1) (ppm)	Th (1) (ppm)
1	84.0	70	2.00	13.1	11.9	11.0	71	0.84	1.50	7.9
3	82.0	78	2.00	13.5	11.4	11.2	66	1.00	1.60	8.3
5	86.0	77	1.80	13.9	12.9	11.1	77	1.00	1.30	8.6
7	79.0	76	1.70	13.5	12.6	10.6	74	1.00	1.50	8.4
9	74.0	82	2.00	13.2	12.6	10.3	73	1.00	1.40	8.2
11	83.0	72	2.30	13.2	12.9	10.3	74	1.00	1.20	8.2
13	80.0	77	2.40	13.0	12.7	10.0	71	0.94	1.20	8.4
15	73.0	78	2.30	11.2	12.5	10.0	70	0.92	1.30	7.8
17	68.0	62	3.60	11.2	11.3	10.0	67	0.91	1.10	7.4
19	46.0	39	3.40	10.0	9.6	10.4	58	0.55	1.30	5.6
21	27.0	27	2.00	7.2	7.5	11.7	39	0.42	1.50	3.9
23	17.0	18	1.00	6.0	6.3	13.3	28	0.10	1.50	3.2
25	14.0	13	0.46	5.2	5.8	13.3	21	0.25	1.70	3.0
27	11.0	11	0.29	4.6	5.5	12.3	18	0.20	1.50	2.6
29	5.9	10	0.17	4.2	4.9	12.0	18	0.29	1.40	2.7
31	9.4	12	0.17	4.4	4.8	12.3	17	0.23	1.60	2.5
33	8.6	10	0.19	3.8	4.6	11.2	16	0.26	1.30	2.4
35	6.4	9	0.19	3.3	4.1	10.7	17	0.10	1.40	2.5
37	5.6	10	0.10	3.4	3.9	10.8	17	0.36	1.10	2.7
39	6.3	13	0.11	3.5	3.7	10.0	18	0.25	1.10	2.5
42.5	2.0	7	0.08	3.0	3.2	7.9	19	0.24	0.82	2.0
47.5	4.4	5	0.06	2.7	2.9	7.4	19	0.10	0.84	1.8
52.5	2.0	5	0.05	2.7	2.8	7.1	19	0.10	0.86	1.8
57.5	3.9	5	0.05	2.4	2.6	6.8	19	0.10	0.84	1.5
62.5	6.0	8	0.08	2.4	2.7	6.5	20	0.10	0.73	1.5
67.5	2.0	5	0.02	2.4	2.6	6.7	20	0.10	0.80	1.5
72.5	2.0	7	0.05	2.7	2.9	7.4	20	0.10	0.87	1.7
77.5	8.4	6	0.06	2.5	3.0	8.0	20	0.10	1.00	1.7
82.5	6.7	5	0.07	3.0	3.1	8.7	20	0.24	1.00	1.7
87.5	2.0	5	0.07	2.8	3.0	8.6	20	0.10	1.00	1.6
92.5	7.4	5	0.09	2.9	3.5	10.0	21	0.10	1.10	1.8
97.5	11.0	6	0.07	2.8	3.3	9.4	21	0.10	1.10	1.8

Core MP1

Depth (cm)	Ti (2) (ppm)	U (1) (ppm)	V (2) (ppm)	W (1) (ppm)	Y (2) (ppm)	Yb (1) (ppm)	Zn (1) (ppm)	Zn (2) (ppm)	Zn (3) (ppm)	Zr (2) (ppm)
1	3801	1.9	97	<2	44	4.90	1600.0	1210	939	102
3	3998	1.9	100	<2	41	4.80	1500.0	1141	969	111
5	4153	2.0	101	<2	43	5.50	1400.0	1084	859	119
7	4151	2.0	98	<2	41	5.80	1300.0	1046	822	116
9	4108	2.0	95	<2	38	5.00	1100.0	893	699	118
11	3952	2.0	93	<2	38	5.10	1100.0	884	703	110
13	3986	1.9	90	<2	37	4.20	1100.0	868	667	113
15	3763	1.9	92	<2	37	3.70	1100.0	868	684	107
17	3377	1.8	74	<2	35	4.70	1300.0	1025	827	90
19	2663	1.6	56	<2	38	4.80	1100.0	804	589	68
21	1792	1.2	38	<2	42	3.90	570.0	495	377	45
23	1398	1.3	28	<2	44	3.60	320.0	310	219	36
25	1223	1.2	24	<2	45	3.80	150.0	200	149	31
27	1148	1.1	23	<2	43	3.20	140.0	159	114	31
29	1061	1.0	20	<2	42	2.80	73.0	117	86	27
31	1011	1.1	19	<2	41	2.90	120.0	116	82	27
33	978	1.0	19	<2	40	3.10	110.0	120	88	27
35	956	1.0	18	<2	36	1.80	95.0	116	90	25
37	960	1.0	17	<2	31	2.00	60.0	116	84	24
39	947	1.0	17	<2	28	2.10	65.0	102	80	24
42.5	781	0.8	13	<2	24	1.60	<50	63	48	20
47.5	715	0.7	12	<2	22	1.20	<50	57	43	19
52.5	677	0.8	13	<2	20	<0.5	<50	52	38	18
57.5	665	0.8	11	<2	20	1.40	<50	46	39	19
62.5	662	0.6	11	<2	20	0.89	<50	40	31	21
67.5	620	0.7	9	<2	4	1.40	<50	36	30	18
72.5	670	0.6	11	<2	21	1.30	<50	55	45	20
77.5	716	0.7	13	<2	23	1.50	<50	63	46	21
82.5	685	0.7	12	<2	23	1.10	58.0	61	43	20
87.5	654	0.6	12	<2	25	1.60	62.0	61	45	21
92.5	623	0.7	11	<2	27	2.00	<50	73	52	24
97.5	669	0.7	12	<2	27	1.70	<50	59	41	21

Core MP2

core MP2 Sample #	Depth (cm)	Ag (6) (ppm)	Al (2) (%)	As (1) (ppm)	Au (1) (ppb)	Ba (1) (ppm)	Ba (2) (ppm)	Be (2) (ppm)	Br (1) (ppm)	Ca (2) (%)
MP2-002	1	0.2	6.65	11.0	14.0	480	495	3.2	32.4	0.42
MP2-004	3	0.2	6.60	13.0	13.0	560	508	3.2	35.1	0.41
MP2-006	5	0.2	6.53	14.0	13.0	480	502	3.2	25.7	0.38
MP2-008	7	0.3	5.94	19.0	15.0	440	473	3.4	24.2	0.35
MP2-010	9	0.2	3.76	16.0	12.0	280	282	4.1	45.0	0.24
MP2-012	11	<0.2	3.68	10.0	8.7	200	247	4.1	36.4	0.20
MP2-014	13	<0.2	3.34	5.8	3.8	180	195	3.9	35.6	0.16
MP2-016	15	<0.2	2.96	4.2	3.0	110	160	3.6	41.6	0.15
MP2-018	17	<0.2	2.77	3.9	<2	98	139	3.4	43.3	0.14
MP2-020	19	<0.2	2.72	3.7	<2	110	130	3.3	47.7	0.14
MP2-022	21	<0.2	2.71	3.4	<2	120	125	3.0	48.1	0.14
MP2-024	23	<0.2	2.66	3.7	<2	120	122	2.5	63.4	0.16
MP2-026	25	<0.2	2.33	2.8	3.2	96	116	2.0	80.8	0.17
MP2-028	27	<0.2	2.18	4.0	<2	110	122	1.8	90.5	0.19
MP2-030	29	<0.2	2.03	2.6	<2	96	110	1.6	87.1	0.19
MP2-032	31	<0.2	2.04	2.3	<2	110	107	1.6	89.8	0.18
MP2-034	33	<0.2	2.00	2.3	<2	75	102	1.5	90.4	0.18
MP2-036	35	<0.2	1.93	2.2	<2	78	103	1.5	97.5	0.18
MP2-038	37	<0.2	1.91	2.1	<2	110	102	1.5	91.8	0.19
MP2-040	39	<0.2	1.95	1.8	<2	79	101	1.5	89.4	0.19
MP2-045	42.5	<0.2	1.87	1.5	<2	83	101	1.4	85.0	0.19
MP2-050	47.5	<0.2	1.81	1.7	<2	89	106	1.3	102.0	0.19

Depth (cm)	Cd (2) (ppm)	Cd (3) (ppm)	Ce (1) (ppm)	Ce (2) (ppm)	Co (1) (ppm)	Co (2) (ppm)	Co (3) (ppm)	Cr (1) (ppm)	Cr (2) (ppm)	Cr (2a) (ppm)
1	2.4	2.1	85	94	17.0	23	15	95.0	109	111
3	2.4	2.1	96	103	22.0	24	16	120.0	114	117
5	2.2	2.0	110	105	22.0	24	17	130.0	122	115
7	2.4	2.1	85	101	29.0	31	22	278.0	272	263
9	1.2	1.0	93	103	40.0	45	31	1350.0	1309	1231
11	0.8	0.7	100	115	41.0	46	33	722.0	662	618
13	0.4	0.4	99	119	16.0	11	12	82.0	88	84
15	0.4	0.3	97	110	10.0	11	7	28.0	26	24
17	0.3	0.2	89	110	9.5	10	7	8.0	13	11
19	0.3	0.2	87	108	8.6	9	6	20.0	10	9
21	0.2	0.2	79	98	7.3	9	6	8.0	13	11
23	0.2	0.2	87	98	10.0	9	5	20.0	14	13
25	0.2	0.2	75	80	10.0	8	5	8.0	13	11
27	0.3	0.2	71	74	10.0	9	5	31.0	26	23
29	0.2	0.1	64	72	8.2	7	5	20.0	11	10
31	0.1	0.1	63	71	6.4	7	4	8.0	10	8
33	0.1	0.1	62	71	6.0	6	4	8.0	7	7
35	0.1	0.1	61	67	5.6	6	4	8.0	7	8
37	0.2	0.1	57	65	6.1	6	4	8.0	10	8
39	0.1	0.1	55	67	4.4	6	4	8.0	10	9
42.5	0.1	0.1	44	62	3.7	6	3	8.0	7	6
47.5	0.1	0.1	53	60	1.0	5	3	16.0	7	7

Core MP2

Depth (cm)	Cs (1) (ppm)	Cu (2) (ppm)	Cu (3) (ppm)	Dy (2) (ppm)	Eu (1) (ppm)	Fe (1) (%)	Fe (2) (%)	Fe (3) (%)	Ga (2) (ppm)	Hf (1) (ppm)
1	4.1	107	78	6.9	1.80	5.80	5.80	5.01	20	4.50
3	4.4	97	77	7.1	1.80	6.50	5.74	5.07	21	5.00
5	4.5	87	66	6.9	2.40	6.10	5.38	4.77	21	5.50
7	3.7	91	64	6.7	2.80	5.80	5.81	5.03	20	4.10
9	2.0	64	44	7.3	2.50	3.90	4.15	3.14	15	2.50
11	1.7	45	33	8.2	3.40	3.80	4.07	3.31	12	2.50
13	1.7	28	21	8.3	2.90	2.50	2.71	2.04	7	1.90
15	1.4	20	15	7.7	2.90	1.70	1.97	1.38	7	1.60
17	1.1	15	11	7.6	2.30	1.40	1.62	1.05	7	1.20
19	1.0	14	10	7.4	2.60	1.40	1.55	1.07	6	1.10
21	1.3	12	9	6.9	2.40	1.30	1.55	1.07	6	0.74
23	1.0	12	9	6.5	2.10	1.70	1.40	0.97	6	1.40
25	1.0	11	8	5.4	1.90	1.40	1.23	0.84	5	1.70
27	1.2	17	10	4.9	2.50	1.60	1.32	0.86	5	1.40
29	0.6	12	8	4.7	1.80	1.20	1.14	0.72	5	0.86
31	0.6	11	8	4.7	2.00	1.10	1.06	0.69	4	1.00
33	0.6	10	7	4.7	1.90	1.00	0.96	0.62	5	0.68
35	0.3	10	8	4.5	1.70	1.00	0.94	0.64	5	0.62
37	0.5	10	8	4.4	2.10	0.94	0.93	0.60	4	1.10
39	0.5	11	8	4.6	1.20	1.00	0.94	0.64	4	0.70
42.5	0.4	10	7	4.3	1.60	0.90	0.86	0.60	4	1.40
47.5	0.5	11	8	4.1	1.10	0.86	0.81	0.57	4	0.20

Depth (cm)	Hg(18) (ppb)	K (2) (%)	La (1) (ppm)	La (2) (ppm)	Li (2) (ppm)	LOI (%)	Lu (1) (ppm)	Mg (2) (%)	Mn (2) (%)	Mn (3) (ppm)
1	323	1.71	39.0	42	42.9	17.0	0.69	0.68	0.13	865
3	328	1.70	43.0	45	42.7	16.6	0.63	0.68	0.13	880
5	357	1.61	42.0	44	41.7	16.5	0.78	0.63	0.13	870
7	487	1.45	37.0	42	38.3	20.4	0.74	0.56	0.14	871
9	623	0.67	37.0	42	22.4	26.2	0.56	0.26	0.12	826
11	369	0.58	40.0	45	19.9	23.3	0.58	0.23	0.22	1910
13	201	0.41	36.0	44	15.9	23.9	0.52	0.16	0.09	579
15	159	0.30	33.0	40	12.6	27.1	0.47	0.11	0.08	514
17	139	0.21	31.0	38	10.8	28.5	0.37	0.08	0.08	476
19	141	0.19	31.0	38	10.4	28.5	0.39	0.08	0.07	468
21	132	0.19	28.0	34	10.1	28.1	0.31	0.08	0.07	456
23	134	0.19	30.0	34	10.2	31.2	0.27	0.08	0.08	488
25	127	0.15	26.0	29	7.9	36.2	0.29	0.07	0.08	544
27	127	0.16	29.0	28	7.3	38.2	0.20	0.08	0.08	556
29	116	0.12	23.0	27	6.0	39.1	0.23	0.06	0.08	509
31	119	0.12	23.0	26	6.1	38.5	0.28	0.06	0.07	498
33	116	0.10	22.0	26	5.5	37.5	0.19	0.05	0.07	454
35	NA	0.10	23.0	26	5.0	38.5	0.24	0.05	0.07	455
37	NA	0.10	22.0	25	5.6	38.2	0.24	0.06	0.07	448
39	103	0.10	21.0	26	5.5	38.3	0.16	0.06	0.06	435
42.5	110	0.09	18.0	24	5.0	38.7	0.18	0.05	0.05	389
47.5	109	0.09	20.0	24	4.8	41.9	0.13	0.05	0.05	393

Core MP2

Depth (cm)	Mo (2) (ppm)	Mo (5) (ppm)	Na (1) (%)	Na (2) (%)	Nb (2) (ppm)	Ni (2) (ppm)	Ni (3) (ppm)	P (2) (ppb)	Pb (2) (ppm)	Pb (3) (ppm)
1	6	2	1.60	1.71	10	32	17	1569	298	242
3	7	2	1.80	1.77	12	32	17	1584	313	255
5	5	2	1.80	1.51	12	32	17	1666	311	254
7	7	3	1.50	1.35	10	36	19	1804	324	258
9	10	3	0.79	0.75	6	21	11	1667	305	223
11	6	3	0.66	0.64	5	16	9	1381	214	155
13	6	3	0.45	0.45	4	9	7	1242	125	85
15	5	3	0.34	0.35	3	8	5	1200	77	51
17	5	3	0.28	0.27	2	7	5	1192	57	35
19	6	3	0.24	0.23	2	7	4	1224	49	32
21	5	3	0.24	0.23	2	7	4	1245	41	28
23	5	3	0.26	0.22	3	7	4	1216	33	22
25	5	2	0.23	0.20	3	7	4	1066	25	16
27	4	2	0.31	0.23	2	8	4	988	33	19
29	4	2	0.21	0.19	2	7	4	956	20	12
31	3	2	0.23	0.21	2	6	4	953	17	12
33	4	2	0.21	0.18	2	7	4	975	18	9
35	5	2	0.23	0.20	2	7	4	939	15	9
37	4	2	0.22	0.20	2	8	4	912	15	8
39	5	2	0.20	0.19	2	7	4	906	16	8
42.5	4	2	0.17	0.16	2	7	4	838	7	5
47.5	4	2	0.20	0.19	2	7	4	818	10	5

Depth (cm)	Rb (1) (ppm)	Rb (2) (ppm)	Sb (1) (ppm)	Sc (1) (ppm)	Sc (2) (ppm)	Sm (1) (ppm)	Sr (2) (ppm)	Ta (1) (ppm)	Tb (1) (ppm)	Th (1) (ppm)
1	73.0	70	1.90	10.9	12.2	10.3	71	0.94	1.30	7.6
3	78.0	69	2.30	12.6	12.7	11.4	74	1.20	1.40	8.6
5	79.0	71	2.40	14.0	12.7	10.7	75	0.94	1.30	8.4
7	69.0	61	2.80	11.9	12.0	9.4	70	0.88	1.30	7.1
9	33.0	25	1.80	7.4	7.6	11.4	41	0.43	1.20	4.1
11	23.0	22	1.10	7.1	7.2	13.0	34	0.54	1.60	4.1
13	17.0	15	0.52	5.6	6.3	12.7	24	0.32	1.50	3.2
15	11.0	11	0.29	4.8	5.5	12.3	20	0.39	1.50	2.8
17	12.0	8	0.20	4.4	4.9	11.8	18	0.29	1.50	2.5
19	14.0	7	0.18	4.4	4.7	12.0	17	0.32	1.50	2.7
21	11.0	9	0.19	3.7	4.4	11.0	18	0.37	1.40	2.7
23	14.0	10	0.17	3.9	4.1	12.0	18	0.33	1.40	2.8
25	7.5	10	0.12	3.4	3.4	9.3	20	0.27	1.10	2.4
27	15.0	6	0.23	3.5	3.3	9.0	22	0.38	1.20	2.2
29	9.2	5	0.11	2.9	3.0	7.8	21	0.10	1.00	1.8
31	6.0	5	0.07	2.9	3.0	7.8	20	0.22	0.93	2.0
33	7.0	5	0.09	2.8	2.9	7.8	20	0.36	1.00	1.9
35	2.0	5	0.10	2.7	2.9	7.7	20	0.10	1.00	1.9
37	2.0	5	0.08	2.8	2.8	7.4	20	0.21	0.91	1.9
39	7.5	5	0.10	2.7	2.8	7.4	20	0.23	0.92	1.9
42.5	4.4	6	0.06	2.3	2.7	6.6	19	0.20	0.84	1.6
47.5	4.4	5	0.08	2.5	2.6	6.8	21	0.29	0.72	1.6

Core MP2

Depth (cm)	Ti (2) (ppm)	U (1) (ppm)	V (2) (ppm)	W (1) (ppm)	Y (2) (ppm)	Yb (1) (ppm)	Zn (1) (ppm)	Zn (2) (ppm)	Zn (3) (ppm)	Zr (2) (ppm)
1	3884	1.9	95	<2	40	4.30	1200.0	1054	958	102
3	3913	2.2	95	2.30	45	4.40	1400.0	1028	934	103
5	3831	2.0	90	<2	40	5.30	1200.0	922	845	105
7	3532	1.8	80	<2	38	4.70	1100.0	966	878	107
9	1988	1.3	42	<2	41	4.00	570.0	509	417	61
11	1803	1.3	38	<2	43	4.30	410.0	363	310	55
13	1225	1.2	24	<2	43	3.20	270.0	240	193	43
15	1225	1.1	24	<2	42	3.20	150.0	164	144	39
17	1086	1.1	20	<2	40	2.80	100.0	118	98	31
19	1041	1.0	19	<2	40	2.60	94.0	125	101	30
21	1023	1.1	18	<2	36	2.10	100.0	128	107	30
23	1033	1.1	17	<2	32	1.70	120.0	135	114	29
25	916	1.0	15	<2	27	1.80	72.0	102	83	26
27	879	0.8	15	<2	24	1.70	120.0	149	124	25
29	773	0.9	13	<2	23	1.30	<50	108	85	23
31	760	0.8	13	<2	22	0.91	<50	71	57	22
33	733	0.7	12	<2	22	1.50	<50	58	42	20
35	718	0.9	12	<2	21	1.60	<50	21	17	20
37	712	0.7	12	<2	21	1.10	<50	23	20	19
39	714	0.7	12	<2	21	1.40	<50	29	26	20
42.5	681	0.7	11	<2	20	1.30	<50	24	21	18
47.5	668	0.6	10	<2	19	0.20	<50	24	22	18

Core GP1

core GP1 Sample #	Depth (cm)	Ag (6) (ppm)	Al (2) (%)	As (1) (ppm)	Au (1) (ppb)	Ba (1) (ppm)	Ba (2) (ppm)	Be (2) (ppm)	Br (1) (ppm)	Ca (2) (%)
GP1-002	1	0.3	4.86	12.0	5.4	210	248	3.0	73.0	0.31
GP1-004	3	0.3	4.87	11.0	<2	190	252	2.8	66.6	0.31
GP1-006	5	0.3	4.82	11.0	4.6	200	245	2.8	67.1	0.30
GP1-008	7	0.3	5.06	11.0	<2	220	277	3.0	57.2	0.31
GP1-010	9	0.4	5.13	13.0	7.0	240	276	3.1	59.8	0.29
GP1-012	11	0.3	5.16	14.0	7.0	230	272	3.1	54.7	0.27
GP1-014	13	0.3	5.42	14.0	6.0	250	304	2.7	43.5	0.27
GP1-016	15	0.3	5.63	11.0	8.7	240	332	2.5	41.5	0.28
GP1-018	17	0.3	5.83	10.0	7.5	260	349	2.5	37.4	0.28
GP1-020	19	0.4	5.33	7.8	7.7	200	275	2.6	52.6	0.24
GP1-022	21	0.4	5.67	8.5	7.1	230	310	2.6	42.6	0.25
GP1-024	23	0.3	5.09	6.9	4.3	170	232	2.9	44.8	0.20
GP1-026	25	0.3	4.17	4.9	4.2	130	154	2.6	97.9	0.23
GP1-028	27	0.3	4.27	4.8	<2	150	146	2.7	89.4	0.21
GP1-030	29	0.5	4.89	5.7	11.0	120	197	2.3	61.1	0.20
GP1-035	32.5	0.3	4.65	5.0	13.0	140	198	2.1	75.2	0.22
GP1-040	37.5	0.3	4.00	3.3	4.1	130	152	1.9	101.0	0.21
GP1-045	42.5	0.3	3.61	2.6	<2	100	146	1.7	126.0	0.22
GP1-050	47.5	0.3	3.72	2.9	<2	110	160	1.7	128.0	0.23
GP1-055	52.5	0.3	3.78	2.4	<2	90	189	1.3	122.0	0.23
GP1-060	57.5	0.3	3.28	2.6	<2	120	165	1.2	146.0	0.27
GP1-065	62.5	0.3	3.21	2.0	<2	150	167	1.2	145.0	0.29
GP1-070	67.5	0.2	3.25	2.0	<2	100	167	1.2	132.0	0.27
GP1-075	72.5	0.3	3.20	1.9	<2	130	174	1.2	134.0	0.29
GP1-080	77.2	0.3	3.31	2.1	<2	130	185	1.5	158.0	0.31
GP1-085	82.5	0.2	3.11	2.1	<2	160	181	1.5	145.0	0.29
GP1-090	87.5	0.3	3.23	1.9	<2	130	189	1.6	153.0	0.30
GP1-095	92.5	0.3	3.30	1.9	<2	130	189	1.7	147.0	0.30
GP1-100	97.5	0.3	3.26	2.2	<2	120	194	1.8	158.0	0.32
GP1-105	102.5	0.3	3.14	1.6	<2	150	191	2.1	167.0	0.32
GP1-110	107.5	0.3	3.05	1.5	<2	53	162	2.2	129.0	0.29
GP1-115	112.5	0.2	2.96	1.4	<2	79	140	2.1	124.0	0.27
GP1-120	117.5	0.3	3.00	1.5	<2	85	135	2.3	122.0	0.27
GP1-125	122.5	0.3	3.23	1.5	<2	120	145	2.4	108.0	0.28
GP1-130	127.5	0.3	3.49	2.4	<2	140	152	2.6	131.0	0.29

Core GP1

Depth (cm)	Cd (2) (ppm)	Cd (3) (ppm)	Ce (1) (ppm)	Ce (2) (ppm)	Co (1) (ppm)	Co (2) (ppm)	Co (3) (ppm)	Cr (1) (ppm)	Cr (2) (ppm)	Cr (2a) (ppm)
1	0.4	0.3	97	89	21.0	21	12	39.0	28	27
3	0.4	0.3	82	85	25.0	21	11	31.0	28	26
5	0.5	0.3	81	87	21.0	20	12	28.0	27	26
7	0.4	0.4	78	85	18.0	20	12	33.0	-1	29
9	0.5	0.4	72	89	20.0	22	13	21.0	31	29
11	0.4	0.3	78	90	31.0	32	19	27.0	31	27
13	0.3	0.3	70	85	27.0	31	18	35.0	32	30
15	0.4	0.3	64	85	28.0	29	17	31.0	33	27
17	0.2	0.1	65	84	21.0	25	14	34.0	31	26
19	0.2	0.2	84	91	13.0	17	10	33.0	30	27
21	0.3	0.2	76	91	20.0	24	14	36.0	31	28
23	0.2	0.2	75	98	23.0	25	16	24.0	25	21
25	0.3	0.2	76	90	12.0	15	8	30.0	22	20
27	0.4	0.2	88	98	13.0	18	10	<15	22	21
29	0.2	0.1	75	84	18.0	21	12	30.0	27	24
32.5	0.2	0.1	65	72	22.0	25	14	36.0	26	24
37.5	0.1	0.1	65	69	13.0	16	8	25.0	22	21
42.5	0.2	0.1	61	66	7.9	13	7	35.0	18	18
47.5	0.2	0.1	49	60	8.9	12	6	20.0	21	20
52.5	0.2	0.1	48	49	5.5	9	5	35.0	21	20
57.5	0.1	0.1	45	52	1.0	5	3	<15	18	16
62.5	0.1	0.1	46	53	1.0	5	2	19.0	17	16
67.5	0.2	0.1	42	54	1.0	3	2	26.0	17	16
72.5	0.2	0.2	44	54	1.0	5	2	<15	17	16
77.2	0.2	0.2	42	55	1.0	3	1	<15	18	17
82.5	0.2	0.1	50	54	1.0	3	2	19.0	19	17
87.5	0.2	0.1	51	56	1.0	3	2	<15	17	16
92.5	0.2	0.2	48	61	1.0	5	2	<15	17	15
97.5	0.3	0.2	56	62	1.0	5	3	22.0	19	18
102.5	0.3	0.2	44	58	1.0	3	2	<15	17	16
107.5	0.2	0.1	47	57	1.0	3	2	20.0	17	16
112.5	0.3	0.2	52	63	1.0	4	3	<15	17	14
117.5	0.3	0.2	57	66	4.7	4	2	<15	18	15
122.5	0.2	0.2	57	69	1.0	4	2	<15	19	17
127.5	0.2	0.2	63	71	1.0	5	3	<15	19	16

Core GP1

Depth (cm)	Cs (1) (ppm)	Cu (2) (ppm)	Cu (3) (ppm)	Dy (2) (ppm)	Eu (1) (ppm)	Fe (1) (%)	Fe (2) (%)	Fe (3) (%)	Ga (2) (ppm)	Hf (1) (ppm)
1	3.3	43	33	7.8	4.80	3.80	3.16	2.26	14	3.30
3	3.4	43	31	7.4	3.80	3.20	3.10	2.08	14	3.10
5	3.5	41	31	7.5	3.20	3.00	3.00	2.04	13	2.50
7	3.6	46	37	7.5	4.10	3.40	3.40	2.39	15	3.00
9	4.3	47	38	8.1	4.10	3.20	3.23	2.32	15	2.80
11	3.8	45	34	8.1	3.20	3.00	3.12	2.17	13	3.20
13	4.8	41	31	7.5	2.60	3.00	3.28	2.32	10	3.00
15	4.9	39	30	6.9	2.70	2.90	3.36	2.29	18	3.10
17	5.2	36	28	6.9	2.50	3.10	3.41	2.33	16	3.90
19	4.3	35	29	8.0	3.40	2.60	2.73	1.95	13	3.20
21	4.6	35	27	7.9	3.10	2.60	3.13	2.16	16	3.30
23	3.3	33	29	9.6	3.50	1.80	2.22	1.64	11	2.30
25	2.1	29	22	7.9	3.70	1.90	2.11	1.43	9	1.50
27	2.1	28	21	9.0	4.50	1.90	1.95	1.30	9	2.20
29	3.1	27	20	8.1	2.50	2.50	2.55	1.68	13	2.00
32.5	2.9	24	18	6.7	2.90	3.50	3.63	2.47	12	2.40
37.5	2.2	23	18	6.2	2.60	2.80	2.90	1.92	9	1.20
42.5	1.8	25	18	5.8	2.10	2.20	2.11	1.44	9	1.80
47.5	2.2	23	18	5.5	3.40	2.30	2.27	1.49	8	1.60
52.5	3.2	19	13	4.6	2.10	1.90	1.85	1.09	11	1.40
57.5	1.8	21	14	4.6	1.70	1.40	1.30	0.83	6	1.80
62.5	2.2	19	15	4.8	1.90	1.30	1.21	0.79	8	1.50
67.5	1.9	19	14	4.8	2.10	1.20	1.21	0.80	7	1.70
72.5	1.4	19	15	4.7	1.90	1.20	1.19	0.82	7	0.20
77.2	2.2	20	16	5.0	2.10	1.30	1.20	0.83	7	1.30
82.5	2.0	19	15	4.9	1.10	1.20	1.15	0.76	7	1.80
87.5	2.3	21	15	5.1	2.30	1.30	1.16	0.75	6	1.00
92.5	1.7	21	16	5.6	2.80	1.20	1.15	0.76	6	1.10
97.5	2.0	22	17	5.9	3.10	1.10	1.15	0.79	7	0.20
102.5	2.3	23	17	5.8	2.00	1.20	1.07	0.71	6	1.50
107.5	1.8	24	18	5.8	2.20	1.00	0.94	0.64	6	1.50
112.5	1.1	29	22	5.6	2.50	0.88	0.88	0.62	4	0.75
117.5	1.7	27	19	5.9	3.10	1.10	0.99	0.65	5	1.00
122.5	1.4	29	24	6.5	3.30	1.10	0.92	0.63	5	1.20
127.5	2.4	30	22	6.9	3.70	1.40	1.09	0.75	5	1.30

Core GP1

Depth (cm)	Hg(18) (ppb)	K (2) (%)	La (1) (ppm)	La (2) (ppm)	Li (2) (ppm)	LOI (%)	Lu (1) (ppm)	Mg (2) (%)	Mn (2) (%)	Mn (3) (ppm)
1	195	0.68	42.0	39	16.7	30.1	0.40	0.27	0.06	340
3	228	0.71	37.0	37	17.2	29.7	0.50	0.28	0.06	306
5	204	0.67	36.0	38	16.9	29.0	0.35	0.27	0.06	321
7	314	0.80	36.0	37	19.7	26.6	0.48	0.32	0.06	341
9	216	0.79	35.0	39	19.8	26.4	0.27	0.31	0.06	356
11	293	0.78	37.0	40	19.3	26.1	0.49	0.30	0.06	363
13	246	0.93	34.0	37	22.2	23.7	0.32	0.34	0.07	381
15	261	1.05	33.0	36	23.9	22.4	0.46	0.37	0.07	393
17	261	1.10	32.0	36	24.8	21.6	0.40	0.38	0.07	392
19	251	0.80	36.0	39	19.6	26.3	0.40	0.29	0.06	367
21	253	0.95	34.0	39	22.8	24.9	0.36	0.34	0.07	376
23	223	0.62	36.0	41	16.3	26.9	0.34	0.23	0.06	330
25	141	0.33	35.0	39	8.6	37.0	0.39	0.14	0.06	334
27	155	0.31	35.0	41	9.4	35.8	0.24	0.14	0.05	283
29	295	0.52	31.0	36	15.3	29.3	0.24	0.21	0.05	283
32.5	299	0.53	27.0	30	15.3	33.6	0.33	0.21	0.06	321
37.5	244	0.33	28.0	29	9.2	36.6	0.33	0.14	0.05	272
42.5	162	0.25	28.0	28	6.5	42.2	0.27	0.11	0.05	269
47.5	151	0.29	26.0	27	7.4	42.5	0.31	0.13	0.05	259
52.5	135	0.41	22.0	22	9.4	40.4	0.40	0.15	0.05	241
57.5	169	0.27	21.0	23	7.1	47.6	0.11	0.13	0.05	280
62.5	162	0.26	21.0	23	7.5	47.5	0.24	0.13	0.04	248
67.5	149	0.26	21.0	23	7.5	45.6	0.02	0.13	0.04	217
72.5	158	0.26	20.0	23	7.7	47.1	0.16	0.13	0.04	210
77.2	144	0.26	22.0	25	7.9	48.1	0.02	0.14	0.04	194
82.5	133	0.26	21.0	25	8.2	46.6	0.13	0.13	0.02	170
87.5	147	0.26	24.0	25	8.6	48.5	0.21	0.14	0.02	160
92.5	131	0.26	25.0	26	9.1	46.8	0.26	0.13	0.02	149
97.5	127	0.27	27.0	28	10.0	49.0	0.22	0.14	0.02	148
102.5	126	0.26	26.0	28	10.2	48.5	0.25	0.13	0.02	147
107.5	109	0.22	24.0	27	8.9	43.8	0.22	0.12	0.02	120
112.5	91	0.19	26.0	30	7.1	43.7	0.22	0.11	0.02	117
117.5	N/A	0.18	29.0	31	6.4	42.3	0.19	0.11	0.02	116
122.5	106	0.20	26.0	32	7.9	42.4	0.02	0.11	0.02	125
127.5	106	0.22	34.0	33	8.3	42.1	0.29	0.11	0.02	136

Core GP1

Depth (cm)	Mo (2) (ppm)	Mo (5) (ppm)	Na (1) (%)	Na (2) (%)	Nb (2) (ppm)	Ni (2) (ppm)	Ni (3) (ppm)	P (2) (ppb)	Pb (2) (ppm)	Pb (3) (ppm)
1	2	2	0.80	0.64	7	28	12	1202	142	107
3	3	2	0.70	0.67	6	26	12	1164	141	98
5	2	2	0.67	0.63	6	24	11	1170	130	97
7	3	2	0.80	0.76	7	26	13	1154	157	142
9	2	2	0.72	0.74	7	26	14	1152	153	141
11	2	2	0.70	0.72	6	29	14	1136	154	135
13	2	2	0.79	0.85	8	23	13	1068	183	160
15	2	2	0.92	0.94	9	21	11	1027	321	197
17	2	2	1.00	0.99	9	19	10	976	197	177
19	2	2	0.72	0.72	8	17	8	1147	137	112
21	2	2	0.81	0.83	9	18	9	1112	160	146
23	2	2	0.50	0.54	6	18	11	1169	115	97
25	2	<2	0.29	0.29	3	16	7	1182	44	34
27	2	2	0.24	0.25	5	16	8	1244	49	37
29	2	2	0.42	0.43	6	16	8	1316	169	150
32.5	2	2	0.46	0.44	6	16	8	1304	194	165
37.5	<2	2	0.30	0.27	3	13	7	1378	50	37
42.5	2	2	0.23	0.20	5	13	7	1480	18	15
47.5	2	2	0.23	0.21	5	13	7	1561	10	8
52.5	2	2	0.30	0.27	6	11	6	1670	7	7
57.5	2	2	0.20	0.18	4	10	5	1685	8	5
62.5	2	<2	0.19	0.16	4	11	6	1614	2	4
67.5	2	2	0.19	0.16	4	12	5	1578	<2	4
72.5	<2	2	0.17	0.16	4	12	6	1558	2	5
77.2	2	2	0.16	0.15	4	12	6	1717	<2	5
82.5	2	2	0.15	0.13	4	12	6	1583	<2	4
87.5	2	2	0.16	0.13	4	12	6	1666	3	5
92.5	2	2	0.16	0.13	4	13	6	1647	2	5
97.5	2	2	0.15	0.13	4	14	7	1669	2	4
102.5	2	2	0.14	0.12	4	13	7	1814	<2	4
107.5	2	2	0.12	0.11	4	12	6	1846	3	4
112.5	2	2	0.12	0.11	2	15	9	1742	2	4
117.5	<2	2	0.13	0.10	2	15	7	1674	<2	3
122.5	<2	2	0.11	0.11	5	18	7	1771	<2	4
127.5	2	2	0.17	0.15	2	15	6	1904	2	4

Core GP1

Depth (cm)	Rb (1) (ppm)	Rb (2) (ppm)	Sb (1) (ppm)	Sc (1) (ppm)	Sc (2) (ppm)	Sm (1) (ppm)	Sr (2) (ppm)	Ta (1) (ppm)	Tb (1) (ppm)	Th (1) (ppm)
1	29.0	34	1.00	10.6	9.2	10.0	47	0.46	1.60	5.2
3	34.0	31	1.00	9.3	8.9	10.0	48	0.30	1.40	5.4
5	26.0	29	0.92	9.2	8.9	10.0	45	0.47	1.50	5.2
7	32.0	36	1.20	9.5	9.4	9.4	53	0.48	1.50	5.4
9	39.0	34	1.40	8.5	9.9	10.8	52	0.58	1.60	5.7
11	32.0	34	1.10	9.0	10.0	10.6	50	0.43	1.60	5.5
13	42.0	38	1.00	10.0	10.4	9.4	54	0.51	1.30	5.8
15	43.0	48	1.10	10.1	10.7	8.8	60	0.70	1.30	5.7
17	51.0	52	1.00	10.2	11.0	8.4	63	0.67	1.20	5.8
19	39.0	37	0.78	10.0	10.0	10.2	47	0.52	1.60	5.5
21	49.0	45	1.00	10.0	10.9	9.5	54	0.49	1.40	5.7
23	29.0	25	0.50	8.7	10.4	11.1	38	0.55	1.80	5.3
25	15.0	15	0.32	6.6	7.3	10.1	28	0.39	1.30	4.3
27	10.0	16	0.27	6.8	7.9	11.4	26	0.24	1.70	4.5
29	23.0	24	0.42	7.9	8.9	10.1	34	0.45	1.50	5.2
32.5	20.0	27	0.40	7.5	8.1	7.9	37	0.44	1.20	4.4
37.5	12.0	17	0.21	6.8	6.6	7.8	29	0.37	1.10	4.1
42.5	10.0	13	0.15	6.2	6.0	7.1	29	0.32	1.00	3.8
47.5	10.0	15	0.18	6.5	6.5	6.5	30	0.29	0.92	3.8
52.5	19.0	19	0.16	6.3	6.1	5.4	36	0.42	0.75	3.5
57.5	12.0	13	0.12	5.1	5.2	5.0	37	0.29	0.70	3.0
62.5	12.0	13	0.12	5.2	5.1	5.2	39	0.10	0.84	3.1
67.5	8.4	11	0.09	5.0	5.3	5.1	40	0.32	0.79	2.9
72.5	10.0	9	0.10	4.3	5.2	5.0	42	0.21	0.74	2.9
77.2	13.0	11	0.10	5.1	5.3	5.9	43	0.44	0.85	3.2
82.5	12.0	14	0.14	5.2	5.3	5.6	42	0.34	1.00	3.2
87.5	16.0	14	0.13	5.6	5.4	5.9	42	0.40	0.87	3.1
92.5	8.1	12	0.10	5.8	5.6	6.5	42	0.35	0.93	3.1
97.5	15.0	16	0.11	5.7	5.7	6.6	43	0.22	1.00	3.0
102.5	14.0	11	0.10	6.1	5.6	6.5	42	0.10	1.00	2.6
107.5	13.0	13	0.10	4.9	5.3	6.4	36	0.10	0.94	2.2
112.5	8.6	11	0.14	4.8	5.2	6.8	34	0.10	1.00	2.4
117.5	7.8	8	0.12	5.5	5.2	7.3	33	0.10	0.91	2.9
122.5	2.0	13	0.10	4.9	5.8	7.2	34	0.10	1.10	2.8
127.5	10.0	10	0.14	5.7	6.1	9.3	36	0.10	1.40	3.5

Core GP1

Depth (cm)	Ti (2) (ppm)	U (1) (ppm)	V (2) (ppm)	W (1) (ppm)	Y (2) (ppm)	Yb (1) (ppm)	Zn (1) (ppm)	Zn (2) (ppm)	Zn (3) (ppm)	Zr (2) (ppm)
1	2416	1.7	94	<2	44	2.40	160.0	210	171	60
3	2417	1.6	93	<2	41	2.40	250.0	239	184	59
5	2382	1.5	84	<2	43	2.20	140.0	204	158	58
7	2651	1.7	108	<2	41	2.30	170.0	207	171	66
9	2675	2.0	96	<2	45	1.90	170.0	217	179	67
11	2675	1.9	83	<2	46	2.30	190.0	197	161	67
13	2647	1.9	78	<2	41	2.10	160.0	180	145	75
15	3515	1.8	78	<2	39	1.90	130.0	188	149	84
17	3744	1.9	77	<2	39	1.70	84.0	147	118	87
19	2852	1.8	63	<2	43	2.10	110.0	133	110	67
21	3265	1.8	71	<2	43	1.90	110.0	138	114	75
23	2395	1.9	52	<2	50	2.20	96.0	104	92	61
25	1559	1.5	44	<2	43	1.20	55.0	130	104	38
27	1551	1.7	39	<2	48	1.20	160.0	167	130	39
29	2097	1.8	47	<2	43	1.50	55.0	132	104	52
32.5	2046	1.6	46	<2	35	1.70	52.0	108	84	50
37.5	1562	1.3	36	<2	33	1.70	97.0	124	97	37
42.5	1413	1.3	32	<2	31	1.10	77.0	103	81	32
47.5	1633	1.4	36	<2	29	1.20	74.0	104	80	35
52.5	1979	1.3	40	<2	25	1.20	95.0	109	81	40
57.5	1552	1.2	32	<2	36	0.20	57.0	104	79	32
62.5	1543	1.2	32	<2	24	1.30	62.0	112	86	31
67.5	1562	1.1	32	<2	25	0.68	<50	116	85	31
72.5	1560	1.1	31	<2	25	1.30	<50	98	74	31
77.2	1617	1.3	33	<2	27	0.20	<50	120	91	32
82.5	1623	1.3	32	<2	26	1.00	<50	112	83	31
87.5	1656	1.2	32	<2	27	1.30	<50	97	71	31
92.5	1612	1.3	31	<2	29	1.20	<50	100	76	34
97.5	1635	1.3	33	<2	32	1.30	64.0	97	73	33
102.5	1583	1.2	31	<2	32	1.10	<50	88	67	31
107.5	1261	1.2	27	<2	31	0.84	<50	88	65	27
112.5	1002	1.2	25	<2	32	1.20	<50	92	69	24
117.5	99	1.2	24	<2	32	0.20	<50	84	61	24
122.5	1089	1.2	25	<2	35	0.94	<50	100	78	27
127.5	1182	1.5	26	<2	36	1.00	86.0	115	88	29

core GP2 Sample #	Depth (cm)	Ag (6) (ppm)	Al (2) (%)	As (1) (ppm)	Au (1) (ppb)	Ba (1) (ppm)	Ba (2) (ppm)	Be (2) (ppm)	Br (1) (ppm)	Ca (2) (%)
GP2-002	1	<0.2	4.77	12.0	<2	220	247	3.0	80.9	0.31
GP2-004	3	<0.2	4.97	12.0	4.5	240	266	3.1	69.9	0.32
GP2-006	5	<0.2	5.03	12.0	6.0	230	256	3.1	63.0	0.29
GP2-008	7	<0.2	5.13	13.0	4.6	230	262	3.1	59.6	0.29
GP2-010	9	<0.2	5.61	12.0	7.8	300	317	2.7	47.6	0.29
GP2-012	11	<0.2	5.70	11.0	8.3	310	317	2.6	53.4	0.28
GP2-014	13	<0.2	4.99	7.6	5.0	210	233	2.7	74.3	0.25
GP2-016	15	<0.2	4.81	5.6	8.9	160	182	2.6	72.0	0.21
GP2-018	17	<0.2	4.84	5.1	16.0	210	214	2.3	78.8	0.23
GP2-020	19	<0.2	4.61	5.7	7.9	190	198	2.2	90.0	0.23
GP2-022	21	<0.2	3.77	3.1	<2	130	149	1.8	135.0	0.22
GP2-024	23	<0.2	3.77	3.6	<2	160	160	1.8	151.0	0.24
GP2-026	25	<0.2	3.81	2.7	<2	150	167	1.8	146.0	0.24
GP2-028	27	<0.2	3.96	2.7	<2	160	177	1.7	140.0	0.23
GP2-030	29	<0.2	3.83	2.4	<2	160	183	1.4	143.0	0.24
GP2-035	32.5	<0.2	3.25	2.4	<2	140	166	1.2	190.0	0.28
GP2-040	37.5	<0.2	3.24	2.0	<2	170	172	1.3	168.0	0.28
GP2-045	42.5	<0.2	3.19	2.1	<2	110	163	1.3	154.0	0.28
GP2-050	47.5	<0.2	3.24	2.4	<2	140	178	1.3	162.0	0.30
GP2-055	52.5	<0.2	3.28	1.7	<2	160	186	1.4	162.0	0.31
GP2-060	57.5	<0.2	3.28	2.0	<2	180	189	1.5	171.0	0.31
GP2-065	62.5	<0.2	3.33	2.2	<2	170	192	1.6	172.0	0.32
GP2-070	67.5	<0.2	3.26	1.6	<2	170	186	1.7	170.0	0.32
GP2-075	72.5	<0.2	3.25	1.9	<2	180	185	1.8	169.0	0.32
GP2-080	77.5	<0.2	3.28	2.1	<2	190	209	2.0	191.0	0.34
GP2-085	82.5	<0.2	3.27	2.1	<2	170	195	2.2	198.0	0.33
GP2-090	87.5	<0.2	3.83	4.8	<2	170	214	2.1	145.0	0.30

Depth (cm)	Cd (2) (ppm)	Cd (3) (ppm)	Ce (1) (ppm)	Ce (2) (ppm)	Co (1) (ppm)	Co (2) (ppm)	Co (3) (ppm)	Cr (1) (ppm)	Cr (2) (ppm)	Cr (2a) (ppm)
1	0.5	0.4	82	85	19.0	22	12	16.0	55	51
3	0.5	0.4	73	84	17.0	22	12	24.0	41	35
5	0.5	0.3	80	92	21.0	24	14	<15	45	40
7	0.4	0.4	80	95	31.0	32	19	22.0	44	40
9	0.4	0.3	70	86	21.0	27	18	23.0	45	40
11	0.3	0.2	76	84	20.0	23	13	30.0	32	41
13	0.3	0.2	87	93	18.0	22	11	21.0	27	38
15	0.2	0.2	86	91	17.0	20	10	34.0	26	50
17	<0.2	<0.2	73	76	15.0	20	9	27.0	45	44
19	<0.2	<0.2	73	75	17.0	22	11	40.0	39	37
21	<0.2	<0.2	59	65	9.3	12	5	43.0	38	35
23	0.2	<0.2	62	65	11.0	10	5	47.0	41	41
25	0.2	0.2	54	62	6.7	9	5	24.0	43	39
27	0.2	<0.2	49	56	8.1	10	4	17.0	48	44
29	<0.2	<0.2	45	47	8.7	8	4	<15	41	38
32.5	0.3	<0.2	42	51	1.0	5	2	27.0	40	35
37.5	0.3	0.2	49	50	1.0	5	2	21.0	17	39
42.5	0.2	0.2	48	50	5.7	7	4	<15	43	39
47.5	0.2	0.2	47	52	2.5	5	2	22.0	16	41
52.5	0.2	<0.2	42	51	1.0	5	2	<15	17	53
57.5	0.2	0.2	54	53	1.0	5	2	<15	17	35
62.5	0.2	0.2	51	55	1.0	3	2	19.0	17	12
67.5	0.2	0.2	50	58	1.0	4	2	23.0	18	12
72.5	0.3	0.2	51	59	1.0	4	2	<15	16	13
77.5	0.3	0.2	46	58	1.0	3	2	<15	16	14
82.5	0.2	0.2	53	58	3.8	4	2	<15	16	14
87.5	0.3	0.3	62	63	8.3	9	5	<15	22	17

Depth (cm)	Cs (1) (ppm)	Cu (2) (ppm)	Cu (3) (ppm)	Dy (2) (ppm)	Eu (1) (ppm)	Fe (1) (%)	Fe (2) (%)	Fe (3) (%)	Ga (2) (ppm)	Hf (1) (ppm)
1	3.0	50	30	7.5	2.80	3.60	3.36	2.22	13	3.20
3	2.7	53	33	7.3	2.70	3.40	3.53	2.42	13	3.00
5	2.7	49	30	8.2	3.60	2.90	3.01	2.02	13	3.00
7	2.9	48	30	8.1	3.00	2.70	2.92	1.88	14	2.40
9	3.6	45	30	7.3	3.10	2.90	3.17	2.33	15	3.00
11	4.0	38	24	7.3	3.10	3.50	2.95	2.13	15	3.50
13	3.1	35	22	8.2	2.50	2.30	2.31	1.51	12	2.30
15	2.1	30	21	8.7	3.90	2.00	2.24	1.56	9	2.10
17	2.6	27	17	7.0	2.60	3.20	3.30	2.12	13	1.90
19	2.3	30	20	6.7	3.00	3.40	3.40	2.33	12	2.30
21	1.6	26	17	5.9	2.30	2.20	2.15	1.40	9	1.60
23	1.8	32	17	5.8	2.50	2.00	1.87	1.21	7	2.00
25	1.7	26	18	5.7	3.30	1.90	1.98	1.29	8	1.70
27	2.7	24	14	5.1	2.30	2.20	2.11	1.42	9	2.10
29	2.7	21	14	4.8	2.30	2.00	1.75	1.06	9	0.20
32.5	2.0	21	12	4.2	2.10	1.50	1.24	0.74	8	2.60
37.5	1.8	22	13	4.4	1.90	1.20	1.16	0.68	8	0.20
42.5	1.8	18	12	4.6	1.30	1.10	1.15	0.70	7	1.40
47.5	1.5	22	13	4.9	1.60	1.10	1.13	0.70	8	1.70
52.5	1.6	21	13	4.8	2.20	1.20	1.14	0.72	8	1.40
57.5	1.7	22	14	5.1	1.90	1.20	1.16	0.70	8	1.90
62.5	1.7	22	15	5.5	2.60	1.10	1.09	0.70	6	1.10
67.5	1.8	22	15	5.7	2.60	1.10	1.04	0.72	4	1.70
72.5	1.2	23	16	6.0	2.60	1.20	1.08	0.70	6	0.82
77.5	1.8	25	17	6.1	2.00	1.20	1.06	0.67	7	1.60
82.5	1.8	26	18	6.2	1.20	1.30	1.06	0.67	6	1.70
87.5	2.4	33	22	6.0	2.90	2.10	1.93	1.21	9	1.70

Depth (cm)	Hg(18) (ppb)	K (2) (%)	La (1) (ppm)	La (2) (ppm)	Li (2) (ppm)	LOI (%)	Lu (1) (ppm)	Mg (2) (%)	Mn (2) (%)	Mn (3) (ppm)
1	203	0.68	35.0	38	15.7	30.5	0.65	0.29	0.06	306
3	199	0.76	32.0	37	17.3	28.7	0.62	0.32	0.06	330
5	206	0.74	36.0	40	18.9	28.1	0.67	0.31	0.06	299
7	219	0.75	34.0	40	19.1	27.5	0.61	0.28	0.06	287
9	240	0.99	31.0	38	23.7	24.0	0.60	0.35	0.06	333
11	241	0.97	33.0	38	23.3	24.6	0.60	0.34	0.06	311
13	212	0.63	35.0	39	16.0	30.9	0.61	0.23	0.05	269
15	232	0.46	34.0	39	13.8	31.1	0.61	0.19	0.05	271
17	286	0.57	28.0	33	16.5	33.3	0.54	0.22	0.06	286
19	240	0.51	29.0	32	14.3	33.4	0.55	0.20	0.05	301
21	154	0.28	27.0	30	7.8	40.0	0.34	0.12	0.05	251
23	157	0.28	28.0	29	7.2	43.2	0.46	0.13	0.04	266
25	151	0.29	25.0	29	7.6	44.4	0.28	0.13	0.04	271
27	142	0.37	22.0	25	8.8	40.8	0.44	0.15	0.04	243
29	136	0.38	20.0	23	9.4	41.6	0.40	0.15	0.04	235
32.5	173	0.27	19.0	23	7.4	49.2	0.39	0.13	0.05	252
37.5	151	0.28	21.0	23	8.1	47.4	0.30	0.14	0.03	252
42.5	134	0.25	21.0	23	7.2	46.8	0.30	0.13	0.03	221
47.5	146	0.27	21.0	24	8.1	47.6	0.35	0.14	0.03	206
52.5	131	0.27	22.0	25	7.8	48.6	0.49	0.14	0.03	196
57.5	140	0.28	23.0	25	8.7	47.4	0.44	0.14	0.03	177
62.5	140	0.28	23.0	25	9.3	48.3	0.41	0.14	0.02	167
67.5	131	0.26	23.0	25	8.9	48.5	0.37	0.14	0.02	159
72.5	125	0.26	23.0	26	9.2	47.5	0.55	0.14	0.02	152
77.5	127	0.30	22.0	27	11.6	49.8	0.35	0.15	0.02	155
82.5	124	0.28	24.0	28	10.8	48.6	0.34	0.14	0.02	160
87.5	160	0.46	26.0	27	13.0	40.6	0.50	0.20	0.03	238

Depth (cm)	Mo (2) (ppm)	Mo (5) (ppm)	Na (1) (%)	Na (2) (%)	Nb (2) (ppm)	Ni (2) (ppm)	Ni (3) (ppm)	P (2) (ppb)	Pb (2) (ppm)	Pb (3) (ppm)
1	6	2	0.73	0.67	6	44	14	1167	149	103
3	4	2	0.78	0.76	6	32	14	1126	160	114
5	4	2	0.69	0.70	6	32	14	1139	142	98
7	4	2	0.68	0.70	6	32	16	1145	145	109
9	3	2	0.86	0.89	8	28	13	1051	200	180
11	3	2	0.92	0.87	8	23	11	1056	193	173
13	4	<2	0.60	0.57	6	23	9	1147	115	81
15	3	2	0.43	0.41	5	25	9	1295	123	91
17	6	<2	0.53	0.50	6	22	7	1301	216	172
19	5	<2	0.49	0.46	5	22	8	1304	110	79
21	7	<2	0.29	0.26	3	18	6	1461	31	24
23	6	<2	0.27	0.24	4	22	6	1509	24	18
25	7	2	0.23	0.22	4	24	7	1589	15	13
27	5	2	0.28	0.26	4	25	7	1678	8	10
29	5	2	0.27	0.27	4	19	6	1760	7	7
32.5	5	2	0.20	0.19	5	21	5	1685	7	5
37.5	6	2	0.21	0.19	5	36	5	1599	4	5
42.5	5	2	0.19	0.17	3	24	6	1495	3	4
47.5	5	2	0.19	0.17	5	25	6	1560	7	4
52.5	5	<2	0.18	0.16	3	30	6	1652	5	4
57.5	4	<2	0.18	0.16	5	23	6	1610	12	6
62.5	4	2	0.17	0.15	4	11	6	1632	3	4
67.5	4	2	0.15	0.14	1	11	6	1578	<2	4
72.5	3	2	0.15	0.13	4	12	7	1557	2	5
77.5	3	2	0.13	0.14	4	14	7	1738	5	4
82.5	2	2	0.15	0.14	5	12	7	1858	6	6
87.5	4	2	0.41	0.35	5	17	9	1553	61	41

Depth (cm)	Rb (1) (ppm)	Rb (2) (ppm)	Sb (1) (ppm)	Sc (1) (ppm)	Sc (2) (ppm)	Sm (1) (ppm)	Sr (2) (ppm)	Ta (1) (ppm)	Tb (1) (ppm)	Th (1) (ppm)
1	32.0	29	1.10	9.2	9.3	11.8	47	0.44	1.50	5.4
3	34.0	31	1.10	9.0	9.5	10.8	51	0.46	1.40	5.2
5	30.0	30	1.10	9.4	9.8	12.4	48	0.41	1.50	5.4
7	37.0	30	0.92	9.2	9.9	12.0	48	0.53	1.60	5.6
9	41.0	43	1.00	10.0	10.8	10.5	58	0.62	1.40	5.8
11	49.0	46	1.00	10.5	10.9	12.1	56	0.88	1.50	6.6
13	31.0	30	0.56	9.2	9.5	12.5	40	0.51	1.70	5.5
15	25.0	22	0.41	8.9	9.1	12.7	32	0.39	1.70	5.3
17	32.0	25	0.43	8.2	8.8	10.0	38	0.32	1.40	5.3
19	27.0	22	0.44	8.2	8.3	10.0	37	0.57	1.40	5.1
21	13.0	15	0.21	6.4	6.4	9.2	30	0.51	1.10	4.2
23	8.2	18	0.25	6.5	6.4	9.1	30	0.21	1.30	4.4
25	13.0	16	0.19	6.4	6.7	8.2	31	0.40	1.10	4.1
27	20.0	19	0.19	6.3	6.8	7.4	32	0.32	1.00	4.3
29	19.0	22	0.17	5.6	6.3	6.9	34	0.30	1.10	3.9
32.5	11.0	5	0.12	5.2	5.5	6.8	38	0.40	0.88	3.6
37.5	13.0	15	0.11	5.7	5.5	6.6	39	0.36	1.00	3.4
42.5	12.0	14	0.11	5.1	5.2	6.5	39	0.25	0.93	3.2
47.5	16.0	12	0.08	5.4	5.6	6.6	42	0.33	1.00	3.2
52.5	9.2	11	0.09	5.4	5.6	6.5	44	0.34	1.00	3.2
57.5	13.0	14	0.09	6.1	5.7	7.0	43	0.41	0.91	3.3
62.5	14.0	15	0.12	5.8	5.9	7.2	43	0.21	0.89	3.4
67.5	12.0	14	0.10	5.8	5.7	7.4	42	0.29	1.00	3.2
72.5	11.0	13	0.11	5.7	5.7	8.0	42	0.41	1.00	3.2
77.5	13.0	16	0.13	5.4	6.0	7.8	44	0.22	1.10	3.3
82.5	14.0	11	0.14	5.7	6.0	8.8	43	0.27	1.30	3.3
87.5	28.0	18	0.47	7.2	7.0	8.8	46	0.40	1.20	4.2

Depth (cm)	Ti (2) (ppm)	U (1) (ppm)	V (2) (ppm)	W (1) (ppm)	Y (2) (ppm)	Yb (1) (ppm)	Zn (1) (ppm)	Zn (2) (ppm)	Zn (3) (ppm)	Zr (2) (ppm)
1	2328	1.6	119	<2	41	4.10	220.0	196	137	60
3	2498	1.6	131	<2	41	3.90	230.0	190	133	66
5	2451	1.8	89	<2	46	4.50	180.0	185	131	64
7	2513	1.7	82	<2	46	3.60	170.0	187	141	65
9	3228	1.8	86	<2	41	3.80	210.0	182	136	79
11	3295	2.1	72	<2	41	4.40	140.0	142	108	82
13	2388	1.9	57	<2	45	3.80	92.0	129	88	60
15	2010	1.8	48	<2	47	4.30	81.0	98	66	51
17	2198	1.6	51	<2	38	3.30	51.0	104	68	56
19	2028	1.6	62	<2	37	3.60	120.0	113	86	50
21	1494	1.4	37	<2	31	1.90	81.0	105	82	36
23	1498	1.5	38	<2	32	2.10	64.0	118	91	36
25	1569	1.3	38	<2	32	3.10	86.0	138	101	37
27	1860	1.5	43	<2	28	2.50	94.0	129	90	42
29	1895	1.4	41	<2	26	0.20	<50	137	97	42
32.5	1555	1.4	33	<2	25	0.20	120.0	95	64	33
37.5	1600	1.2	33	<2	25	2.30	53.0	101	75	34
42.5	1463	1.4	31	<2	25	0.20	91.0	101	80	31
47.5	1555	1.2	33	<2	26	2.00	95.0	103	74	33
52.5	1560	1.2	33	<2	26	2.00	61.0	92	65	34
57.5	1648	1.3	36	<2	27	1.80	150.0	109	77	35
62.5	1656	1.2	32	<2	28	2.30	72.0	84	62	37
67.5	1562	1.4	30	<2	29	2.80	<50	95	74	33
72.5	1531	1.2	30	<2	31	2.30	53.0	94	73	35
77.5	1712	1.5	33	<2	32	2.20	99.0	90	66	38
82.5	1593	1.4	31	<2	33	0.20	52.0	77	55	39
87.5	1903	1.5	67	<2	32	2.90	130.0	116	88	48

core LPW Sample #	Depth (cm)	Ag (6) (ppm)	Al (2) (%)	As (1) (ppm)	Au (1) (ppb)	Ba (1) (ppm)	Ba (2) (ppm)	Be (2) (ppm)	Br (1) (ppm)	Ca (2) (%)
LPW-002	1.0	<0.2	3.80	12.0	<2	120	135	2.3	59.5	0.36
LPW-004	3.0	<0.2	3.78	13.0	<2	160	133	2.3	61.8	0.36
LPW-006	5.0	<0.2	3.79	12.0	<2	110	121	2.3	58.3	0.39
LPW-008	7.0	<0.2	3.80	12.0	<2	120	116	2.3	60.0	0.39
LPW-010	9.0	<0.2	3.78	12.0	<2	89	118	2.2	55.9	0.38
LPW-012	11.0	<0.2	3.76	12.0	<2	96	101	2.2	56.1	0.42
LPW-014	13.0	<0.2	3.89	12.0	<2	93	106	2.2	55.8	0.45
LPW-016	15.0	<0.2	3.96	12.0	<2	69	104	2.2	50.7	0.47
LPW-018	17.0	<0.2	3.97	14.0	<2	100	107	2.3	55.2	0.50
LPW-020	19.0	<0.2	4.04	12.0	<2	120	109	2.3	51.4	0.54
LPW-022	21.0	<0.2	3.98	12.0	<2	120	113	2.3	53.3	0.53
LPW-024	23.0	<0.2	4.09	12.0	<2	96	105	2.4	51.1	0.54
LPW-026	25.0	<0.2	4.00	13.0	<2	97	104	2.5	49.4	0.56
LPW-028	27.0	<0.2	3.85	13.0	<2	100	104	2.4	50.8	0.57
LPW-030	29.0	<0.2	3.80	14.0	<2	110	98	2.4	51.6	0.58
LPW-035	32.5	<0.2	3.15	14.0	<2	95	78	2.1	47.0	0.47
LPW-040	37.5	<0.2	3.96	13.0	<2	100	102	2.6	42.9	0.60
LPW-045	42.5	<0.2	4.00	14.0	<2	97	105	2.7	42.2	0.65
LPW-050	47.5	<0.2	3.89	15.0	<2	120	109	2.6	46.9	0.68
LPW-055	52.5	<0.2	3.72	15.0	<2	64	94	2.7	44.7	0.69
LPW-060	57.5	<0.2	3.91	15.0	<2	76	100	3.0	42.7	0.70
LPW-065	62.5	<0.2	3.69	14.0	<2	120	105	2.9	41.9	0.73
LPW-070	67.5	<0.2	3.64	14.0	<2	68	100	3.0	40.0	0.75
LPW-075	72.5	<0.2	3.69	14.0	<2	70	92	3.2	37.9	0.75
LPW-080	77.5	<0.2	3.52	13.0	<2	80	99	3.2	35.6	0.75
LPW-085	82.5	<0.2	3.45	14.0	<2	120	114	3.3	35.2	0.78
LPW-090	87.5	<0.2	3.49	15.0	<2	130	118	3.1	30.7	0.84
LPW-095	92.5	<0.2	3.19	12.0	<2	95	107	3.4	34.4	0.73
LPW-100	97.5	<0.2	3.16	11.0	<2	62	78	3.2	43.5	0.76
LPW-105	102.5	<0.2	3.22	10.0	<2	64	72	3.0	39.4	0.79
LPW-110	107.5	<0.2	3.38	8.1	<2	69	67	3.4	38.7	0.84
LPW-115	112.5	<0.2	3.08	8.1	<2	65	67	3.4	39.9	0.77
LPW-120	117.5	<0.2	2.89	7.8	<2	75	63	3.4	37.8	0.75
LPW-125	122.5	<0.2	2.62	7.4	<2	<50	59	3.4	36.6	0.72
LPW-130	127.5	<0.2	2.49	6.0	<2	<50	57	3.4	35.7	0.73
LPW-135	132.5	<0.2	2.46	7.5	<2	54	55	3.2	40.4	0.74
LPW-140	137.5	<0.2	2.55	7.7	<2	<50	56	3.3	41.2	0.79

Depth (cm)	Cd (2) (ppm)	Cd (3) (ppm)	Ce (1) (ppm)	Ce (2) (ppm)	Co (1) (ppm)	Co (2) (ppm)	Co (3) (ppm)	Cr (1) (ppm)	Cr (2) (ppm)	Cr (2a) (ppm)
1.0	0.6	0.4	63	65	30.0	30	19	<15	20	15
3.0	0.5	0.4	61	65	29.0	31	19	<15	22	16
5.0	0.6	0.5	62	69	28.0	30	18	<15	21	17
7.0	0.6	0.5	62	66	29.0	30	19	<15	19	16
9.0	0.5	0.4	60	65	27.0	31	19	<15	19	15
11.0	0.6	0.5	63	64	32.0	34	20	<15	18	15
13.0	0.5	0.4	60	63	28.0	31	19	<15	18	15
15.0	0.5	0.4	57	64	27.0	31	19	<15	19	15
17.0	0.6	0.5	65	66	29.0	32	19	<15	20	15
19.0	0.5	0.4	66	67	30.0	32	19	<15	21	15
21.0	0.6	0.5	63	66	28.0	28	18	<15	21	15
23.0	0.7	0.5	66	67	30.0	32	19	<15	20	15
25.0	0.6	0.5	63	66	35.0	37	22	<15	19	14
27.0	0.6	0.5	60	66	38.0	38	22	<15	20	16
29.0	0.6	0.5	69	70	41.0	42	26	<15	22	15
32.5	0.5	0.6	62	54	50.0	42	31	<15	15	11
37.5	0.6	0.5	66	67	31.0	34	20	<15	20	14
42.5	0.6	0.5	60	68	34.0	42	26	<15	21	14
47.5	0.5	0.5	70	68	75.0	73	45	17.0	20	14
52.5	0.7	0.6	75	66	47.0	46	28	<15	19	13
57.5	0.8	0.7	75	73	32.0	36	23	<15	21	15
62.5	0.6	0.5	64	71	70.0	67	45	<15	19	14
67.5	0.7	0.6	65	70	44.0	46	31	<15	16	14
72.5	0.7	0.6	67	71	35.0	35	23	<15	19	13
77.5	0.8	0.7	65	71	46.0	50	35	<15	17	14
82.5	0.7	0.6	66	71	86.0	89	58	<15	17	13
87.5	0.8	0.7	62	72	160.0	171	135	<15	17	13
92.5	1.0	0.8	54	65	47.0	51	35	<15	17	12
97.5	0.9	0.7	59	59	26.0	26	19	<15	15	12
102.5	0.9	0.7	56	63	36.0	35	25	21.0	15	11
107.5	1.1	0.9	58	65	19.0	19	13	21.0	14	12
112.5	1.1	0.9	61	67	24.0	23	17	<15	12	12
117.5	1.0	0.9	58	63	16.0	17	13	19.0	11	11
122.5	1.0	0.9	53	60	16.0	12	13	<15	11	11
127.5	1.1	0.9	45	59	13.0	15	11	<15	11	11
132.5	1.0	0.8	51	57	14.0	15	11	<15	10	9
137.5	1.1	0.9	57	60	21.0	22	17	<15	12	10

Depth (cm)	Cs (1) (ppm)	Cu (2) (ppm)	Cu (3) (ppm)	Dy (2) (ppm)	Eu (1) (ppm)	Fe (1) (%)	Fe (2) (%)	Fe (3) (%)	Ga (2) (ppm)	Hf (1) (ppm)
1.0	1.5	14	12	5.0	1.90	5.30	5.40	4.28	12	1.90
3.0	1.9	14	12	4.9	2.10	5.50	5.43	4.50	12	0.92
5.0	1.7	14	11	5.0	2.00	5.20	5.30	4.35	11	1.90
7.0	1.6	14	12	4.9	1.90	5.20	5.26	4.38	12	1.80
9.0	1.3	14	11	4.8	1.90	5.00	5.30	4.35	12	1.40
11.0	1.3	14	11	4.6	1.50	5.30	5.47	4.57	13	1.00
13.0	1.3	15	12	4.5	1.70	5.40	5.31	4.43	13	1.00
15.0	1.1	12	11	4.6	1.40	5.50	5.41	4.64	12	0.75
17.0	1.4	14	11	4.7	1.60	5.90	5.57	4.75	13	1.50
19.0	1.3	15	11	4.6	2.30	5.50	5.26	4.39	13	1.60
21.0	1.4	14	12	4.6	2.20	4.40	4.35	3.60	12	2.70
23.0	1.2	15	12	4.6	1.70	5.20	4.87	4.00	12	1.90
25.0	1.0	14	12	4.6	1.00	5.60	5.45	4.58	13	1.50
27.0	1.4	14	11	4.6	1.70	6.00	5.77	4.82	13	1.00
29.0	1.3	14	12	4.6	1.40	5.90	5.62	4.88	13	2.20
32.5	1.2	12	12	3.2	1.80	5.90	4.70	4.83	11	1.30
37.5	1.2	15	12	4.9	1.70	6.30	6.00	5.23	12	1.20
42.5	1.3	15	12	5.1	1.70	6.10	6.06	5.16	13	0.77
47.5	1.5	14	12	4.9	1.10	7.00	6.01	5.37	12	1.20
52.5	1.2	14	11	4.8	1.80	6.60	5.75	5.04	12	1.20
57.5	1.4	16	13	5.1	2.40	6.40	6.02	5.31	12	1.30
62.5	1.0	15	12	5.1	2.30	5.30	5.12	4.58	12	1.40
67.5	1.0	15	12	4.9	1.90	4.90	5.15	4.39	10	1.10
72.5	0.9	16	13	5.0	2.10	4.80	4.95	4.18	9	0.69
77.5	1.1	16	13	5.0	1.10	4.40	4.68	4.04	6	0.55
82.5	1.1	16	12	4.8	1.40	4.30	4.57	3.75	9	1.30
87.5	0.8	15	12	5.9	1.50	5.70	6.26	5.44	9	1.00
92.5	1.0	16	13	4.7	1.70	2.90	3.29	2.72	6	0.20
97.5	0.9	16	13	4.2	1.50	2.70	2.59	2.10	5	0.72
102.5	0.7	15	12	4.2	1.70	2.00	2.16	1.73	4	0.80
107.5	0.8	17	13	4.5	1.80	2.20	2.31	1.84	4	1.20
112.5	0.8	18	13	4.6	1.80	2.00	2.00	1.58	5	0.65
117.5	0.7	18	13	4.2	1.80	1.60	1.71	1.33	3	1.00
122.5	0.7	18	13	4.2	1.70	1.50	1.63	1.30	4	0.83
127.5	0.5	19	14	4.1	1.90	1.10	1.37	1.07	3	0.20
132.5	0.7	19	14	3.8	1.20	1.20	1.12	0.92	2	0.60
137.5	0.9	18	14	4.2	1.90	1.60	1.68	1.30	4	0.20

Depth (cm)	Hg(18) (ppb)	K (2) (%)	La (1) (ppm)	La (2) (ppm)	Li (2) (ppm)	LOI (%)	Lu (1) (ppm)	Mg (2) (%)	Mn (2) (%)	Mn (3) (ppm)
1.0	NA	0.37	23.0	23	12.2	32.0	0.26	0.15	0.25	1960
3.0	157	0.37	22.0	23	12.1	32.2	0.37	0.15	0.25	2220
5.0	142	0.32	23.0	25	10.7	32.7	0.36	0.13	0.24	2110
7.0	149	0.31	24.0	25	10.3	32.8	0.40	0.13	0.23	1910
9.0	144	0.31	22.0	26	10.3	32.3	0.35	0.13	0.23	1850
11.0	134	0.26	22.0	25	8.9	32.6	0.28	0.11	0.21	1670
13.0	130	0.26	23.0	24	9.3	33.2	0.32	0.12	0.21	1780
15.0	139	0.26	20.0	25	9.0	33.4	0.25	0.12	0.21	1800
17.0	130	0.26	23.0	25	9.5	33.5	0.27	0.12	0.21	1730
19.0	143	0.27	23.0	26	10.3	33.8	0.24	0.12	0.18	1560
21.0	141	0.26	24.0	25	10.7	33.2	0.33	0.12	0.18	1550
23.0	135	0.26	25.0	26	10.5	33.5	0.32	0.12	0.18	1540
25.0	120	0.25	24.0	26	9.8	33.3	0.33	0.11	0.16	1640
27.0	113	0.24	25.0	26	9.4	33.1	0.26	0.11	0.20	1550
29.0	105	0.23	25.0	26	9.0	33.3	0.40	0.11	0.18	1590
32.5	86	0.18	25.0	22	6.8	46.1	0.29	0.09	0.15	1580
37.5	115	0.24	25.0	28	9.6	32.4	0.29	0.11	0.18	1550
42.5	120	0.24	23.0	28	9.8	32.6	0.36	0.11	0.20	1620
47.5	118	0.23	25.0	31	9.2	31.9	0.35	0.11	0.20	1600
52.5	117	0.21	26.0	27	8.4	31.9	0.37	0.10	0.17	1460
57.5	113	0.22	28.0	30	9.3	31.9	0.35	0.11	0.17	1410
62.5	98	0.23	28.0	32	9.3	30.9	0.29	0.11	0.17	1360
67.5	102	0.21	25.0	28	8.8	30.8	0.34	0.11	0.17	1290
72.5	85	0.20	27.0	33	8.7	31.0	0.29	0.10	0.15	1010
77.5	84	0.20	25.0	30	8.5	29.9	0.32	0.10	0.15	1000
82.5	85	0.19	25.0	29	8.5	29.6	0.23	0.10	0.20	1700
87.5	86	0.18	24.0	30	8.5	28.8	0.25	0.10	1.59	12700
92.5	75	0.17	21.0	28	8.4	28.3	0.24	0.09	0.17	1360
97.5	69	0.16	23.0	27	7.6	28.3	0.29	0.09	0.10	703
102.5	70	0.15	23.0	27	7.1	28.8	0.30	0.09	0.09	628
107.5	79	0.15	25.0	29	7.1	29.7	0.31	0.09	0.10	672
112.5	56	0.14	27.0	30	7.2	29.1	0.34	0.09	0.10	657
117.5	60	0.13	24.0	28	7.0	28.0	0.28	0.08	0.09	595
122.5	56	0.12	22.0	28	6.6	27.5	0.26	0.08	0.08	534
127.5	55	0.12	20.0	30	6.4	27.3	0.27	0.07	0.07	498
132.5	52	0.11	23.0	26	6.1	27.4	0.22	0.08	0.07	457
137.5	57	0.12	24.0	28	6.2	27.1	0.27	0.07	0.08	570

Depth (cm)	Mo (2) (ppm)	Mo (5) (ppm)	Na (1) (%)	Na (2) (%)	Nb (2) (ppm)	Ni (2) (ppm)	Ni (3) (ppm)	P (2) (ppb)	Pb (2) (ppm)	Pb (3) (ppm)
1.0	4	2	0.21	0.20	4	14	10	2006	34	23
3.0	4	2	0.22	0.20	2	14	8	2031	33	22
5.0	4	2	0.18	0.16	2	14	8	2135	22	16
7.0	3	2	0.17	0.15	2	14	8	2151	20	15
9.0	4	2	0.16	0.16	2	16	8	2112	26	16
11.0	4	2	0.15	0.13	3	17	9	2128	17	10
13.0	3	2	0.14	0.13	2	17	8	2088	18	10
15.0	4	3	0.13	0.13	2	16	8	2117	14	10
17.0	3	3	0.14	0.13	3	15	8	2159	18	10
19.0	4	3	0.15	0.14	2	16	8	2191	15	8
21.0	3	2	0.17	0.14	3	17	9	2070	15	10
23.0	3	2	0.15	0.13	3	18	9	2181	16	9
25.0	4	2	0.14	0.13	2	18	10	2212	15	9
27.0	5	2	0.15	0.13	2	18	9	2172	16	9
29.0	4	2	0.12	0.12	2	22	12	2194	15	8
32.5	4	3	0.12	0.09	2	18	12	1829	12	8
37.5	4	3	0.13	0.12	2	18	9	2290	13	8
42.5	4	3	0.13	0.12	2	18	10	2238	16	9
47.5	5	3	0.14	0.12	2	24	13	2162	15	8
52.5	4	3	0.14	0.11	2	20	11	2229	15	8
57.5	4	3	0.13	0.12	2	18	10	2466	14	8
62.5	4	3	0.13	0.12	2	28	15	2314	11	8
67.5	4	2	0.13	0.11	2	20	11	2421	10	8
72.5	4	2	0.12	0.11	1	19	10	2612	10	7
77.5	4	2	0.11	0.11	1	21	11	2485	11	8
82.5	5	2	0.11	0.11	1	37	14	2348	9	7
87.5	6	4	0.11	0.10	1	37	21	1833	16	7
92.5	3	2	0.10	0.10	1	26	15	2151	9	7
97.5	3	2	0.10	0.10	1	21	11	2160	9	7
102.5	3	2	0.11	0.10	1	24	14	2138	6	7
107.5	3	2	0.11	0.10	1	19	10	2394	6	7
112.5	2	2	0.12	0.10	1	23	13	2116	7	7
117.5	2	<2	0.11	0.10	1	21	11	1948	5	7
122.5	2	<2	0.09	0.08	1	21	12	1738	6	6
127.5	3	<2	0.09	0.08	1	19	11	1652	5	6
132.5	3	<2	0.09	0.08	1	20	12	1557	3	5
137.5	3	2	0.09	0.09	1	21	12	1629	5	5

Depth (cm)	Rb (1) (ppm)	Rb (2) (ppm)	Sb (1) (ppm)	Sc (1) (ppm)	Sc (2) (ppm)	Sm (1) (ppm)	Sr (2) (ppm)	Ta (1) (ppm)	Tb (1) (ppm)	Th (2) (ppm)
1.0	22.0	17	0.37	6.0	5.9	6.7	29	0.34	0.84	1
3.0	16.0	16	0.45	6.2	5.8	6.7	29	0.21	0.83	1
5.0	14.0	18	0.27	5.6	5.5	6.7	28	0.24	1.00	1
7.0	17.0	15	0.32	5.8	5.5	7.0	27	0.53	0.85	1
9.0	15.0	15	0.24	5.4	5.6	6.5	28	0.27	0.73	1
11.0	13.0	11	0.16	5.2	5.1	6.7	27	0.41	0.76	1
13.0	10.0	11	0.15	5.2	4.8	6.5	27	0.38	0.80	1
15.0	8.6	14	0.13	4.6	5.0	6.4	28	0.33	0.81	1
17.0	14.0	14	0.18	5.0	5.1	7.2	29	0.32	0.84	1
19.0	18.0	10	0.14	5.3	5.1	7.1	30	0.36	0.74	1
21.0	6.7	14	0.18	5.3	5.1	7.0	30	0.30	0.89	1
23.0	16.0	12	0.12	5.4	5.1	7.1	30	0.43	0.94	1
25.0	12.0	16	0.12	5.2	5.1	6.9	31	0.44	0.89	1
27.0	8.4	13	0.13	5.2	5.0	7.0	31	0.32	0.95	1
29.0	13.0	10	0.14	5.4	4.8	6.9	30	0.10	0.85	1
32.5	7.7	10	0.14	5.3	4.1	6.8	25	0.33	0.83	1
37.5	11.0	10	0.13	5.6	5.1	6.9	32	0.36	0.79	1
42.5	12.0	14	0.14	5.0	5.1	7.0	33	0.24	0.76	1
47.5	13.0	10	0.13	5.6	5.0	7.9	35	0.36	1.00	1
52.5	11.0	6	0.19	5.7	4.9	7.2	35	0.31	0.76	1
57.5	10.0	11	0.14	6.0	5.2	7.8	35	0.10	0.87	1
62.5	14.0	10	0.14	5.5	5.2	7.4	37	0.26	0.86	5
67.5	5.4	11	0.12	5.2	5.1	7.0	38	0.24	1.00	1
72.5	5.9	10	0.12	5.2	5.2	7.3	38	0.34	0.79	3
77.5	11.0	8	0.13	4.8	5.0	6.9	41	0.10	0.81	3
82.5	6.8	10	0.11	4.7	4.9	7.3	45	0.10	0.81	3
87.5	5.4	7	0.12	4.4	4.8	6.9	47	0.10	0.85	3
92.5	6.4	8	0.13	3.9	4.7	6.8	46	0.20	0.84	3
97.5	2.0	8	0.12	4.2	4.3	7.5	42	0.10	0.83	4
102.5	4.6	8	0.12	4.0	3.9	6.9	44	0.10	0.69	3
107.5	5.0	6	0.10	4.0	4.3	7.3	45	0.10	0.89	1
112.5	6.4	6	0.13	4.3	4.3	7.6	46	0.10	1.00	5
117.5	5.8	7	0.13	3.8	4.1	7.2	46	0.10	0.72	1
122.5	5.0	6	0.10	3.4	3.9	6.7	45	0.10	0.78	1
127.5	4.5	5	0.11	3.1	3.7	6.2	46	0.10	0.73	1
132.5	2.0	7	0.13	3.2	3.4	6.9	46	0.23	0.87	8
137.5	7.0	6	0.13	3.3	3.5	7.0	46	0.10	0.82	5

Depth (cm)	Ti (2) (ppm)	U (1) (ppm)	V (2) (ppm)	W (1) (ppm)	Y (2) (ppm)	Yb (1) (ppm)	Zn (1) (ppm)	Zn (2) (ppm)	Zn (3) (ppm)	Zr (2) (ppm)
1.0	1854	1.0	44	<2	25	1.40	230.0	223	181	52
3.0	1857	1.1	44	<2	24	2.30	210.0	213	177	50
5.0	1766	0.9	40	<2	24	2.00	240.0	220	177	48
7.0	1727	1.0	39	<2	24	2.50	250.0	221	184	46
9.0	1704	1.0	41	<2	24	1.30	170.0	204	167	41
11.0	1510	0.9	37	<2	24	2.10	200.0	210	177	36
13.0	1605	0.9	36	<2	22	1.90	200.0	226	184	37
15.0	1615	1.0	36	<2	22	1.50	190.0	201	165	36
17.0	1645	1.2	38	<2	22	1.80	240.0	241	195	38
19.0	1692	1.0	39	<2	24	2.10	320.0	255	212	39
21.0	1665	1.0	37	<2	22	1.60	200.0	261	218	39
23.0	1640	1.1	37	<2	22	1.80	230.0	267	216	37
25.0	1612	1.0	37	<2	22	2.10	240.0	272	223	36
27.0	1569	1.1	37	<2	22	1.50	290.0	261	212	36
29.0	1518	1.0	36	<2	22	2.10	320.0	275	233	34
32.5	1152	0.9	28	<2	18	1.70	310.0	211	217	28
37.5	1473	1.0	36	<2	24	1.70	230.0	248	206	37
42.5	1540	0.9	36	<2	24	1.70	320.0	276	223	36
47.5	1457	1.0	35	<2	23	2.20	330.0	254	213	36
52.5	1378	1.0	33	<2	23	2.20	300.0	273	227	84
57.5	1425	0.9	36	<2	25	2.00	390.0	304	263	35
62.5	1385	0.9	34	<2	25	2.40	340.0	286	241	33
67.5	1355	0.7	34	<2	25	2.10	360.0	305	245	33
72.5	1254	0.8	32	<2	25	2.50	380.0	315	255	32
77.5	1185	0.8	31	<2	25	1.60	300.0	341	274	31
82.5	1070	0.8	30	<2	25	2.40	400.0	356	267	32
87.5	1070	0.8	30	<2	25	2.00	350.0	356	290	32
92.5	979	0.7	27	<2	25	1.60	350.0	391	318	26
97.5	898	0.7	24	<2	24	1.90	420.0	361	291	26
102.5	876	0.7	21	<2	23	1.20	350.0	344	288	22
107.5	918	0.7	23	<2	25	2.00	410.0	391	318	24
112.5	850	0.8	22	<2	25	2.00	430.0	396	319	23
117.5	776	0.7	21	<2	24	1.70	400.0	391	324	21
122.5	683	0.6	20	<2	24	2.00	370.0	408	323	20
127.5	637	0.6	18	<2	23	1.60	420.0	408	333	19
132.5	555	0.7	14	<2	23	1.10	380.0	402	316	17
137.5	594	0.7	16	<2	24	2.00	460.0	412	331	17

Appendix D: Pollen and spore count

Core QV2

depth	3	7	11	13	17	21	25.5	32
Species								
Picea	40	44	42	39	33	32	40	30
Abies	2	1	1	1	1		2	1
Pinus	1							
Populus	3	2	3	2			2	1
Tilia	2	2		1				1
Betula	40	80	71	84	72	80	57	58
Acer	11	7	3	7	3	1	3	
Alnus	23	38	44	38	32	49	39	30
Polypodiaceae	62	88	63	76	97	95	90	80
Lycopodium	8	13	9	9	8	7	4	9
Salix	6	5	2	3	4	2		2
Osmunda			1	1				
Ericaceae								
Juniperus			1	1				
Epilobium								
Taraxacum	11	7	6	11	10	6	10	18
Rumex	16	8	18	24	24	14	20	21
Stellaria	1				2			1
Gramineae	120	86	84	81	90	86	116	115
Asteraceae	7	12	3	13	9	9	16	6
Chenopodiaceae							1	
Myrica gale	2	5	7	6	11	14	6	5
Thalictrum	3	2	4	3	2		2	
Sphagnum	30	61	60	64	61	66	49	32
Equisetum	8	3	15	16	27	27	22	54
Nemopanthus	2	1	1	4	8	4		3
Carex							3	1
Isoetes	5	3	4	7		2	16	6
Nymphaeaceae	2	5	5	6	6	7	1	6
Stratiotes	1		2	1		2		4
Nuphar								
Eriocaulon								
Potamogeton	3		2					
total pollen and spores	409	473	451	498	500	503	499	484
Corroded	14	12	15	8	10	12	16	10
Unknown	6	7	7	4	3	10	4	9
Indeterminable	20	15	19	17	20	21	20	21
lycopodium spike for pollen	343	270	212	199	280	275	174	341
total lycopodium spike added	24200	24200	24200	24200	24200	24200	24200	24200
Soot	71	62	25	59	55	65	10	35
Charcoal	2487	1914	884	1609	1540	1524	441	424
Spike for charcoal and soot	238	174	66	110	183	168	95	174

Core QV2

depth	38	44	52.5	57.5	62.5	67.5	72.5	77.5
Species								
Picea	41	45	69	73	88	103	114	106
Abies	2	3	4	12	13	25	25	34
Pinus						4	3	2
Populus	2		3			1		
Tilia		1						
Betula	52	70	74	87	106	84	80	84
Acer	1							
Alnus	23	35	32	25	42	35	22	61
Polypodiaceae	60	52	98	90	76	72	72	54
Lycopodium	6	11	5	9	6	6	8	6
Salix	1	1	1	2		1		2
Osmunda			1	1	1	1	1	1
Ericaceae			1			1	1	
Juniperus								
Epilobium				1	1			
Taraxacum	9	9	6	1	10	5		
Rumex	24	19	35	20	20	18	6	17
Stellaria	1		1		3	5		
Gramineae	137	96	92	70	90	46	30	19
Asteraceae	13	14	8	11	14	4	7	7
Chenopodiaceae					1			
Myrica gale	3	8	3	7	9	6	8	7
Thalictrum	2	1	5	4	4	9	4	2
Sphagnum	27	46	60	43	48	54	37	24
Equisetum	23	7	6	11	2	2	1	7
Nemopanthus	1	1	1		3		1	
Carex			2	14	1	1	15	
Isoetes	36	5	76	66	89	25	22	57
Nymphaeaceae	4	3	3	6	6	4	2	3
Stratiotes	2	1	3	1	3			
Nuphar				1	1			
Eriocaulon								
Potamogeton								
total pollen and spores	470	428	589	555	637	512	459	493
Corroded	15	12	12	20	20	20	10	13
Unknown	9	11	5	11	26	5	2	
Indeterminable	10	10	10	11	9	14	10	3
lycopodium spike for pollen	201	267	165	135	104	143	212	196
total lycopodium spike added	24200	24200	24200	24200	24200	24200	24200	24200
Soot	14	19	6	7				
Charcoal	555	305	300	211	82	28	20	18
Spike for charcoal and soot	114	166	155	135	104	133	212	196

Core QV2

depth	82.5	87.5	92.5	102.5	107.5	112.5	122.5	132.5
Species								
Picea	111	119	127	116	132	136	146	137
Abies	17	42	50	23	20	11	27	38
Pinus	1	4	8	3	9	1	16	14
Populus					1	1		
Tilia								
Betula	102	117	117	143	131	96	103	108
Acer								
Alnus	53	22	14	26	28	14	20	16
Polypodiaceae	44	26	24	18	35	32	29	29
Lycopodium		4	2	1	3	5	3	2
Salix						2		
Osmunda		2						
Ericaceae			2					
Juniperus								
Epilobium	1				1			
Taraxacum								
Rumex	2	3				2		3
Stellaria				2				
Gramineae	13	3		1		2		4
Asteraceae	3	5	2	9	5	3	1	3
Chenopodiaceae								
Myrica gale	11	3	6	8	10	11	7	5
Thalictrum	1	2	1	5	4	2	2	1
Sphagnum	20	7	11	10	12	21	21	28
Equisetum		3			2	2	1	3
Nemopanthus		1					1	2
Carex	1		2		1			1
Isoetes	44	20	10	20	18	17	10	13
Nymphaeaceae	1	1		1	2	3		3
Stratiotes	1			1		1	1	
Nuphar		3						
Eriocaulon	1							
Potamogeton								
total pollen and spores	427	387	376	387	414	362	388	410
Corroded	21	12	12	22	15	23	14	10
Unknown	7	1		3	3	3	3	
Indeterminable	5	11	8	4	13	9	5	6
lycopodium spike for pollen	96	96	94	84	95	100	4	107
total lycopodium spike added	24200	24200	24200	24200	24200	24200	24200	24200
Soot								
Charcoal	26	5			2			10
Spike for charcoal and soot	96	96	94	84	95	100	91	107

Core QV2

depth	142.5	152.5	162.5	172.5	192.5	197.5
Species						
Picea	157	146	151	136	124	139
Abies	31	57	25	67	44	35
Pinus	9	17	3	8	15	8
Populus		1			1	1
Tilia						
Betula	113	98	110	104	114	115
Acer						
Alnus	18	14	18	10	24	28
Polypodiaceae	31	24	26	18	21	19
Lycopodium	4	3	3	1		6
Salix						
Osmunda	1	2			1	3
Ericaceae						
Juniperus						
Epilobium						
Taraxacum						
Rumex				3		
Stellaria						
Gramineae	1	2		1		2
Asteraceae	10	4	5	3	6	8
Chenopodiaceae						
Myrica gale	8	4	15	5	6	7
Thalictrum	9	2	2		10	5
Sphagnum	7	16	18	13	1	13
Equisetum		3		3		
Nemopanthus						
Carex		1			3	1
Isoetes	38	23	20	22	33	
Nymphaeaceae	1	3	1	3	6	6
Stratiotes	3					
Nuphar					2	
Eriocaulon						
Potamogeton						
total pollen and spores	441	420	397	397	411	396
Corroded	13	7	15	6	12	19
Unknown	6	2	3	4	5	2
Indeterminable	7	11	8	10	11	11
lycopodium spike for pollen	101	83	89	98	67	94
total lycopodium spike added	24200	24200	24200	24200	24200	24200
Soot						
Charcoal		3	1	2	1	
Spike for charcoal and soot	101	83	89	98	67	94

Core LP5

depth	1	3	7	11	15	19	21	23	27
Species									
Picea	72	58	67	53	40	49	74	76	71
Abies	14	7	16	7	7	3	10	10	13
Pinus									
Populus		1			1	2	1	2	
Acer	2	1	2	2		2	1	2	
Betula	49	73	95	92	98	63	71	59	83
Alnus	29	33	30	31	44	42	22	42	49
Polypodiaceae	64	64	67	99	107	84	60	46	31
Lycopodium	5	8	18	11	7	8	4	4	6
Salix	3	2	2	3		5	3	1	3
Osmunda	1	1	3	1	1		3		1
Ericaceae									
Juniperus	3	2	2	3	5	2	1	3	1
Botarychium	1		2						
Taraxacum	7	7	1	4	6	1	3	3	
Rumex	8	10	8	15	17	18	15	4	11
Stellaria		1	1	2		1			1
Gramineae	82	81	40	49	54	86	65	66	41
Asteraceae	13	13	5	9	8	9	13	16	11
Polygonum		1					1		
Carex	4		1	2					3
Myrica gale	10	2	19	10	6	4	16	8	9
Thalictrum	7	5	10	12	10	8	15	5	15
Sphagnum	64	27	113	68	83	44	57	42	51
Equisetum	6	5		16	18	25	9	7	17
Nemopanthus	1	1	2		2	1	4	1	4
Isoetes	4	6		8	6	8	14	10	16
Nymphaeaceae	6	11	11	6	8	5	6	4	1
Stratiotes	1	1		1	4		2	3	8
Nuphar								3	
Eriocaulon								1	
Potamogeton		2		1	1	1		1	
total pollen and spores	456	423	515	505	533	471	470	419	446
Corroded	9	15	6	10	15	12	10	10	17
Unknown	5	11	6	7	7	9	6	5	8
Indeterminable	13	16	11	14	13	15	12	14	5
lycopodium spike counted	235	276	307	237	175	165	192	188	133
total lycopodium spike added	24200	24200	24200	24200	24200	24200	24200	24200	24200
Soot	63	41	40	18	22	11	5	2	1
Spike for soot	165	211	226	99	147	84	86	43	33
Charcoal	19	21	20	14	28	17	35	19	8
Spike for charcoal	137	31	179	63	93	57	49	43	33

Core LP5

depth	29	32.5	37.5	42.5	47.5	52.5	57.5	62.5	67.5
Species									
Picea	86	93	79	59	89	96	107	98	113
Abies	13	16	15	14	33	25	27	21	22
Pinus						2	3	2	4
Populus									
Acer						1			
Betula	90	60	91	88	77	80	96	116	113
Alnus	35	39	33	44	49	51	25	31	19
Polypodiaceae	82	63	73	66	80	39	26	22	36
Lycopodium	8	3	14	8	4	1	2	1	2
Salix	4	2	4	2	3	1	1		2
Osmunda	2	2	1	1	4		1		1
Ericaceae	1								
Juniperus					1	3	1		
Bothrychium					1				
Taraxacum	1		5	1					1
Rumex	14	13	11	21	9	4	4		
Stellaria		1	1		1			1	
Gramineae	32	38	23	29	7	3	1	2	3
Asteraceae	6	14	12	11	5	8	9	10	7
Polygonum									
Carex		1	1	1	2	2	5	1	5
Myrica gale	19	14	14	19	17	16	11	10	14
Thalictrum	11	13	6	13	10	8	9	9	7
Sphagnum	55	38	55	31	44	20	28	21	36
Equisetum	11	18	9	9	7	11		6	
Nemopanthus	2	1		2					
Isoetes	26	21	13	24	8	11	7	8	4
Nymphaeaceae	3	3	4	2	4		2	1	
Stratiotes		5	1			3			
Nuphar		2	1	1		2	3	1	1
Eriocaulon				2	1		1	1	
Potamogeton		2							
total pollen and spores	501	462	466	448	456	387	369	362	390
Corroded	7	18	16	20	16	13	7	10	11
Unknown	4	7	3	8	8	12	2	20	5
Indeterminable	16	9	14	8	9	15	7	10	12
lycopodium spike counted	168	164	159	153	255	156	103	122	107
total lycopodium spike added	24200	24200	24200	24200	24200	24200	24200	24200	24200
Soot	2	3	2	7					
Spike for soot	168	164	153	153	255	156	103	122	107
Charcoal	19	12	18	18	24	10	10	4	3
Spike for charcoal	168	164	153	153	255	156	103	122	107

Core LP5

depth	72.5	87.5	112.5
Species			
Picea	137	133	130
Abies	18	14	17
Pinus	2		1
Populus			
Acer			
Betula	93	103	86
Alnus	27	24	28
Polypodiaceae	25	40	18
Lycopodium	7		5
Salix	4	2	
Osmunda	2		
Ericaceae			
Juniperus			3
Bothrychium			
Taraxacum			
Rumex		2	
Stellaria		1	1
Gramineae		1	
Asteraceae	5	7	15
Polygonum			
Carex	1	1	3
Myrica gale	7	12	9
Thalictrum	8	8	7
Sphagnum	26	33	16
Equisetum	1	2	2
Nemopanthus			
Isoetes	13	4	22
Nymphaeaceae		5	2
Stratiotes	6	3	6
Nuphar	1		
Eriocaulon	2		
Potamogeton			
total pollen and spores	385	395	371
Corroded	16	15	14
Unknown	7	4	14
Indeterminable	7	6	3
lycopodium spike counted	130	86	85
total lycopodium spike added	24200	24200	24200
Soot			
Spike for soot	130	86	85
Charcoal			13
Spike for charcoal	130	86	85

Core MP1

depth	1	7	11	17	21	27	31	37
Species								
Picea	38	25	26	34	33	53	54	117
Abies				1		2	6	2
Pinus	1							
Populus	2	4	3	1	2	2		1
Acer	1	1	2	1	3			
Betula	35	50	49	32	63	113	103	128
Alnus	30	36	37	30	37	32	23	27
Polypodiaceae	57	43	24	23	25	24	51	32
Lycopodium	7	4	3	8	6	13	4	11
Salix	5	2	7	5	6	9	5	3
Osmunda			1	1	5	5	6	3
Salix		1		2		3	6	2
Juniperus	1			2				1
Taraxacum	5	3	2	2	3		1	
Rumex	8	9	4	12	10	8	4	7
Stellaria					1			5
Gramineae	133	148	140	167	104	56	55	11
Asteraceae	5	4	5	3	3	5	1	4
Polygonum			2					
Carex		6	10	3	9	11	11	4
Myrica gale	7	13	4	8	4	12	11	10
Thalictrum	3	2	1	1		2	2	
Sphagnum	19	48	25	32	20	13	51	17
Equisetum	19	24	2	10	1	18	38	22
Sparganium	52	25		2				
Isoetes	2		3					
Nymphaeaceae	1	2		2		5		2
Stratiotes								
Nuphar			1			1	2	1
Ericaulon			1		1	2	4	1
Pediastrum	134	238	336	306	103	7	3	2
total pollen and spores	431	450	352	382	336	389	438	411
Corroded	2	1	1	1	6	5	2	4
Unknown	0	1	1	5	4	3	3	1
Indeterminable	11	8	3	5	3	8	1	12
lycopodium spike counted	249	312	188	339	302	207	213	411
total lycopodium spike added	24200	24200	24200	24200	24200	24200	24200	24200
Charcoal	367	499	80	640	126	23	6	18
Soot	97	115	35	37	11			
spike for charcoal and soot	249	312	188	339	302	207	213	411

Core MP1

depth	42.5	77.5	97.5
Species			
Picea	124	130	144
Abies	8	7	3
Pinus			
Populus	1	2	3
Acer		1	
Betula	110	140	126
Alnus	37	12	13
Polypodiaceae	21	11	9
Lycopodium	3	5	3
Salix	1		
Osmunda	1		
Salix		1	1
Juniperus			3
Taraxacum			
Rumex	5	3	2
Stellaria	3	1	1
Gramineae	7	2	7
Asteraceae	1		1
Polygonum			
Carex	4	1	8
Myrica gale	10	3	6
Thalictrum			
Sphagnum	22	14	14
Equisetum	3	2	5
Sparganium			2
Isoetes	1	1	
Nymphaeaceae	3		
Stratiotes			
Nuphar	1		2
Ericaulon	3		1
Pediastrum	1	1	1
total pollen and spores	369	336	354
Corroded	4	1	1
Unknown	6	4	1
Indeterminable	10	10	5
lycopodium spike counted	191	145	107
total lycopodium spike added	24200	24200	24200
Charcoal	13	5	3
Soot			
spike for charcoal and soot	191	145	107

Core GP1

depth	3	7	11	13	17	21	23	29	32.5
Species									
Picea	102	65	27	107	90	102	201	57	74
Abies	2	1	2	1	7	3	17		5
Pinus				1	2		7	1	3
Populus									
Acer		1	2	1	1	1	1	3	3
Betula	155	144	191	123	123	125	150	172	114
Alnus	23	49	35	18	27	25	17	42	74
Polypodiaceae	4	5		7	4	7	3		9
Lycopodium	2	1	4	2	4	6	4	1	2
Salix				2	3	1	5	2	4
Osmunda				1	1		3		
Ericaceae		1	3	2	2	6	3		1
Taraxacum	1	2	5	4	1	2			2
Rumex	1	4	6	4	2	4	4	4	10
Gramineae	16	39	48	45	48	42	5	12	19
Asteraceae	1	1	2	3	3	3		1	1
Polygonum					1				
Carex		2		2	1	3	1	1	
Myrica gale	6	6	14	9	4	7	5	3	5
Thalictrum						1		1	
Sphagnum	4			10	5		1		
Equisetum	6	12	33	6	2	4	3	18	17
Sparganium		1	2	1	1	3		1	1
Isoetes	4	10		3	8	9	3		
Nymphaeaceae		1		1	2				
Numphar							1		
Eriocaulon	1		1		1			2	1
Pediastrum						1			
total pollen and spores	328	345	375	353	343	354	434	321	345
Corroded		4	10		1	4	3	9	3
Unknown	1	3	5		4	4		1	2
Indeterminable	3	7	1	8	6	2	2		3
Soot	55	73	60	93	401	51	49	44	19
Charcoal	102	106	93	250	395	125	40	53	68
lycopodium spike counted	212	135	234	225	203	214	204	246	192
lycopodium spike added	24200	24200	24200	24200	24200	27000	24200	24200	24200

Core GP1

depth	102.5	107.5	112.5	117.5	122.5	127.5
Species						
Picea	184	148	187	151	124	132
Abies	2	19	7	10	5	5
Pinus		4	18	4		
Populus					2	
Acer	1		3		3	3
Betula	160	130	118	111	156	153
Ulnus	3	13	31	22	32	58
Polypodiaceae		9	4	3		1
Lycopodium		1	1	1		4
Salix	1			1	2	1
Osmunda				1		
Ericaceae	1	1				
Taraxacum						
Rumex	1	2	1	1		
Gramineae	1	5		4		2
Asteraceae	1					1
Polygonum			1			
Carex	3	3		1	1	1
Myrica gale	3	4	2	3	2	9
Thalictrum				1		
Sphagnum		4	2	3		
Equisetum		5	15	5	67	31
Sparganium	6				3	5
Isoetes			10	3	5	
Nymphaeaceae				1		1
Numphar						
Eriocaulon	2		1		1	1
Pediastrum						
total pollen and spores	369	348	401	326	403	408
Corroded	4	3	1	2	4	3
Unknown		4			4	
Indeterminable	4	4	5	6	3	5
Soot						
Charcoal	1	20	16	8	3	10
lycopodium spike counted	56	79	169	145	94	89
lycopodium spike added	24200	27000	24200	24200	24200	24200

Core GP1

depth	37.5	42.5	47.5	52.5	62.5	62.5	72.5	87.5	97.5
Species									
Picea	66	99	122	141	182	95	122	151	152
Abies	1	2	14	9	9	6	11	6	4
Pinus	1	1	1	3	5	2	1		5
Populus									
Acer	2	1				4	2	1	1
Betula	113	101	98	128	117	184	206	141	153
Alnus	70	91	55	20	5	9	10	4	5
Polypodiaceae		1	3	4	2			1	2
Lycopodium	3	1		3	1				
Salix	4	1		3		2		1	1
Osmunda	1		1	3					1
Ericaceae	2		3	3	1				
Taraxacum									
Rumex	3				2			2	1
Gramineae	23	17	12	3		1	1	3	
Asteraceae	2	2		1					
Polygonum									
Carex	3	4		3		2	1	3	2
Myrica gale	10	7	5	6	1	6	5	1	4
Thalictrum	1								
Sphagnum	9		9	9					1
Equisetum	7	48	4		1			1	
Sparganium						1	1	1	
Isoetes	2	1	1	1		1		2	1
Nymphaeaceae		1							
Numphar			1						
Eriocaulon	1	1				1	1		2
Pediastrum									
total pollen and spores	324	379	329	340	326	314	361	318	335
Corroded	1	2			1	6	2	3	1
Unknown	1	2	1	6	2	1	1	1	1
Indeterminable	10	9	9	3	2	6	3	2	5
Soot	524	4	1						
Charcoal	72	5	12	10	2	1	1		3
lycopodium spike counted	230	141	104	114	57	94	93	85	53
lycopodium spike added	27000	24200	24200	24200	27000	27000	24200	24200	24200

Core LPW

depth	1	5	11	15	19	23	27	29	42.5
Species									
Picea	135	161	198	195	209	201	190	199	164
Abies	23	26	28	23	32	17	11	8	7
Pinus	5	4	3	2	3	5	4		8
Tsuga									
Larix	0	3	0	1	1	2	3	2	0
Betula	73	53	39	70	80	50	55	73	83
Acer					1	1			
Alnus	33	17	11	8	10	10	6	8	15
Juniperus									1
Ericaceae	5	5			4	2	1	3	2
Lycopodium	5	2	2	1	5	5	2	6	
Salix	2					1			
Osmunda	2			1	1				2
Botarychium					1			1	
Gramineae	4	5	2	1	1	1	1	3	
Rumex	2	3	5	1	4	3	3	3	2
Asteraceae	2		1						1
Chenopodiaceae		2	1		1				
Myrica gale	11	9	5	7	6	3	8	1	10
Polypodiaceae	29	8	14	4	18	6	16	11	10
Nymphaeaceae	2	1	1	1	1	1	1	5	0
Stratiotes	1		1					2	
Thalictrum	2								
Sphagnum	50	18	32	19	25	15	18	19	30
Equisetum	8	12	8	30	40	33	15	20	14
Cyperaceae	7	7	6	9	8	4	15	8	12
Isoetes	202	198	235	301	173	147	191	95	117
Nemopanthus		1							
total pollen and spore	603	535	592	674	624	507	540	467	478
Corroded	10	7	8	9	14	11	10	15	8
Indeterminable	11	11	13	10	6	9	13	17	12
Soot	2								
Charcoal	41	14	28	14	4	7	6	4	14
lycopodium spike counted	405	336	431	274	352	234	152	251	231
lycopodium spike added	24200	24200	24200	24200	24200	24200	24200	24200	24200

Core LPW

depth	57.5	72.5	87.5	97.5	102.5	117.5	137.5
Species							
Picea	198	196	210	133	181	191	177
Abies	18	8	18	5	10	2	5
Pinus	3	8	6	1	3		4
Tsuga						1	
Larix	0	0	0		1	0	0
Betula	68	72	61	129	79	88	133
Acer							
Alnus	11	7	8	21	13	6	11
Juniperus							
Ericaceae	1		2	1		2	
Lycopodium	5	2	3	3	1	5	5
Salix		1					
Osmunda		1			6		4
Botarychium							
Gramineae	4	1		2	1	2	1
Rumex	1		2	1		4	2
Asteraceae				1			
Chenopodiaceae				1			2
Myrica gale	3	8	8	4	6	8	8
Polypodiaceae	17	10	10	7	11	4	11
Nymphaeaceae	1	0	2	3	0	5	0
Stratiotes			2			2	
Thalictrum					1		1
Sphagnum	16	19	18	7	9	17	6
Equisetum	10	28	31	22	10	17	17
Cyperaceae	3	6	4		10	8	4
Isoetes	140	120	90	31	64	51	28
Nemopanthus							
total pollen and spore	499	487	475	372	406	413	419
Corroded	13	14	13	11	7	10	14
Indeterminable	11	6	11	10	9	14	13
Soot							
Charcoal	2	2	2	24	5	5	5
lycopodium spike counted	193	225	154	86	170	190	153
lycopodium spike added	24200	24200	24200	24200	27000	24200	24200

Appendix E: Diatom data for Core QV2

depth	5	28	73	127.5	167.5
Species					
Achnanthes affinis (Hustedt '72, page 381)				1	
Achnanthes arcus (Germain pg 66)				1	
Achnanthes levanderi var. levanderi (Pirla)				2	1
Achnanthes conspicua (Foged, 1980)		1			
Achnanthes delicatula (Germain)					1
Achnanthes detha (PIRLA)					1
Achnanthes flexula (Patrick '66 pg 286)					1
Achnanthes minutissima (Smol pg 193)	7		10	2	6
Achnanthes saxonia (Germain)		1	11	1	1
Achnanthes lanceolata (Germain)	1				
Achnanthes kryophila (Cleve-Euler fig 550, pg 233)				3	2
Achnanthes marginulata (PIRLA)		2	2	1	3
Achnanthes microcephala (Germain, pg 110)		1			1
Achnanthes linearis (Hustedt '72, page 381)		1	1	5	5
Achnanthes sp. 8 PIRLA (PIRLA)		1			1
Actinella punctata			1		
Anomoeoneis exillis var. lanceolata (Smol pg 196)				4	
Anomoeoneis exillis var. exillis (Smol pg 196)				1	
Anomoeoneis vitrea (Germain pg 164)	1		8	4	1
Anomoeoneis serians (Patrick '66 pg 429)					3
Anomoeoneis serians var. brachysira (Germain)				1	
Asterionella formosa (PIRLA pl 27)	61	128	11	8	8
Asterionella raifsil var. americana (PIRLA)	1			1	
Cocconeis placentula (germain pg 102)	1	1			
Cyclotella andancesis var. andancesis (Ross '81)	7				
Cyclotella andancesis var. bauzilensis (Ross '81, pg 36, pl 4)	4				
Cyclotella perforata (Ross '81, pg 23)	5				
Cyclotella stelligera	9		42	32	98
Cyclotella memeghiniana (Foged '82, pg 104)		3			
Cyclotella sp. 2 PIRLA (PIRLA)	4				
Cymbella amphioxya (PIRLA)		1			
Cymbella cesatii (PIRLA)			1		
Cymbella gracilis (Krammer '82, pg 102)		1	2	1	2
Cymbella minuta (Krammer '82 pg 541)		3	3	1	
Diatoma anceps (Patrick '66, pg 166)	1				
Diatoma elongatum (Germain pg 52)	163	35			
Diatoma hiemale (Cleve-Euler fig 329)					1
Diatoma vulgare (Patrick '66, pg 166)	19	13			
Eunotia exigua (Germain pg 88)	1		6	3	4
Eunotia faba (Germain)					1
Eunotia incisa ? (var. 4 PIRLA)					2
Eunotia incisa var. 2 PIRLA (PIRLA)				1	
Eunotia tenella (Germain pg 88)			3		5
Eunotia paludosa var. genuina (Cleve-Euler fiG 441)				1	
Eunotia pectinalis (Germain)			2	2	

depth	5	28	73	127.5	167.5
Eunotia pectinalis var. minor (Germain)				6	1
Eunotia meisteri			1	1	2
Eunotia curvata (PIRLA)			1	4	2
Eunotia curvata var. subarcuata (PIRLA)				4	
Eunotia praenana (Cleve-Euler pg 158)				1	
Eunotia praerupta (Foged '82 pg 116)		1	4		2
Eunotia polydentula var. perminata (Cleve-Euler fig 429)			1	2	3
Eunotia septentrionalis (PIRLA)					1
Eunotia tassiae var. pilula (Cleve-Euler fig 434 e)				1	
Eunotia tenelloides				1	
Eunotia vanheurcku (Foged '81 pg 206)				5	
Eunotia venerisi (Germain)			2	1	2
Eunotia sp. 35 PIRLA (PIRLA)		1			
Fragilaria breistriata var. capitata (PIRLA)		2			
Fragilaria breistriata (Germain)		2		2	3
Fragilaria capucina (Germian)	1	12	5		9
Fragilaria capucina var. valvaric (Germain)				3	
Fragilaria construents (Germain)		9	10		11
Fragilaria construents var. pumila (PIRLA)				3	
Fragilaria hungarica var. tumida (PIRLA)				1	
Fragilaria intermedia (Germain pg 64)	1	4			
Fragilaria lata (PIRLA)				1	
Fragilaria pinnata (Germain pg 66)				2	
Fragilaria producta (Germain pg 62)			1		
Fragilaria virescens	1	15	10		8
Fragilaria virescens var. exigua (PIRLA)				17	
Frustulia rhomboudes var. saxonia (Germain pg 140)			1	5	4
Frustulia rhomboudes var. viridula					1
Gomphonema angustatum var. producta (Germain)	3	1	2		4
Gomphonema gracile (Germain)				1	
Gomphonema parvulum (Germain)	1				
Melosira lirata var. lirata (PIRLA)		5	3	3	7
Melosira distans var. humilis (PIRLA)		3			
Melosira distans var. niveloides (PIRLA)			36	61	64
Melosira distans var. nivalis		1	1	1	1
Melosira distans var. tenella			1		1
Melosira distans var. distans (PIRLA)				1	2
Melosira italica var. italica					1
Melosira italica subsp. subartica (PIRLA)	1			1	
Melosira perglabra var. florinine (PIRLA)			2	13	
Melosira ambigua (PIRLA)			2		
Melosira ambigua var. ambigua (PIRLA)	2				
Melosira pseudoamericana (PIRLA)		1	5	4	2
Melosira undulata var. normanni (Smol pg 27)					3
Meridion circula		1	1		
Meridion circulare var. constricta (Germain pg 56)		1		4	
Meridion circulare	1				1
Navicula arvensis (Patrick '6 pg 556)	1				
Navicula adisjuncta var. anglica (Foged '77 pg 182)					1
Navicula conferavaacea var. peregrina (Patrick '66 pg 554)				1	1

depth	5	28	73	127.5	167.5
Navicula cuspidata (Germain)				1	
Navicula heimansii (PIRLA)				2	
Navicula minima (Nova Hedwiga vol 30 pg 25??)				1	
Navicula pseudoscutiformis (PIRLA)				1	
Navicula pupula (PIRLA)			1	1	
Navicula radiosa (Germain)			1		
Navicula subrhynchocephala (Foged '78)	1				
Navicula viridula var. rostella (Germain pg 178)		1		2	
Navicula sp. 3 PIRLA (PIRLA)		1			
Navicula sp. 6 PIRLA (PIRLA)				1	
Navicula sp. 31 PIRLA (PIRLA)				1	1
Neidium affine (PIRLA)				1	
Nitzschia gracilis (Germain pg 346)					2
Nitzschia hantzschiana (Germain)				2	1
Nitzschia palea (Germain pg 350)	3	4	2	1	
Nitzschia palea var. tenuirostris (Germain)	2				
Nitzschia paleacea (Germain pg 350)		1			
Pinnularia appendiculata (Germain)				1	
Pinnularia divergens (Germain)					1
Pinnularia var. PIRLA (PIRLA)					1
Pinnularia subcapitata var. stauroneiformis (Cleve-Euler fig 1090 d)			1		
Stauroneis phenicenteron (Germain pg 154)		1		1	
Stenopterobia anceps				1	
Surirella avata (Foged '81 pg 311)	1				
Synedra acus (Foged '80 pg 104)	8	6	6	3	8
Synedra acus var. angustissima (Germain)	1				
Synedra minscula (Foged pg 138)				2	
Synedra rumpens (Germain pg 80)	1	3	6	5	4
Synedra tabulata var. ?? (cleve-Euler fig 392)				4	1
Synedra ulna var. dancia (Germain pg 74)		2			1
Synedra vaucheriae (Germain)	3	5			
Synedra palchella (Germain)		1			
Synedra parasitica (Foged '79)	1				
Synedra sp. 2 PIR:A (PIRLA)				1	
Tabellaria fenestrata var. fenestrata (Koppen '75 pg 241)				1	
Tabellaria flocculosa var. linearis (PIRLA)		16			
Tabellaria flocculosa str. III sensu (PIRLA)	1	6			
Tabellaria flocculosa (Kalbe '80 pg 126)	4	3	95	42	13
Tabellaria quadriseptata (PIRLA)	1	1		1	
Thalassiosira fluviatilis (Foged '82 pg 156)				1	
Unknowns	3	8	2	14	2
Achnanthes A		4			
Achnanthes B		1			
Achnanthes C		1			
Achnanthes D	1	1			
Navicula A		1			
Navicula B	1				
Navicula C	1				
Navicula D			1		
Pinnularia A	1				

Appendix F: Dating methods for Core QV2

This appendix provides, in more detail the process that was applied to obtain the dates for core QV2. Dating was carried out by Dr. Peter Appleby, the director of Environmental Radioactivity Research Centre, at The University of Liverpool, Liverpool, UK.

Table F.1 shows the depths of the samples that Dr. Appleby examined. For those depths not listed the dates were interpolated. Column one shows the midpoint interval for the samples that were analyzed. Column two and three are the LOI and percent dry matter for each sample, respectively. The dry bulk density (DBD - dry weight/wet volume), column 4 was calculated using the equation:

$$DBD = SD*PDW/[PDW+SD*(1-PDW)]$$

where SD = density of solids (2.6 g cc^{-1})
PDW = percent dry weight

Column 5, the Cumulative Dry Weight (W), is a measure of the cumulative dry weight above each core depth, independent of compaction or water content ("It is literally the total mass of dry sediment above each linear depth level, per unit area of cross-section of the core." (Appleby, personal communication) It is calculated using the equation:

$$M2 = M1 + 0.5*(DBD1+DBD2)*(X2-X1)$$

where;
M1 = cumulative dry weight at depth X1 and
DBD1 = is the dry bulk density at depth X1.

Table F.1. LOI, dry matter content, dry bulk density and cumulative dry weight for core QV2.

Depth (cm)	LOI (%) (%)	dry matter (%)	Dry bulk density (g/cm^3)	Cumulative dry weight (g/cm^2)
3.0	18.0	22.0	0.2544	0.7633
5.0	17.0	29.0	0.3530	1.4693
7.0	15.0	36.0	0.4625	2.3942
9.0	14.0	38.0	0.4960	3.3862
11.0	14.0	40.0	0.5306	4.4474
13.0	14.0	41.0	0.5484	5.5441
15.0	13.0	43.0	0.5847	6.7136
17.0	13.0	42.0	0.5664	7.8464
19.0	13.0	40.0	0.5306	8.9076
21.0	13.0	41.0	0.5484	10.0043
23.0	13.0	40.0	0.5306	11.0655
25.5	14.0	40.0	0.5306	12.3921
28.0	15.0	40.0	0.5306	13.7186
30.0	15.0	39.0	0.5132	14.7449
34.0	15.0	38.0	0.4960	16.7288
38.0	16.0	34.0	0.4300	18.4487
40.0	16.0	31.0	0.3831	19.2148
46.0	22.0	21.0	0.2412	20.6618
48.8	19.0	21.0	0.2412	21.3371
52.5	20.0	24.0	0.2816	22.3790
62.5	25.0	15.0	0.1653	24.0315
72.5	35.0	14.0	0.1532	25.5635

Table F.2. ^{226}Ra data for selective samples.

Depth (cm)	cum dry mass (g/cm^2)	^{226}Ra conc (Bq/Kg)	std error
5.0	1.3764	49.27	2.75
9.0	3.0744	38.89	1.48
13.0	5.163	39.89	1.83
19.0	8.339	34.29	0.89
23.0	10.5224	36.06	1.19
25.5	11.8489	46.41	1.61
46.0	20.6083	37.95	1.06
52.5	22.3072	39.57	1.45
62.5	24.5414	38.11	1.5
72.5	26.0155	36.62	1.9

Table F.3 shows the raw ^{210}Pb activities (in Bq kg^{-1}, column 2). The data are a combination of data collected by Dr. P. Appleby and data from Becquerel Laboratories in Mississauga. The data was combined, by Dr. Appleby, in order to date core QV2 more precisely.

Columns 3 and 4 are the unsupported ^{210}Pb and cumulative unsupported ^{210}Pb respectively. Unsupported ^{210}Pb is calculated from total ^{210}Pb minus ^{226}Ra, while the cumulative unsupported ^{210}Pb, column 4, was calculated by numerical integration of column 3 with respect to column 5 in Table F.1. Interpolated values for ^{226}Ra were used for those samples that were not examined for ^{226}Ra. Columns 5 through 7 are the standard errors for the data.

Table F.3. ^{210}Pb analysis and standard errors for core QV2.

Depth	^{210}Pb data (Bq kg^{-1})			^{210}Pb Standard errors		
	total	unsup-ported	cumulat-ive unsupp.	Total	Unsup-ported	cumulative unsupp.
1						
3	280.0	228.86	2391.2	39.20	39.31	250.4
5	206.1	156.83	3573.4	15.33	15.57	341.5
7	130.0	85.97	4563.1	29.90	29.97	381.9
9	102.1	63.33	5278.9	9.26	9.38	443.8
11	160.0	120.66	6225.5	30.40	30.45	480.5
13	104.0	64.13	7226.7	9.46	9.64	558.1
15	92.0	53.98	7900.2	15.60	15.67	572.4
17	70.0	33.84	8408.9	28.00	28.03	610.3
19	61.6	27.33	8744.4	5.51	5.58	665.0
21	70.0	34.82	9079.7	11.20	11.25	669.9
23	58.9	22.82	9390.7	6.56	6.67	678.9
25.5	74.5	28.09	9728.3	6.89	7.08	684.5
28	66.0	20.62	10050.9	9.20	9.33	692.0
30	71.0	26.45	10296.1	11.40	11.5	700.7
34	63.0	20.10	10761.9	12.60	12.68	729.7
38	66.0	24.75	11173.4	9.90	9.98	761.4
40	62.0	21.57	11361.7	9.90	9.98	767.9
46	61.5	23.57	11784.4	6.29	6.38	781.7
48.5	60.0	21.30	11918.0	11.40	11.47	785.4
52.5	49.0	9.45	12076.6	4.96	5.17	790.5
62.5	39.8	1.67	12200.6	6.47	6.64	797.8
72.5	30.3	-6.30	12164.1	7.03	7.28	805.6
73			12180.0			

Table F.4, below, illustrates the calculated ages using

the CRS method of dating. Column 3 is cumulative unsupported ^{210}Pb (Bq/m^2) from interpolation from column 5, Table F.3. It is cumulative from the bottom up rather than top down. Thus cumulative values at an interval are subtracted from total inventory estimated at 11709 Bq/m^2 (Report on the Radiometric Dating of Quidi Vidi Lake: core QV2).

Column 4 is the age in years (t) calculated using the equation:

$$t=(1/k)*\ln(Ao/A)$$

where: A is the cumulative activity of unsupported ^{210}Pb
Ao is the estimated ^{210}Pb inventory for the whole core
k is the decay constant = 0.03114

Note, however, that the core was treated as three unique sections, below 34 cm, 34 to 25.5 cm, and above 25.5 cm. Column 7 is the date of each interval. Date=1992-age.

Though this model was applied it most likely does not represent the actual events that have occurred. In fact the ^{137}Cs profile indicates that the intervals of 25.5 and 34 cm correspond to 1963 and 1954 AD, respectively. These intervals were used to break the core into three parts in which the ^{210}Pb supply to each section was calculated (see below).

Prior to 1954 the ^{210}Pb flux was quite normal at 153 Bq m^{-2}y^{-1} (Report on the Radiometric Dating of Quidi Vidi Lake: Core QV2). The flux increases to 317 Bq M^{-2}y^{-1} for the period

1954-1963 and to 487 Bq $m^{-2}y^{-1}$ for the period 1963-1992. Thus

Table F.4. Calculated dates using the CRS model.

Depth (cm)	cum. dry mass (g/cm)	cum. unsup. ^{210}Pb (Bq/M^2)	age (yr)	error (yr)	date (AD)
1.0					
3.0	0.7954	9788.8	7.0	1	1985.0
5.0	1.3932	8606.6	11.0	2	1981.0
7.0	2.2086	7616.6	15.2	2	1976.8
9.0	3.1671	6901.2	18.1	2	1973.9
11.0	4.1942	5953.5	23.0	3	1969.0
13.0	5.2797	4953.3	29.0	3	1963.0
15.0	6.4202	4279.8	33.0	4	1959.0
17.0	7.5787	3771.1	37.0	4	1955.0
19.0	8.6757	3435.6	40.0	4	1952.0
21.0	9.7547	3100.3	43.3	5	1948.7
23.0	10.8337	2789.3	46.7	5	1945.3
25.5	12.1602	2451.7	50.8	5	1941.2
28.0	13.4845	2129.1	55.3	5	1936.7
30.0	14.5265	1883.9	59.4	5	1932.6
34.0	16.5279	1418.1	68.3	5	1923.7
38.0	18.3628	1006.6	78.8	6	1913.2
40.0	19.1758	818.3	85.2	7	1906.8
46.0	21.0486	395.6	109.5	13	1882.5
48.5	21.6449	211.2	129.0	14	1863.0
52.5	22.6799	77.8	161.0	14	1831.0

each part was treated as an entity, applying the CRS model to each section to create a composite chronology (Oldfield and Appleby, 1984).

The ^{210}Pb flux for each section was calculated using the following;

$$\Delta A = P/\lambda[\exp(-\lambda t_2) - \exp(-\lambda t_1)]$$

where:
P is the ^{210}Pb flux
ΔA is the cumulative unsupported ^{210}Pb in the section,
λ is the inverse of the decay constant (1/0.03114),
t_1 and t_2 ages of the top and bottom of the section of core,

The piecewise CRS model was applied to each section. For each section that spanned t_1 to t_2 the cumulative unsupported ^{210}Pb for the time span t_1 to t was calculated using;

$$\delta A = A(0)e^{-\lambda t} - A_1 \text{ (column 3, Table 4)}$$

where
$A(0) = P/\lambda$ and $A_1 = A(0)\exp(-\lambda t_1)$

The age of the sediment then can be calculated using the equation;

$$t = (1/k)(\ln(A(0)/(\delta A + A_1)$$

For the three sections, the following has been used to calculate the age of the sediment.

Pre-1954 (> 34 cm depth)
$t_1 = \infty$, $t_2 = 38$ y, $\Delta A = 1505$ Bq m^{-2}, $P = 153$ Bq m^{-2}y^{-1},
$A(0) = 4913$ Bq m^{-2}, $A_1 = 0$

1954-1963 (25.5-34 cm depth)
$t_1 = 38$ y, $t_2 = 29$ y, $\Delta A = 1008$ Bq m^{-2}, $P = 317$ Bq m^{-2}y^{-1},
$A(0) = 10178$ Bq m^{-2}, $A_1 = 3117$

1963-1992 (0-25.5 cm depth)
$t_1 = \infty$, $t_2 = 38$ y, $\Delta A = 1505$ Bq m^{-2}, $P = 153$ Bq m^{-2}y^{-1},
$A(0) = 4913$ Bq m^{-2}, $A_1 = 0$

Table F.5 shows the results using the piece-wise CRS method.

Table F.5. Calculated ages and dates using the three part CRS model on core QV2.

Depth (cm)	Age (years)	Date (AD)
3.0	5.1	1986.9
5.0	7.9	1984.1
7.0	10.5	1981.5
9.0	12.5	1979.5
11.0	15.4	1976.6
13.0	18.7	1973.3
15.0	21.2	1970.8
17.0	23.2	1968.8
19.0	24.6	1967.4
21.0	26	1966
23.0	27.4	1964.6
25.5	29	1963
28.0	31.5	1960.5
30.0	33.6	1958.4
34.0	38	1954
38.0	49	1943
40.0	55.7	1936.3
46.0	79	1913
48.5	92.2	1899.8
52.5	122.1	1869.9

Appendix G: relative and absolute analytical accuracy

ICP total concentrations for controls, standards and ranges in this study
Units are in ppm except for Al, Ca, Fe, K, Mg, Na and LOI which are in % and P which is in ppt

element	LKSD-1	study range	LKSD-2	study range	LKSD-3	study range	LKSD-4	study range
Ba	430	408 - 413	780	773 - 786	680	676 - 690	330	318 - 330
Be	1.1	0.6 - 0.7	2.5	1.8 - 1.9	1.9	1.6 - 1.6	1	0.7 - 0.8
Ce	27	26 - 30	108	115 - 117	90	90 - 95	48	46 - 50
Co	11	12 - 13	17	20 - 21	30	31 - 33	11	12 - 13
Cr	31	29 - 31	57	53 - 56	87	79 - 93	33	30 - 34
Cu	44	43 - 44	37	36 - 37	35	34 - 35	31	30 - 33
Dy	3.4	2.8 - 3.2	7.3	6.1 - 6.7	4.9	4.2 - 4.4	3.7	3.0 - 3.6
Fe	2.8	2.79 - 2.80	4.3	4.36 - 4.50	4	4.15 - 4.23	2.8	2.97 - 3.18
La	16	15 - 16	68	64 - 68	52	49 - 50	26	25 - 27
Li	7	6.9 - 7.4	20	22.5 - 23.1	25	25.6 - 28.9	12	12.6 - 13.1
LOI	23.5	15.2 - 23.2	12.3	11.6 - 11.9	11.8	11.5 - 11.8	40.8	38.8 - 40.7
Mn	700	700 - 700	2020	2000 - 2200	1440	1500 - 1500	500	500 - 600
Mo	10	11 - 13	<5	3 - 8	<5	2 - 5	<5	3 - 7
Nb	7	2 - 4	8	8 - 8	8	7 - 9	9	2 - 3
Ni	16	17 - 17	26	31 - 33	47	60 - 61	31	38 - 41
Pb	82	77 - 86	44	42 - 46	29	25 - 27	91	90 - 106
Rb	24	21 - 24	85	76- 82	78	71 - 74	28	19 - 23
Sc	9	8.5 - 9.2	13	13.7 - 14.8	13	13.2 - 14.5	7	7.5 - 8.5
Sr	250	260 - 267	220	237 - 245	240	244 - 257	110	123 - 128
Th	2.2	1 - 3	13.4	9 - 12	11.4	8 - 10	5.1	1 - 8
Ti	3010	2697 - 2899	3460	3311 - 3376	3330	3029 - 3145	2270	1771 - 1943
V	50	46 - 51	77	79 - 79	82	83 - 84	49	49 - 50
Y	19	19 - 20	44	39 - 40	30	26 - 27	23	21 - 22
Zn	331	314 - 324	209	205 - 210	152	144 - 145	194	185 - 194

element	D-1	study range	D-3	study range	D-4	study range
Al	4.9	4.84 - 4.96	3.1	2.99 - 3.11	3.28	3.26 - 3.31
Ba	170	170 - 170	1072	1066 - 1077	353	345 - 353
Be	3.1	3.0 - 3.2	2.8	2.7 - 2.8	2.5	2.4 - 2.5
Bi	1.8	1 - 3	5	5 - 5	4	3 - 5
Ca	0.29	0.28 - 0.30	0.41	0.40 - 0.42	0.18	0.17 - 0.18
Cd	0.6	0.6 - 0.7	2.2	2.1 - 2.2	1.3	1.2 - 1.3
Ce	76	76 - 76	138	138 - 138	138	137 - 139
Co	9.5	8 - 11	21	21 - 21	55	54 - 55
Cr	15	15 - 15	9	8 - 10	16	15 - 17
Cr2a	10.5	9 - 12	8	6 - 9	15	15 - 15
Cu	13	13 - 13	3	3 - 3	12	11 - 12
Dy	4.8	4.7 - 4.9	6.1	5.5 - 6.6	4.3	3.2 - 5.4
Fe	3	2.96 - 3.05	6.3	6.19 - 6.35	7.1	6.95 - 7.25
Ga	8.5	8 - 9	8	7 - 8	11	10 - 11
K	0.19	0.19 - 0.20	0.09	0.09 - 0.09	0.1	0.09 - 0.10
La	38	37 - 39	48	47 - 48	47	46 - 47
Li	3.1	3.1 - 3.1	7.1	7.1 - 7.1	7.1	7.0 - 7.2
LOI	35.9	35.6 - 36.1	13.2	13.1 - 13.3	14.9	14.8 - 15.0
Mg	0.1	0.09 - 0.10	0.06	0.06 - 0.06	0.06	0.06 - 0.06
Mn	100	100-100	4650	4590-4720	2950	2900-3000
Mo	12	11 - 13	52	51 - 53	9	8 - 10
Na	0.21	0.21 - 0.22	0.07	0.06 - 0.07	0.07	0.06 - 0.07
Nb	3	3 - 3	2	2 - 2	1	1 - 1
Ni	7	6 - 8	5	4 - 5	10	10 - 10
P	1482	1467 - 1498	564	558 - 569	867	867 - 867
Pb	14	13 - 14	49	48 - 49	47	45 - 48
Rb	9	7 - 9	7	5 - 8	<5	-5
Sc	5.6	5.2 - 5.9	4.6	4.3 - 4.9	6.1	5.9 - 6.3
Sr	25	24 - 25	81	80 - 82	28	27 - 28
Th	10	8 - 11	12	9 - 14	6	4 - 7
Ti	1370	1362 - 1378	692	691 - 692	843	839 - 846
V	43	42 - 44	44	44 - 44	67	67 - 67
Y	34	33 - 35	45	44 - 46	28	28 - 28
Zn	81	79 - 83	86	86 - 86	112	110 - 113

Neutron Activation controls for total concentration

	D-1	study range	D-3	study range	D-4	study range	D-5	study range
As	1.8	1.6 - 2.0	2.3	2.0 - 2.4	1.3	1.2 - 1.3	1.0	0.7 - 0.7
Au	1.0	1.0	1.0	1.0	1.0	1.0	1.0	1.0
Ba	69.0	57 - 74	743.0	570 - 680	255.0	200 - 250	108.0	82 - 82
Br	74.5	66.6 - 78.4	15.7	15 - 16	36.0	35.3 - 38.5	22.8	21.3 - 22.7
Ce	76.0	65 - 83	115.0	90 - 110	114.0	110 - 120	38.0	32 - 35
Co	6.5	5.5 - 9.1	14.0	13 - 17	44.0	44 - 51	6.8	6.3 - 6.5
Cr	19.0	8 - 25	18.0	8 - 8	22.0	8 - 8	14.0	8 - 8
Cs	0.5	0.2 - 0.7	0.6	0.4 0.9	0.5	0.2 - 0.6	0.5	0.4 - 0.8
Eu	1.0	1.3 - 2.2	1.0	1.4 - 2.2	0.9	1.3 - 1.8	0.5	0.58 - 0.65
Fe	2.7	3.0 - 3.4	4.6	5.0 - 5.6	5.3	6.2 - 6.4	2.1	2.2 - 2.3
Hf	0.7	0.85 - 1.30	0.4	0.20 - 0.65	0.3	0.2 - 0.2	0.5	0.58 - 0.65
La	35.9	36 - 40	36.4	33 - 43	36.8	36 - 41	15.5	16 - 16
Lu	0.5	0.02 - 0.22	0.8	0.02 - 0.02	0.3	0.02 - 0.16	0.2	0.02 - 0.02
Mo	8.4	6.3 - 8.8	47.1	42 - 44	5.7	5.6 - 6.9	2.5	2.5 - 2.5
Na	0.2	0.25 - 0.26	0.1	0.05 - 0.07	0.1	0.07 - 0.09	0.1	0.08 - 0.09
Ni	5.4	5.0 - 5.0	5.0	5 - 5	7.0	5.0	5.5	5.0
Rb	8.1	6.4 - 10.0	4.4	2.0 - 9.4	2.8	2.0 - 5.1	5.0	5.8 - 7.0
Sb	0.2	0.14 - 0.17	0.2	0.12 - 0.19	0.2	0.15 - 0.15	0.1	0.07 - 0.08
Sc	4.5	5.5 - 6.3	3.0	3.4 - 4.0	4.0	5.0 - 5.6	2.5	3.0 - 3.1
Se	1.5	1.0	1.0	1.0	1.0	1.0	1.1	1.0
Sm	6.0	5.1 - 6.2	5.6	4.4 - 5.6	5.8	5.4 - 6.3	3.1	2.6 - 2.6
Ta	0.4	0.22 - 0.47	0.2	0.10 - 0.30	0.2	0.10 - 0.23	0.2	0.10 - 0.21
Tb	1.0	0.71 - 1.00	1.1	0.88 - 1.00	0.8	0.62 - 0.83	0.4	0.28 - 0.33
Th	7.8	6.5 - 7.5	12.4	11.3 - 11.9	7.0	6.7- 6.9	3.6	3.4 - 3.4
U	19.7	15.2 - 17.5	46.6	41.1 - 42.8	11.4	10.4 - 10.6	4.3	4.0 - 4.1
W	1.0	1.0	1.0	1.0	1.0	1.0	1.0	1.0
Yb	2.0	1.4 - 3.9	3.0	2.0 - 3.7	1.4	1.1 - 2.6	0.7	0.20 - 0.63
Zn	56.0	25 - 69	45.0	25 - 51	61.0	62 - 76	33.0	25 - 25
Zr	100.0	100.0	100.0	100.0	100.0	100.0	100.0	140.0

	D-6	study range	D-7	study range
As	12.7	13 - 13	14.0	14 - 15
Au	1.3	1.0	1.0	1.0
Ba	4750.0	4610 - 4920	109.0	84 - 130
Br	5.9	6.2 - 6.3	47.8	46.8 - 49.4
Ce	132.0	140 - 160	265.0	262 - 286
Co	4.3	4.0 - 5.6	33.0	36 - 42
Cr	31.0	30 - 38	33.0	8 - 8
Cs	5.2	5.3 - 6.3	0.8	0.8 - 1.3
Eu	0.6	0.7 - 2.0	0.7	1.1 - 2.2
Fe	1.2	1.5 - 1.7	9.6	12.2 - 13.0
Hf	5.3	5.7 - 7.5	2.2	2.3 - 3.3
La	52.4	56 - 65	61.6	64 - 73
Lu	4.8	6.12 - 6.64	0.6	0.53 - 1.0
Mo	3.6	4.4	2.6	3.3
Na	0.5	0.62 -0.70	0.2	0.25 - 0.28
Ni	5.9	5.0	5.4	5.0
Rb	133.0	120 - 130	16.4	10 -27
Sb	2.2	2.1 - 2.3	0.5	0.51 - 0.54
Sc	1.2	1.4 - 1.7	3.2	4.1 - 4.3
Se	1.0	1.0	1.0	1.0
Sm	22.0	22.3 - 25.6	16.8	15.6 - 20.2
Ta	2.7	2.6 - 2.9	0.7	0.56 - 0.66
Tb	8.1	7.5 - 7.7	3.0	2.5 - 2.8
Th	11.3	11.5 - 12.1	9.5	9.1 - 10.1
U	10.5	10.0 - 10.4	4.7	4.3 - 4.6
W	3.6	3.4 - 4.6	1.0	1.0
Yb	28.0	24.5 - 41.4	5.1	3.7 - 6.6
Zn	949.0	1100 - 1300	82.0	61 - 160
Zr	130.0	100.0	104.0	140.0

	LKSD-1	study range	LKSD-2	study range	LKSD-3	study range	LKSD-4	study range
Ag	0.6	1.0	0.8	1.0	2.7	1.0 - 3.6	<0.5	1.0
As	40.0	36.6 - 40.0	11.0	10 - 11	27.0	25.6 - 28.3	16.0	13 - 14
Au	5.0	4.4 - 5.0	3.0	1.0 - 3.3	3.0	3.3 - 4.3	2.0	1.0 - 5.0
Ba	430.0	420 - 460	780.0	690 - 800	680.0	650 - 730	330.0	93 - 140
Br	11.0	12 - 14	18.0	19 - 21	16.0	16 - 19	49.0	47.6 - 51.9
Ce	27.0	32 - 33	108.0	110 - 120	90.0	90 - 100	48.0	43 - 49
Co	11.0	10 - 12	17.0	18 - 25	30.0	36 - 42	11.0	11 - 13
Cr	31.0	31 - 44	57.0	63 - 77	87.0	100 - 110	33.0	26 - 39
Cs	1.5	0.7 - 0.7	3.0	2.2 - 3.1	2.3	2.1 - 2.5	1.7	1.0 - 1.4
Eu	0.9	1.0 - 1.0	1.9	0.8 - 1.9	1.5	0.25 - 2.4	1.1	1.1 - 1.5
Fe	2.8	3.4 - 3.8	4.3	4.3 - 5.0	4.0	4.5 - 5.1	2.8	3.0 - 3.3
Hf	3.6	4.4 - 5.3	7.0	7.1 - 8.2	4.8	5.2 - 5.7	2.8	2.4 - 3.7
La	16.0	16 - 18	68.0	59 - 71	52	47 - 54	26.0	23 - 24
Lu	0.4	0.32 - 0.52	0.6	0.02 - 0.94	0.4	0.02 - 0.58	0.5	0.02 - 0.02
Mo	10.0	11.5	<5	2.5	<5	2.5	<5	2.5
Ni	16.0	5 - 22	26.0	5 - 32	47.0	35 - 54	31.0	5 - 29
Rb	24.0	29- 30	85.0	78 - 92	78.0	68 - 78	28.0	23 - 25
Sb	1.2	1.2 - 1.2	1.1	1.0 - 1.1	1.3	1.2 - 1.3	1.7	1.4 - 1.6
Sc	9.0	10.0 - 11.3	13.0	13.2 - 14.7	13.0	12.3 - 15.2	7.0	6.9 - 8.0
Sm	4.0	4.1 - 4.4	11.0	10.8 - 13.0	8.0	7.9 - 10.0	5.0	3.0 - 3.7
Ta	0.3	0.28 - 0.31	0.8	0.68 - 0.83	0.7	0.55 - 0.79	0.4	0.25 - 0.41
Tb	0.6	0.59 - 0.69	1.4	1.2 - 1.4	1.0	0.62 - 1.00	1.2	0.57 - 0.62
Th	2.2	2.2 - 2.3	13.4	12.3 - 13.3	11.4	11.0 - 12.1	5.1	4.5 - 4.6
U	9.7	10.3 - 11.0	7.6	7.4 - 7.9	4.6	4.8 - 5.1	31.0	27.2 - 29.5
W	<4	1.0	<4	1	<4	1.0	<4	1.0
Yb	2.0	3.1 - 4.0	4.0	3.0 - 5.7	2.7	2.0 - 4.3	2.0	1.2 - 2.7
Zn	331.0	480 - 510	209.0	210 - 250	152.0	170 - 200	194.0	150 - 240
Zr	134.0	100.0	254.0	220 - 290	178.0	100.0	105.0	100.0

Partial element levels for controls

element	LKSD-1	sample range	LKSD-2	sample range	LKSD-3	sample range	LKSD-4	sample range
Cd	1.2	0.8 - 1.0	0.6	0.6	0.4	0.4	1.9	1.3 - 1.5
Co	8.0	5.0 - 7.0	16.0	12.0	30.0	23.0	9.0	6.0 - 7.0
Cu	44	27 - 33	36	27.0	34.0	27.0	31.0	20 - 24
Fe	1.8	1.21 - 1.34	3.7	3.2	3.6	3.3	2.6	1.93 - 2.17
Mn	410.0	284 - 315	1840.0	1670.0	1300.0	1012.0	420.0	322 -334
Ni	12	8 - 10	23	17	46	35	31	21 - 23
Pb	83	57 - 63	34	28	21	17	91	61 - 66
Zn	335	233 - 291	205	176	151	133	195	132 - 155

element	D-1		D-3		D-4		D-5	
Cd	0.6	0.4 - 0.5	2.1	2.0 -2.2	1.4	1.1 - 1.3	0.3	0.1 - 0.2
Co	6	5 - 5	14	13 - 14	43	39- 41	6	5 - 5
Cu	12	10 - 10	5	5 - 6	13	12 - 13	8	6 - 7
Fe	2.34	2.08 - 2.13	5.1	3.81 - 3.90	6.36	4.52 - 4.95	2.2	1.88 - 2.00
Mn	544	621 - 646	43900	38950	28600	25100	240	226 - 246
Ni	6	3 - 3	4	3 - 3	6	6 - 7	5	4 - 4
Pb	17	13 - 13	35	34 - 35	34	34 - 34	9	7 - 8
Zn	64	66 - 67	62	76 - 77	92	96 - 100	51	47 - 48

element	D-6	
Cd	4.1	3.5 - 3.5
Co	3	4 - 4
Cu	289	284 - 285
Fe	1.04	0.85 - 0.93
Mn	3140	2030 - 2460
Ni	12	10 - 11
Pb	1500	1550 - 1580
Zn	836	828 - 873

Mercury cold vapour atomic absorption spectrophotometry

element	LKSD-1	sample range	LKSD-2	sample range	LKSD-3	sample range	LKSD-4	sample range
Hg	98.0	100-127	154.0	144-176	276.0	266-326	165.0	164-172

Appendix H:
Dry sediment Influx and Wet Sedimentation Rates

depth (cm)	Date (A.D.)	influx g/cm^2 * yr	Wet sedimentation rate cm * yr
1.0	1992.00	0.088	0.38
3.0	1989.40	0.195	0.81
5.0	1986.9	0.214	0.70
7.0	1984.1	0.315	0.77
9.0	1981.5	0.477	1.00
11.0	1979.5	0.359	0.70
13.0	1976.6	0.324	0.60
15.0	1973.3	0.464	0.81
17.0	1970.8	0.582	1.01
19.0	1968.8	0.789	1.44
21.0	1967.4	0.749	1.39
23.0	1966.0	0.771	1.43
25.5	1964.6	0.829	1.56
28.0	1963.00	0.519	0.98
30.0	1960.45	0.501	0.96
32.0	1958.37	0.551	1.07
34.0	1956.50	0.402	0.80
36.0	1954.00	0.187	0.40
38.0	1949.0	0.146	0.33
40.0	1943.0	0.122	0.30
42.0	1936.3	0.098	0.27
44.0	1929.0	0.081	0.25
46.0	1921.0	0.069	0.25
48.5	1913.0	0.045	0.19
52.5	1899.8	0.035	0.13
57.5	1869.9	0.067	0.27
62.5	1851.1	0.052	0.27
67.5	1832.3	0.044	0.27
72.5	1813.5	0.042	0.27
77.5	1794.7	0.037	0.27
82.5	1775.9	0.037	0.27
87.5	1757.1	0.005	0.04
92.5	1620.00	0.005	0.04
97.5	1482.00	0.005	0.04
102.5	1345.00	0.005	0.04
107.5	1207.00	0.005	0.04

depth (cm)	Date (A.D.)	Dry sediment influx g/cm^2 * yr	Wet sedimentation rate cm * yr
112.5	1071.00	0.005	0.04
117.5	933.00	0.005	0.04
122.5	796.00	0.005	0.04
127.5	658.00	0.005	0.04
132.5	521.00	0.005	0.04
137.5	384.00	0.005	0.04
142.5	246.00	0.005	0.04
147.5	109.00	0.005	0.04
152.5	-27.00	0.005	0.04
157.5	-165.00	0.005	0.04
162.5	-302.00	0.005	0.04
167.5	-439.00	0.005	0.04
172.5	-577.00	0.005	0.04
177.5	-714.00	0.005	0.04
182.5	-851.00	0.005	0.04
187.5	-988.00	0.006	0.04
192.5	-1126.00	0.006	0.04
197.5	-1263.00	-0.001	-0.00